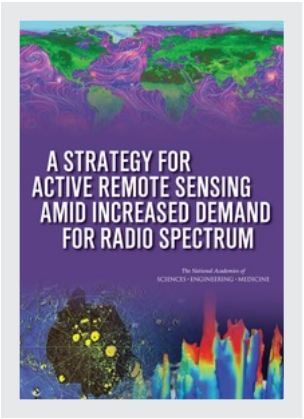

A Strategy for Active Remote Sensing Amid Increased Demand for Radio Spectrum

DETAILS

247 pages | 7 x 10 | PAPERBACK
ISBN 978-0-309-37305-0 | DOI 10.17226/21729

CONTRIBUTORS

Committee on a Survey of the Active Sensing Uses of the Radio Spectrum; Board on Physics and Astronomy; Division on Engineering and Physical Sciences; National Academies of Sciences, Engineering, and Medicine

A STRATEGY FOR ACTIVE REMOTE SENSING AMID INCREASED DEMAND FOR RADIO SPECTRUM

Committee on a Survey of the Active Sensing Uses of the Radio Spectrum

Board on Physics and Astronomy

The National Academies of
SCIENCES • ENGINEERING • MEDICINE

THE NATIONAL ACADEMIES PRESS
Washington, DC
www.nap.edu

THE NATIONAL ACADEMIES PRESS 500 Fifth Street, NW Washington, DC 20001

This study was supported by the National Aeronautics and Space Administration under Contract NNH10CD04B, TO#6. Any opinions, findings, conclusions, or recommendations expressed in this publication are those of the author(s) and do not necessarily reflect the views of the organizations or agencies that provided support for the project.

International Standard Book Number-13: 978-0-309-37305-0
International Standard Book Number-10: 0-309-37305-0

Additional copies of this report are available for sale from the National Academies Press, 500 Fifth Street, NW, Keck 360, Washington, DC 20001; (800) 624-6242 or (202) 334-3313; http://www.nap.edu.; and from the Board on Physics and Astronomy, National Academies of Sciences, Engineering, and Medicine, 500 Fifth Street, N.W., Washington, DC 20001, Internet: http://www.national-academies.org/bpa.

Printed in the United States of America

Suggested citation: National Academies of Sciences, Engineering, and Medicine. 2015. *A Strategy for Active Remote Sensing Amid Increased Demand for Radio Spectrum*. Washington, DC: The National Academies Press.

The National Academies of
SCIENCES • ENGINEERING • MEDICINE

The **National Academy of Sciences** was established in 1863 by an Act of Congress, signed by President Lincoln, as a private, nongovernmental institution to advise the nation on issues related to science and technology. Members are elected by their peers for outstanding contributions to research. Dr. Ralph J. Cicerone is president.

The **National Academy of Engineering** was established in 1964 under the charter of the National Academy of Sciences to bring the practices of engineering to advising the nation. Members are elected by their peers for extraordinary contributions to engineering. Dr. C. D. Mote, Jr., is president.

The **National Academy of Medicine** (formerly the Institute of Medicine) was established in 1970 under the charter of the National Academy of Sciences to advise the nation on medical and health issues. Members are elected by their peers for distinguished contributions to medicine and health. Dr. Victor J. Dzau is president.

The three Academies work together as the **National Academies of Sciences, Engineering, and Medicine** to provide independent, objective analysis and advice to the nation and conduct other activities to solve complex problems and inform public policy decisions. The Academies also encourage education and research, recognize outstanding contributions to knowledge, and increase public understanding in matters of science, engineering, and medicine.

Learn more about the National Academies of Sciences, Engineering, and Medicine at **www.nationalacademies.org**.

COMMITTEE ON A SURVEY OF THE ACTIVE SENSING USES OF THE RADIO SPECTRUM

FAWWAZ ULABY, University of Michigan, *Chair*
SUSAN AVERY, Woods Hole Oceanographic Institute
COLEMAN BAZELON, The Brattle Group
WILLIAM BRISTOW, University of Alaska, Fairbanks
DONALD B. CAMPBELL, Cornell University
MARIE COLTON, NOAA Great Lakes Environmental Research Laboratory (retired)
SANDRA CRUZ-POL, University of Puerto Rico-Mayaguez (resigned August 2014)
LENNARD FISK, University of Michigan
ALBIN GASIEWSKI, University of Colorado, Boulder
JEFFREY HERD, MIT Lincoln Laboratory
LINWOOD JONES, University of Central Florida
PAUL KOLODZY, Kolodzy Consulting
ROBERT PALMER, University of Oklahoma
DEAN PASCHEN, First RF Co.
MICHAEL SPENCER, Jet Propulsion Laboratory, California Institute of Technology
DAVID LONG, Brigham Young University, *consultant to the committee*

Staff

DAVID B. LANG, Senior Program Officer, *Study Director*
JAMES C. LANCASTER, Director, Board on Physics and Astronomy
LINDA WALKER, Program Coordinator
BETH DOLAN, Financial Associate

Preface

To support the presidential initiative for Spectrum Management for the 21st Century, a review of current and future needs of scientific users of the spectrum is in order. In recent years, the explosion of new wireless technologies has significantly increased the demand for access to the radio spectrum. The increased demand has led to discussions in both government and industry about new ways of thinking about spectrum allocation and use.

Scientific users of the radio spectrum (such as radio astronomers and Earth scientists using remotely sensed data) have an important stake in the policies which will result from this activity. A survey of the scientific uses of the spectrum up to 3 THz by passive (receive-only) means was conducted by the National Research Council (NRC), resulting in "Spectrum Management for Science in the 21st Century" (SMS). Identifying the potentially dire interference situation posed to NASA's in-orbit and planned passive remote sensing observatories and to the National Science Foundation's ground-based radio astronomy observatories, the report had a significant amount of impact in the Administration and Congress.

NASA requested that the NRC immediately embark on a similar study to explore the current and planned scientific use of the spectrum by active means and the current and potential vulnerabilities and problem areas therein. This information will assist spectrum management decision makers in balancing the requirements of the scientific users of the spectrum with other interests.

With funding from NASA, the NRC convened the Committee on a Survey of the Active Scientific Use of the Radio Spectrum to conduct this study and issue a report. The committee first met in Washington, D.C. on August 15-16, 2013, at

which it heard from government policymakers. The subsequent 3 meetings over the following year featured discussions with experts and stakeholders from academia, government labs, industry, and foreign interests. In particular, the committee organized a one-day workshop to gather information on radiofrequency interference experiences by operating spaceborne active remote sensing platforms. This workshop was held at the Jet Propulsion Laboratory on November 8, 2013, and an account of the meeting is provided in the appendix to this report.

In the course of its discussions the transmission of collected data arose (for example, NASA's Deep Space Network) as a possible topic for the committee to include in its report. However, after discussion, the committee and sponsors concluded that, while crucial in its own right, that it is outside of the committee's purview and expertise and thus should not be treated in this report. Both the sponsor and committee agreed that an in-depth look at data transmission could indeed be a separate and valuable study following this one.

In writing its report the committee presents the scientific and technical bases for the multiple applications of active remote sensing in separate chapters: the atmosphere; the oceans; the land surfaces; space physics; and radar astronomy. These chapters (Chapters 2-6) also summarize the spectrum usage for each remote sensing and radiofrequency interference environment for each application. A later chapter (Chapter 8) discusses in greater detail radiofrequency interference issues for active sensing instruments. Finally, Chapter 7 provides an overview of spectrum allocation policies and the frequency assignment process, and Chapter 9 knits the report together by recommending unilateral and cooperative strategies for enhanced usage of the spectrum by all parties, including commercial interests.

This report provides useful information and guidance to engineers who operate the current suite of spacecraft and those who will build future observatories; scientists who use the information gleaned by these spacecraft; policymakers who must balance multiple competing priorities; and the telecommunications industry which is facing ever-increasing demand. The forward-looking approach laid out in this report allows scientists to continue to provide the nation and world with an improving understanding of Earth and the local solar system while working cooperatively alongside other spectrum users in an era of ever-increasing demand for bandwidth.

Acknowledgment of Reviewers

This report has been reviewed in draft form by individuals chosen for their diverse perspectives and technical expertise, in accordance with procedures approved by the Report Review Committee of the National Academies of Sciences, Engineering, and Medicine. The purpose of this independent review is to provide candid and critical comments that will assist the institution in making its published report as sound as possible and to ensure that the report meets institutional standards for objectivity, evidence, and responsiveness to the study charge. The review comments and draft manuscript remain confidential to protect the integrity of the deliberative process. We wish to thank the following individuals for their review of this report:

William J. Blackwell, Massachusetts Institute of Technology,
V. Chandra Chandrasekar, Colorado State University,
Bryan Huneycutt, Jet Propulsion Laboratory,
David L. Hysell, Cornell University,
Kenneth Jezek, The Ohio State University,
Jean-Luc Margot, University of California, Los Angeles,
James J. Reis, Fugro EarthData,
Gregory Rosston, Stanford Institute for Economic Policy Research,
David T. Sandwell, Scripps Institute of Oceanography,
Robert J. Serafin, National Center for Atmospheric Research, and
Paul Siqueira, University of Massachusetts.

Although the reviewers listed above have provided many constructive comments and suggestions, they were not asked to endorse the conclusions or recommendations nor did they see the final draft of the report before its release. The review of this report was overseen by Ken Kellermann, National Radio Astronomy Observatory, who was responsible for making certain that an independent examination of this report was carried out in accordance with institutional procedures and that all review comments were carefully considered. Responsibility for the final content of this report rests entirely with the authoring committee and the institution.

Contents

Summary

The Committee on a Survey of the Active Sensing Uses of the Radio Spectrum was tasked with: (1) documenting the importance of active remote sensing, particularly for the purpose of serving societal needs; (2) documenting the threats, both current and future, to the effective use of the electromagnetic spectrum required for active remote sensing; and (3) offering specific recommendations for protecting and making effective use of the spectrum required for active remote sensing.

Active remote sensing is defined as the use of a transmitter and at least one receiver to measure (sense) the transmission or scattering properties of a medium at radio frequencies. These measurements discern the physical state of the medium through which the signal passes or is scattered by. The media of interest encompass Earth's atmosphere (including the ionosphere), oceans, and land surfaces, as well as extraterrestrial objects.

This report concentrates on active remote sensing at radio frequencies, which is the portion of the electromagnetic spectrum from near 0 Hz to 300 GHz. Measurements in this range have direct societal benefits. Active remote sensing measurements can be either transmission measurements, in which the transmit and receive antennas usually point at each other; or scattering measurements, where the transmitted signal reflects from the medium and is received by an antenna co-located with the transmitter (the backscatter mode), or by a non-colocated receiver (the bistatic mode). Active remote sensing is performed by ground-based, airborne, or satellite platforms, or combinations thereof.

Demand for spectrum is growing quickly, spurred by advanced, affordable electronics and mobile wireless technology. The proliferation of wireless technology

has also meant increasing interference to active remote sensing systems, particularly in the L- and C-bands.

Regulators are using reallocation, spectrum sharing, and higher spectral efficiency to try to make the desired spectrum available.

Wireless communication systems have already demonstrated the ability to share the spectrum. While it has not yet occurred, it should be possible for Earth active remote sensing systems to operate in existing communication bands, although limitations exist, to provide scientists with access to improved observations and thus an improved understanding of Earth.

Several letter-designation schemes are in common use for sub-bands within and adjacent to the radio bands and are used in this report: HF band (3-30 MHz); VHF band (30-300 MHz); UHF band (300 MHz to 1 GHz); L-band (1-2 GHz); S-band (2-4 GHz); C-band (4-8 GHz); X-band (8-12 GHz); K_u-band (12-18 GHz); K-band (18-27 GHz); K_a-band (27-40 GHz); V-band (40-75 GHz); W-band (75-110 GHz); and millimeter-wave band (110-300 GHz).[1]

THE IMPORTANCE OF ACTIVE REMOTE SENSING

Active remote sensing is a principal tool used to study and to predict short- and long-term changes in the environment of Earth—the atmosphere, the oceans and the land surfaces—as well as in the near-space environment of Earth. All of these measurements are essential to understanding terrestrial weather, climate change, solid Earth processes, space weather hazards, inventory and tracking of space debris, and threats from asteroids. Active remote sensing measurements are also of great benefit to society, as we pursue the development of a technological civilization that is economically viable and seek to maintain the quality of our life.

Specific examples of the importance of different types of active remote sensing measurements to science and society include these:

- Active remote sensing of the atmosphere can save lives and protect property from severe storms, as well as provide a deeper understanding of upper-atmospheric winds and global circulation to scientists.
- Active microwave sensors provide unique measurements of ocean currents, waves, and wind speed and direction and are complementary to passive microwave and visible and infrared (IR) measurements. Applications include global weather prediction, storm and hurricane warning, wave forecasting, coastal storm surge, ship routing, commercial fishing, and coastal currents and wave monitoring. These applications are vital to the interests of the United States.

[1] The committee has used the IEEE Standard Letter Designations for Radar-Frequency Bands.

- Spaceborne, airborne, and surface-operated active remote sensing measurements with radar, including real-aperture radars, synthetic-aperture radars (SARs), and scatterometers, provide essential data over land-use and ice critical to our understanding of global change and environmental management and weather forecasting, all of which are important for a wide range of scientific, commercial, and defense applications, such as urban planning, agriculture, forestry, water management, topography, sea ice mapping, earthquake and volcano studies, post-disaster assessment, and spatial intelligence.
- Active remote sensing of the ionosphere is essential for understanding the basic physics of this near-space region but also for predicting the impacts of space weather events on our electricity-dependent society.
- Active remote sensing through planetary radar astronomy continues to make important contributions to our understanding of the solar system, planning for space missions to extraterrestrial objects, and in particular for the tracking and characterization of near-Earth asteroids that may pose a threat to society.

However, many of these benefits are not easy to fully internalize in a market system, so the value of active sensing is very difficult to compare with commercial systems. For example, benefits from advances in weather prediction might be hard to internalize such that private entities would not invest sufficiently in the prediction systems. Also, basic research such as this develops knowledge, which is a public good, and is again hard to fully internalize in a market system. Furthermore, scientific discoveries can lead to many different types of social benefits.

Current and Future Threats to the Effective Use of Spectrum Required for Active Remote Sensing

In all cases the frequencies utilized by active remote sensing are determined by the physics of the phenomena that are being studied. The frequencies were carefully chosen to best reveal the underlying physics, and in most cases considerable expense has been incurred in facilities and technology to operate in the chosen frequency range. For each type of measurement, it may be very difficult to relocate operations into other frequency bands. Thus, given that ongoing active remote sensing measurements are essential to protect the future of society, there must be effective access for these measurements to the required spectrum.

There are primarily two spectrum issues that can impact active science sensors. Like passive sensors, active sensors can experience radio-frequency interference (RFI) from other radio services. Conversely, and unlike passive systems, active

systems also transmit signals and are hence subject to operational restrictions to ensure that they do not interfere with other services. With growing demand for and use of the spectrum growing rapidly, both of these spectrum issues are generating concerns about the successful operation of current and planned active science sensors.

Specific examples of current interference and potential future interference include these:

- In several cases, transmit restrictions imposed on active science sensors have significantly impeded the ability to collect the desired science data (as in the operational restrictions imposed on the European Space Agency's [ESA's] BIOMASS mission), degraded the science data (an example being the deep spectral waveform notches required on the GeoSAR sensor flown on aircraft), or significantly driven up costs (as for the NASA Soil Moisture Active-Passive mission). Conservative interference standards in some bands can make science operations difficult. Restrictions imposed in the lower frequency UHF and L-bands are increasing with time. (Finding 8.2)
- The RFI environment has been observed to be growing worse in some bands. Within the heavily used and well-studied L-band allocation of 1215-1300 MHz, the amount of RFI observed worldwide has steadily increased over time. This trend has been detected by a series of L-band SARs operated by the Japan Aerospace Exploration Agency (JAXA) spanning the years 1992-2011. ESA has reported an increase in RFI at the C-band. (Finding 8.4)
- Established, high-value science radar measurements at the C-band face near-term threats due to the planned expansion of commercial services in the Earth Exploration-Satellite Service-Active spectrum allocation. The proposed 5350-5470 MHz Radio Local Access Network (RLAN) service will severely limit science performed by the ESA's Sentinel-1 Constellation (Copernicus Program) and the Canadian Radarsat-2 and RadarSat Constellation Mission (RCM) constellations. The broad-band, noise-like nature of RLAN emitters is difficult or impossible to mitigate. (Finding 8.7)
- There are multiple bands allocated to Earth-Exploration Satellite Service-Active where only portions of the band are being used or that are not being used at all. With constant pressure to accommodate new services, it may be more difficult to establish new science in these bands in the future. (Finding 8.10)
- For nearly four decades ocean-sensing radar systems have coexisted with the global communications and radar infrastructure. Recently there have been more instances of RFI to active sensors from communications and navigation systems at the C-band and lower frequencies. So far the impact

of degraded sensor performance or loss of data has been manageable over most regions of the world through the application of aggressive RFI mitigation techniques. (Chapter 3 "Findings and Recommendations")

- RFI has not been a significant impediment to planetary radar astronomy observations to date. However, as bandwidth requirements increase due to the need to image near-Earth asteroids at high spatial resolution, RFI could pose a significant problem in the future. To facilitate high-spatial-resolution imaging of small near-Earth asteroids, frequency assignments with bandwidths of 60 MHz to 120 MHz are required. The NASA JPL Goldstone radar currently has an assignment of 200 MHz centered at 8.600 GHz. (Finding 6.2)

It should be noted that whereas active science sensors routinely report interference from other non-science sources, science sensors appear to rarely interfere with other services. The only documented instance to come to the attention of the committee of an active science sensor actually interfering with the operations of another service was the radar on the NASA CloudSat mission, which can interfere with radio astronomy measurements (another science service).

One of the reasons for this lack of interference from active remote sensing users is the resistance of communications systems to interference from radar systems with narrow pulse waveforms and low duty cycles, which are typical characteristics of scientific and operational radars.

Current RFI mitigation techniques work best for interfering signals that have sparse spectral or temporal occupancy—for example, signals that are close to being a continuous wave or having short, widely separated pulses. The more that sources, or aggregates of sources, resemble broadband white noise, the more difficult the interference is to mitigate with known techniques. Consequently, active remote sensing is able to share more effectively with some services than with others, depending on the nature of the interfering signal. So far, current RFI mitigation techniques have able to significantly reduce the impact of interference on science in the UHF, L-, and C-bands, and few problems with RFI, generally, have been experienced with the science measurements made at frequencies above the C-band.

It should also be noted that one of the difficulties with characterizing the impact of RFI on active remote sensing space instruments is the incompleteness of information regarding current emitters world-wide, as well as the evolving nature of the RFI environment over time. There is currently a lack of good metrics for quantifying the degradation of science measurements for the full variety of active instrument types (e.g., scatterometers, altimeters, SARs, interferometers, and sounders). This makes it very difficult to accurately quantify how a given active sensor might be impacted by RFI, how the RFI might be mitigated, and how the spectrum might be shared.

Recommendations for the Protection and Effective Use of the Spectrum Required for Active Remote Sensing

The recommendations of how to protect and effectively use the spectrum required for active remote sensing fall into the following categories: (1) actions by the science community; (2) actions by federal agencies; (3) possible actions by the telecommunications industry; (4) opportunities for spectrum sharing; and (5) recommended increases in the spectrum allocated for scientific active remote sensing.

Actions by the Science Community

Merit alone will not assure that the spectrum required is available for the scientific community. Scientific interests must be actively engaged in the spectrum allocation and assignment process to assure that science needs are met. (Finding 7.2) This will require ongoing efforts to ensure active remote sensing is balanced with competing interests in the regulatory processes, and to make more information available about the value of active remote sensing:

- The science community should increase its participation in the International Telecommunications Union (ITU), the National Telecommunications and Information Administration (NTIA), and the Federal Communications Commission (FCC) spectrum management processes. This includes close monitoring of *all* spectrum management issues to provide early warning for areas of concern. It also requires regular filings in regulatory proceedings and meetings with decision makers. This will build credibility for the science community and ensure a seat at the table for spectrum-related decision making that impacts the science community. (Recommendation 7.1)
- For the spectrum management process to be effective, the science community, NASA, the National Oceanic and Atmospheric Administration (NOAA), the National Science Foundation (NSF), and the U.S. Department of Defense (DOD) should also articulate the value of the science-based uses of radiofrequency spectrum. Such value will include both economic values, through enabling commerce or reducing the adverse economic impacts of natural phenomenon, and noneconomic values that come from science research. (Recommendation 7.2)
- The next decadal surveys in solar and space physics and Earth science should address the future spectrum needs for their communities. (Recommendation 7.4)

Actions by Federal Agencies

Actions for federal agencies responsible for supporting the scientific use of active remote sensing, and for overseeing spectrum allocations, include these:

- NASA should lead an effort to significantly improve characterization of the RFI environment that affects active science measurements. This effort should also involve other agencies involved in active remote sensing, including NOAA, NSF, and perhaps DOD, as well as the agencies regulating these activities—the FCC and the NTIA—and include the use of (1) modeling, (2) dedicated ground-based and airborne characterization campaigns, and (3) data mining of currently operating science sensors. To the extent possible, this effort should be a collaborative one with other space and science agencies of the world. (Recommendation 8.1)
- NASA should lead a community effort to construct a set of metrics that relate to the various RFI environments encountered and the associated degradation in science performance for each major class of instruments employed in active remote sensing. (Recommendation 8.2)
- NASA and NSF should conduct a formal survey of the space physics research community to determine future spectrum needs. (Recommendation 5.3)
- NOAA should conduct a full assessment of the recent World Radiocommunication Conference (WRC) 2012 results regarding ground-based high-frequency radars to ensure that the planned build-out needs of the U.S. high-frequency over-the-horizon radar observing system can be adequately met. (Recommendation 3.1)
- Coastal ocean dynamics applications radar (CODAR) would benefit from allocated bandwidths larger than 25 kHz near 4.438-4.488 MHz. The FCC should reinstate an experimental licensing process for CODAR to allow for future engineering research progress and exploratory science advances. (Finding 3.2 and Recommendation 3.2)
- Radar systems meeting specific criteria for pulse repetition, maximum pulse width, and duty cycle should be permitted by the FCC or the NTIA to operate as secondary users in communications bands, where minimal interference to the communications operations would be expected to occur. (Recommendation 9.3)
- The Office of Science and Technology Policy should adjudicate the possibility of time and frequency sharing between ESA BIOMASS and DOD's Space Object Tracking Radar (SOTR) system. (Recommendation 4.1)
- Given the importance of the educational CubeSat program for the development of the aerospace workforce, and for the development of small satellite

technology, NSF, NASA, the FCC, and the NTIA should undertake a concerted and coordinated effort to eliminate impediments in the spectrum allocation process that are currently impeding the success of educational CubeSats. (Recommendation 7.3)

Possible Actions by the Telecommunications Industry

There are certain actions the telecommunications industry should consider, for their own benefit and for the benefit of active remote sensing users:

- The use of millimeter-wave frequencies for short-wave femtocell-sized[2] communications would significantly increase network capacity by an order of magnitude, thereby reducing pressure on the spectrum and therefore on the active remote sensing users, as well. (Finding 9.3)
- The wireless industry should consider pursuing the femtocell approach by developing towers, networks, and the like to add the use of millimeter-wave frequencies for communications in 6G and up communication standards. (Recommendation 9.2)

Opportunities for Spectrum Sharing

There are actions by the scientific community that would facilitate spectrum sharing:

- From the perspective of efficient spectrum usage, the active sensing community would benefit from the consolidation of the L-, C-, and S-band radar assets of NOAA and the FAA to a single multi-function radar at the S-band, as proposed by the Multifunction Phased Array Radar program. (Finding 9.1)
- The committee recommends an investigation of spatial frequency re-use techniques (e.g., 7-to-1 spatial frequency saving) to reduce the total S-band spectrum requirements. The existing L-band spectrum should be maintained for Earth imaging radar use. (Recommendation 9.1)

Recommended Increases in the Spectrum Allocated for Scientific Active Remote Sensing

Some modest increases in spectrum allocations for scientific active remote sensing would be highly beneficial:

[2] Femtocells are discussed in Chapter 9.

- The FCC and the NTIA should support access to the frequency bands that best support the extraction of ocean-related information from ocean science remote sensing observations. (Recommendation 3.3)
- Coastal ocean dynamics applications radar (CODAR) would benefit from allocated bandwidths larger than 25 kHz near 4.438-4.488 MHz. The FCC should reinstate an experimental licensing process for CODAR to allow for future engineering research advances and exploratory science advances. (Finding 3.2 and Recommendation 3.2)
- If deemed worthwhile by the astronomy community, and if the NSF considers it appropriate, NSF should seek frequency assignments in the relevant bands for the proposed Green Bank and upgraded Arecibo radar systems to facilitate high-spatial-resolution imaging of small near-Earth asteroids. (Recommendation 6.1)

1

Introduction

ACTIVE SENSING SCENARIOS

Active sensing encompasses the use of a transmitter and at least one receiver to measure (sense) the transmission or scattering properties of a medium at radio frequencies. In transmission measurements, the transmit and receive antennas usually are pointed towards one another and located on opposite sides of the transmission medium, as shown in Figure 1.1(A). Scattering measurements are performed by a radar operated in either a *monostatic* (backscatter) mode—wherein the transmit and receive antennas are colocated, as shown in Figure 1.1(B)—or in a *bistatic* (oblique) mode as shown in Figure 1.1(C). Hence, the term active sensing encompasses both *transmission measurements* and *radar remote sensing*. The measurements are intended to discern information about the physical state of the medium of interest. In Earth active sensing, the media of interest include the terrestrial environment, the ocean surface, and the atmosphere (including the ionosphere). Another branch of active sensing is radar astronomy, wherein the targets of interest are extraterrestrial objects.

Figure 1.2 depicts active sensing measurement scenarios relevant to Earth remote sensing. They include upward-looking backscatter measurements made by weather radars; downward-looking backscatter measurements made by satellite-borne radars; upward-looking backscatter measurements of the ionosphere, and bistatic observations of the ocean surface realized by measuring the bistatically scattered illumination due to an orbiting transmitter such as a Global Position-

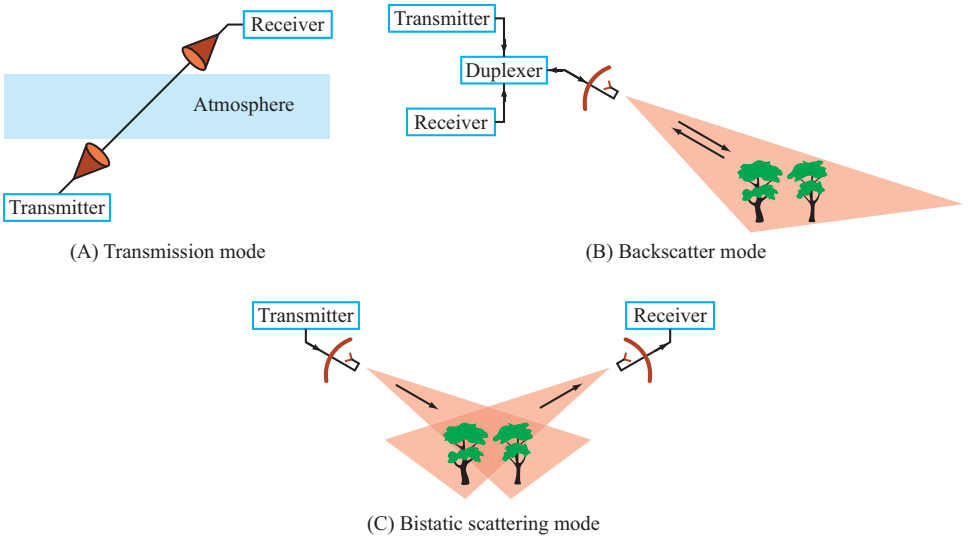

FIGURE 1.1 Active sensing measurement scenarios.

ing System. The receiver may be stationary and located at a coastline or may be onboard an orbiting satellite.

Similarly, astronomical observations may be performed either monostatically or bistatically (see Figure 1.3). A feature common to all active sensing systems is the use of an artificially generated signal radiated by a transmit antenna. This is in contrast to passive sensing, wherein the medium under observation is itself the transmission or emission source; a passive sensor consists of only a receiver configured to measure the naturally generated thermal radiation from the observed medium or reflected radiation from other sources.

THE RADIO SPECTRUM

The electromagnetic spectrum (Figure 1.4) spans many decades in frequency (or wavelength), with the radio part constituting the frequency range from near 0 Hz to 300 GHz. Some of the applications of the radio spectrum—including communication, navigation, broadcasting, radar, and passive remote sensing—are summarized in Figure 1.5. The radio spectrum is divided into 11 individual bands, the three highest of which (UHF, SHF, and EHF) comprise the microwave band extending between 0.3 GHz and 300 GHz (or, equivalently, between 1 m and 1 mm in wavelength).

The top part of Figure 1.4 provides a spectral plot of atmospheric opacity

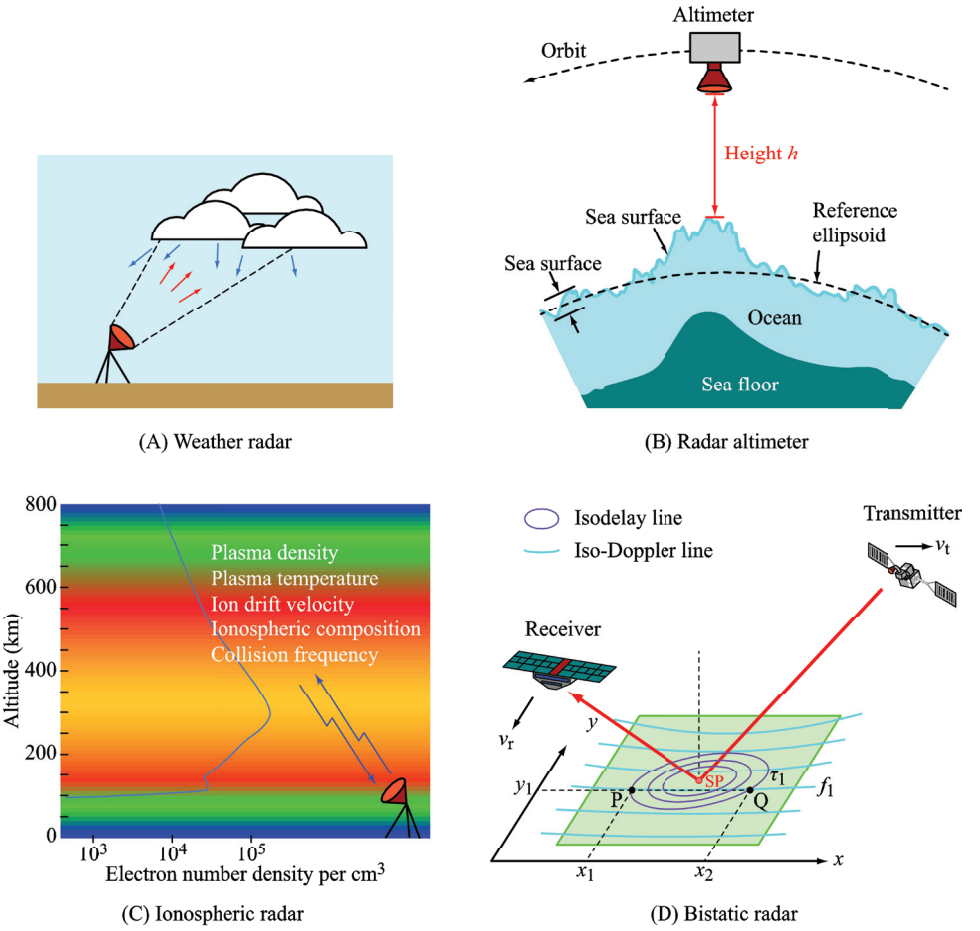

FIGURE 1.2 Active sensing measurement scenarios relevant to Earth remote sensing. SOURCE: (B) and (D) Fawwaz T. Ulaby and David G. Long, *Microwave Radar and Radiometric Remote Sensing*, University of Michigan Press, Ann Arbor, Mich., 2014. With permission of the authors. (A) and (C) generated by the committee.

under clear-sky conditions. Transmission between Earth's surface and outer space is limited to frequencies within the electromagnetic atmospheric windows in the visible, infrared, and radio regions of the spectrum. Among these windows, only the radio window allows successful transmission through the atmosphere under cloud-cover conditions.

Atmospheric transmissivity is the inverse of atmospheric opacity. The plot shown in Figure 1.6 displays atmospheric transmissivity as a function of electro-

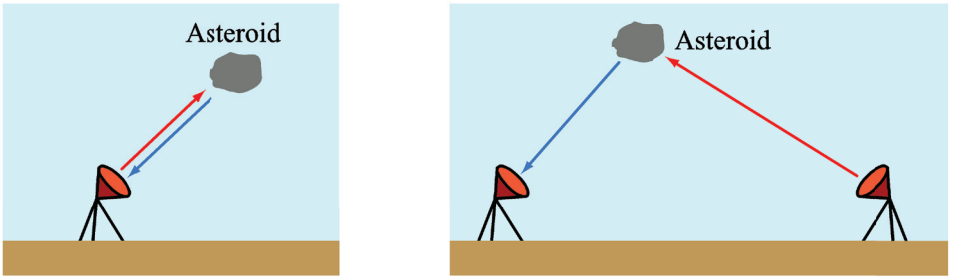

FIGURE 1.3 Radar astronomy uses backscatter and bistatic scattering measurements to extract complementary information about extraterrestrial targets.

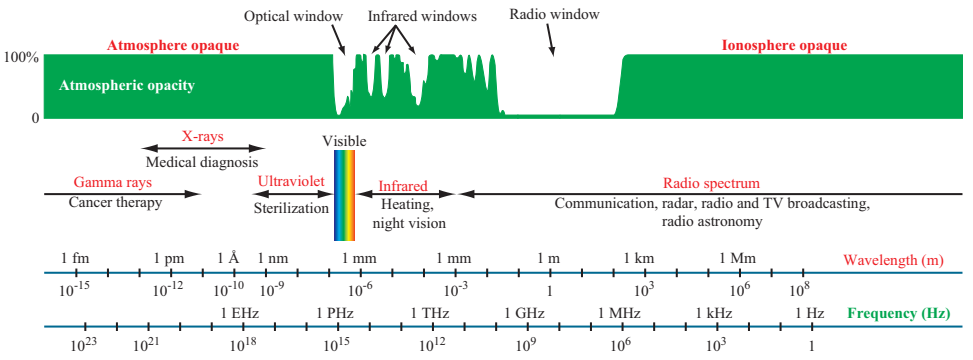

FIGURE 1.4 The electromagnetic spectrum. Atmospheric opacity for Earth is shown along the top. SOURCE: Fawwaz T. Ulaby and David G. Long, *Microwave Radar and Radiometric Remote Sensing*, University of Michigan Press, Ann Arbor, Mich., 2014. With permission of the authors.

magnetic frequency for the microwave band (300 MHz-300 GHz). The ionosphere is opaque to the transmission of electromagnetic waves at all frequencies below about 15 MHz, depending on ionospheric conditions. Atmospheric transmissivity plays a key role in frequency selection for both active and passive sensing within or through the atmosphere. For example, because of water-vapor absorption near 22 and 183 GHz and oxygen absorption near 58 and 119 GHz, these frequencies are used almost exclusively for passive sensing observations of the atmosphere. In contrast, because at frequencies between about 300 MHz and 20 GHz the atmo-

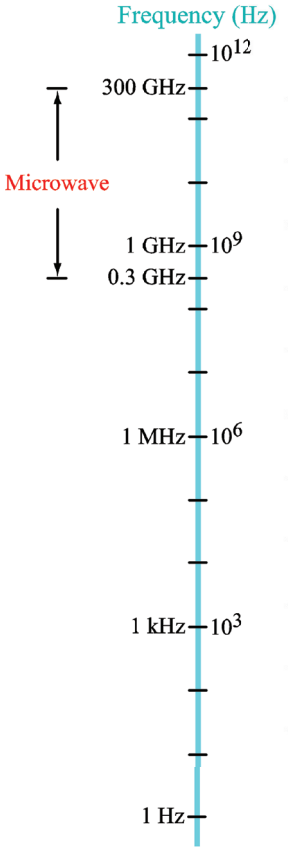

Band	Applications
Extremely High Frequency (30–300 GHz)	Radar, advanced communication systems, remote sensing, radio astronomy
Super High Frequency (3–30 GHz)	Radar, satellite communication systems, aircraft navigation, radio astronomy, remote sensing
Ultra High Frequency (300 MHz – 3 GHz)	TV broadcasting, radar, radio astronomy, microwave ovens, cellular telephone
Very High Frequency (30–300 MHz)	TV and FM broadcasting, mobile radio communication, air traffic control
High Frequency (3–30 MHz)	Shortwave broadcasting
Medium Frequency (300 kHz – 3 MHz)	AM broadcasting
Low Frequency (30–300 kHz)	Radio beacons, weather broadcast stations for air navigation
Very Low Frequency (3–30 kHz)	Navigation and position location
Ultra Low Frequency (300 Hz – 3 kHz)	Audio signals on telephone
Super Low Frequency (30–300 Hz)	Ionospheric sensing, electric power distribution, submarine communication
Extremely Low Frequency (3–30 Hz)	Detection of buried metal objects
	Magnetotelluric sensing of the Earth's structure

FIGURE 1.5 The radio spectrum and some of its applications. SOURCE: Fawwaz T. Ulaby and David G. Long, *Microwave Radar and Radiometric Remote Sensing*, University of Michigan Press, Ann Arbor, Mich., 2014. With permission of the authors.

sphere is essentially transparent and signal attenuation is tolerable in atmospheric "windows," sensors observing Earth's surface through the atmosphere are operated either at frequencies below 20 GHz or at those within the transmission windows shown in Figure 1.6. Short-range radar applications such as vehicle anticollision radars operate at 77 GHz, where atmospheric attenuation helps minimize interference from distant radars.

Several letter-designation schemes are in common use for sub-bands within

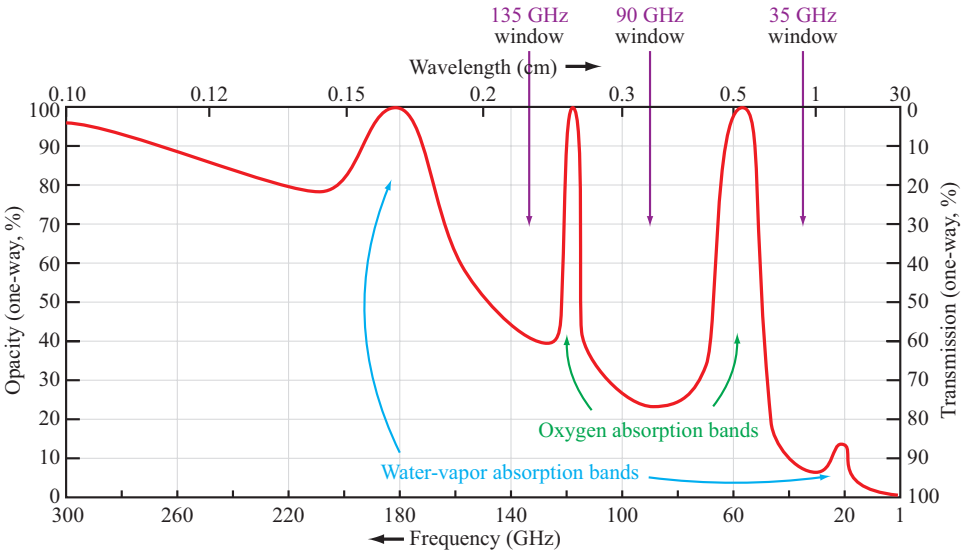

FIGURE 1.6 Percentage transmission through Earth's atmosphere, along the vertical direction, under clear sky conditions. SOURCE: Fawwaz T. Ulaby and David G. Long, *Microwave Radar and Radiometric Remote Sensing*, University of Michigan Press, Ann Arbor, Mich., 2014. With permission of the authors.

and adjacent to the microwave band. Two such schemes are described in Table 1.1. The first, an unofficial set used extensively by the microwave remote-sensing community, starts with the P-band (0.225-0.39 GHz) and concludes with the W-band (56-100 GHz). The second set, officially known as the IEEE radar bands, covers the spectral range from 1 GHz to 110 GHz. Because many sensor systems are organized by letter sub-band, it is impractical to entirely exclude the use of such designations in this report. To avoid confusion, however, the associated frequency or frequency interval is always included explicitly.

SCIENTIFIC APPLICATIONS AND SOCIETAL BENEFITS

Chapters 2-4 provide overviews of how active sensing systems are used to extract information about the state of Earth's atmosphere and its ocean and land surfaces. Separate chapters provide similar information on ionospheric sensing (Chapter 5) and radar astronomy (Chapter 6). A summary of the physical parameters measureable by active sensing is available in Box 1.1. The associated applica-

TABLE 1.1 Common Band Designations

Band	Remote-Sensing Community Frequency Range	IEEE Radar Frequency Range
HF	3-30 MHz	3-30 MHz
VHF	30-300 MHz	30-300 MHz
UHF	0.3-3 GHz	0.3-3 GHz
P	0.225-0.39 GHz	—
L	0.39-1.55 GHz	1-2 GHz
S	1.55-4.2 GHz	2-4 GHz
C	4.2-5.75 GHz	4-8 GHz
X	5.75-10.9 GHz	8-12 GHz
K_u	10.9-22 GHz	12-18 GHz
K	—	18-27 GHz
K_a	22-36 GHz	27-40 GHz
Q	36-46 GHz	—
V	46-56 GHz	40-75 GHz
W	56-100 GHz	75-110 GHz

NOTE: HF, high frequency; IEEE, Institute of Electrical and Electronics Engineers; UHF, ultrahigh frequency; VHF, very high frequency.

tions extend from the purely scientific, such as the study of the interior structure of planets, to the applications that are essential for health, safety, and commerce.

FREQUENCY ALLOCATIONS

The radio spectrum is used by many types of services, from radio and TV broadcasting to wireless phone communication; weather, military, and remote sensing radars; and radio and radar astronomy, among many others. The services concerned with scientific uses of the spectrum are listed in Table 1.2. Active sensing, the subject of the present study, encompasses the following:

- *Radar remote sensing* operates under the Earth Exploration Satellite Service (EESS/active).
- *Radar astronomy* operates under the Radiolocation Service.
- *Weather radar* operates under the Radiolocation Service.
- *Ionospheric sounding* operates under the Meteorological Aids Service.

Regulatory Allocation Process

As discussed in detail in Chapter 7, radio regulations and frequency allocations are developed at both national and international levels. At the international level, regulations are formulated by the Radiocommunication Sector of the International Telecommunications Union (ITU-R). The process is described in some detail in

BOX 1.1
Selected Applications of Active Sensing Systems

Radar Remote Sensing

Geology—tectonics, seismology, volcanism, geodesy, structure, lithology.

Hydrology—soil moisture, watershed mapping, flood mapping, mapping of surface water (ponds, lakes, rivers), snow mapping.

Agriculture—crop mapping, agricultural-practice monitoring, identifying field boundaries, monitoring growth and harvest progress, identifying stress areas, rangeland monitoring, water problems—same as hydrology.

Forests—monitoring cutting, mapping fire damage, identifying stress areas, vegetation density, and biomass.

Cartography—topographic mapping, land-use mapping, monitoring land-use changes, urban development.

Polar regions (cryosphere)—monitoring and mapping sea ice, detecting and tracking icebergs, mapping glacial ice sheets, monitoring glacial changes, including measuring velocity.

Ocean—measuring wave spectra, monitoring oil spills, monitoring ship traffic and fishing fleets, wind speed and direction measurement, rain, clouds, measuring currents, undersea mapping.

Weather Radar

Quantitative precipitation estimation (aka rainfall estimation), flash flood warnings, severe storm warnings, forensic meteorology for the insurance industry, risk mitigation, aviation/transportation safety—wind shear detection, television weather forecasts, mesoscale meteorology, numerical weather prediction via data assimilation, urban meteorology.

Ionospheric Sounding

Ionospheric plasma density structure, plasma dynamics, upper atmospheric heating, storms and substorms, radio propagation, ground-satellite communication impacts, radiation belt impacts on spacecraft, GPS disruptions, ground-induced currents in pipelines and power systems.

Astronomy

Precision orbits for impact assessment and mitigation of potentially hazardous near-Earth asteroids, surface and interior properties of near-Earth asteroids, interior structure of planets and satellites, support for space missions, evolution of the solar system, surface properties of the terrestrial planets and the Moon.

the National Research Council *Handbook of Frequency Allocation and Spectrum Protection for Scientific Uses.*[1]

[1] National Research Council, *Handbook of Frequency Allocation and Spectrum Protection for Scientific Uses*, The National Academies Press, Washington, D.C., 2007.

TABLE 1.2 Science Services

Service	Abbreviation	Description of Service
Active Sensing Services		
Earth Exploration—Satellite Service	EESS	Remote sensing from orbit, both active and passive, and the data downlinks from these satellites
Meteorological Satellite Service	MetSat	Weather satellites
Radiolocation Service	RLS	Radar astronomy, weather radar
Support Services		
International Global Navigation Satellite System (GNSS) Service	IGS	Accurate position and timing data
Meteorological Aids Service	MetAids	Radio communications for meteorology, e.g., weather balloons, ionospheric sounding
Space Operations Service	SOS	Radio communications concerned exclusively with the operation of spacecraft—in particular, space tracking, space telemetry, and space telecommand
Space Research Service	SRS	Science satellite telemetry and data downlinks, space-based radio astronomy, and other services

The aforementioned handbook describes the frequency allocation process within the United States as follows:

> Non-federal-government use of the spectrum is regulated by the *Federal Communications Commission* (FCC). Federal government use is regulated by the *National Telecommunications and Information Administration* (NTIA), which is part of the U.S. Department of Commerce. Most, if not all, spectrum use for scientific research is under shared federal government/non-federal-government jurisdiction. Many federal agencies have spectrum-management offices—for example, the Department of Defense (DOD), National Aeronautics and Space Administration (NASA), and the National Science Foundation (NSF). The Interdepartment Radio Advisory Committee (IRAC) is a standing committee that advises NTIA with respect to the spectrum needs and use by departments and agencies of the U.S. government.
>
> The U.S. administration has set up national-level study groups, working parties, and task groups that mirror those that operate within the ITU-R. For example, U.S. Working Party 7C (U.S. WP7C), part of U.S. Study Group 7, develops U.S. positions and draft documents concerning remote sensing. These documents are reviewed by the United States International Telecommunication Advisory Committee (ITAC) and, if approved, are forwarded by the U.S. Department of State to the ITU-R as input for international meetings.

TABLE 1.3 EESS (Active) Frequency Allocations

Band Designation	Frequency Band as Allocated in Article 5 of the Radio Regulations	Application Bandwidths				
		Scatterometer	Altimeter	Imager	Precipitation Radar	Cloud Profile Radar
P-band	432-438 MHz			6 MHz		
L-band	1,215-1,300 MHz	5-500 kHz		20-85 MHz		
S-band	3,100-3,300 MHz		200 MHz	20-200 MHz		
C-band	5,250-5,570 MHz	5-500 kHz	320 MHz	20-320 MHz		
X-band	8,550-8,650 MHz	5-500 kHz	100 MHz	20-100 MHz		
X-band	9,300-9,900 MHz	5-500 kHz	300 MHz	20-600 MHz		
K_u-band	13.25-13.75 GHz	5-500 kHz	500 MHz		0.6-14 MHz	
K_u-band	17.2-17.3 GHz	5-500 kHz			0.6-14 MHz	
K-band	24.05-24.25 GHz				0.6-14 MHz	
K_a-band	35.5-36 GHz	5-500 kHz	500 MHz		0.6-14 MHz	
W-band	78-79 GHz					0.3-10 MHz
W-band	94-94.1 GHz					0.3-10 MHz
mm-band	133.5-134 GHz					0.3-10 MHz
mm-band	237.9-238 GHz					0.3-10 MHz

Table 1.3 lists frequency bands and associated bandwidths used for spaceborne active sensors operating in the EESS, per Recommendation ITU-R RS.577-7 of the ITU. Contained in the overall list are the bands commonly used for each of the five types of active sensors on satellite platforms—namely, scatterometers, altimeters, imagers, precipitation radars, and cloud profiling radars. More detail about individual bands is available in Appendix C.

Radars used for astronomical observations use bands allocated to the Radiolocation Service. Table 1.4 lists bands used by current systems as well as those associated with potential new planetary radar systems under consideration for the future. The bands commonly used for radar ionospheric studies are listed in Table 1.5.

Scientific Basis for Frequency Choices

The choice of frequency, or combination of multiple frequencies, for sensing a particular physical parameter in Box 1.1 is dictated by three factors:

- *The transmission spectrum of the medium between the radar and the target of interest.* As noted earlier in connection with Figure 1.6, the atmosphere is essentially transparent to electromagnetic wave propagation at frequencies between 100 MHz and 20 GHz and partially transparent within the

TABLE 1.4 Radar Astronomy Frequency Bands

Transmitting Location	Frequency (GHz)	Bandwidth (MHz)	Power	Receive Location
A. Current Planetary Radar Systems				
Arecibo, Puerto Rico	2.380	20	1.0 MW average	Arecibo, Puerto Rico GBT, Green Bank, West Virginia VLA, Socorro, New Mexico LRO, Lunar orbit
	0.430	0.6	2.5 MW peak, 150 kW average	Arecibo, Puerto Rico GBT, Green Bank, West Virginia
Goldstone, California, DSS-13	7.190	80	80 kW average	Goldstone, California GBT, Green Bank, West Virginia Arecibo, Puerto Rico
Goldstone, California, DSS-14	8.560	50	500 kW average	Goldstone, California GBT, Green Bank, West Virginia Arecibo, Puerto Rico VLA, Socorro, New Mexico 10 VLBA sites
B. Potential New Planetary Radar Systems				
GBT, Green Bank, West Virginia	8.6	100	500 kW average	GBT, Green Bank, West Virginia VLA, Socorro, New Mexico Goldstone, California
Arecibo, Puerto Rico	4.6	50	500 kW average	Arecibo, Puerto Rico GBT, Green Bank, West Virginia
Goldstone, California, DSS-14	8.60	120	1.0 MW average	Goldstone, California GBT, Green Bank, West Virginia Arecibo, Puerto Rico

NOTE: Close asteroid observations require bistatic operation. GBT, Green Bank Telescope; LRO, Lunar Reconnaissance Orbiter; VLA, Very Large Array; VLBA, Very Long Baseline Array.

transmission windows centered at 35, 90, and 135 GHz. Hence, microwave satellite sensors used to observe Earth's surface are limited to frequencies within these bands. The specific choice of frequency within an atmospheric transmission window is usually dictated by factor (b), namely the physical mechanism responsible for the process that is remotely observed.

- *Scattering mechanism.* Water droplets in a nonprecipitating cloud are much smaller than those in rain. Consequently, different frequencies are best suited for measuring the water content of a water cloud as opposed to the rainfall rate of a precipitating cloud. In the frequency allocations list of Table 1.3, the frequencies associated with precipitation radar extend between 13.25 GHz and 36 GHz, whereas those associated with cloud profiles extend between 78 GHz and 238 GHz.

TABLE 1.5 Ionospheric Radar Frequency Bands

Radar	Location	Frequency/Bandwidth	Power	License
SuperDARN	Global	8-20 MHz instantaneous BW 60 kHz	10 kW	Within the United States—FCC experimental noninterference
Digisonde	Global	2-30 MHz	500 W	
Arecibo ISR	Arecibo, Puerto Rico	430 MHz, 500 kHz BW	2.5 MW	NTIA
Millstone Hill ISR	Westford, Massachusetts	440.0, 440.2, 440.4 MHz, 1.7 MHz BW	2.5 MW	NTIA noninterference
PFISR	Poker Flat, Alaska	449.5 MHz, 1 MHz BW	2 MW	NTIA Primary
RISR	Resolute Bay, Nunavut, Canada	442.9 MHz, 4 MHz BW	2 MW	Industry Canada
Sondrestron	Kangerlussuaq, Greenland	1287-1293 MHz, 1 MHz BW	3.5 MW	
Homer VHF	Homer, Alaska	29.795 MHz, 100 kHz BW	15 kW	FCC experimental noninterference
Jicamarca ISR	Jicamarca, Peru	49.92 MHz, 1 MHz BW	6 MW	Peruvian
HAARP	Gakona, Arkansas	2.6-9.995 MHz instantaneous BW 200 kHz	3.6 MW CW	NTIA

NOTE: BW, bandwidth; CW, continuous wave; FCC, Federal Communications Commission; HAARP, High Frequency Active Auroral Research Program; ISR, Ionosondes and Incoherent-Scatter Radar; NTIA, National Telecommunications and Information Administration; PFISR, Poker Flat, Alaska, Incoherent-Scatter Radar; RISR, Resolute Incoherent Scatter Radar; VHF, very high frequency.

Similar arguments apply to the choice of frequencies for radar measurements of other physical parameters (Figure 1.7). From a radar perspective, a vegetation canopy is a "cloud" of branches and leaves whose sizes and dielectric properties dictate the nature of the scattering within the vegetation volume, and consequently, the optimum choice of frequencies for measuring biomass or for penetrating the canopy to sense the moisture content of the soil surface beneath it. Ocean scattering depends on the spatial spectrum of waves on the ocean surface relative to λ. Radar scattering by the ionosphere is strongly dependent on the plasma density, the strength of the ambient magnetic field, and the frequency and polarization direction of the incident radar wave. In radar astronomy, the degree of scattering by the surface of a planet or satellite is related to the scale of roughness of the surface relative to λ.

- *Hardware, cost, and operational constraints.* The cost and feasibility of a radar design often are constrained by two critical system parameters: the operating

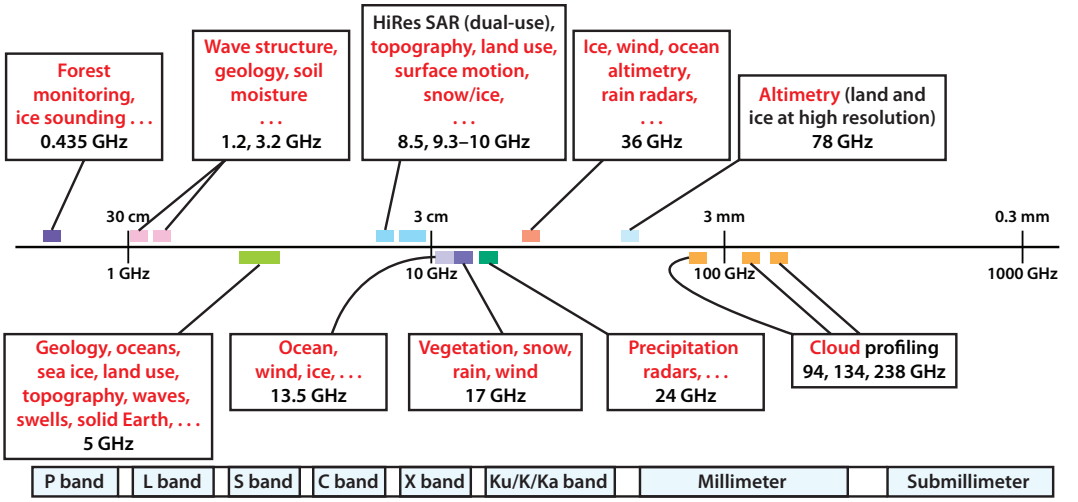

FIGURE 1.7 The choice of frequencies for satellite active sensing is dictated by the physics of the relevant scattering mechanism.

frequency and the average transmit power. Increasing the frequency from 10 GHz, for example, to 100 GHz (while keeping antenna size and all other specifications the same), leads to a substantial increase in cost because transmitter and receiver technology is much better developed at 10 GHz than at 100 GHz. By the same token, because of technology improvements over the past two decades, some systems that were considered unfeasible for satellite operation in the 1990s are now under consideration for future missions.

Transmitter power is a critically important factor for radar astronomy. Because of the long distance between Earth-based radars and their intended targets, it is necessary to transmit signals with powers on the order of megawatts, which requires the use of special types of klystrons. Advances in klystron technology leading to successful operation at higher frequencies and/or higher power has led to proposed upgrades of current radar astronomy facilities as noted in Table 1.4. Higher average power allows for wider bandwidths, which provide for better spatial resolution.

RADIO-FREQUENCY INTERFERENCE AND MITIGATION OPPORTUNITIES

Radio-frequency interference (RFI) refers to the unintended reception of a signal transmitted by an auxiliary source. Active sensors use transmitters and receivers,

so an active sensor may act as the source of interference to a communication system, a passive sensing system, or another radar system, or the receiver of the active sensor may be the recipient of an unintended signal radiated by an external source. Chapter 8 provides a review of the available information on documented occurrences of RFI, organized by frequency band, starting with the HF band (3-30 MHz) and concluding with the W-band (56-100 GHz). One of the conclusions deduced from the review is that while there is evidence that RFI occurs fairly frequently at the C-band and lower frequencies, its occurrence is rare at higher frequencies. Moreover, the preliminary evidence suggests that active sensing instruments do not normally cause RFI to other users but that other users have negatively impacted the performance of active sensing instruments.

Another topic alluded to in Chapter 8 is RFI mitigation and the degree to which mitigation techniques have been applied successfully. This is followed in Chapter 9 with a detailed examination of the various tools available for avoiding or mitigating RFI, and the limitations thereof.

2

Active Earth Remote Sensing for Atmospheric Applications

INTRODUCTION

This chapter covers active sensing of the atmosphere using both ground-based and satellite-borne radars. Owing to the vast expanse of weather, hydrometeors, and atmospheric gases, in situ measurements are not sufficient to obtain all of the critical data necessary for forecasting, warning, and monitoring of the weather and atmosphere worldwide, especially at high altitudes. In order to collect the necessary data, active remote sensing of the atmosphere is conducted from both ground- and satellite-based radar systems.

Our climate is changing faster than ever, breaking the normal cycles established since before the beginning of human civilization.[1] Recent extreme weather events in the United States have received significant attention on both traditional and social media sites (Figures 2.1 and 2.2). It has therefore become more imperative than ever to monitor our atmosphere with all of the remote sensing tools available in order to best mitigate and adapt to changes in our climate, as well as to develop enhanced models that can better predict future weather patterns. Active ground-based and satellite sensors are a critical part of this monitoring. Environmental

[1] C. Field and N. Diffenbaugh, Changes in ecologically critical terrestrial climate conditions, *Science* 341(6145):486-492, 2013; "Stanford climate scientists warn that the likely rate of change over the next century will be at least 10 times quicker than any climate shift in the past 65 million years" (B. Carey, "Climate change on pace to occur 10 times faster than any change recorded in past 65 million years, Stanford scientists say," *Stanford Report*, August 1, 2013, http://news.stanford.edu/news/2013/august/climate-change-speed-080113.html).

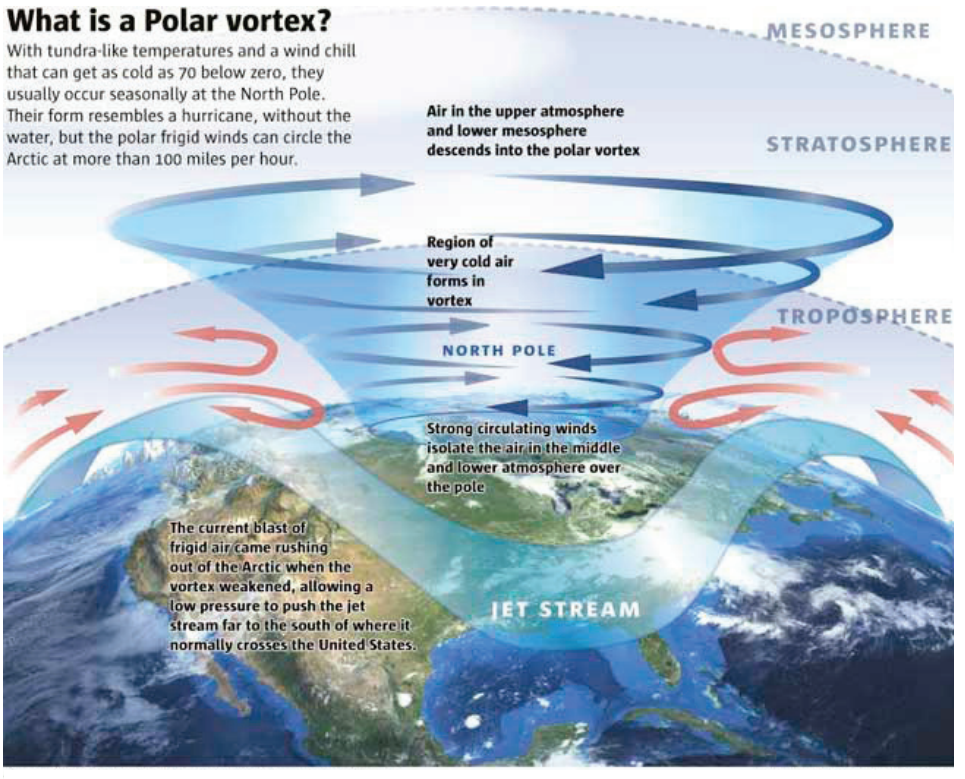

FIGURE 2.1 Record temperatures and extreme weather such as the polar vortex event of winter of 2014. SOURCE: Courtesy of Mike Nelson, 7News KMGH-TV.

measurements available from remote sensing will help us to better quantify the environment and its changes and understand the interactions that affect our climate, including human activities.

The measurement of atmospheric variables is needed because they play an important role in heat transport, cloud genesis, winter storms formation, hurricane and cyclone formation, and other atmospheric events. Some of the fundamental atmospheric variables that can be retrieved and monitored by active sensors include vapor and liquid water content, wind vectors, cloud cover, rainfall rate, precipitation type, and ice cloud content.

To develop and enhance climate/weather models, it is necessary to have a global atmospheric database of geophysical parameters, which can then be used to evaluate risk management options and develop preparedness plans, thereby reducing the risks of disasters. By incorporating knowledge about projected climate changes, we

FIGURE 2.2 The 2014 polar vortex induced extreme events, an example of which is displayed in this photo of the Schuylkill River in Philadelphia. SOURCE: Shuvaev, "Ice Formations on the Schuylkill River in Philadelphia," January 7, 2014, Wikipedia file: Frozen Schuylkill River, Philadelphia 2014.JPG, Creative Commons Attribution-ShareAlike 3.0 Unported license.

can enhance our mitigation/adaptation response and help make informed decisions to reduce vulnerability to extreme events. The database also supports the development of improved weather prediction models.

The sensors discussed in this chapter are an important part of the nation's (and the world's) infrastructure for monitoring the Earth system. In order to observe the intended phenomena, however, these sensors require access to various windows of the electromagnetic spectrum. Without this access they become unable to support their many societal and scientific applications. Recent efforts to minimize spectral usage while remaining bound by the physical constraints of electromagnetism are discussed, following an introduction to the layers of the atmosphere and the instruments used to observe them.

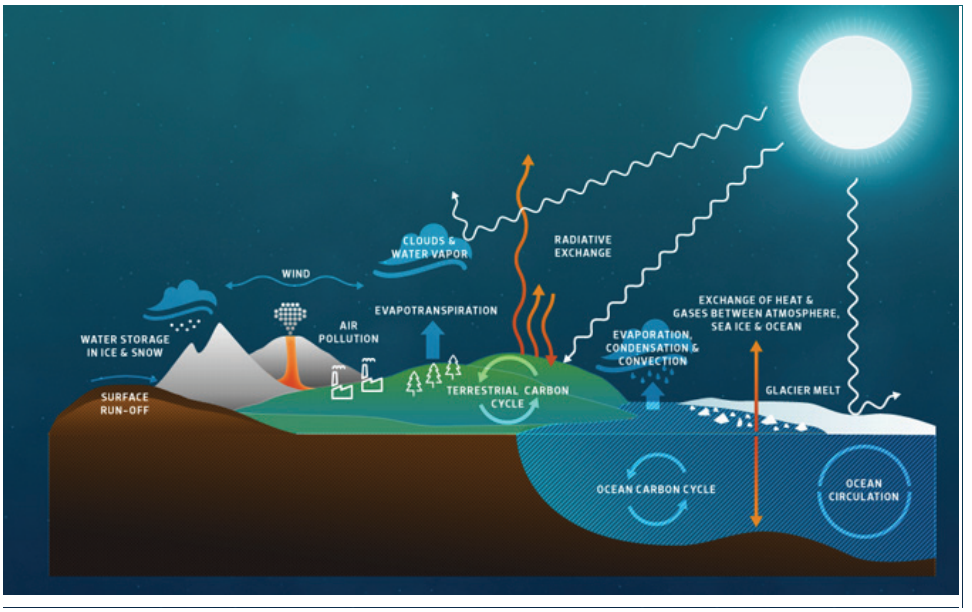

FIGURE 2.3 Climate models incorporate air/ocean/land interactions and processes. SOURCE: Koshland Science Museum of the National Academy of Sciences, "How Do Climate Models Work?" Earth Lab Online Exhibit, https://www.koshland-science-museum.org/, Copyright © 2011 National Academy of Sciences. All rights reserved.

LAYERS OF THE ATMOSPHERE AND SCIENTIFIC APPLICATIONS

From a scientific perspective, the atmosphere is segmented into layers (troposphere, stratosphere, mesosphere, and thermosphere) based on temperature characteristics as a function of height, with temperature defined as the average random kinetic energy of the molecules in the particular atmospheric stratum. Based on expected values across the globe, the temperature profile of the so-called "standard atmosphere" is shown in Figure 2.4. Distinct temperature gradients exist in each layer, which can have a significant effect on the stability of the atmosphere and therefore the type of phenomena observed.

Troposphere

The troposphere is the layer closest to Earth's surface where most species of plants and animals live. Owing to the abundance of moisture from evaporation of rivers, lakes, and oceans, and the general instability caused by the decrease in temperature as a function of height, the troposphere contains virtually all of what

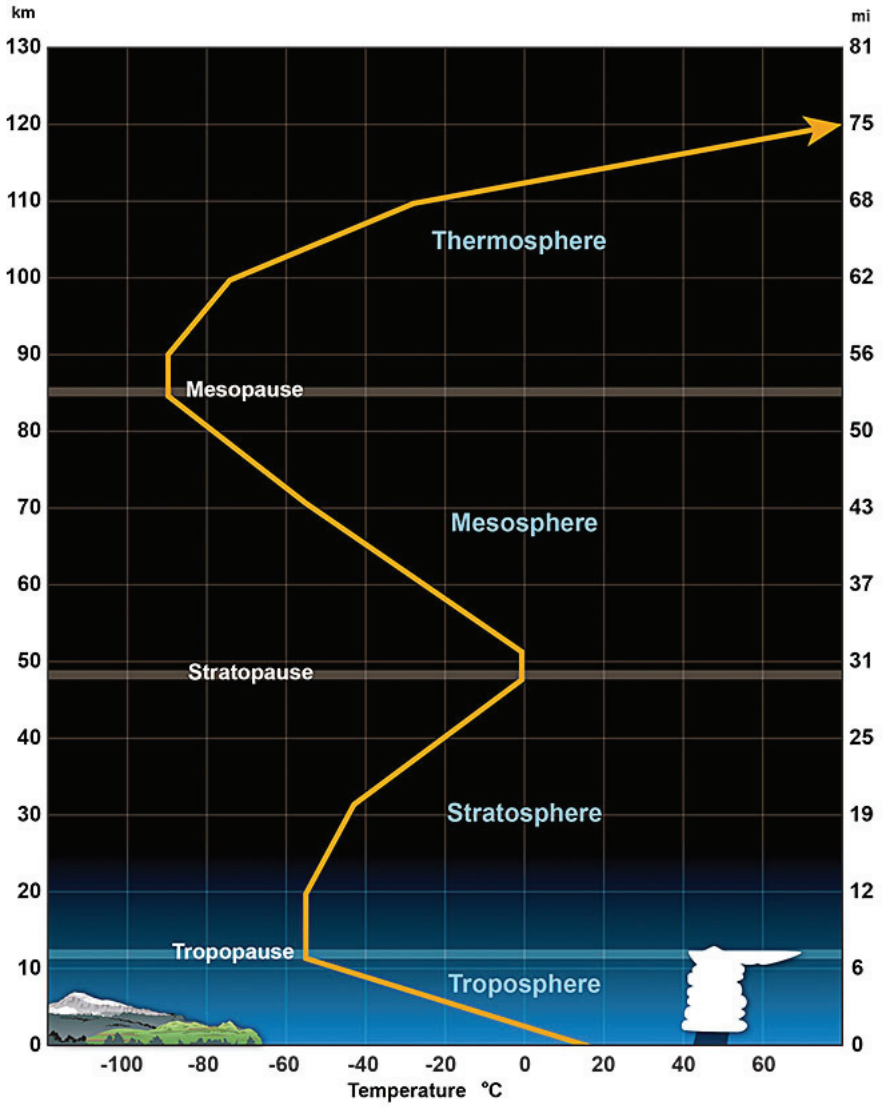

FIGURE 2.4 Temperature profile of the standard atmosphere as a function of height. Layers of the atmosphere are denoted on the figure along with transition layers. SOURCE: NOAA, National Weather Service, "Standardized Temperature Profile" [image], page last modified March 5, 2013, http://www.srh.noaa.gov/jetstream/atmos/atmprofile.htm.

is generally called "weather" (not to be confused with "space weather," which occurs in the upper atmosphere). From severe storms and tornadoes throughout North America to hurricanes in the Atlantic Ocean, the troposphere is where these violent phenomena occur. In addition, droughts, floods, heat waves, and winter storms are manifest in the troposphere and can also have a significant impact on the environment.[2] For these reasons, natural activity in the troposphere has arguably the most significant impact on life and property.[3]

In the troposphere, the majority of scientific applications focus on observations and prediction of weather events. Surface-based observations include meteorological sensor stations (wind, temperature, moisture, etc.) and advanced Doppler weather radars, which can characterize precipitation over hundreds of kilometers. These data are often fed into numerical weather prediction (NWP) models, which are used to forecast severe weather, such as tornadoes and hail, hours in advance. Of course, the accuracy of forecasts is constantly improving through intensive research; however, this improvement is becoming increasingly dependent on data assimilation techniques that rely on accurate products from Doppler radar among other data sources.[4] Weather radar products include rainfall rate, hydrometeor classification, and tornado classification, for example. It should also be emphasized that many of these radar products are used for value-added commercial markets and to broadcast to satisfy the public.

Stratosphere

The layer just above the troposphere is the stratosphere, where temperature begins to increase with height due to absorption of solar radiation by atmospheric ozone. This increase in temperature causes general stability in this layer, resulting in layered ("stratiform") clouds rather than the strong convective clouds seen in the troposphere. Due to this stability and the existence of the jet stream, long-range airline traffic generally takes advantage of flying in the lower stratosphere to increase fuel economy.

The stratosphere can also exhibit extreme wind shear, which causes turbulent

[2] S.A. Changnon, R.A. Pielke Jr., D. Changnon, R.T. Sylves, and R. Pulwarty, Human factors explain the increase losses from weather and climate extremes, *Bulletin of the American Meteorological Society* 81(3):437-442, 2000.

[3] K.M. Simmons and D. Sutter, *The Economic and Societal Impacts of Tornadoes,* American Meteorological Society, Boston, Mass., 2011.

[4] D.J. Stensrud, M. Xue, L.J. Wicker, K.E. Kelleher, M.P. Foster, J.T. Schaefer, R.S. Schneider, S.G. Benjamin, S.S. Weygandt, J.T. Ferree, and J.P. Tuell, Convective-scale warn-on-forecast system: A vision for 2020, *Bulletin of the American Meteorological Society* 90(10):1487-1499, 2009.

instabilities.[5] These phenomena have a major impact on the momentum budget and must be taken into account when modeling global atmospheric fields. General circulation models (GCMs) depend on measurements of stratospheric parameters, but these are very difficult to obtain using ground-based sensors (compared with measuring those in the troposphere) due to lower moisture level and cloud density. Radar remote sensing techniques are largely based on scattering from turbulent eddies in this region, and can be used to estimate the three-dimensional wind field throughout the stratosphere. This scattering mechanism, along with specific radar systems used to observe the stratosphere, are discussed in subsequent sections.

Mesosphere

Within the mesosphere, temperature generally decreases as a function of height—similar to the troposphere. The upper part of the mesosphere is the coldest region of the atmosphere, with temperatures reaching as low as minus 100°C. Although moisture levels are extremely low, these low temperatures can cause deposition of water vapor and the formation of ice clouds. Since these clouds are visible only at night, when the Sun is illuminating the clouds but not Earth's surface, they are called "noctilucent clouds." In addition to being the highest known clouds, ionization of this region can cause associated radar echoes that are unexpectedly intense. These echoes were discovered in the 1990s and were appropriately termed Polar Mesospheric Summer Echoes (PMSE) since seasonal circulation patterns cause the lowest temperatures at these altitudes to occur in the northern hemisphere summer.[6] It is also important to note that climate change may be part of the cause of the increasing observations of noctilucent clouds after the Industrial Revolution due to a possible increase in moisture and a simultaneous decrease in temperature at these high altitudes; this is in contrast to warmer temperatures at lower altitudes.

The mesosphere is extremely difficult to observe since standard radiosonde balloons cannot reach these heights. Furthermore, radar techniques are limited to the upper reaches of the mesosphere where PMSE are observed. In the lower mesosphere, appropriately called the "gap" region, low atmospheric density and limited ionization contribute to a dearth of effective remote sensing techniques.

[5] W.K. Hocking, Measurement of turbulent eddy dissipation rates in the middle atmosphere by radar techniques: A review, *Radio Science* 20(6):1402-1422, 1985.

[6] J.Y.N. Cho and J. Rottger, An updated review of polar mesosphere summer echoes: Observation, theory, and their relationship to noctilucent clouds and subvisible aerosols, *Journal of Geophysical Research* 102(D2):2001-2020, 1997.

Thermosphere

As seen in Figure 2.4, temperature in the thermosphere increases rapidly with height due to absorption of solar radiation, which also causes molecules in the thermosphere to become electrically charged. This charged region, called the ionosphere, scatters electromagnetic waves effectively, providing a physical mechanism for remote sensing. Ionosphere and thermosphere science is discussed in detail in the section "Ionosphere–Thermosphere Science" in Chapter 5.

ATMOSPHERIC SCATTERING/REFLECTION MECHANISMS

Electromagnetic wave scattering and/or reflection in the atmosphere are a consequence of several physical mechanisms. The present section provides a brief overview of these mechanisms along with the physical limitations they impose on remote sensing techniques.

Rayleigh/Mie Scattering

Several active remote sensing techniques are based on scattering from distinct objects in the atmosphere. As discussed in later sections, weather radars are designed so that their transmitted electromagnetic waves are scattered primarily by hydrometeors (e.g., raindrops, ice crystals, hailstones). By far the most prevalent hydrometeor in the lower atmosphere is rain. Cloud droplets are created by either condensation of water vapor directly onto cloud condensation nuclei (CCN), forming a liquid drop, or by a deposition process with subsequent melting. Once formed, the primary mechanism for increasing the size of droplets is through collision and coalescence. As the liquid drop falls, it interacts with the wind field, causing drag forces to deform the drop and eventually break it up as shown in Figure 2.5. Because of these chaotic processes, a wide distribution of drop sizes exists in the atmosphere. From cloud droplets to intense convective storms, liquid water drops range from approximately 5 microns to just over 8 millimeters in diameter.[7] It is important to note that these physically driven sizes dictate the design of radars used to obverse the raindrops.

If raindrops are assumed to be spherical (which is not always true for very large drops), the scattering of electromagnetic waves is well understood. The simplest case is for wavelengths much larger than the diameter of the sphere. In this situation of Rayleigh scattering, the amount of energy scattered from the drop depends on the sixth power of the drop diameter. In other words, larger drops backscatter more

[7] K. Andsager, K.V. Beard, and N.F. Laird, Laboratory measurements of axis ratios for large raindrops, *Journal of Atmospheric Science,* 56: 2673-2683, 1999.

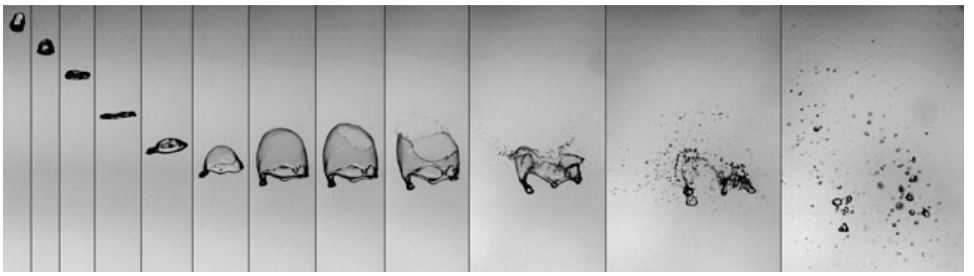

FIGURE 2.5 Snapshots of a raindrop falling through the atmosphere. The deformation and eventual breakup due to drag forces are clearly observed. SOURCE: Reprinted by permission from Macmillan Publishers Ltd: Nature Physics, E. Villermaux and B. Bossa, Single-drop fragmentation determines size distribution of raindrops, *Nature Physics* 5(9):697-702, 2009, copyright 2009.

energy than do smaller drops, which is not always the case when the wavelength is closer to the drop diameter. For this reason, it is highly desirable to design radars that operate in the Rayleigh regime.

In severe weather events, it is possible to observe hydrometeors with sizes that place the scattering outside the Rayleigh regime. For example, hailstones can be quite large (several centimeters), and in this case the scattering can become resonant, causing oscillations in the magnitude of the scattered electromagnetic energy. This phenomenon is called Mie scattering, and it is usually not desirable to design a weather radar for operation under these conditions.

The choice of optimum frequencies is different for precipitation radar than for cloud radar. This is because the radar backscattering cross section of a spherical or quasi-spherical water droplet is governed by Rayleigh scattering if $r/\lambda < 0.1$ (where r is the radius of the droplet and λ is the electromagnetic wavelength), and then transitions into Mie scattering as r/λ approaches and exceeds 1. In the Rayleigh regime, the backscattering cross section is proportional to $(r/\lambda)4$, so it is advantageous to operate a radar such that r/λ is close to 0.1 for the largest size of droplet radii expected for the medium under consideration. At longer wavelengths the scattering cross section becomes too small for detection, while at shorter wavelengths (the Mie regime) scattering exhibits a resonance pattern as a function of (r/λ), leading to ambiguous estimates of water content or precipitation rate.

Bragg Scattering

Atmospheric turbulence can be caused by a variety of mechanical forcing mechanisms such as wind shear, thermally driven convection, etc. As a consequence of this chaotic process, a continuum of turbulent eddy sizes is created and exists

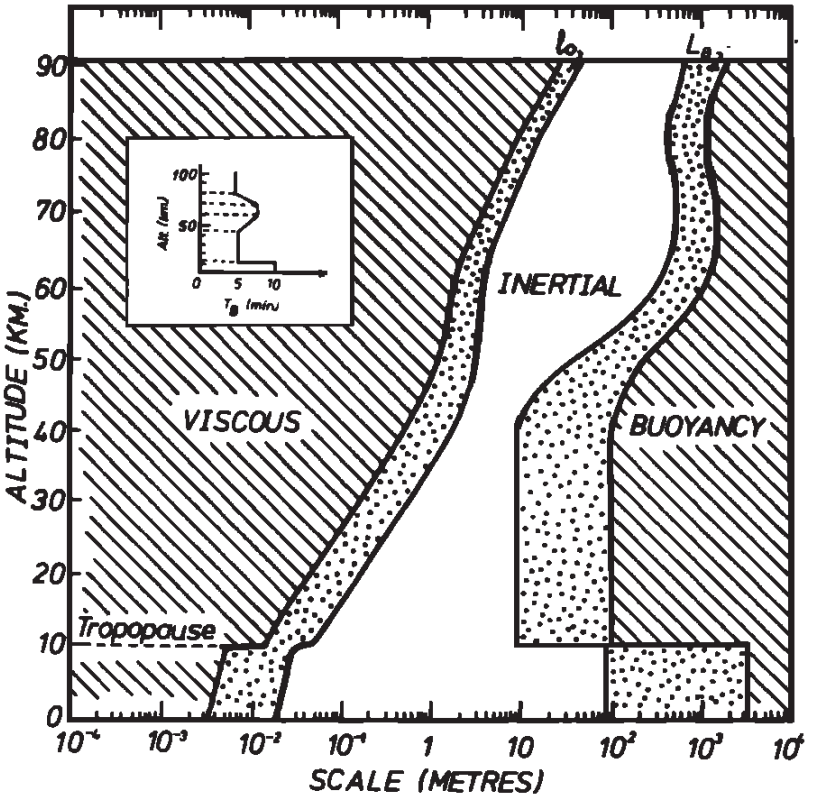

FIGURE 2.6 Typical scales of turbulence in the atmosphere. For profiling radars, it is advantageous to operate at a wavelength that corresponds to a Bragg scale in the inertial subrange of turbulence. SOURCE: W.K. Hocking, "Measurement of turbulent energy dissipation rates in the middle atmosphere by radar techniques: A review," *Radio Science*, November 1985.

in the atmosphere.[8] This turbulence mixes various temperature and moisture regions of the atmosphere, creating a more homogeneous fluid. Much theoretical and empirical research has been accomplished in this field over many decades, and a reasonable understanding has emerged of the generation mechanisms as well as turbulent scale limitations. In an important review article, Hocking summarizes the theory behind quantifying turbulent intensity.[9] He also explains how turbulent scales vary as a function of height and the range of potential eddy sizes. These results are reproduced in Figure 2.6.

[8] T.E. Faber, *Fluid Dynamics for Physicists*, Cambridge University Press, Cambridge, United Kingdom and New York, N.Y., 1995.

[9] Hocking, 1985.

As is evident from the curve, the scales of isotropic turbulence (called the inertial subrange) gradually increase with height. An abrupt change occurs at the transition region between the troposphere and stratosphere due to the large temperature inversion at that altitude, which has a significant impact on atmospheric stability and therefore the generation of turbulence. The key point to recognize is that the atmosphere limits the scales of turbulence that can exist, and that these scales vary with altitude from centimeters in the troposphere to hundreds of meters in the mesosphere.

In the absence of hydrometeors in the atmosphere, radar remote sensing is still possible through a phenomenon called Bragg scattering. When turbulent eddies exist at a scale of half the wavelength of the electromagnetic wave, constructive Bragg scattering can occur, resulting in a measurable amount of backscattered energy. Of course, this is only possible when the turbulence mixes parts of the atmosphere with different temperatures and moisture levels, which largely control the radio refractive index in the lower atmosphere. The intensity of the backscattered signal is proportional to the intensity of the turbulence and the variations in the refractive index. It is this Bragg scattering mechanism that drives the design of profiling radars, also known as mesosphere-stratosphere-troposphere (MST) radars.

Fresnel Reflection (or Partial Reflection)

In the upper atmosphere, large-scale vertically stratified discontinuities in the refractive index can cause what is called Fresnel reflection or partial reflection. Unlike the lower atmosphere, these refractive index variations are primarily caused by discontinuities in electron density in the ionosphere. In addition, meteor ablation in the upper mesosphere–lower thermosphere can leave long plasma trails, which can also cause Fresnel reflections for particular wavelengths of electromagnetic waves.

For the ionosphere, efficient scales for Fresnel reflection dictate radar wavelengths on the order of hundreds of meters resulting in the use of the medium frequency (MF)[10] or high frequency (HF) bands.[11] For the case of meteor trail reflections, shorter wavelengths in the VHF band (for example, tens of meters) are the most effective. In all cases, it is important to note that the physics of the particular region of the atmosphere to be observed drives the design of all remote sensing techniques.

[10] See Figure 1.5 for definitions of the radio spectrum bands.

[11] A.H. Manson, J.B. Gregory, and D.G. Stephenson, Winds and wave motions (70-100 km) as measured by a partial reflection radiowave system, *Journal of Atmospheric and Terrestrial Physics* 35:2055-2067, 1973.

GROUND-BASED RADAR SYSTEMS USED TO OBSERVE THE ATMOSPHERE

The design of an atmospheric radar system begins with an understanding of the region of the atmosphere to be observed and the physics of the potential scattering/reflection mechanisms that may occur in that region. As described in the previous sections, the distinct layers of the atmosphere encompass a variety of phenomena and characteristics. Therefore, the radars used to observe these layers have correspondingly distinct designs. Once the scattering/reflection mechanism is understood, the actual design of the system can begin, involving major decisions about operation frequency, bandwidth, transmit power, etc. The following sections provide a brief summary of the main upward-looking radars used to observe the atmosphere, from the troposphere to the thermosphere.

Weather Radar

The term weather radar describes the suite of radars used to remotely observe precipitation; these radar designs are largely based on the Rayleigh scattering assumption. Almost all modern weather radars have Doppler capability, allowing for an estimate of radial velocity in addition to the backscattered intensity. Furthermore, recent improvements to operational robustness have made dual-polarization weather radars more commonplace. In fact, the extremely successful WSR-88D radar network (NEXRAD), operated by the U.S. National Weather Service,[12] of which an example is shown in Figure 2.7, has been recently upgraded to dual polarization, making it the world's largest network of such radars. With this capability, more accurate rainfall estimates are possible, in addition to the promise of hydrometeor classification. It should also be mentioned that weather radars often observe scattering from insects in the lower atmosphere even when there is no actual precipitation. As a result, it becomes possible to use this type of scattering as a tracer of the wind field under clear-air conditions, which is invaluable for short-term prediction of convection initiation.

Since severe storms are primarily confined to the troposphere, the altitude coverage of weather radars is also limited to this atmospheric layer. Using a pencil beam, weather radars are scanned for a full 360 degrees of azimuth and then sequentially positioned to several higher elevation angles in order to fill the volume of interest.[13] This type of volume scanning is used by the NEXRAD network and has proven successful in providing the data forecasters need to protect lives and

[12] T.D. Crum and R.L. Alberty, The WSR-88D and WSR-88D operational support facility, *Bulletin of the American Meteorological Society* 74(9):1669-1687, 1993.

[13] R.J. Doviak and D.S. Zrnic, *Doppler Radar and Weather Observations*, 2nd Edition, Dover, Mineoloa, N.Y., 2006.

FIGURE 2.7 Photograph of a WSR-88D radar (NEXRAD) operated by the U.S. National Weather Service. SOURCE: NOAA.

property.[14] In addition, these data are available in real time and are used freely by commercial companies, TV stations, and the general public.

Because of the expected range of hydrometeor sizes in storms, the optimal wavelength for a weather radar is in the S-band. For example, the NEXRAD network is allocated for primary use in the 2.7-2.9 GHz band. At this wavelength,

[14] K.M. Simmons and D. Sutter, WSR-88D radar, tornado warnings, and tornado casualties, *Weather and Forecasting* 20(3):301-310, 2005.

Rayleigh scattering is a valid assumption that allows for simpler rainfall estimation and for little attenuation of the electromagnetic wave. Nevertheless, commercial and some research weather radars operate in the C- and X-bands (~5 GHz and 10 GHz, respectively). Often, these wavelengths are chosen for mobile applications, where minimizing the overall size of the radar antenna is important. Higher frequencies allow for smaller antennas while providing good angular resolution.

It should be emphasized that the commercial weather industry relies heavily on C-band radars and plays an important role in directly alerting the public of severe weather. TV meteorologists are usually the first authority to whom the public reaches out for weather information. Commercial C-band weather radars have a very similar design to other weather radars, such as NEXRAD, with comparable beamwidths, bandwidths, etc. The key different is the wavelength, which makes them more susceptible to atmospheric attenuation and resonance scattering effects. In addition, commercial weather radars typically use magnetron transmitters, which have less controlled spectral leakage compared to klystron and solid-state transmitters.

Range resolution is controlled by the bandwidth of the radar. For weather radar, the typical range resolution is 100 m, requiring approximately 1-2 MHz of bandwidth depending on the specific pulse shape used. Peak power levels can be as high as 1 MW for large systems with duty cycles of approximately 0.1 percent. As mentioned earlier, the beam shape is always a pencil beam requiring extensive scanning in both azimuth and elevation in order to provide complete volumetric coverage.

Cloud Radar

In many ways, a cloud radar is similar to a weather radar. The former is typically used to observe nonprecipitating clouds, which are made up of extremely small droplets.[15] In order to obtain the required sensitivity and to avoid extreme attenuation by atmospheric gases, cloud radars normally operate in the K_a- and W-bands (35 GHz and 94 GHz, respectively). At these frequencies, Rayleigh scattering dominates the backscatter from clouds. A prime example of the use of cloud radars is the Department of Energy's (DOE's) Atmospheric Radiation Measurement (ARM) program, which boasts numerous cloud radars used for climate studies, among other scientific applications.

Although some cloud radars have scanning capability, many are fixed in the vertical position. For such a configuration, the goal is to follow the temporal evo-

[15] P. Kollias, E.E. Clothiaux, M.A. Miller, B.A. Albrecht, G.L. Stephens, and T.P. Ackerman, Millimeter-wavelength radars: New frontier in atmospheric cloud and precipitation research, *Bulletin of the American Meteorological Society* 88(10):1608-1624, 2007.

lution of the clouds by allowing advection to provide the sampling. Using such a technique allows for a simpler pedestal design, but separating the temporal from the dynamical evolution of the cloud structure can be a challenge.

As mentioned, the K_a- and W-bands are typically used for cloud radars. Range (or height in the case of a vertically pointing radar) resolution is often better than for weather radars, so bandwidth requirements can approach approximately 5 MHz. Normal pulsed waveforms are common with peak power levels of 100 kW for K_a-band systems and near 1 kW for W-band systems. As with weather radars, cloud radars use a pencil beam and sometimes have dual-polarization capabilities.

Wind Profiling Radar

Measuring winds in the upper atmosphere is fundamental to our understanding of global circulation and for numerical modeling. Conventional means of measuring the winds include launching radiosondes, which can be used to infer the wind profile as the balloons rise. Due to advection, radiosondes drift horizontally, thereby providing a less than ideal profile of the wind and other atmospheric states. Nevertheless, radiosondes are launched around the world at the same time twice per day. This synchronized sampling provides global data with a 12-hour temporal resolution.

Wind profiling radars, also known as MST radars, were conceived as a technology to provide wind profiles in the upper atmosphere with a much better temporal resolution than radiosondes. Boundary layer radars (BLR) are much smaller (~1-2 m aperture) and are designed to scatter from turbulence in the lowest 1-3 km of the atmosphere. Both MST radars and BLRs are based on Bragg scattering from refractive index discontinuities in the atmosphere, mostly caused by turbulence.[16] Given the expected scales of turbulence, wind profiling radars must operate in the VHF, UHF, and L-bands. In the boundary layer, the L-band is the wavelength of choice, while VHF and UHF wavelengths are used for higher-altitude coverage with MST radars. One of the most sophisticated MST radars in the world is located in Shigaraki, Japan, and operated by Kyoto University. The MU (middle and upper atmosphere) radar, shown in Figure 2.8, has an aperture with a diameter of approximately 100 meters, made up of hundreds of crossed-Yagi antennas.[17,18] Phased-array beam steering is usually used with these large wind-profiling radars.

[16] See, for example, R.F. Woodman, Spectral moment estimation in MST radar, *Radio Science* 20(6):1185-1195, 1985.

[17] S. Fukao, T. Sato, T. Tsuda, S. Kato, K. Wakasugi, and T. Makihira, The MU radar with an active phased array system: 1. Antenna and power amplifiers, *Radio Science* 20(6):1155-1168, 1985.

[18] S. Fukao, T. Tsuda, T. Sato, S. Kato, K. Wakasugi, and T. Makihira, The MU radar with an active phased array system: 2. In-house equipment, *Radio Science* 20(6):1169-1176, 1985.

FIGURE 2.8 The MU radar in Shigaraki, Japan. This example of an MST radar has an antenna field with an overall aperture diameter of approximately 100 m. SOURCE: Hiroyuki Hashiguchi, Kyoto University.

Wind profiling radars are designed to direct the radar beam near vertical, thereby providing a profile of both the horizontal and vertical wind components. The horizontal wind component is obtained by steering the beam slightly off vertical using a method called Doppler beam swinging. Range resolution is normally not better than 150 meters, requiring an approximate 1 MHz bandwidth. Given the weak echoes from clear-air turbulence, peak power levels are as high as 1 MW with approximately 0.2 percent duty cycles. As is the case with most atmospheric radars, wind profilers use a pencil beam, but in this case a typical beamwidth is 5-10 degrees.

High-Frequency/Medium-Frequency Radar

Studies of the mesosphere and thermosphere require robust remote sensing techniques. Standard radiosondes can reach altitudes of only 15-20 kilometers. MST radars can be designed to observe this region, but require extremely high transmit powers, with correspondingly high cost, resulting in a limited number of

FIGURE 2.9 The Saura MF Radar antenna field in Andoya, Norway. SOURCE: Chris Adami, ATRAD/IAP Saura MF Radar, Andoya, Norway.

such systems across the globe. Fortunately, a technique based on Fresnel reflection was developed in the 1970s that requires much less transmit power at a lower cost.[19] These HF/MF radars operate in these bands but also at lower VHF frequencies (1-60 MHz), given their strong sensitivity to partial reflections from ionized layers in the mesosphere and thermosphere.

Given wavelengths of up to hundreds of meters, unique antennas have been developed using coaxial cables strung among a set of large poles. An example of such a system is shown in Figure 2.9. The radar transmission is directed vertically with a fairly large (~20 degrees) beamwidth. By receiving the reflected signal on several spatially separated antennas, cross-correlation techniques can be used to find the delay of the diffraction pattern on the ground, thereby providing a method to estimate the horizontal velocity. This so-called Spaced Antenna Drift method has been used for decades with HF/MF radars[20] as well as with wind profiling radars.

[19] Manson et al., 1973.
[20] Manson et al., 1973.

Range resolution is not a huge design constraint with these radars, so the typical bandwidths are ~1 MHz. Peak transmit power is approximately 10-200 kW with duty cycles less than 1 percent.

Meteor Radar

As with HF/MF radars, meteor radars were developed in order to obtain wind measurements in the upper mesosphere and lower thermosphere. Although the physical mechanism by which meteor radars operate is the same as HF/MF radars (Fresnel reflection), the source phenomenon is quite different. As thousands of meteors come into the atmosphere every day, most burn or "ablate" in the 80-100 kilometer region. This ablation process leaves behind a meteor trail, which drifts with the prevailing winds. By transmitting an electromagnetic wave perpendicular to these almost linear trails, Fresnel reflection occurs and can be used to detect the trails and to estimate their radial velocity. The angular position is determined using interferometry, and when combined with the velocity information from numerous meteors, it can be used to estimate the three-dimensional wind field at these altitudes. These relatively low-cost "meteor radars" operate most effectively at 20-60 MHz, and can provide estimates of winds, meteor concentration, and atmospheric temperature.[21]

Since meteor trails can be created over a wide range of angles, and Fresnel reflection requires a perpendicular orientation, the transmit beam of a meteor radar is extremely wide (~100 degrees). At least three small receive antennas (typically crossed-Yagi design) are used for interferometric processing in order to estimate the angular position of the echo. When combined with range gating, the three-dimensional position can then be determined. The bandwidth requirement is typically less than 1 MHz. Peak power levels range from 8 kW to 40 kW, with duty cycles less than 1 percent.

Summary of Current Ground-Based Radar Systems

A summary of general atmospheric radar characteristics is provided in Table 2.1. As should be evident, these radars do not require significant bandwidth in comparison to extremely high-resolution scientific applications or broadband wireless needs. The unique aspect of atmospheric remote sensing is that the physics of the atmosphere drives the choice of the operating frequency. As discussed previously, for example, the range of possible hydrometeor sizes is limited by drag forces,

[21] S.K. Avery, J.P. Avery, T.A. Valentic, S.E. Palo, M.J. Leary, and R.L. Obert, A new meteor echo detection and collection system: Christmas Island mesospheric wind measurements, *Radio Science* 25(4):657-669, 1990.

TABLE 2.1 Summary of Typical Atmospheric Radar Characteristics

Radar Type	Characteristics
Weather Radar	
Scattering/reflection	Rayleigh, Mie
Altitude coverage	0-15 km, usually confined below the tropopause with volume coverage to ranges 0-450 km
Frequency	2.7-2.9 GHz, ~5 GHz, ~10.0 GHz in the S-, C-, and X-bands, respectively
Bandwidth	<1-2 MHz
Antenna	Parabolic dish, pencil beam, 1 degree beamwidth, dual-polarization
Peak power	20 kW-1 MW
Duty cycle	<0.1%
Cloud Radar	
Scattering/reflection	Rayleigh, Mie if precipitating clouds are observed
Altitude coverage	0-30 km, includes high-level clouds in the stratosphere
Frequency	~35 GHz, ~94 GHz
Bandwidth	<5 MHz
Antenna	Parabolic dish, pencil beam, some scanning but usually vertically pointing, typical 1 degree beamwidth, dual-polarization
Peak power	100 kW (35 GHz), 1 kW (94 GHz)
Duty cycle	<0.1%
Wind Profiling Radar	
Scattering/reflection	Bragg
Altitude coverage	0-400 km, upper height depends on sensitivity and ionospheric state
Frequency	~50 MHz, ~400 MHz (MST radars), ~915 MHz or ~1.3 GHz (boundary layer radars)
Bandwidth	<1 MHz
Antenna	Large phased array, pencil beam, typical 3-5 degree beamwidth, ± 10 degree zenith angles
Peak power	500 kW-1 MW
Duty cycle	<0.2%
HF/MF Radar	
Scattering/reflection	Fresnel
Altitude coverage	70-100 km, depends on ionospheric state
Frequency	~1-60 MHz
Bandwidth	<1 MHz
Antenna	Various dipole designs, 20 degree beamwidth
Peak power	10-200 kW
Duty cycle	<1%
Meteor Radar	
Scattering/reflection	Fresnel
Altitude coverage	80-100 km, altitudes of meteor ablation
Frequency	~20-60 MHz
Bandwidth	<1 MHz
Antenna	Crossed-Yagi, ~100 degree beamwidth for all-sky coverage, interferometer
Peak power	8-40 kW
Duty cycle	<1%

collision/coalescence processes, etc. Therefore, the radar wavelength of choice is dictated by these physical mechanisms.

Future Trends and Concepts—Ground-Based Radar

Recently, some innovative weather-radar ideas have been developed that are relevant to the spectrum usage challenge. The first is the so-called Multifunction Phased Array Radar (MPAR) program, which envisions replacing the aging radar infrastructure in the United States with phased-array radar technology.[22] The Federal Aviation Administration (FAA) and the National Oceanic and Atmospheric Administration (NOAA) partnered to develop the idea of deploying a fleet of phased-array radars of a single design to accomplish the missions of several disparate radars currently operated by these two federal agencies. Significant advantages would be gained through such a concept, including rapid-update weather observations that are fundamentally important for mitigating severe weather. From an economic standpoint, an advanced radar network with a common design, replacing several systems with distinct parts, maintenance procedures, etc., would inherently have much lower maintenance and operation costs. Another extremely important advantage of an MPAR system relevant to this study would be its spectral efficiency. By the simple fact that several radars, all in different frequency bands (L-, C-, and S-bands), would be replaced with a radar in a single band (S-band), significant reduction in spectrum usage would be realized. With the rapid growth of broadband wireless and its ever-increasing need for bandwidth, this advantage of the MPAR concept cannot be overstated. Of course, it should also be stated that many commercial weather radars are currently operating at C-band wavelengths, and the MPAR program will not be replacing these radars.

Funded by the National Science Foundation, the Center for the Collaborative Adaptive Sensing of the Atmosphere (CASA) was established with the goal of predicting severe weather using advanced radar technology in conjunction with numerical weather prediction models.[23] An important aspect of the CASA radar concept, called distributed collaborative adaptive sensing (DCAS), is to use a network of low-cost X-band radars, which provides the important advantage of coverage of the lower troposphere, the source of severe weather that directly impacts life and property. Longer-range radars (e.g., NEXRAD) are more sig-

[22] D.S. Zrnić, J.F. Kimpel, D.E. Forsyth, A. Shapiro, G. Crain, R. Ferek, J. Heimmer, W. Benner, T.J. McNellis, and R. J. Vogt, Agile-beam phased array radar for weather observations, *Bulletin of the American Meteorological Society* 88(11):1753-1766, 2007.

[23] D. McLaughlin, D. Pepyne, V. Chandrasekar, B. Philips, J. Kurose, M. Zink, K. Droegemeier, S. Cruz-Pol, F. Junyent, J. Brotzge, D. Westbrook, et al., Short-wavelength technology and the potential for distributed networks of small radar systems, *Bulletin of the American Meteorological Society* 90(12):1797-1817, 2009.

nificantly impacted by Earth's curvature, where the radar beam propagates to progressively higher altitudes at farther ranges. Using a much larger number of shorter-range X-band radars, a DCAS network could observe much closer to the ground, while at the same time providing much higher spatial and temporal resolutions.

SATELLITE-BASED RADAR SYSTEMS USED TO OBSERVE THE ATMOSPHERE

Meteorological data are extremely important for weather forecasting, including the monitoring and prediction of extreme droughts, mudslides, hurricanes, and winter storms. To be of value, precise measurements over wide areas are required. Satellites offer a unique perspective from which to measure atmospheric information over the globe. Satellite sensors provide critical information about current conditions, storm formation, and the evolution of weather events. Their data are also essential for feeding climate and weather prediction models used to understand interactions within the entire biosphere—croplands, forests, lakes, oceans, and the like, including urban and coastal areas.

Radar remote sensing instruments operating from satellites are particularly effective in the observation of precipitation, clouds, and near-surface winds over the ocean, providing invaluable data of environmental parameters that are vital for a wide variety of scientific, commercial, and military applications and that enhance our ability to protect human life and property. Active sensors can provide measurements day or night, independent of solar illumination. Furthermore, because the microwave spectrum offers a wide range of penetration depths, the use of multiple-frequency observations can provide three-dimensional (3D) information about the microphysical properties of clouds and rain.

Meteorological Satellite Radar Systems

The Tropical Rain Mapping Mission (TRMM) precipitation radar (PR) is the first meteorological radar to be launched in space for mapping 3D rain distributions. Launched in 1997 into a low-inclination (35 degree) orbit, the PR uses a K_u-band (13.8 GHz) radar to measure rainfall over a 50 km swath with 4-5 km horizontal and 250 m vertical resolution. An example of the PR pass over a hurricane is given in Figure 2.10.

The CloudSat satellite, launched in 2006, a member of NASA's A-Train platforms, carried a 94 GHz radar designed for vertically profiling clouds and precipitation along its nadir track. The mission goal is to provide the first global survey of the vertical structure of clouds and profiles of cloud liquid water and ice water

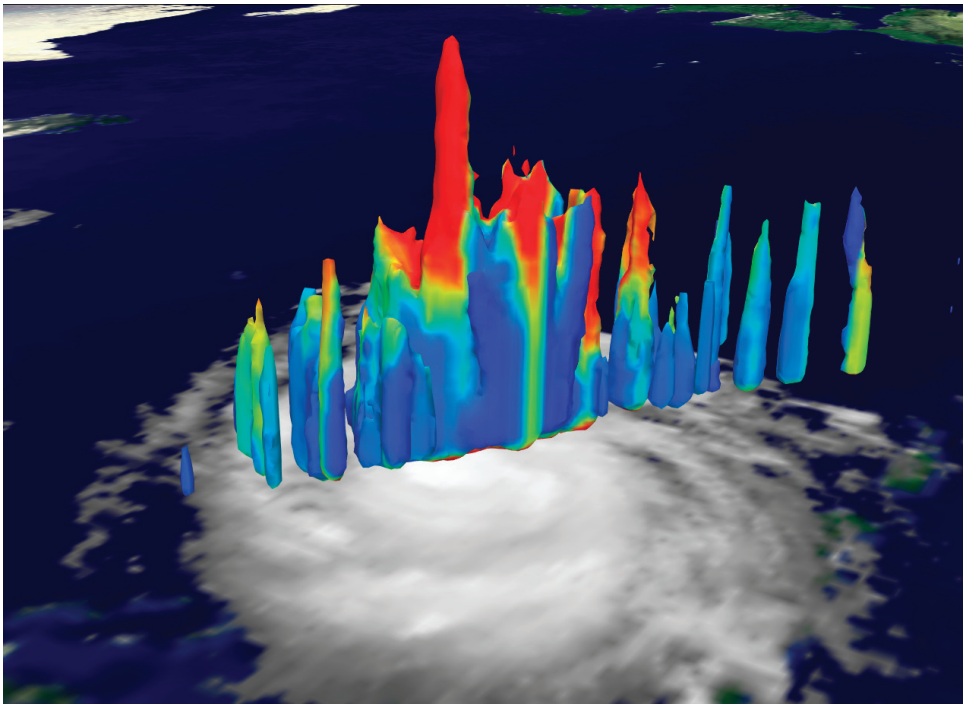

FIGURE 2.10 Examples of PR 3D imagery for a hurricane. SOURCE: NASA/Goddard Space Flight Center Scientific Visualization Studio; see NASA, "Hurricane Bonnie from TRMM and GOES with Cloud Tower: August 22, 1998," December 31, 1998, http://svs.gsfc.nasa.gov/goto?211.

content, filling a recognized, critical gap in the measurements and understanding of clouds for weather and climate research.

The follow-on mission to the TRMM is the Global Precipitation Mission (GPM), launched in February 2014. The GPM dual-frequency precipitation radar (DPR) uses two frequencies, 13.6 GHz (KuPR) and 35.5 GHz (KaPR). The KaPR is useful for detecting light precipitation. Measurements at the two frequencies can observe both strong rain in the tropics and light rain and snow in high latitudes. They also deliver the ability to estimate the drop size distribution (DSD). This information cannot be acquired using only one frequency as in TRMM, hence the accuracy of precipitation volume estimation is significantly improved. The first DPR image released is shown in Figure 2.11. Thus, future missions will be multifrequency.

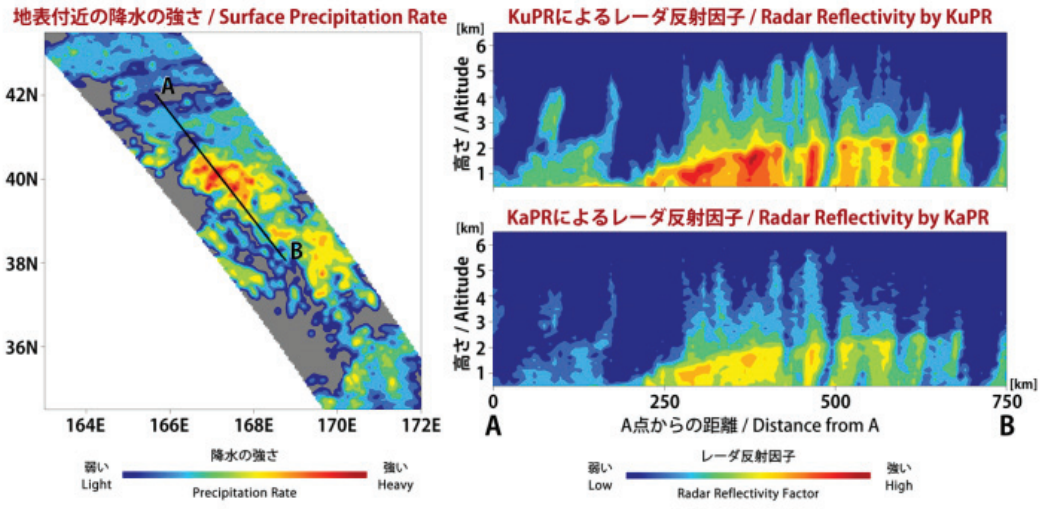

FIGURE 2.11 Examples of DPR 3D imagery for a hurricane. SOURCE: JAXA/NASA.

Scientific and Operational Applications

TRMM's observations are critical to the study of precipitation and associated storms and climate processes in the tropics. Scientists using the data have been able to determine the time and space varying characteristics of tropical rainfall, convective systems, and storms and how these are related to variations in the global water and energy cycles. The satellite also helps us build a long record of near-global precipitation characteristics, which is critical to understanding Earth's natural mechanisms and cycles. Additionally, the availability of real-time TRMM data has allowed monitoring of tropical cyclones, assimilation of precipitation information into weather forecast models, and other contemporaneous hydrological applications. The continuation of the TRMM data set will be the objective of the GPM.

Satellite Ocean Wind Sensors

The International Space Station (ISS) RapidScat instrument is the third K_u-band wind scatterometer in the SeaWinds series. The QuikSCAT instrument operated from 1999 until 2009. RapidScat was launched to the ISS in September 2014 as a cost-effective replacement for QuikSCAT. It measures ocean winds to support weather prediction, monitor hurricanes, and perform basic research. QuikScat's measurements were so essential to the prediction community that when QuikSCAT

stopped collecting wind data in late 2009, NASA's Jet Propulsion Laboratory (JPL) created the RapidScat instrument from the test hardware that was originally built to test QuikSCAT. This hardware was then launched to the ISS for a fraction of the cost and time it would have taken to build and launch a new satellite. Recently, RapidSCAT monitored the very active 2014-2015 winter on the East Coast and the extended typhoon season in the Pacific.

Summary of Current and Future Satellite-Based Sensors

Tables 2.2 and 2.3 list several current and planned future satellite missions that use active sensors to remotely sense the atmosphere. The sensors typically obtain 2D or 3D images of atmospheric winds and precipitation. In addition to supporting basic scientific research, the data are operationally used in numerical weather forecasting and are especially vital during tropical cyclones for monitoring and predicting land-falling hurricanes and predicting storm intensity.[24] These sensors provide data used to retrieve the motion of ice and rain within storms and to support climate studies and hurricane evolution studies and other scientific applications.

SPECTRUM USAGE REQUIREMENTS FOR SATELLITE-BASED SENSING

Atmospheric transmission windows impose restrictions on what frequencies can be used for remote sensing atmospheric parameters.[25] In addition, some frequencies are desirable (or undesirable) owing to their sensitivity to specific physical parameters of interest such as ice, rain, and particulates. These considerations lead to the selection of the operational frequencies commonly used for active atmospheric sensing. As indicated in Tables 2.3 and 2.4, the typical bands used by current and future atmospheric sensors extend from the L-band (1.2 GHz) into the millimeter-wave bands such as the W-band (94 GHz).

The bandwidth necessary to satisfy spatial resolution requirements for current and planned cloud and precipitation radars are typically between 0.6 and 60 MHz for precipitation radars and 0.3 and 10 MHz for cloud radars.

Because of the size, weight, and power limitations of spacecraft-borne sensors, they must limit their transmit power. The echo signals are typically very small and

[24] National Academy of Public Administration, *Forecast for the Future: Assuring the Capacity of the National Weather Service*, Washington, D.C., 2013, http://www.napawash.org/wp-content/uploads/2013/05/ForecastfortheFuture-AssuringtheCapacityoftheNationalWeatherService.pdf.

[25] International Telecommunication Union, "Frequency Bands and Required Bandwidths Used for Spaceborne Active Sensors Operating in the Earth Exploration-Satellite (Active) and Space Research (Active) Services," REC. ITU-R RS.577-7, 2009.

TABLE 2.2 Current Active Atmospheric Sensor Missions

Instrument	Frequency Band (GHz)	Launch	Description and Comments
GPM[a] Core Observatory[b]	13.6 (K_u- band) 35.5 (K_a-band) 35-36 GHz	February 2014	Near-global liquid and solid precipitation to improve climate predictions, follow-on for TRMM. DPR active/passive sensor light to heavy rain. Simultaneous measurements at the K_a-/K_u-bands will provide new information on DSD (NASA/JAXA).
ATTREX (airborne)	1.25 (L-band)	2011	Measures tropopause layer water vapor with Dual-frequency Airborne Precipitation Radar (NASA).[c]
CloudSAT (CPR)[d]	94-GHz (W-band) nadir-looking 94-94.1 GHz	2006	Measures rain and clouds to study their impact on Earth's radiation budget and climate change. NASA/Canadian Space Agency (CSA) mission.
HS3 (airborne) — (Hurricane and Severe Storm Sentinel)[e]	13.47, 13.91 33.72, 35.56 (K_a/K_u-band), HIWRAP[f] Doppler radar	2012	Maps the 3D tropospheric and atmospheric winds, precipitation field and ocean surface wind field of tropical cyclones, hurricane development, monitoring, storm intensity prediction. Motion of ice and rain within storms (NASA).
TRMM (PR)	13.8 GHz (K_u-band) 13.4-14 GHz	1997	Measures rainfall in the tropics and subtropics for a better understanding of cloud formation, rain, floods, and droughts and how the winds drive ocean currents (NASA/JAXA).
METOP ASCAT series	5.4 GHz (C-band)	2007	Measure near-surface wind speed and direction over the global oceans. Monitor severe weather events such as hurricanes and typhoons (ESA).
ISS-RapidScat	13.6 (K_u-band)	2014	Diurnal cycle observation of global near-surface winds and rain over the ocean (NASA/JPL).

NOTE: ASCAT, Advanced Scatterometer; ATTREX, Airborne Tropical Tropopause Experiment; ESA, European Space Agency; HIWRAP, High-Altitude Imaging Wind and Rain Airborne Profiler; JAXA, Japan Aerospace Exploration Agency; METOP, Meteorological Operational satellite program.

[a] NASA, "Constellation Partners," http://pmm.nasa.gov/GPM/constellation-partners, accessed June 2, 2015.

[b] NASA, "Global Precipitation Measurement: Core Observatory," http://www.nasa.gov/sites/default/files/files/GPM_Mission_Brochure.pdf, accessed June 2, 2015.

[c] NASA, "Dual-Frequency Airborne Precipitation Radar (PR-2)," https://espo.nasa.gov/missions/attrex/instrument/PR-2, accessed June 2, 2015.

[d] Colorado State University, "The Cloud Profiling Radar (CPR)," http://cloudsat.atmos.colostate.edu/instrument, accessed June 2, 2015.

[e] NASA, "HS3 Mission Overview," http://www.nasa.gov/mission_pages/hurricanes/missions/hs3/overview/#.UuQ_C2TD8YI, accessed June 2, 2015.

[f] H. Kramer, "HIWRAP (High-Altitude Imaging Wind and Rain Airborne Profiler)," Earth Observation Portal, https://directory.eoportal.org/web/eoportal/airborne-sensors/hiwrap, accessed June 2, 2015.

TABLE 2.3 Future Active Atmospheric-Sensing Satellite Missions

Instrument	Frequency Band (GHz)	Launch	
Earthcare (CPR)[a]	94.05 (W-band)[b]	Late 2015	Clouds and aerosols (lidar/radar) cloud profiling radar (CPR)—(ESA/JAXA/NICT), doppler providing sensitivity of -36 dBZ.[c]
Aerosol/Cloud/Ecosystems (ACE), Doppler NASA radar	35.6 GHz (K_a-band) and 94.1 GHz (W-band)	2020+	Measures cloud ice and rain, will help to answer emerging science questions associated with aerosols, clouds, air quality, and global ocean ecosystems (NASA).[d]
Ocean Surface Vector Wind (OSVW)	5.4 GHz (C-band) and 13.2 GHz (K_u-band)	TBD	Measure near-surface wind speed and direction and rain rate over the global oceans. Monitor severe weather events such as cyclones (NASA/NOAA).[e]

NOTE: NICT, National Institute of Information and Communications.

[a] AXA, "Earth Cloud, Aerosol and Radiation Explorer (EarthCARE)," November 29, 2012, http://www.jaxa.jp/projects/sat/earthcare/index_e.html.

[b] P. Foster, J. Hartmann, H. Horie, and R. Wylde, "Performance Verification of the 94 GHz Quasi-Optical-Feed for EarthCARE's Cloud Profiling Radar," *Proceedings of the 5th ESA Workshop on Millimeter Wave Technology and Applications and 31st ESA Antenna Workshop*, May 18-20, 2009, Noordwijk, The Netherlands, ESA WPP-300, 2009.

[c] ESA, "EarthCARE," https://earth.esa.int/web/guest/missions/esa-future-missions/earthcare, accessed June 3, 2015.

[d] NASA, "ACE Science Working Group (SWG) Workshop," November 2014, http://dsm.gsfc.nasa.gov/ace/.

[e] P.S. Chang, Z. Jelenak, J.M. Sienkiewicz, R. Knabb, M.J. Brennan, D.G. Long, and M. Freeberg, Operational use and impact of satellite remotely sensed ocean surface vector winds in the marine warning and forecasting environment, *Oceanography* 22(2):194-207, 2009.

therefore vulnerable to interference. Active atmospheric sensors are designed to meet their performance requirements so long as RFI does not exceed the interference criteria specified in Recommendation ITU-R RS.1166, where *I/N* refers to the ration of interference to noise power. According to the said recommendation,

> Performance criteria for active sensors is defined in terms of the precision of measurement of physical parameters and the availability of measurements free from harmful interference. Interference criteria are stated in terms of the interfering signal power not to be exceeded in a reference bandwidth for more than a given percentage of time.

TABLE 2.4 Commonly Used Bands for Active Atmospheric Sensing by Sensor Type

Altimeter	Wind Scatterometer	Precipitation Radar	Cloud Radar
(C) 5.25-5.57 GHz (K_u) 13.25-13.75 GHz	(C) 5.4-5.5 GHz (K_u) 13.25-13.75 GHz	(K_u) 13.25-13.75 GHz (K_u) 17.2-17.3 GHz (K) 24.05-24.25 GHz (K_a) 35.5-36.0 GHz	(W) 94.0-94.1 GHz (mm) 133.5-134.0 GHz (mm) 237.9-238.0 GHz
Weather prediction, scientific studies	Weather prediction, severe storms, scientific studies, hurricanes	Hurricanes, severe storms, scientific studies	Hurricanes, severe storms, scientific studies

SOURCE: Bryan Huneycutt, Jet Propulsion Laboratory.

TABLE 2.5 Interference Sensitivity for Precipitation and Cloud Radars[a]

	Interference Criteria		Data Availability Criteria (%)	
Sensor Type	Performance Degradation	I/*N* (dB)	Systematic	Random
Precipitation radar	7% increase in minimum rainfall rate	–10	N/A	99.8
Cloud profile radar	10% degradation in minimum cloud reflectivity	–10	99	95

NOTES: I/N, interference to noise power ratio.

[a] International Telecommunication Union, "Performance and Interference Criteria* for Active Spaceborne Sensors," Recommendation RS.1166-4, 2009, http://www.itu.int/rec/R-REC-RS.1166-4-200902-I.

Table 2.5 summarizes the maximum allowable interference levels for current precipitation radars based on Recommendation ITU-R RS.1166 for each operating frequency. Interference levels exceeding these values would degrade, or may entirely prevent, collection of useful measurements.

Table 2.6 summarizes the maximum allowable interference levels for current precipitation radars based on Recommendation ITU-R RS.1166 for each operating frequency.

ECONOMIC AND SOCIETAL VALUE

According to NOAA, "NOAA's National Weather Service forecasts, warnings, and the associated responses result in a $3 billion savings in a typical hurricane season. Two-thirds of this savings, $2 billion, is attributed to the reduction in

TABLE 2.6 Maximum Interference Power Level for Specific Active Bands Used in Current Precipitation Radars[a]

Frequency (GHz)	Interference Power Level (dBW)
13.75-13.790	–90
13.790-13.793	–115
13.793-13.805	–150
13.805-13.808	–115
13.808-13.850	–90
13.85-13.86	–70
35.5-36.0	–152
94.0-94.1, 133.5-134, 237.9-238 (CR)	–155 (over 300 kHz)

[a] International Telecommunication Union, "Performance and Interference Criteria* for Active Spaceborne Sensors," Recommendation RS.1166-4, 2009, http://www.itu.int/rec/R-REC-RS.1166-4-200902-I.

storm-related deaths, and one-third of this savings, $1 billion, to a reduction in property-related damage."[26]

Although NASA's missions are mostly scientific, not operational, its active sensors provide important meteorological and space weather data in near-real time that is also used to improve forecasting, monitoring, and mitigation planning.[27]

Table 2.7 lists some of the yearly savings that accrue to industries like agriculture and railways and to society in general given in the NOAA report. Active remote sensing contributes to these annual savings by providing data to weather services and continually improving the understanding of Earth's processes.

FINDINGS AND RECOMMENDATIONS

Finding 2.1: Whether measured from the ground or space, active remote sensing of the atmosphere provides immense scientific and operational value to society. From saving lives and protecting property from severe storms to facilitating a deeper understanding of upper atmospheric winds and global circulation (as examples), active remote sensing cannot be replaced by any other observational technology.

Radar wind profiling of the atmosphere exploits scattered energy from temperature and moisture discontinuities caused by turbulence. Owing to the viscous characteristics of the atmosphere, however, these discontinuities exist only over cer-

[26] NOAA, *Economic Statistics for NOAA*, 5th ed., April 2006, http://www.publicaffairs.noaa.gov/pdf/economic-statistics-may2006.pdf.

[27] National Academy of Public Administration, *Forecast for the Future,* 2013.

TABLE 2.7 Estimated Financial Savings to the U.S. Economy to which Active Atmospheric Sensing Contributes

Yearly Savings Estimate	Quote
$175 million, electric utilities	U.S. electricity producers save $185 million annually using 24-hour temperature forecasts to improve the mix of generating units that are available to meet electricity demand. Incremental benefits are relevant in assessing the merits of investments that will improve forecast accuracy.[a]
$418 million per °F, electric utilities	Errors in temperature and precipitation forecasting for even benign meteorological events such as local or regional heat or cold waves can cost U.S. utilities approximately $1.14 million per degree Fahrenheit daily as a result of an impaired ability to match energy supplies with demand.[b]
$312-$354 million, agriculture	Benefits to U.S. agriculture by altering planting decisions based on improved El Niño forecasts have been estimated at $312 million to $354 million annually, throughout El Niño, normal, and La Niña years. Costs associated with errors in predicting the onset of regional climate changes could thus easily amount to hundreds of millions of dollars per year.[c]
$78-$177 million per 1°C, many industries	The incremental benefit of an improvement in temperature forecast accuracy is estimated to be about $1.85 million per percentage point of improvement per year. For a 1°C improvement in accuracy, the benefit is about $78 million per year (or a $49 million benefit for a 1°F improvement). It is estimated that a perfect forecast would add $99 million to these savings.[d]
$13.4 million, railways	For every $1 that railway companies spend in acquiring NOAA climate data, they receive a $16,000 savings in infrastructure costs that would be required to maintain their own climate database storage, archiving, and reporting system. After extrapolating these savings to the entire Class I freight railroad sector, the potential benefits are approximately $14 million.[e]

NOTE: All values have been changed to 2014 dollars.

[a] National Weather Service, "Value of a Weather-Ready Nation," National Oceanic and Atmospheric Administration, last revised September 13, 2011, http://www.nws.noaa.gov/com/weatherreadynation/files/Weather-Econ-Stats.pdf.

[b] National Research Council, *Handbook of Frequency Allocations and Spectrum Protection for Scientific Uses*, The National Academies Press, Washington, D.C., 2007.

[c] National Oceanic and Atmospheric Administration, *Economic Statistics for NOAA*, 5th Ed., Silver Spring, Md., April 2006.

[d] T. Teisberg, R. Weiher, and A. Khotanzad, The economic value of temperature forecasts in electricity generation, *Bulletin of the American Meteorological Society* 86:1765-1771, 2005.

[e] Centrec Consulting Group, LLC, *Economic Value of Selected NOAA Products within the Railroad Sector*, Report prepared for NOAA's National Climatic Data Center, Savoy, Ill., June 2005.

tain length scales. This type of scattering (Bragg backscattering is one) can only be observed at particular radio frequency bands. Similar physically based constraints exist for other atmospheric remote sensing techniques, such as turbulence, rain, and clouds.

Finding 2.2: The frequency bands used for active remote sensing of the atmosphere are selected to optimize the detection of specific physical features and phenomena. In general, observations at approximately 50, 400, and 900 MHz and 3, 10, 14, 35, 90, 140, and 210 GHz (very roughly every octave in frequency) are needed.

Recommendation 2.1: Because of the immense impact on society and for the sake of atmospheric science, the current frequency allocations for active remote sensing of the atmosphere should be preserved and strongly protected.

3

Active Earth Remote Sensing for Ocean Applications

INTRODUCTION

A wide variety of operational (near-real-time) and research (non-real-time) active sensing systems are used for scientific, commercial, and government applications. These applications include fundamental meteorological and oceanographic research for understanding air/sea interactions that govern the exchange of fluxes of heat, mass, and momentum, which are physical processes required for oceanic and atmospheric modeling. Applications include global weather prediction, storm and hurricane warning, wave forecasting, coastal storm surge, ship routing, commercial fishing, coastal current and wave monitoring, and climate change. For these ocean applications, active and passive microwaves provide a different and unique response to oceanic geophysical parameters that cannot be obtained using infrared or visible sensors.

Table 3.1 lists the applicable oceanic geophysical parameters that can be measured with active microwave sensors, which can be grouped into airborne/spaceborne sensors and ground-based sensors. The first category includes three general classes of radar sensors: (1) synthetic-aperture radar (SAR) systems/side-looking airborne radar (SLAR) and interferometric SAR (InSAR), (2) scatterometers (Scat), and (3) altimeters (Alt). The ground-based category consists of HF band radars. All of these remote sensing systems are special-purpose radars that respond to physical scales of ocean roughness from tens of meters to centimeters. Since the dominant ocean electromagnetic (EM) scattering mechanism is Bragg scattering, this requires a wide operating frequency range from the HF band (3-50 MHz) to

TABLE 3.1 Oceanic Parameters Remotely Sensed by Active Microwave Sensors

	Sensor			
Oceanic Parameter	Alt	Scat	SAR	HF Radar
Significant wave height	X			
Ocean wave spectrum			X	X
Surface wind speed	X	X	X	X
Surface wind direction		X		
Ocean gravity	X			
Ocean current magnitude	X			X
Ocean current direction				X
Mean sea level	X			
Internal waves			X	
Oil slicks		X	X	
Sea ice extent	X	X	X	
Icebergs		X	X	

the K_u-band (14 GHz). Detailed frequency requirements for the various systems are defined herein.

This section describes the principle of operation for the various classes of active sensors (separated by radar type) and highlights the major applications for each. The discussion begins with a brief overview of the history of active microwave remote sensing for oceanic applications.

HISTORY OF ACTIVE REMOTE SENSING FOR OCEAN APPLICATIONS

Active microwave remote sensing began before World War II, in the 1930s and 1940s, when radar was exploited for military applications. During that period, the environmental signals were regarded as "noise" (e.g., sea-state clutter) that tended to mask the detection of desired surface targets like ships. Later this environmental noise became the signal for the remote sensing technologist who wanted to relate changes in environmental parameters to corresponding changes in the radar back-scattered echo.

Ground-Based High-Frequency Radar Sensors

While D.D. Crombie correctly identified the source of the sea echo observed by HF radars to be the result of coherent scattering by ocean surface waves,[1] efforts to advance both the theory of the phenomenon and its application to providing useful information about the coastal ocean lagged this initial work by a few decades. Donald E. Barrick was the first to offer a supporting theoretical description for the measurements of surface currents by radar.[2] Follow-up studies provided the derivation and interpretation of the nonlinear theory for detecting surface gravity waves (i.e., ocean waves).[3] Such HF radar installations for observing the coastal ocean began to contribute to both scientific research and practical applications in the late 1970s and early 1980s.

Initially, all the deployed research systems utilized phased-array technology. However, the relatively large arrays required to achieve high angular resolution, particularly at the lower frequencies, and the resulting weight of such arrays made these systems challenging to permit, deploy and maintain. To address these difficulties, in the 1970s, the Wave Propagation Laboratory of the National Oceanic and Atmospheric Administration (NOAA) began development of the coastal ocean dynamics applications radar (CODAR) system, which utilized a compact design of colocated antennas. The CODAR system used a crossed-dipole antenna structure along with direction-finding methods to invert the received signals for the azimuthal bearing of surface currents from the dominant backscattered signal.

Airborne/Satellite Radar Sensors for Ocean Applications

During the 1960s and 1970s, the U.S. Naval Research Laboratory performed pioneering laboratory and field measurements,[4] which were later followed by field measurements by NASA,[5] to understand the electromagnetic (EM) scattering of

[1] D.D. Crombie, Doppler spectrum of sea echo at 13.56 Mc./s, Nature 175:681-682, 1955.

[2] D.E. Barrick, First-order theory and analysis of MF/HF/VHF scatter from the sea, *IEEE Transactions on Antennas and Propagation* AP-20(1):2-10, 1972.

[3] D.E. Barrick and B.L. Weber, On the nonlinear theory for gravity waves on the ocean's surface. Part II: interpretation and applications, *Journal of Physical Oceanography* 7(1):11-21, 1977; B.J. Lipa, Inversion of second-order radar echoes from the sea, *Journal of Geophysical Research* 83(C2):959-962, 1978.

[4] N.W. Guinard, and J.C. Daley, An experimental study of a sea clutter model, *Proceedings of the IEEE* 58:543-550, 1970; Guinard et al., Variation of the NRCS of the sea with increasing roughness, *Journal of Geophysical Research* 76:1525-1538, 1971; J.W. Wright, Backscattering from capillary waves with application to sea clutter, *IEEE Transactions on Antennas and Propagation* 14(6):749-754, 1966.

[5] F.G. Bass et al., Very high frequency radiowave scattering by a disturbed sea surface, *IEEE Transactions on Antennas and Propagation* 16(5):554-568, 1968; W.L. Jones, L.C. Schroeder, and J.L. Mitchell,

ocean waves. It was soon recognized that there was a strong cause and effect relationship between ocean sea-state and surface winds, which prompted the development of a theoretical ocean wave spectral model[6] that enabled the development of EM scattering theory for the ocean.[7] As early as the mid-1960s, the pioneering work of Willard J. Pierson and Richard K. Moore[8] suggested the use of space-based radars for measuring ocean waves and wind speed, but it took almost a decade of field experiments using many aircraft-based and surface-based measurements, as well as theoretical developments, before the concept was considered for spaceflight.

The first use by NASA of microwave sensors for ocean observations occurred, primarily as a technology demonstration, on the Skylab mission in 1973-1974.[9] This paved the way for NASA's first oceanographic satellite Seasat-A, which was launched into a polar orbit in 1978.[10] Seasat-A was the first Earth-orbiting satellite to carry four complementary microwave experiments: the radar altimeter (ALT)[11] to measure ocean surface topography; the Seasat-A satellite scatterometer (SASS)[12] to measure ocean wind speed and direction; the passive scanning multichannel microwave radiometer (SMMR)[13] to measure a variety of ocean surface and atmospheric parameters; and SAR[14] to image the ocean surface, polar ice caps, and coastal regions.

Aircraft measurements of the microwave scattering signature of the ocean, *IEEE Transactions on Antennas and Propagation* 25(1):52-61, 1977.

[6] W.J. Pierson and L. Moskowitz, A proposed spectral form for fully developed wind seas based on similarity theory of S.A. Kitaigorodskii, *Journal of Geophysical Research* 69:5191-5203, 1964.

[7] A.K. Fung and K. Lee, A semiempirical sea-spectrum model for scattering coefficients estimation, *IEEE Journal of Oceanic Engineering* 7(4):166-176, 1982.

[8] R.K. Moore and W.J. Pierson, Measuring sea state and estimating surface winds from a polar orbiting satellite, presented at the International Symposium on Electromagnetic Sensing of the Earth from Satellites, Miami Beach, Fla., 1965; R.K. Moore and F.T. Ulaby, The radar radiometer, *Proceedings of the IEEE* 57(4):587-590, 1969.

[9] R.K. Moore et al., Simultaneous active and passive microwave response of the Earth—The Skylab radscat experiment, pp. 189-217 in *Proceedings of the 9th International Symposium on Remote Sensing of Environment*, University of Michigan, Ann Arbor, Mich., 1974.

[10] D.E. Barrick and C.T. Swift, The Seasat microwave instruments in historical perspective, *IEEE Journal of Oceanic Engineering* 2(2):200-206, 1977.

[11] W.F. Townsend, An initial assessment of the performance achieved by the Seasat-1 radar altimeter, *IEEE Journal of Oceanic Engineering* 5(2):80- 92, 1980.

[12] W.L. Grantham, E.M. Bracalente, W.L. Jones, and J.W. Johnson, The Seasat-A satellite scatterometer, *IEEE Journal of Oceanic Engineering* 2(2):200-206, 1977.

[13] E.G. Njoku, J.M. Stacey, and F.T. Barath, The Seasat Scanning Multichannel Microwave Radiometer (SMMR): Instrument description and performance, *IEEE Journal of Oceanic Engineering* 5(2):100-115, 1980.

[14] R.L. Jordan, The Seasat-A synthetic aperture radar system, *IEEE Journal of Oceanic Engineering* 5(2):154-164, 1980.

While originally designed for remote sensing of Earth's oceans, Seasat-A had a large impact in many other areas, including solid Earth science, hydrology, ecology, and planetary science.[15] Following Seasat, several Earth-observing missions were launched in the 1990s by the European Space Agency (ESA) and the National Space Development Agency (NASDA) of Japan. The first and second satellites by ESA were the European remote sensing satellite (ERS-1) in 1991 and ERS-2 in 1995, which carried the active microwave instrument (AMI)—a joint SAR/scatterometer[16] and radar altimeter. The third Earth remote sensing satellite by NASDA was the Advanced Earth Observing Satellite (ADEOS) launched in 1996, which carried the NASA scatterometer (NSCAT)[17] and a passive advanced microwave scanning radiometer (AMSR). Today, there are many satellite microwave ocean-observing systems in orbit used for both research and operational applications. Meteorological agencies throughout the world use both active and passive microwave observations in their numerical weather models and forecasts. Researchers studying global climate change use these data in ocean and atmospheric circulation models to study short- and long-term interactions of the atmosphere and ocean. In recent years, other scientific applications are now using microwave sensor data to study sea and glacial ice, ocean, and land ecology, and other nonoceanic applications.

TECHNICAL BASIS FOR AIRBORNE/SPACEBORNE ACTIVE EARTH REMOTE SENSING OF OCEANS

Because of the global coverage and frequent revisit time provided by polar satellites, they are the platform of choice for the vast majority of oceanic active remote sensing observations. On the other hand, there are a few notable exceptions, such as tropical cyclone (hurricane and typhoon) surveillance, where airborne sensors are used. With the availability of high-flying, long-duration, remotely piloted (unmanned) aircraft, the use of active microwave sensors is becoming an important part of ocean observations for NASA and the National Oceanic and Atmospheric Administration (NOAA) operations and research. Regardless of the platform, the active microwave sensors are very similar and differ primarily in their measurement geometry. The following sections will discuss the technical basis for each category of active microwave sensors.

[15] D. Evans, W. Alpers, A. Cazenave, C. Elachi, T. Farr, D. Glackin, B. Holt, L. Jones, T. Liu, W. McCandless, Y. Menard, R. Moore, and E. Njoku, Seasat—A 25 year legacy of success, *Remote Sensing of Environment* 94(3):287-428, 2005.

[16] E.P.W. Attema, The Active Microwave Instrument on-board the ERS-1 satellite, *Proceedings of the IEEE* 79(6):791-799, June 1991.

[17] Special issue on NSCAT, *Journal of Geophysical Research* 104:11229-11568, 1999.

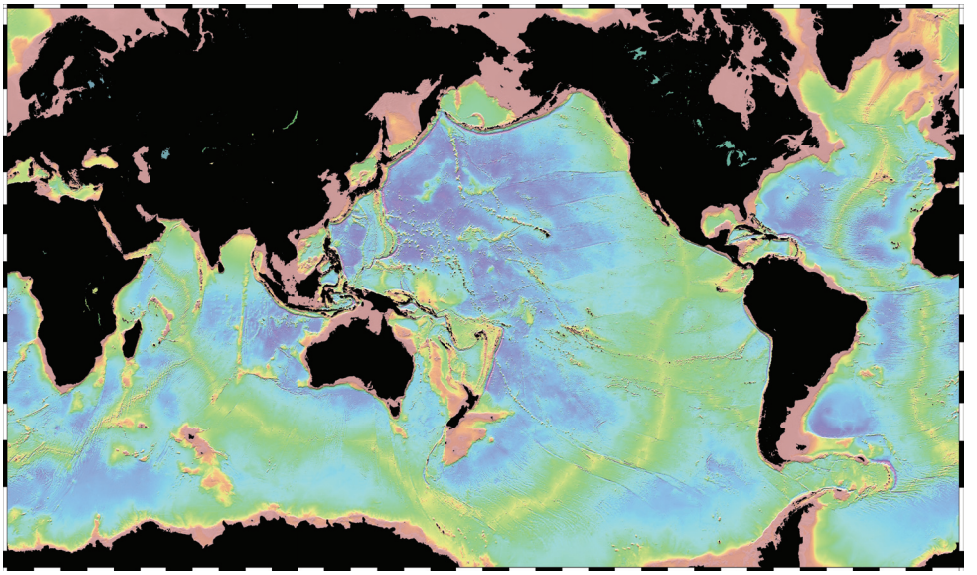

FIGURE 3.1 Ocean gravity field inferred from satellite altimetry, SOURCE: W. Smith and D. Sandwell, "Measured and Estimated Seafloor Topography," World Data Service for Geophysics, Boulder Research Publication RP-1, poster, 34" × 53", 1997; courtesy of W.H.F. Smith and D.T. Sandwell and NOAA's Laboratory for Satellite Altimetry. See also W.H.F. Smith and D.T. Sandwell, Global sea floor topography from satellite altimetry and ship depth soundings, *Science* 277(5334):1956-1962, 1997.

Altimeters

A radar altimeter is a nadir-viewing, short-pulse radar that makes precise measurements of the height of the radar above the ocean surface. This measurement, coupled with knowledge of Earth's gravity field (ocean geoid) and precision orbit determination, allows the measurement of the dynamic ocean topography to a precision of a few centimeters (see Figures 3.1 and 3.2). From ocean topography, ocean currents (circulation) and mean sea level can be determined. Also, by recording the rise time of the return echo, the significant ocean wave height can be measured.

For more than four decades, satellite altimeters have been widely used for the measurement of ocean topography to support oceanographic research and for near-real-time operational applications for wave forecasting, sea-level storm surge, and ocean circulation. A brief history of civilian remote sensing altimeters on spacecraft is presented in Table 3.2.

Satellite altimeters have been widely used for ocean studies and have become

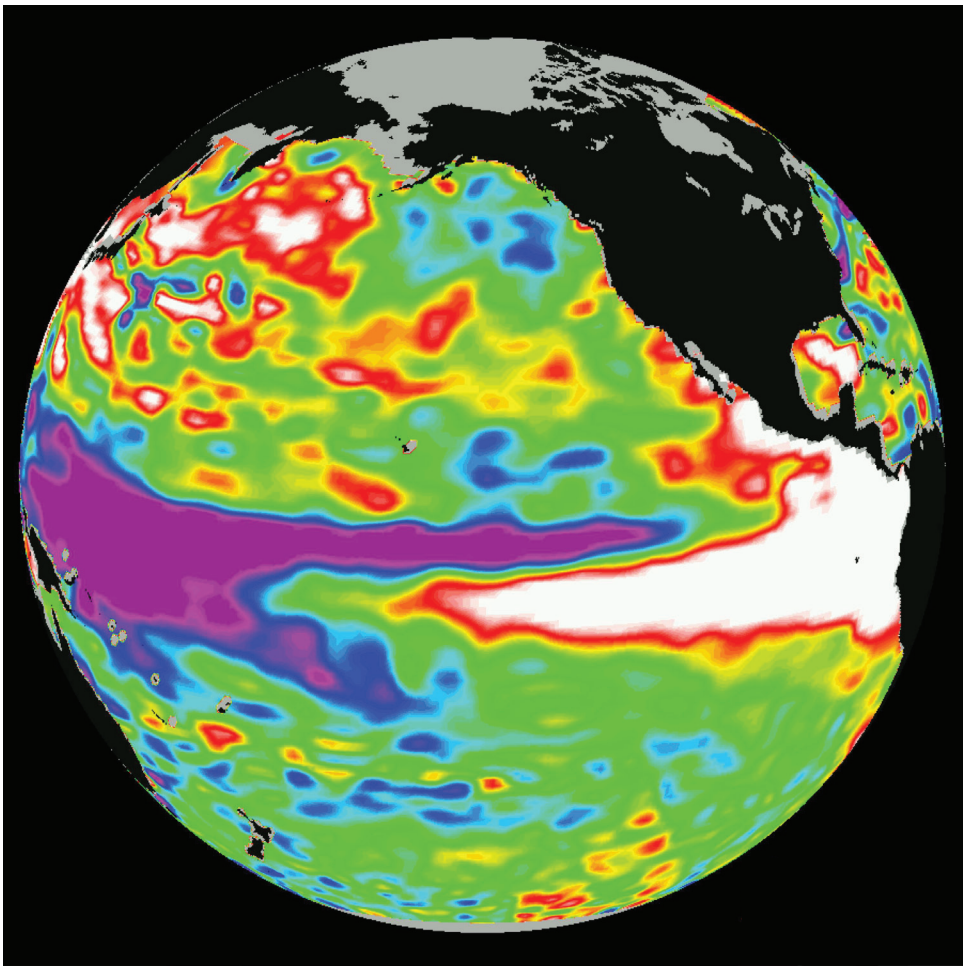

FIGURE 3.2 Ocean surface topography variations derived from satellite altimetry. SOURCE: NASA/JPL; "TOPEX/El Niño Watch—"Double Peak" Pattern Complete," December 1, 1997, PIA01099, http://photojournal.jpl.nasa.gov/catalog/PIA01099.

essential tools for the study of ocean circulation.[18] Satellite altimeters provide very precise measurements of the distance from the satellite to the surface and, coupled with precise orbit determination, very accurate surface topography can be derived. Precision altimetry missions began with TOPEX/Poseidon in 1992 and follow-on missions on Jason-1 and the Ocean Surface Topography Mission (OSTM)/Jason-2.

[18] L.L. Fu and A. Cazenave, *Satellite Altimetry and Earth Sciences: A Handbook of Techniques and Applications*, International GeoPhys Series, Academic Press, San Diego, Calif., 2001.

TABLE 3.2 History of Civilian Remote Sensing Altimeters on Spacecraft

Years	Spacecraft/Instrument	Band	Height Accuracy (cm)[a]
1973	Skylab/S193	K_u	–
1975	Geos3	C	–
1978	Seasat/ALT[b]	K_u	10
1985-1990	Geosatd	K_u	
1991-1996	ERS-1/RA[c]	K_u	
1995-2011	ERS-2/RA[c]	K_u	
1981-2006	TOPEX-Poseidon/SSALT, NRA[c]	C, Ku	5
1998-2008	GFO[c]	C, K_u	
2001-	Jason-1/Poseidon-2[c]	C, K_u	
2002-2008	Envisat/RA-2[c]	K_u	
2006-	CloudSat/CPR[d]	W	5,000
2008-	Jason-2/Poseidon-3[c]	C, K_u	2.5
2010	Cryosat-2/Siral[e]	K_u	
2011-	HaiYang-2[c]	C, K_u	
2013	Saral/AltiK[c]	K_a	

[a] Reported/estimated based on post processing.
[b] Designed for planetary topography measurement.
[c] Primarily designed for ocean topography.
[d] Designed for cloud profiling.
[e] Designed primarily for ice-sheet elevation and sea-ice freeboard.
SOURCE: Adapted from Fawwaz T. Ulaby and David G. Long, *Microwave Radar and Radiometric Remote Sensing*, University of Michigan Press, Ann Arbor, Mich., 2014; with permission of the authors.

This NASA/French National Center for Space Studies (CNES) partnership has produced more than three decades worth of ocean topography data for studying ocean circulation and global climate change associated with sea level rise, which is a sensitive indicator of climate change. Scientific and operational oceanographic applications of altimetry data include determining the geoid; measuring ocean currents; monitoring ocean tides; mapping undersea topography, ocean surface wind speed, and significant ocean wave height; and monitoring large-scale ocean phenomena. Planned developments in altimetry include an improved wide-swath interferometric system[19] to continue the ocean surface topography time series for

[19] B.D. Pollard, E. Rodriguez, L. Veilleux, T. Atkins, P. Brown, A. Kitiyakara, S. Datthanasombat, and A. Prata, The Wide-Swath Ocean Altimeter: Radar interferometry for global ocean mapping with centimeter accuracy, *IEEE Aerospace Conference* 2:1007-1020, 2002; E. Rodriguez, B.D. Pollard, and J.M. Martin, Wide-swath ocean altimetry using radar interferometry, submitted to

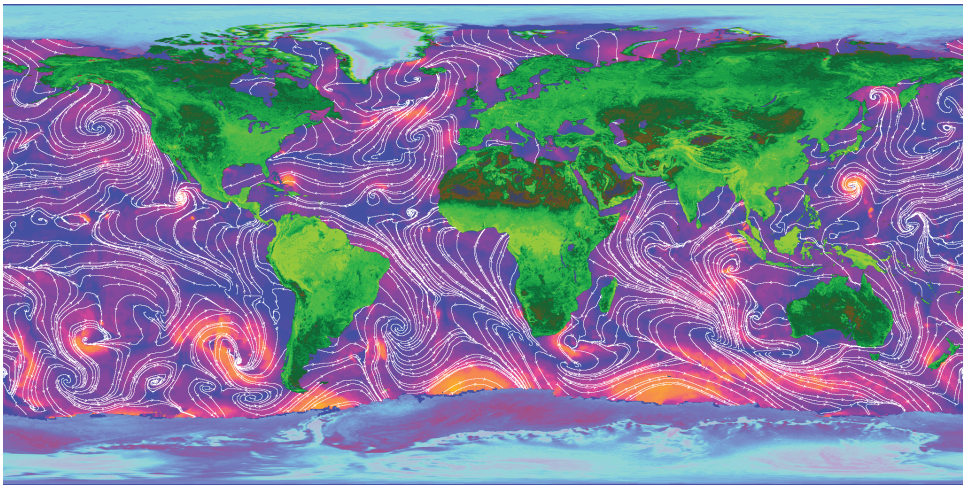

FIGURE 3.3 Scatterometer-derived ocean wind field and radar backscatter over land and ice. Color over land and ice is related to the radar backscatter value, with darker colors indicating lower backscatter. Over the ocean, the color indicates the wind speed with darker colors low wind speeds and lighter colors, high wind speeds. The white lines are streamlines showing wind direction. Note the high wind speed typhoon just south of Japan and the intense storms in the Southern hemisphere. SOURCE: Canadian Space Agency.

assessing climate change. Finally, altimetry data have many operational applications that include U.S. Navy global ocean wave models, NOAA storm surge and coastal flooding models, ocean eddy models, and weather and climate forecasting models on a global scale.

Scatterometers

A scatterometer is a long-pulse radar system that makes an absolute measurement of the Earth-surface-normalized radar cross section, σ^0 (i.e., a radar scattering metric). This technique, which measures the ocean σ^0 at multiple azimuth angles to infer the ocean surface wind vector (speed and direction), is now well established after four decades of research and development. An example of scatterometer-derived global ocean winds is shown in Figure 3.3, where colors represent the wind speed and the arrows show the wind flow patterns.

IEEE Transactions on Geoscience and Remote Sensing, July 1999, http://www.researchgate.net/profile/Jan_Martin7/publication/251800389_Wide-Swath_Ocean_Altimetry_Using_Radar_Interferometry/links/53ebb2630cf250c8947af385.pdf.

TABLE 3.3 History of Satellite Ocean Wind Scatterometers

Platform	Instrument	Agency	Band	Frequency (GHz)	Polarization	Spatial Res (km)	Swath wide (km)	Orbit (km)	Alt Launch Date
Skylab	S-193	NASA	K_u	13.9	VV, HH	16	180	435	May 1973
Seasat	SASS	NASA	K_u	14.6	VV, HH	50	2 × 500	799	June 1978
ERS-1	AMI (wind)	ESA	C	5.3	VV	50	500	784	July 1991
ERS-2	AMI (wind)	ESA	C	5.3	VV	50	500	784	April 1995
ADEOS-1	NSCAT	USA	K_u	14.0	VV, HH	25/50	2 × 600	798	April 1996
QuikScat	SeaWinds	NASA	K_u	13.4	VV, HH	50	1800	800	June 1999
ADEOS-2	SeaWinds	USA	K_u	13.4	VV, HH	50	1800	806	December 2002
MetOp1	ASCAT	ESA/ EUMETSAT	C	5.2	VV	50	2 × 550	720	2005 (estimated)

SOURCE: Glackin, 2004; D.L. Glackin and G.R. Peltzer, *Civil, Commercial, and International Remote Sensing Systems and Geoprocessing*, The Aerospace Press and AIAA, El Segundo, Calif., 1999; Kramer, 2001; Fawwaz T. Ulaby and David G. Long, *Microwave Radar and Radiometric Remote Sensing*, University of Michigan Press, Ann Arbor, Mich., 2014.

A history of satellite wind scatterometers is summarized in Table 3.3. The top panel lists satellite scatterometers and the lower panel depicts the antenna geometry for all satellite wind scatterometers flown in space. To meet the requirement of global ocean coverage in 1-2 days, satellite scatterometers have wide swaths, which result in off-nadir antenna pointing; and the requirement for multiple-azimuth looks is needed in order to recover the surface wind direction from the anisotropic radar backscatter. Note that the antenna configurations are of two types: (1) multiple, fixed fan-beam antennas pointing both forward and aft of the satellite motion and (2) conical scanning dual pencil-beam antennas. Two different frequencies are used: NASA K_u-band 13.4-14.6 GHz and ESA C-band 5.3 GHz.

Recently, ocean salinity measurements from space have been achieved using the active/passive Aquarius instrument aboard the Argentinian SAC-D spacecraft.[20] For this application, the L-band (1.26 GHz) scatterometer provides an important "roughness correction" for the radiometer salinity measurement as well as for measuring ocean wind speed.

Seasat-A, launched in 1978, demonstrated the proof-of-concept of microwave scatterometry for measuring ocean vector winds. Starting with the ERS-1 launch in 1991, there is now a continuous time series of greater than two decades of global scatterometer ocean wind observations. In fact scatterometers are the primary source of global ocean surface wind vectors and wind stress for science applications such as ocean and climate model forcing, air-sea interaction studies, and hurricane studies. Moreover scatterometer data are routinely assimilated in operational numerical weather prediction models at meteorological agencies worldwide, and this has revolutionized the analysis and short-term forecasting of winds over the oceans. Also near real-time (NRT) wind products are produced by NASA/Jet Propulsion Laboratory (JPL) and NOAA's National Environmental Satellite, Data, and Information Service to satisfy national operational requirements. NOAA distributes NRT data products to many operational users.

A National Research Council report noted that "scatterometer measurements have become critical to research and operational applications; that preventing an ocean vector winds data gap is imperative; and that steps must be taken to continue and improve the QuikSCAT ocean vector winds observations by transitioning the technology to an operational system capable of sustaining the measurements for many years."[21]

In addition, the σ^0 measurements from scatterometers have been extensively

[20] D.M. LeVine, G.S.E. Lagerloef, and S.E. Torrusio, Aquarius and remote sensing of sea surface salinity from space, *Proceedings of the IEEE* 98(5):688-703, 2010.

[21] National Research Council, *Earth Science and Applications from Space: National Imperatives for the Next Decade and Beyond*, The National Academies Press, Washington, D.C., 2007.

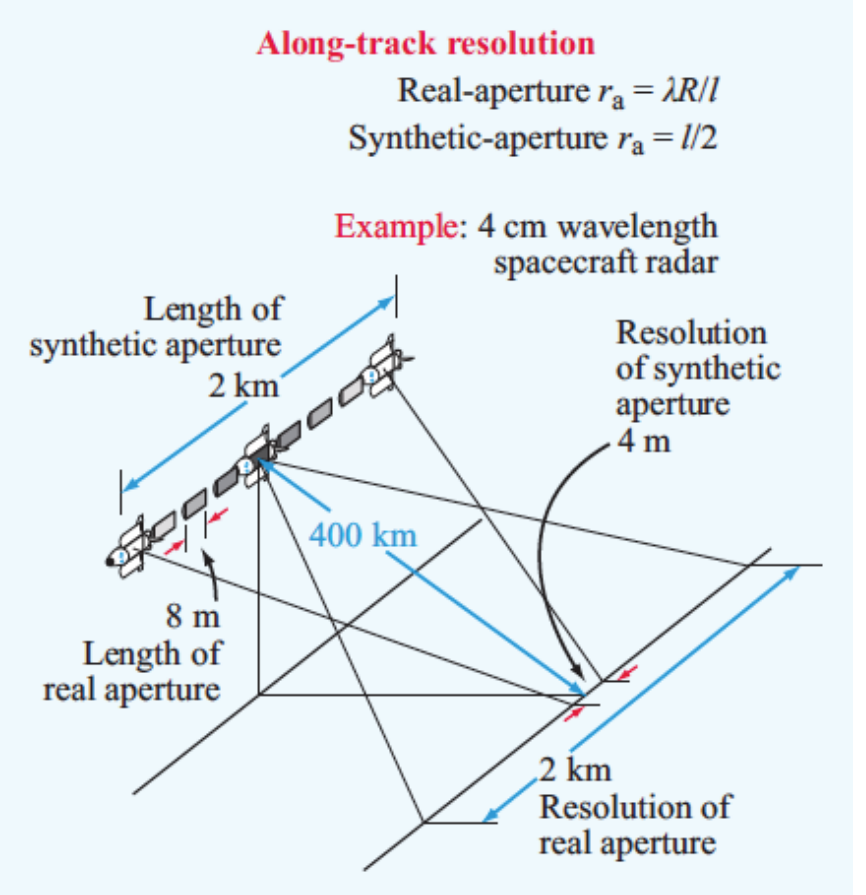

FIGURE 3.4 Illustration of synthetic-aperture principle for radar imaging. Note that R is the distance from the spacecraft to the target, 400 km in this example, and l is the length of the real aperture. SOURCE: Fawwaz T. Ulaby and David G. Long, *Microwave Radar and Radiometric Remote Sensing*, University of Michigan Press, Ann Arbor, Mich., 2014. With permission of the authors.

used for other applications such as the mapping of sea ice type and extent, detection of icebergs, and measuring soil moisture and vegetation density.[22]

Synthetic-Aperture Radar

SAR systems operate by transmitting modulated pulses and using Doppler/range processing to construct backscatter images. Satellite SARs provide the high-

[22] W.T. Liu, Progress in scatterometer applications, *Journal of Oceanography* 58(1):121-136, 2002.

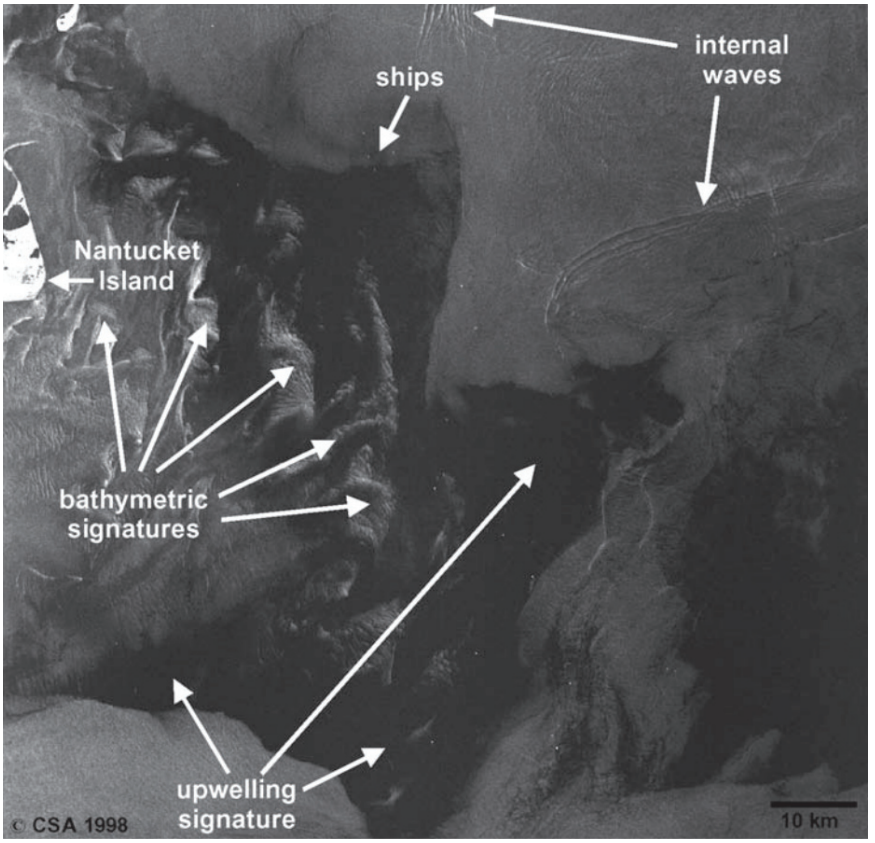

FIGURE 3.5 SAR images of oceanographic features. SOURCE: Canadian Space Agency.

est resolution but are significantly more complex than other radar sensors (e.g., scatterometers and altimeters). Interferometric SAR (InSAR or IFSAR) is a special SAR configuration used to measure topography and the motion of surfaces.

The SAR forms a radar image by coherently combining a time history of radar echoes (amplitude and phase) using a series of inverse Fourier transforms. A major advantage is that the resolution of the SAR in the along-track direction is proportional to the length of the synthetic antenna and independent of the distance. Figure 3.4 illustrates how SAR combines data collected from multiple antenna positions to synthesize a longer effective antenna, thereby achieving high along-track resolution.

Three examples of satellite SAR images for oceanographic applications are given in Figures 3.5-3.7.

Proposals for spaceborne SARs were made in the early 1960s, but the first civil-

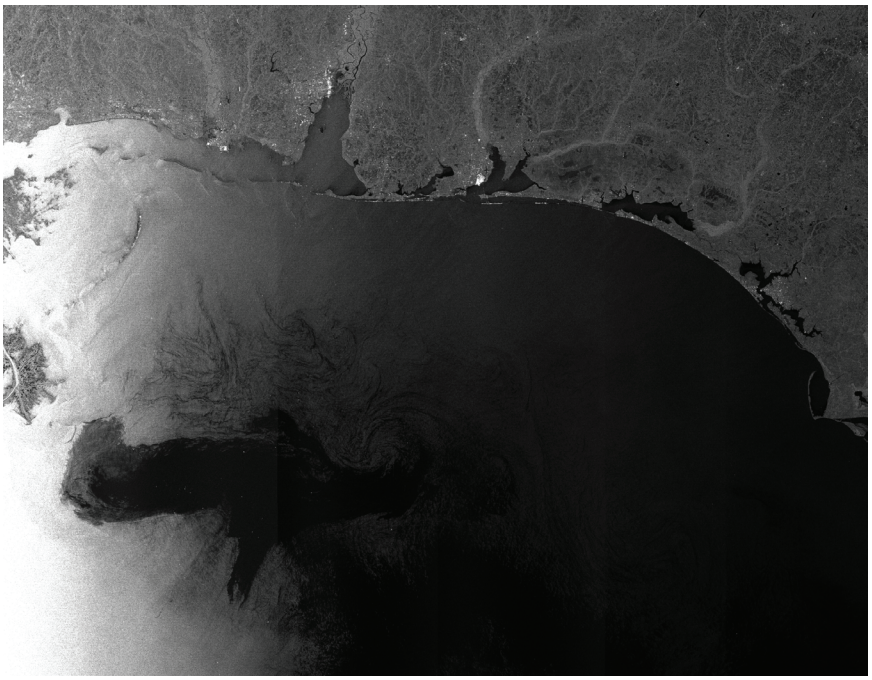

FIGURE 3.6 SAR image of oil spill in Gulf of Mexico. SOURCE: European Space Agency.

ian radar to fly in space was on-board the oceanographic satellite Seasat in 1978.[23] Several space shuttle SAR missions were flown through the 1980s, 1990s, and early 2000s, including the Shuttle Radar Topography Mission (SRTM),[24] which used radar interferometry to measure global surface topography. Many other spaceborne SAR systems launched by Europe, Japan, Canada, and the United States have been flown or are in various planning stages; the history of space-based imaging radars is summarized in Table 3.4.

SARs can be used for many different applications: geology, sea-ice mapping, disaster monitoring, vessel traffic surveillance, crop monitoring, and military applications. SAR imaging at the L-band and the C-band is not significantly affected by meteorological conditions and so can provide data and observations when other instruments cannot. Additionally, SAR interferometry (both dual-pass and single-pass, as used in the SRTM mission) can provide accurate 3D reconstruction of observed areas.

[23] R.L. Jordan, The Seasat-A synthetic aperture radar system, *IEEE Journal of Oceanic Engineering* 5(2):154-163, 1980.

[24] T.G. Farr et al., The Shuttle Radar Topography Mission, *Reviews of Geophysics* 45(2):RG2004, doi:10.1029/2005RG000183, 2004.

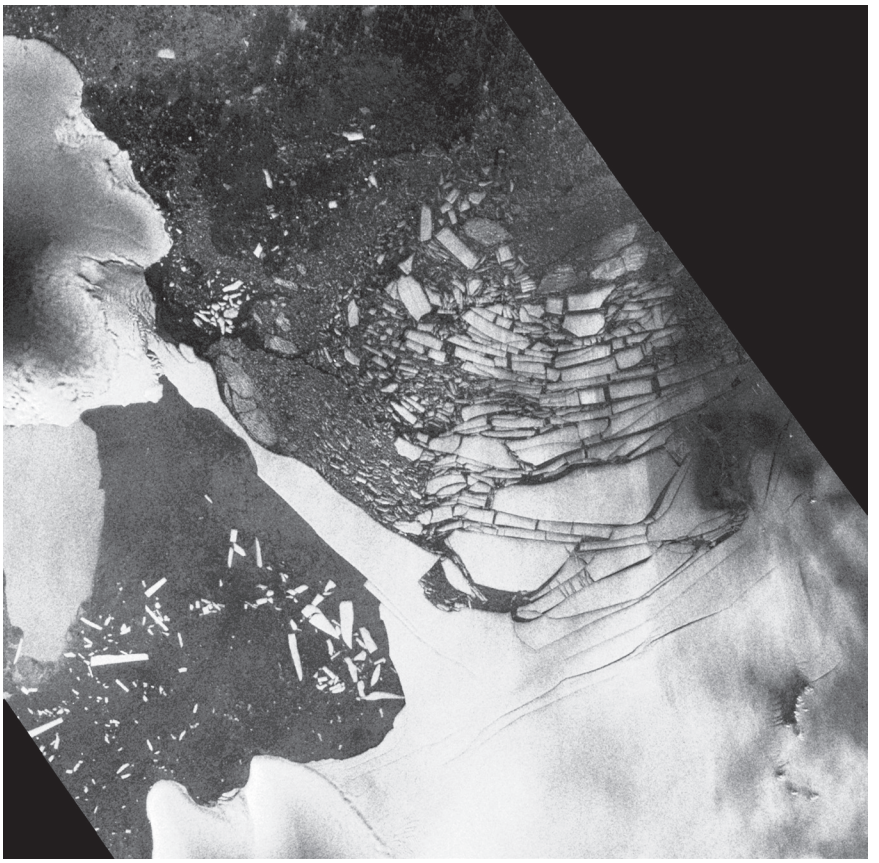

FIGURE 3.7 SAR image of the breakup of an Antarctic ice shelf on the Antarctic Peninsula. SOURCE: Advanced Synthetic Aperture Radar (ASAR) image courtesy the European Space Agency (ESA). The ESA provides additional imagery of the continued breakup of the Wilkins Ice Shelf. See ESA News, "Wilkins Ice Shelf Under Threat," November 28, 2008, http://www.esa.int/Our_Activities/Space_News.

Bistatic Scatterometry

Sensors can usefully operate in a bistatic mode by measuring the signal transmitted by manmade sources after the signal reflects or scatters off a medium or surface of interest.[25] Earth remote sensing platforms will soon begin to take advantage of this mode of operation in earnest.

NASA's Cyclone Global Navigation Satellite System (CYGNSS), due to launch in 2016, will comprise eight small satellites flying in a constellation formation

[25] See Chapter 9 for more discussion of this approach.

TABLE 3.4 History of Space-Based Imaging Radars

Sensor	Operation	Frequency Band (Polarization)	Comments	Institution, Country
Seasat	1978	L (hh)	First civilian SAR satellite, operation for only ca. three months	NASA/JPL, USA
SIRA-A, SIR-B	1981, 1984	L (hh)	Shuttle radar missions	NASA/JPL, USA
ERS-1/2	1991-2000/ 1995-2001	C (vv)	European Remote Sensing Satellite (first European SAR satellite)	ESA, Europe
J-ERS-1	1992-1998	L (hh)	Japanese Earth Resource Satellite (first Japanese SAR satellite)	JAXA, Japan
SIR-C/X-SAR	April and October 1994	L & C (quad) X (vv)	Shuttle imaging radar mission, first demonstration of spaceborne multifrequency SAR	NASA/JPL, USA DLR, Germany ASI, Italy
Radarsat-1	1995-today	C (hh)	First Canadian SAR satellite, swath width of up to 500 km with Scan SAR imaging mode	CSA, Canada
SRTM	February 2000	C (hh+vvv) and X (vv)	Shuttle Radar Topography Mission, first spaceborne interferometric SAR	NASA/JPL, USA DLR, Germany ASI, Italy
ENVISAT/ASAR	2002-2012	C (dual)	First SAR satellite with Transmit/ Receive module technology, swath width up to 400 km	ESA, Europe
ALOS/PALSAR	2006-2011	L (quad)	Advanced Land Observing Satellite (Daichi), swath width up to 360 km	JAXA, Japan
TerraSAR-X/ TanDEM-X	2007-today 2010-today	X (quad)	First bi-static radar in space, resolution up to 1 m, global topography available by end of 2014	DLR/Astrium, Germany

continued

TABLE 3.4 Continued

Sensor	Operation	Frequency Band (Polarization)	Comments	Institution, Country
Radarsat-2	2007-today	C (quad)	Resolution up to: 1 m × 3 m (azimuth × range), swath width up to 500 km	CSA, Canada
COSMO-SkyMed-1/4	2007…2010-today	X (dual)	Constellation of four satellites, up to 1 m resolution	ASI/MID, Italy
RISAT-1/2	2008-today	C (quad)	Follow-on satellite (RISAT-1a) to be launched in 2016, RISAT-3 (L-band) in development	ISRO, India
HJ-1C	2012-today	S (vv)	Constellation of four satellites, first satellite launched in 2012	CRESDA/CAST/NRSCC, China
Kompsat-5	Launch scheduled in 2013	X (dual)	Korea Multi-Purpose Satellite 5, resolution up to 1 m	KARI, Korea
PAZ	Launch scheduled in 2013	X (quad)	Constellation with TerraSAR-X and TanDEM-X planned	CDTI, Spain
ALOS-2	Launch scheduled in 2013	L (quad)	Resolution up to: 1 m × 3 m (azimuth × range), swath width up to 490 km	JAXA, Japan
Sentinel-1a/1b	Launch scheduled in 2013/2015	C (dual)	Constellation of two satellites, swath width up to 400 km	ESA, Europe
Radarsat Constellation-1/2/3	Launch scheduled in 2017	C (dual)	Constellation of three satellites, swath width up to 500 km	CSA, Canada
SAOCOM-1/2	Launch scheduled in 2014-2015	L (quad)	Constellation of two satellites, fully polarimetric	CONAE, Argentina

SOURCE: Fawwaz T. Ulaby and David G. Long, *Microwave Radar and Radiometric Remote Sensing*, University of Michigan Press, Ann Arbor, Mich., 2014; based on Moreira et al., 2013.

that will receive both direct and reflected signals from GPS satellites. In doing so, CYGNSS will measure the ocean surface wind field with high temporal resolution and spatial coverage, under all precipitating conditions and over the full dynamic range of wind speeds experienced in a tropical cyclone, contributing greatly to the improvement of tropical cyclone intensity forecasts. The constellation arrangement will sample the ocean more frequently than a single satellite would be able to, resulting in a highly resolved view of the ocean's surface. The number of observatories and orbital inclination are chosen to optimize the tropical cyclone sampling properties—the result is a dense cross-hatch of sample points on the ground that cover latitudes between ±35 degrees with an average revisit time of 7.0 hours.

GROUND-BASED HF RADARS

The ground-based HF radar is a low-power, chirped, pulse-Doppler radar that measures Bragg scattering from ocean waves in range-gated surface pixels. Since surface gravity waves with wavelengths of 3-30 m are always present on the ocean's surface, Bragg scattering corresponds to frequencies from 3 to 50 MHz. Operational systems typically fall into transmitting frequency categories that include long-range (4-5 MHz and 8 MHz), medium range (11-13 MHz), standard-range (24-26 MHz), and short-range (42-48 MHz). Spatial resolution in the range direction is proportional to the bandwidth of the transmitted signal (e.g., 25 kHz of bandwidth provides radial resolutions of 6 km, and 500 kHz provides resolutions of 250 m), and the azimuthal spatial resolution is governed by the product of the range and the antenna beam width. HF coastal ocean radars are grouped into two classes: direction-finding and phased-array systems. Phased-array systems utilize large multiantenna arrays that synthesize narrow beams, and direction-finding systems utilize wide beam antennas and signal processing algorithms to resolve the azimuthal bearings from the Doppler spectrum of the radar echo.

The operation of the HF radar can be understood by examining the Doppler echo spectrum from a fixed range bin, as shown in Figure 3.8. The largest contribution to the backscattered power (first order return from Bragg resonant waves) is due to scattering from ocean waves whose wavelength is half the wavelength of the radar. In the absence of an ocean surface current, this results in two peaks in the echo power spectrum at ± the frequency of the Bragg wave. Advection of these ocean waves by a surface current produces a Doppler shift in the spectral location of the first-order peaks. Hence, the observed displacement in frequency can be used to infer the radial component of the current along the radar beam propagation direction. Radar returns from the same patch of water using two spatially separated radars enables estimation of the vector current. The Bragg peaks are flanked by a weaker second-order continuum due to double scattering from two freely propagating waves, as well as scattering from nonlinearly bound waves. This continuum

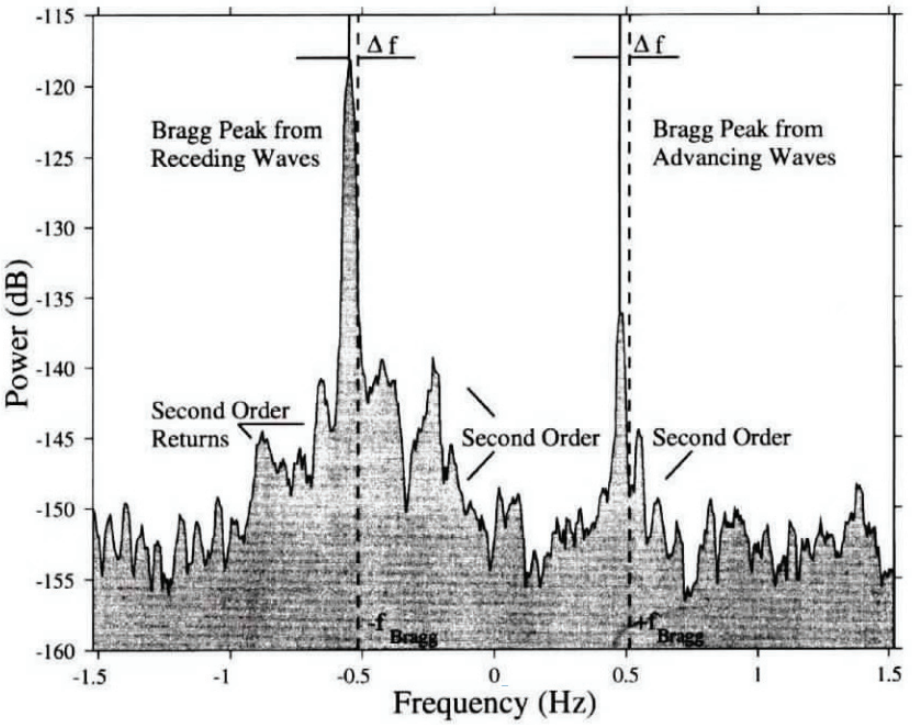

FIGURE 3.8 Example of ocean backscattering Doppler spectrum for a HF radar. Data are for a fixed-range cell with zero ocean surface current. Note that spectral lines occur at ± the Bragg resonant frequency. SOURCE: J.D. Paduan and H.C. Graber, Introduction to high-frequency radar: Reality and myth, *Oceanography* 10(2):36-39, 1997. Courtesy of the Oceanography Society.

contains contributions from all ocean wave components longer than the Bragg waves, and the second-order part of the power spectrum can be inverted to estimate the frequency-direction spectrum of the longer waves[26] and the magnitude and directions of near-surface winds via a wind-wave model.[27]

[26] B.L. Weber and D.E. Barrick, On the nonlinear theory for gravity waves on the ocean's surface. Part I: derivations, *Journal of Physical Oceanography* 7(1):3-10, 1977; L. Wyatt, J. Ledgard, and C.W. Anderson, Maximum-likelihood estimation of the directional distribution of 0.53-Hz ocean waves, *Journal of Atmospheric and Oceanic Technology* 14(3):591-603, 1997.

[27] M.L. Heron and R.J. Rose, On the application of HF ocean radar to the observation of temporal and spatial changes in wind direction, *IEEE Journal of Oceanic Engineering* 11(2):210-218, 1986.

Scientific and Operational Applications

From a scientific perspective, oceanic measurements in the near coastal regions and over the continental shelf are essential for increasing our knowledge about the least observed component of our planetary system—the ocean. The ocean feeds us and provides half our oxygen; it is critical in cycling nutrients, carbon, water, and heat. It regulates our climate. It provides inexpensive transportation of global goods, and it supports economies, from the extractive industries (fisheries, mining, oil and gas) to recreation and tourism.

Further, coastal ocean science aids in decisions about the management of our natural resources, our coastal built environment, and risks/resilience/adaptation in our communities, and it provides important information for making decisions about severe weather events, coastal search and rescue, pollution hazards, and national security. Measuring near-shore and continental shelf ocean currents with high resolution is a high priority for a nation with the majority of its population living within 50 miles of the coast and for the science that is needed to safeguard our ecosystems and our future.

HF radar systems measure large areas of the coastal water, providing excellent maps of surface currents, including both speed and direction. Frequently, HF derived surface current observations are combined with other satellite remote sensing data to examine the coastal ocean in entirely new ways. For example, a collaborative effort among radar operators along the California coast has investigated the utility of combining HF radar with satellite altimetry[28] and NOAA's Advanced Very High Resolution Radiometer (AVHRR) sea surface temperature (SST) imagery to determine the along-shelf wavenumber spectra of surface currents. Results demonstrate that the HF radar observations excelled at producing viable estimates of wave number and frequency spectra of along-shelf velocities, particularly at the important smaller scales where the satellite products become noisy. Also, they showed that HF radar-based currents paired with satellite SST measurements led to observing the spatial structure of complex quantities such as advective heat fluxes at small (1 km) scales within the coastal ocean. From this and other studies it is clear that the HF radar-based surface currents, combined with other remote sensing products such as SST or ocean color, can provide a powerful combined tool for observing the complex circulation present in the coastal ocean and understanding its implications for coastal systems, both natural and anthropogenic.

[28] S.Y. Kim et al., Mapping the U.S. West Coast surface circulation: A multiyear analysis of high-frequency radar observations, *Journal of Geophysical Research* 116(C3), doi 10.1029/2010JC006669, 2011.

RADIO SPECTRUM ISSUES

Radio Frequency Spectrum Characteristics

All of the active remote sensors used for ocean observations are monostatic pulse radars, and, as such, they emit a periodic pulse train of short pulses, each 10^{-3} to 10^{-7} seconds in duration. The radar pulse repetition frequency (PRF) ranges from 10 Hz to 100 KHz, and the duty cycle ranges from 1 percent to 30 percent. For most sensors the spectrum bandwidth is narrow (a few megahertz); however, for altimeters and SARs that use pulse compression, the bandwidths can be hundreds of megahertz. All sensors have a relatively high effective isotropic radiated power (EIRP) that ranges from +40 dBW to +60 dBW.

Possibilities for Spectrum Sharing

Scatterometers

K_u-band scatterometers are long-pulse radars with spinning narrow-beam antennas. Pulse repetition frequencies are generally less than 100 Hz, but the duty cycle can approach 30 percent. The spinning antenna is pointed at a given location for only a few milliseconds. Hence, the probability of a scatterometer interfering with ground or air communications systems is low, so it offers the possibility for spectrum sharing. On the other hand, scatterometers have quite sensitive receivers that can experience interference from ground and airborne communications systems. Because scatterometers make absolute backscatter power measurements, this RF interference (RFI) can be quite degrading and usually results in a loss of data. Fortunately, over the oceans few users share the same frequency bands; however, near the coast significant RFI degradation has been experienced, especially for C-band scatterometers.

C-band scatterometers use range gating and therefore transmit short pulses over nonarticulating fan beam antennas. The PRF is low and the duty cycle is low. However, since the fan beam antennas have very large surface footprints (and there are usually three antennas), the possibility that they will interfere with ground or air communication systems is relatively high for time durations of a few seconds per beam. As was the case for K_u-band scatterometers, these C-band scatterometers also have quite sensitive receivers that can experience interference from terrestrial communications systems; moreover, they operate in the more crowded C-band spectrum region, which have many varied users.

Altimeters

Altimeters are short-pulse radars with very high pulse compression ratios used to achieve nanosecond effective pulse lengths, which means that their spectral width is hundreds of megahertz. The PRFs are in the kilohertz range, the duty cycles are low, and the antennas have narrow beams that point to the nadir. Since these radars average many pulses for range tracking, they are relatively immune to RFI. However they can produce significant interference to ground or air communication systems, but the duration of the interference should last only a few seconds for a given location.

Synthetic Aperture Radars

Because of SAR image processing, SARs are relatively immune to ground-based RFI, except at the L-band. However, since they have broad beam antennas, they have the potential to be significant RFI sources to ground or air communication systems, and the interference could last up to a minute. Further, they frequently employ pulse compression for improved range resolution, which means that their chirp bandwidths are large.

HF/VHF Radar Systems

Since these systems can only operate within the limited HF/VHF range of 3-50 MHz, there needs to be cooperation at the international level to define and protect the spectrum for HF radar operations, and an assessment of the adequacy of the spectrum allocation for future U.S. operational and experimental uses of the technology is needed. At present there is a large installed base of HF/VHF coastal ocean radars in the United States, which are acquired, operated, and maintained almost exclusively by academic researchers for primarily scientific purposes, and the operations of most are subsidized financially by NOAA's Integrated Ocean Observing System (IOOS). Data from the collective system are collated and marketed to users, such as the Coast Guard or other NOAA offices for use in real-time applications. Thus, NOAA-IOOS serves as the present-day coordinating body for HF/VHF radar uses for ocean observations; however, it is crucial that this application be protected by international agreement.

FINDINGS AND RECOMMENDATIONS

Finding 3.1: Ground-based high-frequency coastal ocean radars acquire unique ocean current and wave measurements in the coastal zones. There is a large base of CODARs operated and maintained almost exclusively by academic researchers for

primarily scientific purposes, with most being subsidized financially by NOAA's Integrated Ocean Observing System.

Recommendation 3.1: NOAA should conduct a full assessment of the recent World Radiocommunication Conference 2012 results regarding ground-based high-frequency radars to ensure that the planned build-out needs of the U.S. high-frequency, over-the-horizon radar observing system can be adequately met.

Finding 3.2: CODAR would benefit from allocated bandwidths larger than 25 kHz near 4.438-4.488 MHz.

Recommendation 3.2: The Federal Communications Commission should reinstate an experimental licensing process for coastal ocean dynamics applications radar (CODAR) to allow for future engineering research advances and exploratory science advances.

Finding 3.3: Active microwave sensors provide unique ocean measurements for scientific and operational applications that are vital to the interests of the United States and complementary to passive microwave and visible and infrared sensors.

For nearly four decades, ocean-sensing radar systems have coexisted with the global communications and radar infrastructure. Recently, there have been more instances of RFI to active sensors from communications and navigations systems at the C-band and lower frequencies. So far the degraded sensor performance and loss of data have been manageable over most regions of the world through the application of aggressive RFI mitigation techniques.

Not only are there no viable alternatives to the continuity of active microwave oceanic measurements, but also, emerging requirements for active ocean sensors should be accommodated to allow modest improvements in the capabilities of future systems.

Recommendation 3.3: The Federal Communications Commission and the National Telecommunications and Information Administration should support access to the frequency bands that best support the extraction of ocean-related information from ocean science remote sensing observations.

4

Active Earth Remote Sensing for Land Surface Applications

INTRODUCTION

Active microwave remote sensing has become an essential tool for many science disciplines that seek to observe and understand processes on Earth's land surface. Over the past two decades, over 20 radar missions have been flown by at least 10 international space agencies where the objective was to study and monitor our planet's surface. Because of the recognized value of these measurements and because techniques are ever improving, several nations plan further radar missions to observe the land surface. Many more airborne radar remote sensing instruments have been developed to conduct studies on a regional scale, or as platforms for demonstrating future spaceborne techniques. Active microwave remote sensing has proven valuable across a number of science disciplines and practical applications, including geology, urban planning, agriculture and crop management, forestry and biomass assessment, hydrology and water resource management, weather forecasting, generation of topographic maps, sea ice mapping and glacier studies, earthquake and volcano studies, archaeological investigations, and post-disaster assessment. The unique capabilities and global coverage afforded by spaceborne radar are also making key contributions to understanding the mechanisms of long-term climate change and its impacts. From the standpoint of spectral management, active sensors designed to measure land surface processes routinely utilize a wide range of frequencies.

The first spaceborne synthetic aperture radar (SAR) was flown on the Seasat mission in 1978. The data it returned dramatically indicate the value of radar

remote sensing as a means of characterizing Earth's surface. Active microwave remote sensing offers a number of advantages and unique capabilities in the observation of Earth's surface. As previously mentioned, radar can "see" through clouds and successfully make measurements when the surface is not illuminated by the Sun. Active microwave devices illuminate the surface, and the resultant echoes contain a wealth of information about the terrain that is embedded in the amplitude, delay, Doppler, phase, and polarization characteristics of the reflected signal. Such signal characteristics can be used to obtain a number of important geophysical parameters, which are discussed in the next section.

Different types of radar systems have been used to study the land surface. Some characteristics of each are described at a high level here; several of these sensor types were also described in Chapter 3 in the context of ocean sensing:

- A scatterometer very precisely measures the intensity of the scattered signal scattered from the surface, in terms of the normalized radar cross section (NRCS). As an example, rough surfaces or surfaces with higher backscatter due the volume scattering associated with vegetation will scatter more energy back in the direction of the radar and consequently will appear brighter than smooth surfaces.
- A polarimeter measures the extent to which a surface produces backscatter as a function of polarization. For example, some surfaces may scatter one polarization more strongly than others. Polarimeters also measure the cross-polarized backscatter, or the backscatter component orthogonal to the polarization with which the target was illuminated. Such polarimetric measurements provide another way in which the surface can be characterized. For instance, vegetated surfaces generate a higher cross-polarized backscatter than nonvegetated surfaces.
- A SAR uses the motion of platform on which the radar antenna is mounted, either an aircraft or a spacecraft, to synthesize a much larger effective antenna. This process allows imagery with very high spatial resolution to be obtained. This imagery often has sufficient detail to show ground features on the order of meters, thus making it comparable in resolution to optical sensors. SARs are the dominant form of system for observing land processing.
- Over the past decade, interferometric SAR (InSAR) has matured and become a powerful technique to observe Earth's surface in three dimensions. InSAR is accomplished by observing the same scene from at least two antenna positions in space or time and forming an interferogram. When separated in the cross-track direction, the interferometer can measure topography, and when separated in the along-track direction, it measures the velocity of the surface and targets on the ground. Surface height can

be mapped using topographic InSAR when two antennas observe a scene at (or sufficiently near) the same time. Repeat-pass and differential InSAR represent a category of techniques whereby a location on Earth is observed by a radar at two different times in order to measure the slight changes in the surface over that period. Such systems have demonstrated that motion to within millimeters can be detected, over time periods from days to years, depending on the surface conditions and nature of the surface motion.

- Radar altimeters were discussed at some length in Chapter 3 in the context of ocean surface topography. They can also be used for high accuracy determination of heights over land as well, such as the accumulation of snow and ice in polar regions.
- A radar sounder is used to probe the vertical structure of the sub-surface from an airborne or spaceborne platform. For science applications on Earth, sounders are most often used to probe the interior of ice sheets but can also be used to probe the land subsurface where conditions permit. Ground-penetrating radar (GPR) also uses sounding techniques, but the term usually refers to the case where a sensor is positioned on the surface.

It is important to note that these sensor type designations are not mutually exclusive, and most modern sensors used in land applications have characteristics of more than one type of sensor. For instance, a well-calibrated SAR can function as a high-resolution scatterometer. Scatterometers and SARs typically have multiple polarization channels and thus are also polarimeters while interferometers can be employed as wide-area high-resolution altimeters, and so forth.

The above-described sensor types can also be designed for a wide range of frequencies, depending on what geophysical parameters are to be measured. In general, the lower the frequency, the more penetration into ground, vegetation, or ice. Subsurface sounders consequently operate at frequencies as low as the HF and VHF bands; sensors that probe the ground underneath vegetation typically require the UHF band through the C-band; and measurements that require limited to no penetration typically employ frequencies at the X-band through the K_a-band.

Although the primary focus of this section is the use of radar as a remote sensing tool, it is also important to acknowledge the use of other active techniques that utilize the radio spectrum. Radio ranging between two orbiting satellites is used to precisely measure Earth's gravity field, as is the case with the joint U.S./German Gravity Recovery and Climate Experiment (GRACE). The gravity field contains information on Earth's deep subsurface structure and composition not available by any other means. Such gravity measurements are used in the fields of geodesy, oceanography, seismology, climatology, hydrology, and cryospheric studies. Also, global navigation satellite systems (GNSS) such as GPS provide the means to very precisely locate a point on Earth, and, with differential measurements, allow the

detection of millimetric-scale motions. Consequently, these systems are also highly valuable in the fields of geodesy and seismology. Because these systems use radio frequency methods, they are also susceptible to spectrum concerns such as radio frequency interference (RFI).

Radars are used from both airborne and spaceborne platforms. Airborne radars are operated either as experimental precursors for satellite systems or to augment satellite observations. An example of the latter is NASA's Operation IceBridge, which provides a major survey of Earth's polar ice in both the Arctic and Antarctic oceans. The program, which has been in continuous operation since 2009, generates three-dimensional views of ice sheets, ice shelves, and sea ice. It uses four different airborne radar systems that span in frequency from the VHF band to the K_u-band.

Table 4.1 provides a summary of the currently operating active sensor missions for land applications, and Table 4.2 provides a summary of future such missions.

SCIENCE AND APPLICATIONS OF ACTIVE MICROWAVE REMOTE SENSING OF EARTH'S SURFACE

The Solid Earth: Geology, Geophysics, and Seismology

From the very beginning of the radar remote sensing era, the value of SAR images has been recognized in the field of solid Earth studies.[1] Radar backscatter and polarimetry give insight into the nature of surface materials. Geologists are using radar to map the distribution of different rock types and to understand the history of landform formation and erosion. Radar penetrates vegetation to offer a view of the underlying geological structure, such as the presence of faults or sedimentary strata, which are key features of interest in natural resource exploration. Radar can also penetrate shallow dry surface material to show the underlying rock morphology. Figure 4.1 shows a rather dramatic case of how the early SIR-A radar, operating at the L-band, was able to peer underneath the sand of the Sahara to reveal previously unmapped drainage channels from an earlier, wetter geologic era. This vegetation and surface penetration capability has been applied in the field of archeology as well.

In recent years, the development of powerful interferometric SAR techniques has allowed scientists to study dynamic phenomena associated with the solid Earth, such as those associated with plate tectonics and volcanism.[2] Society's exposure to

[1] C. Elachi, *Spaceborne Radar Remote Sensing: Applications and Techniques*, IEEE Press, New York, N.Y., 1987.

[2] P. Rosen, S. Hensley, I.R. Joughin, F.K. Li, S.N. Madsen, E. Rodriguez, and R.M. Goldstein, Synthetic aperture radar interferometry, *Proceedings of the IEEE* 88(3), 2000.

TABLE 4.1 Current Active Land Applications Satellite Sensor Missions (listed in order of increasing frequency)

Instrument	Frequency band (GHz)	Launch	Description and Comments
SMAP radar[a]	1.26 GHz L-band 1.215-1.30 GHz	January 2015	Makes global measurements of land surface soil moisture and freeze/thaw state; combined with radiometer (1.4 GHz) measurements. (NASA)
ALOS-2 PALSAR-2[b]	1.26 GHz L-band 1.215-1.30 GHz	May 2014	Using L-band synthetic aperture radar, observes forests and land deformation, acquiring image data of the ground surface day and night regardless of the weather. (JAXA)
HJ-1C[c] SAR-S	3.2 GHz S-band 3.1-3.2 GHz	December 2012	Using S-band synthetic aperture radar, detects environment change, climate change observation, soil moisture retrieval, water cycle monitoring. (CAST)
Sentinel-1 (CSAR)[d]	5.4 GHz C-band 5.25-5.57 GHz	May 2013	Using advanced C-band synthetic aperature radar to provide all-weather, day-and-night images of Earth's surface; used to monitor ice loss from ice caps and ice sheets and used to map ground movements related to earthquakes. (ESA)
RISAT-1 C-SAR[e]	5.3 GHz C-band 5.25-5.57 GHz	April 2012	Using C-band SAR to make all-weather as well as day-and-night SAR observation capability in applications such as agriculture, forestry, soil moisture, geology, sea ice, coastal monitoring, object identification, and flood monitoring. (ISRO)
Metop A,B,C ASCAT[f]	5.2 GHz C-band 5.25-5.57 GHz	October 2006	Makes C-band scatterometer measurements of wind speed and direction over the oceans; provide data for ice and land applications, such as sea ice extent, permafrost boundary, desertification. (ESA/EUMETSAT)

continued

TABLE 4.1 Continued

Instrument	Frequency band (GHz)	Launch	Description and Comments
TerraSAR X- SAR[g]	9.65 GHz X-band 9.3-9.9 GHz	June 2007	X-band synthetic aperture radar observation of Earth's surface; for instance, observing vegetation for accurate and up-to-date information about the distribution and composition of, and changes in, types of vegetation forming the basis for many applications; utilizing high spatial resolution. (DLR)
COSMO SkyMed[h]	9.6 GHz X-band 9.3-9.9 GHz	June 2007	Constellation of four satellites for X-band SAR observation of Earth's surface; applications to environment disaster monitoring, observations of oceans and sea coasts, agricultural and forest areas, radar imaging for cartography (ASI)

[a] NASA, "SMAP: Instrument," http://smap.jpl.nasa.gov/observatory/instrument/, accessed June 3, 2015.
[b] JAXA, "Advanced Land Observing Satellite-2 "DAICHI-2" (ALOS-2)," http://global.jaxa.jp/projects/sat/alos2/, accessed June 3, 2015.
[c] Earth Observation Portal, "HJ-1 (Huan Jing-1: Environmental Protection & Disaster Monitoring Constellation)," https://directory.eoportal.org/web/eoportal/satellite-missions/h/hj-1, accessed June 3, 2015.
[d] ESA, "Sentinel-1," https://earth.esa.int/web/guest/missions/esa-operational-eo-missions/sentinel-1, accessed June 3, 2015.
[e] Indian Space Research Organisation, "RISAT-1," http://www.isro.gov.in/Spacecraft/risat-1, accessed June 3, 2015.
[f] CNES, "Jason 1 and 2," http://www.cnes.fr/web/CNES-en/1441-jason.php, accessed June 3, 2015.
[g] DLR, "TerraSAR-X - Germany's radar eye in space," http://www.dlr.de/dlr/en/desktopdefault.aspx/tabid-10377/565_read-436/#/gallery/350, accessed June 3, 2015.
[h] "COSMO-SkyMed Web Site," http://www.cosmo-skymed.it/en/index.htm, accessed June 3, 2015.
NOTE: Acronyms are defined in Appendix D.
SOURCE: Courtesy of Bryan Huneycutt, NASA/JPL.

terrestrial natural hazards is increasing. Large overdue earthquakes will be costly and threaten densely populated regions on the U.S. Western Coast, home to about 50 million people. Volcanic eruptions also endanger many areas of Earth and can disrupt air travel. Radar remote sensing from airborne or spaceborne platforms provides a unique capability for monitoring such hazards. Repeat-pass SAR interferometry is capable of measuring Earth motions at the centimeter or even millimeter level over time, as well as accurately measuring how the land surface

TABLE 4.2 Future Active Land Application Sensing Satellite Missions (listed in order of increasing frequency)[a]

Instrument	Frequency band (GHz)	Planned aunch	Description and Comments
BioMass[b]	0.43 GHz P-band[c]	2018	Measures amount of biomass and forest height will be measured at a resolution of 200 m, and forest disturbances such as clear-cutting at a resolution of 50 m, providing an important tool for sustainable forest management. (ESA)
NI-SAR L-SAR[d]	1.26 GHz L-band 1.215-1.30 GHz (Dual L/S-band)	2020	L-band polarimetric SAR observation and measurements of some of the planet's most complex processes, including ecosystem disturbances, ice-sheet collapse, and natural hazards such as earthquakes, tsunamis, volcanoes and landslides. (NASA/ISRO)
SAOCOM 1A/1B[e]	1.275 GHz L-band 1.215-1.30 GHz	2015/2016	L-band interferometric SAR to obtain soil moisture maps, interferometric topological maps, and to support emergencies. (CONAE)
NI-SAR S-SAR[f]	3.2 GHz S-band 3.1-3.3 GHz (Dual L/S-band)	2020	S-band polarimetric SAR observation and measurements of some of the planet's most complex processes, including ecosystem disturbances, ice-sheet collapse, and natural hazards such as earthquakes, tsunamis, volcanoes and landslides. (NASA/ISRO)
Sentinel 3 SRAL[g]	5.4 GHz C-band 5.25-5.57 GHz (Dual C/K_u-band)	2015	Multimode C/ K_u-band radar; C-band (ionospheric corrections) altimeter mode for ocean surface topography, surface wind speed, surface wave height; and SAR mode for C-band imagery of Earth's surface (ESA)
RadarSAT Constellation Mission (RCM)[h]	5.4 GHz C-band 5.25-5.57 GHz	2018	Constellation of three SARs to improve revisit time over RadarSat 2; main uses in areas of maritime surveillance/ national security and resource management. (CSA)

continued

TABLE 4.2 Continued

Instrument	Frequency band (GHz)	Planned aunch	Description and Comments
Metop-SG-B SCA[i]	5.25 GHz C-band 5.25-5.57 GHz	2022	C-band scatterometer to provide ocean surface wind vectors and land surface soil moisture (ESA/ EUMETSAT)
Paz SAR-X[j]	9.65 GHz X-band 9.3-9.9 GHz	2015	X-band SAR imagery with fine resolution to serve the security and defense needs (INTA)
SCLP X-SAR[k]	9.6 GHz X-band 9.3-9.9 GHz (Dual X/K_u-band)	2030	X-band SAR for the Snow and Cold Land Processes (SCLP) mission to study the hydrology of the snow melting zones. (NASA)
CSG 1/2 SAR[l]	9.6 GHz X-band 9.3-9.9 GHz	2015/ 2016	Constellation of two satellites with X-band SARs as Cosmo-SkyMed Second Generation (CSG) instruments (larger swath and finer spatial and radiometric resolution) (ASI)
Sentinel 3 SRAL[m]	13.6 GHz K_u-band 13.25-13.75 GHz (Dual C/K_u-band)	2015	Multimode C/ K_u-band radar; K_u-band altimeter mode for ocean surface topography, surface wind speed, surface wave height; and SAR mode for K_u-band imagery of Earth's surface (ESA)
Meteor-M SAR[n]	9.6 GHz X-band 9.3-9.9 GHz	2015/ 2016	X-band SAR imagery for observing Earth's surface; monitoring ice fields (RSA)
SCLP K_u-SAR[o]	17.25 GHz K_u-band 17.2-17.3 GHz (Dual X/K_u-band)	2030	K_u-band SAR (the only spaceborne SAR at 17.2 GHz) for the Snow and Cold Land Processes (SCLP) mission to study the hydrology of the snow melting zones. (NASA)
SWOT[p]	35.6 GHz K_a-band 35.5-36.0 GHz	2019	K_a-band interferometric radar to make global survey of Earth's surface water, observe the fine details of the ocean's surface topography, and measure how water bodies change over time. (NASA)

TABLE 4.2 Continued

Instrument	Frequency band (GHz)	Planned aunch	Description and Comments
Signal SAR[q]	35.8 GHz K_a-band 35.5-36.0 GHz	2019	Measures accurately topography and topographic changes associated with mass change or other dynamic effects on glaciers, ice caps and polar ice sheets, complemented with glacier velocity measurements (DLR)

[a] These future missions are a sampling of "potential" future applications that have come to the attention of the ITU-R WP7C, including ones that are just concepts.

[b] ESA, "ESA's Biomass Satellite goes Ahead," February 19, 2015, http://www.esa.int/Our_Activities/Observing_the_Earth/ESA_s_Biomass_satellite_goes_ahead, accessed June 4, 2015.

[c] P. Foster, J. Hartmann, H. Horie, and R. Wylde, "Performance Verification of the 94 GHz Quasi-Optical-Feed for EarthCARE's Cloud Profiling Radar," *Proceedings of the 5th ESA Workshop on Millimeter Wave Technology and Applications and 31st ESA Antenna Workshop*, May 18-20, 2009, Noordwijk, The Netherlands, ESA WPP-300, 2009.

[d] NASA, "NISAR: Technology," http://nisar.jpl.nasa.gov/technology/#, accessed June 4, 2015.

[e] CONAE, "SAOCOM (Satélite Argentino de Observación Con Microondas)," http://www.conae.gov.ar/index.php/english/satellite-missions/saocom/introduction, accessed June 4, 2015.

[f] NASA, "NISAR: Technology," http://nisar.jpl.nasa.gov/technology/#, accessed June 4, 2015.

[g] ESA, "SENTINEL-3 Altimetry: SRAL Instrument," https://sentinel.esa.int/web/sentinel/sentinel-3-altimetry-wiki/-/wiki/Sentinel%20Three%20Altimetry/SRAL+Instrument, accessed June 4, 2015.

[h] Earth Observation Portal, "RCM (RADARSAT Constellation Mission)," https://directory.eoportal.org/web/eoportal/satellite-missions/r/rcm, accessed June 4, 2015.

[i] Earth Observation Portal, "MetOp-SG (MetOp-Second Generation Program)," https://directory.eoportal.org/web/eoportal/satellite-missions/m/metop-sg, accessed June 4, 2015.

[j] Earth Observation Portal, "PAZ SAR satellite mission of Spain," https://directory.eoportal.org/web/eoportal/satellite-missions/p/paz, accessed June 4, 2015.

[k] NASA, "Instrument: SAR-X/Ku," OSCAR, 2014, http://www.wmo-sat.info/oscar/instruments/view/1045.

[l] Earth Observation Portal, "COSMO-SkyMed Second Generation (CSG) Constellation," https://directory.eoportal.org/web/eoportal/satellite-missions/c-missions/cosmo-skymed-second-generation, accessed June 4, 2015.

[m] ESA, "SENTINEL-3 Altimetry: SRAL Instrument," https://sentinel.esa.int/web/sentinel/sentinel-3-altimetry-wiki/-/wiki/Sentinel%20Three%20Altimetry/SRAL+Instrument, accessed June 4, 2015.

[n] Earth Observation Portal, "Meteor-M-1," https://directory.eoportal.org/web/eoportal/satellite-missions/m/meteor-m-1, accessed June 4, 2015.

[o] NASA, "Instrument: SAR-X/Ku," OSCAR, 2014, http://www.wmo-sat.info/oscar/instruments/view/1045.

[p] NASA, "Surface Water & Ocean Topography (SWOT) Mission," https://swot.jpl.nasa.gov/mission/, accessed June 4, 2015.

[q] DLR, "SAR Missions," http://www.dlr.de/hr/en/desktopdefault.aspx/tabid-4622/7621_read-32488/, accessed June 4, 2015.

NOTE: Acronyms are defined in Appendix D.

SOURCE: Courtesy of Bryan Huneycutt, NASA/JPL.

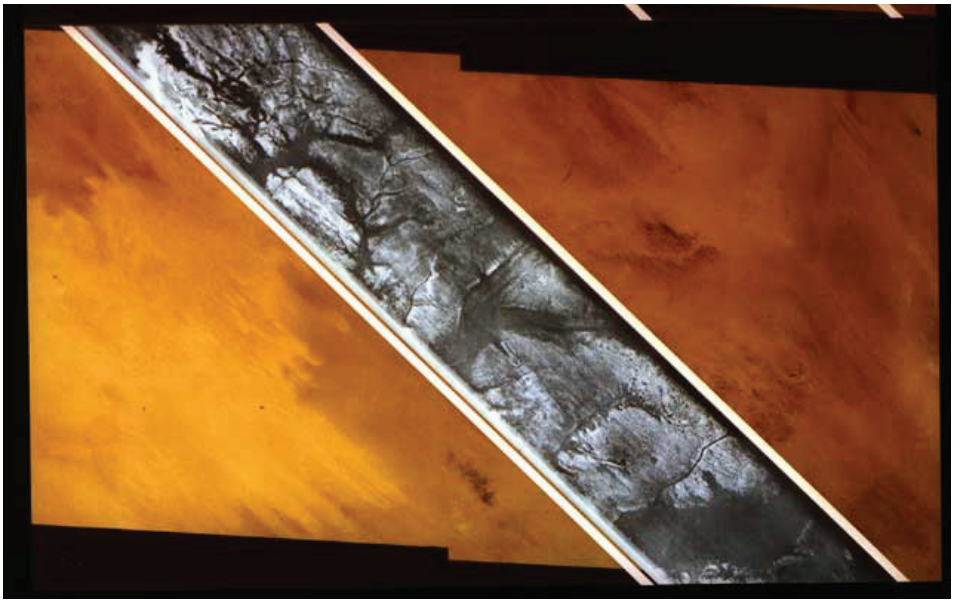

FIGURE 4.1 L-band shuttle imaging radar A (SIR-A) SAR image strip overlaid on optical image of same region in the Sahara. L-band radio waves penetrate the shallow sand to reveal ancient drainage network when the region was much wetter. SOURCE: NASA/JPL; "Shuttle Imaging Radar-A," November 12, 1981, http://www.jpl.nasa.gov/history/index_timeline.htm.

moved after an event. The ground heave and bulging that often precede volcanic eruptions can also be monitored.

Earth deformation measurements have been obtained from space by the European Space Agency's (ESA's) Sentinel satellite (operating at the C-band), the Canadian Space Agency's Radarsat satellites (operating at the C-band), and the Japan Aerospace Exploration Agency PALSAR instrument (operating at the L-band). Currently planned for launch in 2020, the joint NASA/ISRO NISAR mission will operated at the L- and S-bands and is being designed to frequently and consistently monitor all of Earth's major seismic zones. Further, Earth deformation measurements on regional scales and for specific targets of interest have been performed by such sensors as NASA's airborne UAVSAR system (operating at the L-band). Although not a radar remote sensing technique, the use of differential GPS to precisely measure the motion of points on Earth is also critical to the field of seismology. Gravity field measurements made by satellite-to-satellite radio ranging also form a unique data set for the understanding of Earth's deep interior and tectonic processes.

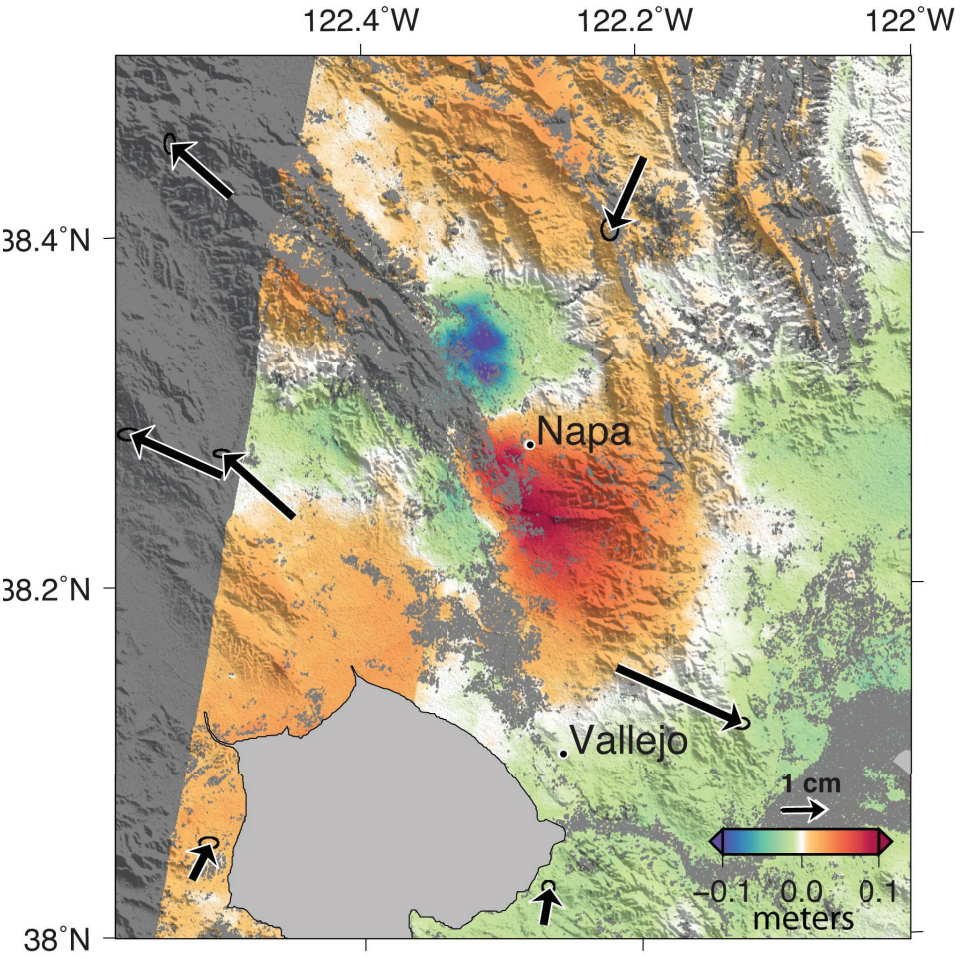

FIGURE 4.2 False color image showing deformation measured from magnitude 6.0 earthquake that struck southern Napa County northeast of San Francisco, California, on August 24, 2014. Repeat-pass interferometric motion data from Italian Space COSMO-SkyMed X-band SAR satellites to calculate a map of the deformation of Earth's surface caused by the earthquake, as shown in this false-color map that has been combined with shaded relief topography (in gray). The red areas south of Napa moved about 10 cm to the east and upward during the earthquake. The dark green and blue areas north of Napa moved about 10 cm to the west and downward due to the earthquake. Black arrows indication motion measured by GPS stations. SOURCE: NASA/JPL-Caltech/ASI/Google Earth, Image PIA18798: NASA Analyses of Global Positioning System Data and Italian Radar Satellite Data Reveal Napa Quake Ground Deformation.

Vegetation: Agriculture, Ecosystems, and Biomass

Radar signals interact with surface vegetation in complex ways. There is varying penetration into the depth of the vegetation cover, depending on the frequency of the radar and the density and water content of the plant matter. The backscattered radar signal is the result of scattering off trunks, stems, and leaves as well as reflections from the ground itself. Particularly when multiple polarizations and phase information are captured, this scattering complexity results in a great richness of information that can be exploited to characterize the vegetation in ways that other sensors cannot. SAR data are used by many nations around the world for agricultural studies and evaluations.[3] Utilizing polarimetry, classification algorithms have been developed to identify the type of crop that is growing, estimate yields, monitor crop health, and aid in the efficient allocation of irrigation resources. Spaceborne radar is also used to study how the expansion of agriculture or urbanization impacts natural ecosystems such as forests and wetlands, the health of which is being increasingly associated with the overall health of the planet.

Deforestation and forest degradation are estimated to account for nearly 20 percent of global greenhouse emissions, more than the global transportation sector and second only to the energy sector.[4] Deforestation and forest degradation contribute to atmospheric greenhouse gas emissions through the combustion of forest biomass, conversion to agricultural or pasture land, logging, and the decomposition of any remaining plant material and soil carbon. It is not well known how Earth's terrestrial biomass is changing and interacting with climate variability. Radar remote sensing provides a means to assess the extent of Earth's biomass over time and is perhaps the most accurate means currently available for estimating global carbon stocks within the above-ground plant matter.[5]

A variety of radar techniques are being employed to assess biomass as well as conduct related measurements of canopy height, vegetation type, and vegetation density. These techniques include polarimetry (Figure 4.3), interferometric height mapping, multiple baseline interferometric tomography, and multifrequency techniques. As an example, the Fugro Earthdata GeoSAR system, designed and built at the Jet Propulsion Laboratory, is able to measure canopy height by comparing simultaneously collected P-band interferometric height data, which penetrates deeply into the vegetation, with X-band interferometric height data, which is more sensitive to the treetops. The difference in these heights is related to the overall

[3] Government of Canada, *Report on International GEO Workshop on Synthetic Aperture Radar (SAR) to Support Agricultural Monitoring*, November 2-4, Alberta, Canada, 2010.

[4] G.R. van der Werf, D.C. Morton, R.S. DeFries, J.G.J. Olivier, P.S. Kasibhatla, R.B. Jackson, G.J. Collatz, and J.T. Randerson, CO_2 emissions from forest loss, *Nature Geoscience* 2:737-738, 2009.

[5] National Research Council, *Earth Science and Applications from Space: National Imperatives for the Next Decade and Beyond*, The National Academies Press, Washington, D.C., 2007.

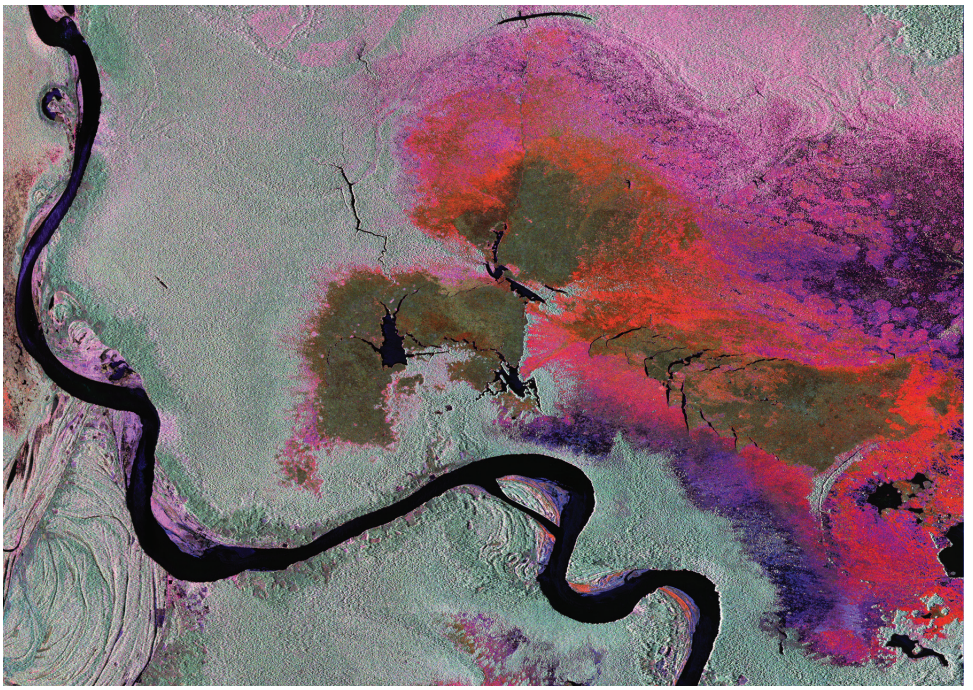

FIGURE 4.3 Polarimetric SAR image of Peru's Pacaya-Samiria National Reserve, measured by NASA's L-band UAVSAR March 17, 2013. Areas by color: black is open water, grayish-green is tropical forest, dark green is low vegetation, perhaps floating vegetation, while red and pink are two different types of inundated vegetation. SOURCE: NASA/JPL; Polarmetric SAR image (channels: HH HV VV) of Peru's Pacaya-Samiria National Reserve (March 17, 2013), http://uavsar.jpl.nasa.gov/education/postcards.html.

heights of the trees. ESA is planning the P-band BIOMASS satellite mission and NASA/ISRO is planning the L-band/S-band NISAR satellite mission. Both are currently planning for launch in 2020 and have global biomass estimation and ecosystem characterization as key science objectives.

Land Surface Hydrology

Terrestrial freshwater is obviously essential to human activity, and there is strong interest in managing this critical resource more effectively. The science of hydrology seeks to understand the movement, distribution, and quality of water on Earth. There is a strong interest in understanding and predicting the conditions that lead to drought, particularly in light of climate change, as well as predicting

extreme events such as floods. In addition to its roles as resource and hazard, water is also important in Earth's climate system.

Land water can exist as surface water bodies such as lakes and rivers, reside in the soil as moisture or permafrost, flow as ground water in aquifers, or rest on top of the surface as snow or ice. In situ methods are often inadequate to characterize the amount and extent of water over broad areas. Consequently, active remote sensing techniques from airborne or spaceborne platforms are a valuable and reliable means to measure water in its various forms over local, regional, or global scales.

Soil Moisture

Soil moisture measurements are used globally for a wide range of applications in hydrology, agriculture, climate monitoring, weather forecasting, and disaster mitigation (including risk forecasting of landslides and flood runoff). An additional application is in the assessment of trafficability of vehicles for defense purposes.

> Soil moisture is also a key control on evaporation and transpiration at the land-atmosphere boundary. Since large amounts of energy are required to vaporize water, soil moisture control also has a significant impact on the surface energy flux. Thus, soil moisture variations affect the evolution of weather and climate particularly over continental regions.[6]

Radar is a demonstrated means of measuring soil moisture because the measured backscatter cross section is a strong and characterizable function of the amount of water in the soil.[7] Further, by means of synthetic aperture processing, soil moisture can be retrieved at high spatial resolution. Relatively low frequencies (primarily the UHF and L-bands, but also the C-band for some applications) are typically utilized for soil moisture measurements because they are able to penetrate vegetation cover and, to varying extents, into the soil itself.

The ESA/EUMETSAT ASCAT C-band scatterometer is being employed to derive a global soil moisture index at coarse resolution globally (Figure 4.4). NASA has developed the Soil Moisture Active Passive (SMAP) mission, scheduled for launch in early 2015. This sensor will employ both radar and radiometer channels at the L-band in order to produce a global soil moisture product at medium resolution. In addition to soil moisture, the SMAP radar will detect whether or not the soil is frozen at high latitudes. The freeze/thaw data are anticipated to become an

[6] SMAP website, http://smap.jpl.nasa.gov/science/, accessed November 25, 2014.

[7] K.C. Kornelsen and P. Coulibaly, Advances in soil moisture retrieval from synthetic aperture radar and hydrological applications, *Journal of Hydrology* 476L:460-489, 2013; D. Entekhabi, E.G. Njoku, P.E. O'Neill, K.H. Kellogg, W.T. Crow, W.N. Edelstein, J.K. Entin, S.D. Goodman, T.J. Jackson, J. Johnson, J. Kimball, et al., The Soil Moisture Active Passive (SMAP) Mission, *Proceedings of the IEEE* 98(5):704-716, 2010.

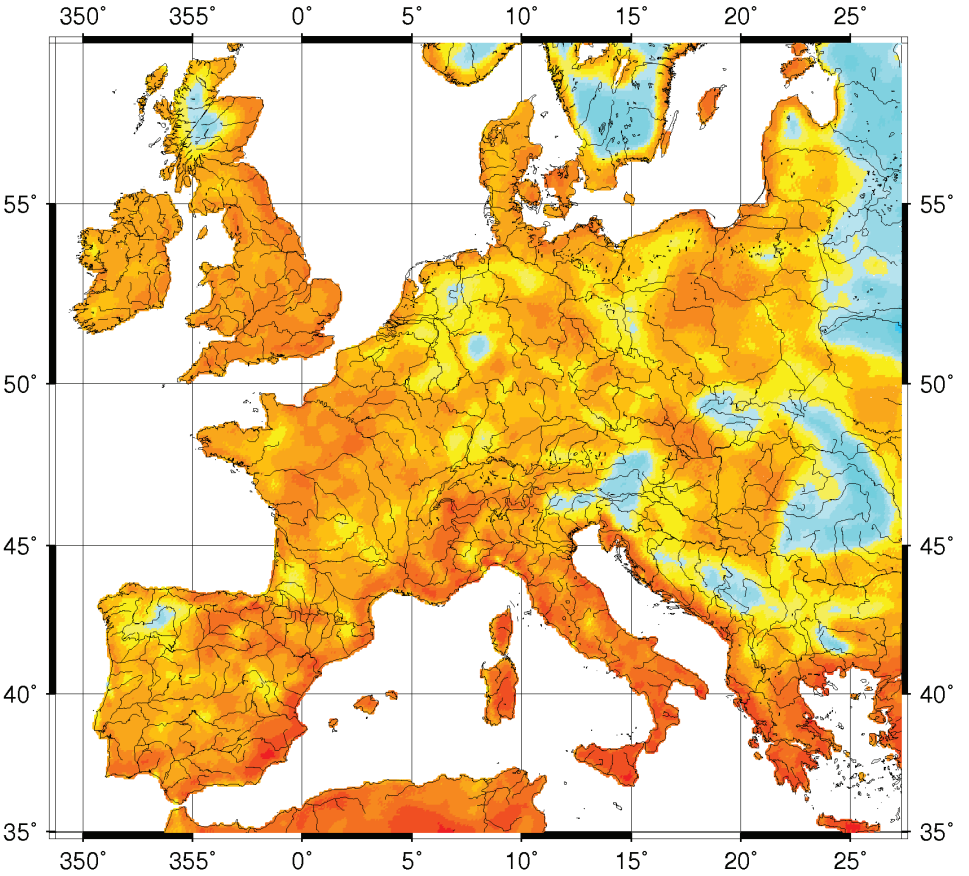

FIGURE 4.4 ASCAT C-band scatterometer derived measurements of soil wetness (expressed as percentage saturation) for the unusually dry European Spring in 2011. SOURCE: EUMETSAT; Metop-A, ASCAT, 15-27 May 2011 UTC Surface Soil Moisture Product (7.5 km^2 box averages).

important scientific predictor of the potential release of methane through anaerobic decomposition of the organic matter stores that have accumulated in boreal arctic tundra over many millions of years. The rapid release of methane from such stores is thought to have serious additional global warming potential. As another example, the Argentine SAOCOM mission, to be launched in 2015, is an L-band polarimetric SAR for which one primary measurement is the regular production of high-resolution soil moisture maps in agricultural regions of significant national interest, such as the pampas. Several other current and planned spaceborne radar missions have soil moisture as one of their measurement objectives. Further, there

are multiple airborne sensors (such as NASA's UAVSAR and PALS instruments) that also are tasked to measure soil moisture.

Although the most commonly used frequency of the L-band can accurately measure soil moisture within a few centimeters of the surface, there is also the scientific need to measure moisture at greater depths. The newly deployed NASA AirMOSS instrument is an airborne SAR operating at the UHF band that measures soil moisture in the "root zone" at greater depths. Root-zone soil moisture impacts carbon uptake because plant roots need water for activating photosynthesis. Root zone soil moisture also impacts carbon release through the respiration processes, where vegetation and organisms in soil consume available organic matter and release CO_2 to the atmosphere.

Surface Water

Observations of the temporal and spatial variations of water stored in rivers, lakes, and wetlands are extremely important to life on the planet, including human life. However, the current understanding of the dynamics of terrestrial surface waters and their interactions with coastal oceans and estuaries is still limited. Radar is able to (1) identify the existence and boundaries of surface water because its backscattering characteristics are distinctly different from that of dry land, and (2) is also capable of determining the level of water bodies to an accuracy of centimeters using interferometric techniques.[8]

The global mapping of surface water dynamics is one of the main objectives of the joint NASA/CNES Surface Water Ocean Topography (SWOT) mission scheduled for launch in 2020. SWOT will employ a near nadir-looking K_a-band interferometric SAR to measure the surface of water bodies. The system will produce water maps which resolve rivers 100 meters wide, lakes 250 m^2 in area, wetlands, and reservoirs, with a water level accuracy of 10 cm. With these capabilities SWOT will contribute to a fundamental understanding of the terrestrial branch of the global water cycle by measuring water storage changes in all wetlands, lakes, and reservoirs, and also by more accurately estimating discharge in rivers.

Groundwater

In many parts of the world rainfall and surface water cannot satisfy the growing demands of the people who live in those regions. Pumping groundwater from subsurface aquifers is therefore relied upon for urban and agricultural needs. Unfortunately, climate change and growing populations are causing increasing stress on

[8] D.E. Alsdorf, E, Rodriguez, and D.P. Lettenmaier, Measuring surface water from space, *Reviews of Geophysics* 45(2), 2007.

groundwater resources around the world. Active remote sensing by airborne or spaceborne radar offer one means of understanding and monitoring groundwater resources.[9] When the surface soil cover is sufficiently dry, radar sounders operating at HF and VHF frequencies can be used to penetrate below the surface and directly observe the extent and dynamics of shallow (<100 m) aquifers. Another technique used to monitor the depletion of aquifers is the observation of surface subsidence via repeat-pass interferometric radar (Figure 4.5). As underground water is depleted, the earth slowly collapses into the cavity that is formed, which is manifested on the surface as a gradual subsidence. Interferometric radar is a unique technique to detect this very subtle lowering of Earth's surface—typically on the order of centimeters—over very wide areas, and has been successfully carried out with several airborne and spaceborne sensors. This technique has been employed extensively from space by the European C-band Envisat and Sentinal-1A systems, and the Japanese L-band PALSAR systems. The joint NASA/ISRO L-band SAR mission (NISAR) is scheduled to launch in 2020 and also has the regular monitoring of aquifer related subsidence as one of its key science objectives. Finally, while not a radar and perhaps not as susceptible to spectrum issues, satellite-to-satellite radio ranging is another indispensable tool to infer groundwater dynamics.

Snow

Measurements of snowpack extent and snow water equivalent (SWE) are critical for water management in many regions, particularly in the Western United States, melt runoff and river height forecasting, and avalanche control and avalanche risk forecasting. Snowpacks also have a big impact on weather and climate by virtue of their high reflectivity and thermally insulating properties, on ecosystems, groundwater uptake, civil and defense trafficability, and heating/cooling needs. Snowpack runoff supplies a large fraction (up to ~80 percent) of the year-round freshwater needs for agricultural and municipal use. Radar imagery from polarimetric SARs or scatterometers operating from the L-band to the K_u-band provide the ability to measure snow over a broad area. Radar sounders operating at the K_u-band have been able to measure snow depth and stratigraphy over ice sheets.[10] In addition to being able to make all-weather measurements through clouds, microwave sensors are able to penetrate into the snow, and thus yield information about snow density, which is directly related to the amount of liquid water produced upon melting. In

[9] D.L. Galloway, K.W. Hudnut, S.E. Ingebritsen, S.P. Phillips, G. Peltzer, F. Rogez, and P.A. Rosen, Detection of aquifer system compaction and land subsidence using interferometric synthetic aperture radar, Antelope Valley, Mohave Desert, California, *Water Resources Research* 34(10):2573-2585, October 1998.

[10] ESA, *CoReH2O: An Earth Explorer to Observe Snow and Ice, Report for Mission Selection*, European Space Agency Productions, Paris, France, 2012.

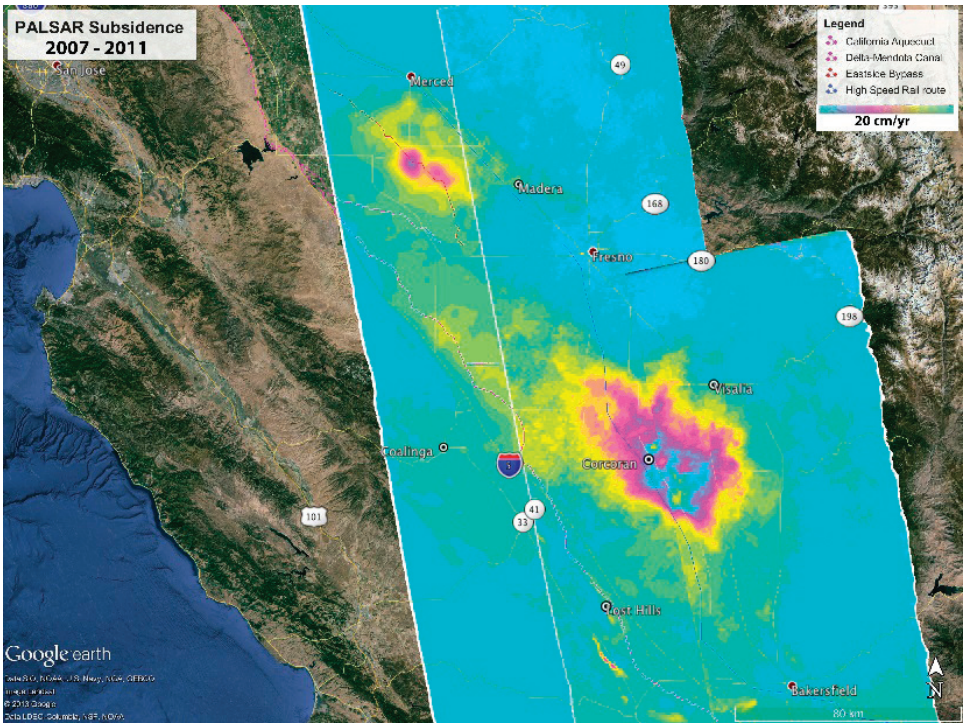

FIGURE 4.5 Subsidence rates in California's southern Central Valley from 2007 to 2011 as measured by Japan's Advanced Land Observing Satellite SAR instrument using repeat-pass interferometry. One full cycle of the color bar equals 20 cm (about 8 in,) per year. NASA is using space-based radar data to monitor groundwater in California. SOURCE: NASA/JPL-Caltech/JAXA/Google Earth, "NASA Responds to California's Evolving Drought," News, February 25, 2014, http://www.jpl.nasa.gov/news/news.php?feature=4057.

addition to sensors already operating, the NRC Earth science decadal survey has called for the development of a dedicated space mission to address snow.[11]

The Cryosphere

The cryosphere covers portions of Earth's surface where water is in solid form, including sea ice, ice sheets, and glaciers. Diminishing glaciers and sea ice are considered by scientists to be an early indicator of global warming. Satellite observations collected over the past three decades show that the summer sea ice

[11] National Research Council, *Earth Science and Applications from Space*, 2007.

cover is decreasing drastically, and ice sheets and glaciers are already melting fast enough to be the largest contributors to sea level rise, with a potential to raise sea level by several tens of centimeters or more in the coming century. The loss of sea ice cover will have a profound effect on life, climate, and commercial activities in the Arctic, while the loss of land ice will impact an important source of water for millions of people. Collectively, these effects mean that despite its remote location, changes in ice have global economic and health implications as climate changes. Accurate projection of the sea level would improve planning of sea walls, dikes, and other mitigation strategies. Largely because of its remote locations and its persistent cloud cover and lack of winter sunlight, active microwave sensors have become a key means of monitoring the cryosphere.

Sea Ice

Due to the strong contrast between backscatter over open water and over sea ice, SARs operating at the L-, C-, and X-bands are especially useful for tracking sea ice floes and estimating the extent and age of the sea ice cover. Radars are particularly adept at differentiating first year ice from multi-year ice conglomerations.[12] End-user applications include monitoring shipping lanes at high latitudes and studying polar climate change, using, for example, the RadarSat or EnviSat series of C-band spaceborne SARs or at the L-band using the Japanese ALOS PALSAR. Combining sea ice extent mapping with radar altimetry provides a means for determining sea ice elevation—also known as freeboard height—and, in turn, sea ice thickness. Sea ice freeboard has been measured using the Cryosat-2 radar altimeter at the K_u-band (Figure 4.6).

Ice Sheets and Glaciers

Earth's two great permanent ice sheets lie over Antarctica and Greenland. The "mass balance" of these ice sheets is the extent to which they are either losing or accumulating new ice. Radar altimeters, such as Cryosat-2, monitor the overall thickness of the ice sheet. The movement and melting of glaciers is the key mechanism for ice sheet mass loss. SAR can not only image the extent of glaciers but can also determine flow speeds of glacier ice by feature tracking over time or by detecting movement directly with repeat-pass interferometry.[13] The penetrative capability of low-frequency radar sounders is utilized to probe the vertical structure of glaciers and ice sheets all the way down to the solid rock base. The

[12] W. Dierking, Sea ice monitoring by synthetic aperture radar, *Oceanography* 26(2):100-111, 2013.

[13] I. Joughin, B.E. Smith, and W. Abdalati, Glaciological advances made with interferometric synthetic aperture radar, *Journal of Glaciology* 56(200):1026-1042, 2010.

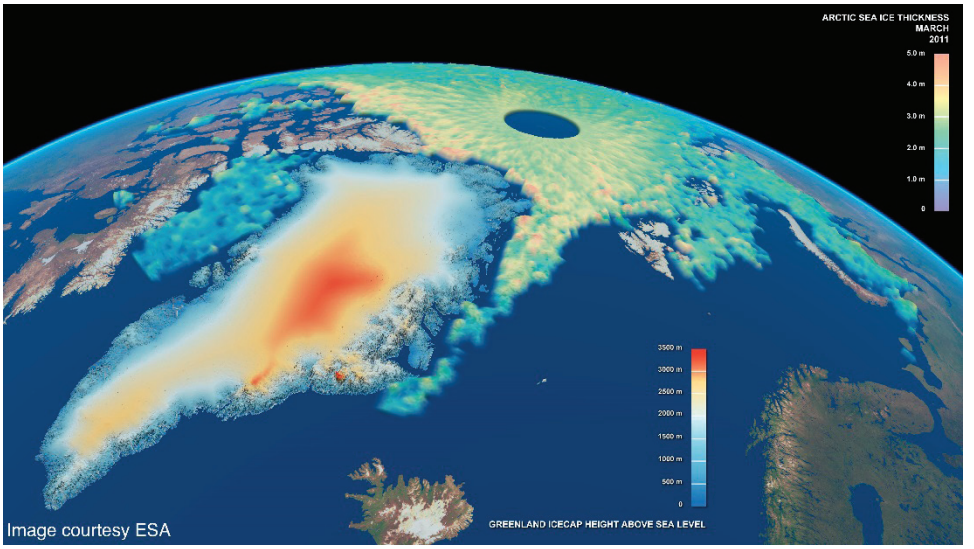

FIGURE 4.6 This map shows Arctic sea ice thickness, as well as the elevation of the Greenland ice sheet, for March 2011. The data come from the European Space Agency CryoSat-2 satellite utilizing a K_u-band altimeter. For the sea ice, green shades indicate thinner ice, while the yellows and oranges indicate thicker ice. SOURCE: Courtesy of Planetary Visions/CPOM/UCL/ESA.

basal structure of glaciers is key to understanding how glaciers move and how the melting mechanisms function. Scatterometers, with their wide area coverage and frequent revisit time, can catch the presence of rapid surface melt events on ice sheets. Finally, gravity field measurements made using satellite-to-satellite radio ranging can yield critical insight into the bulk mass dynamics associated with Earth's ice sheets.

Topographic Mapping

Accurate topographic maps of Earth's surface are essential to many terrestrial science investigations and civil applications. These include watershed delineation for hydrological studies and flood risk mapping, public works planning, forestry and timber management, natural resource exploration, and national security. Interferometric SAR provides a means to generate highly accurate digital elevation models (DEMs) under all weather and lighting conditions.[14] Using this technique,

[14] P. Rosen, S. Hensley, I.R. Joughin, F.K. Li, S.N. Madsen, E. Rodriguez, and R.M. Goldstein, Synthetic aperture radar interferometry, *Proceedings of the IEEE* 88(3), 2000.

multiple SAR images are acquired from two antennas separated in space but as simultaneous as possible. The observed phase difference between these two images is utilized to calculate the vertical height at each point in the scene.

The Shuttle Radar Topography Mission (SRTM) utilized a dual-antenna C-band interferometer that flew aboard the space shuttle *Endeavor* in February 2000. SRTM generated elevation data on a near-global scale and have become widely used by many different research communities. Whereas SRTM utilized two antennas separated by a baseline flying on the same platform, spaceborne DEM work has continued, with free-flying antennas on individual satellites. An example is the DLR X-band TerraSAR-X and TanDEM-X satellites flying in formation (Figure 4.7). These satellites have achieved a global height precision of 2 m at horizontal spacing of approximately 12 m. Airborne SAR interferometers also continue to generate DEMs for special targets at a local and regional scale. The Fugro Earthdata GeoSAR system is dual sided and has a single-pass X-band interferometer and a single-pass UHF interferometer operating simultaneously for two-frequency, two-sided data collection. In vegetated areas, the UHF data can penetrate to near the surface to get ground-level topography, whereas the X-band sensor yields heights higher up in the canopy.

Other Applications: Urban Planning, Disaster Management

The availability of high-resolution SAR imagery has enabled advances in urban planning and land-use management efforts. Information on land use and land cover is an important element in formulating policies on economic, demographic, and environmental issues at the national, regional, and global levels. Mapping land use near the borders of urban areas in a timely and accurate manner is thus of great importance for urban planning, land-use planning, and conservation and management of land resources.[15]

In addition to earthquakes and volcanoes, discussed in the Introduction, SAR interferometry is being used to measure deformation and predict the hazards associated with sinkholes and manmade levies and dams. Regardless of the cause, once a disaster occurs, it is imperative that the extent of the damage be quickly evaluated so that relief efforts can proceed in the most efficient fashion. Again, SAR repeat-pass measurements offer a unique capability to assess the extent of destruction from earthquakes, tsunamis, hurricanes, and floods.[16] When two successive radar images

[15] J. Manoj, S.R. Subramoniam, K.S. Srinivasan, S. Pathak, and J.R. Sharma, Class separability analysis and classifier comparison using quad-polarization radar imagery, *Journal of the Indian Society of Remote Sensing* 41(1):177-182, 2013.

[16] R.J. Dekker, High resolution radar damage assessment after the earthquake in Haiti on 12 January 2010, *IEEE Journal of Selected Topics in Applied Earth Observations and Remote Sensing* 4(4), 2011.

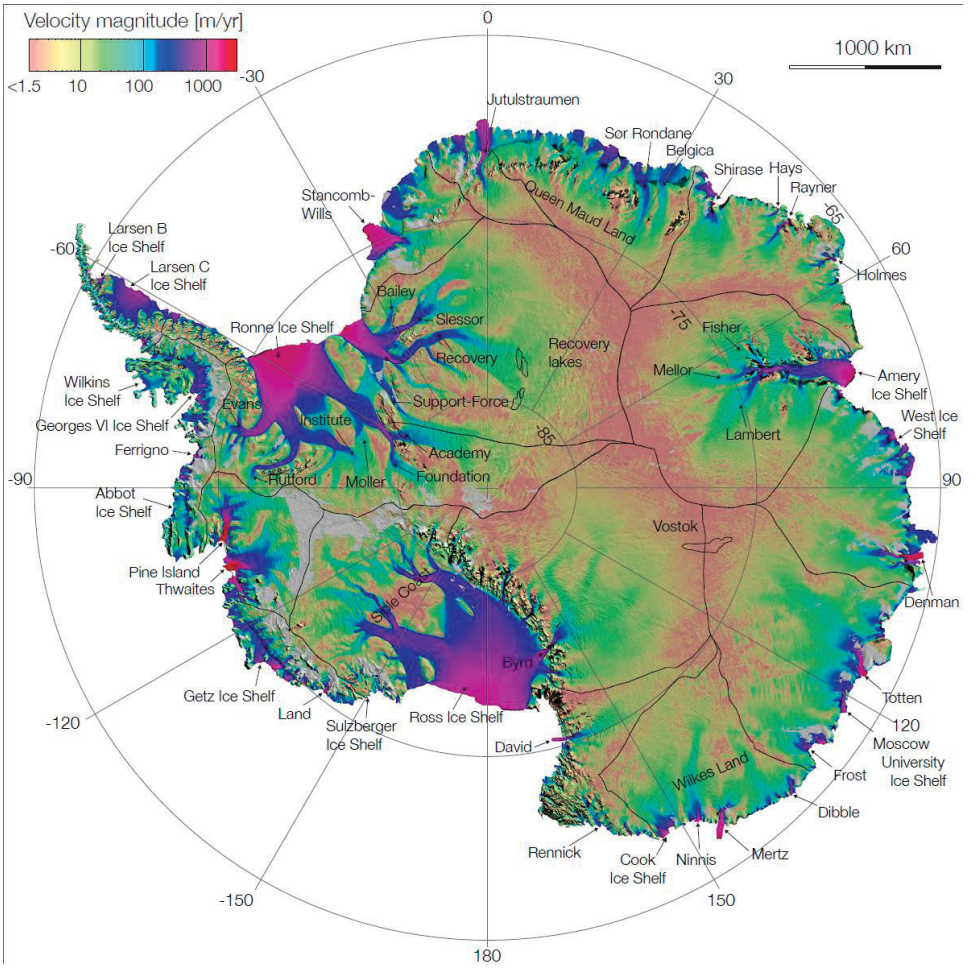

FIGURE 4.7 Velocity of ice flow in Antarctica, derived from radar interferometric data from JAXA's ALOS PALSAR, ESA's Envisat ASAR and ERS-1/2, and CSA's RADARSAT-2 spacecraft. The black lines delineate major ice divides. The grey areas indicate regions where no data was taken. SOURCE: E. Rignot, J. Mouginot, and B. Scheuchl, "MEaSUREs InSAR-Based Antarctica Ice Velocity Map," Sample Data Image, NASA DAAC, National Snow and Ice Data Center, Boulder, Colo., 2011, http://dx.doi.org/10.5067/MEASURES/CRYOSPHERE/nsidc-0484.001. See J. Mouginot, B. Scheuchl, and E. Rignot, Ice flow of the Antarctic ice sheet, *Science* 333(6048):1427-1430, 2011.

of the impacted zone are compared—one before the disaster and the other collected as soon after the disaster as possible—change detection algorithms can be applied to identify such events as collapsed structures or inundated areas. Assessments have been successfully employed for several high-profile recent disasters using a variety of spaceborne SAR assets, including the Christchurch, New Zealand, earthquake in

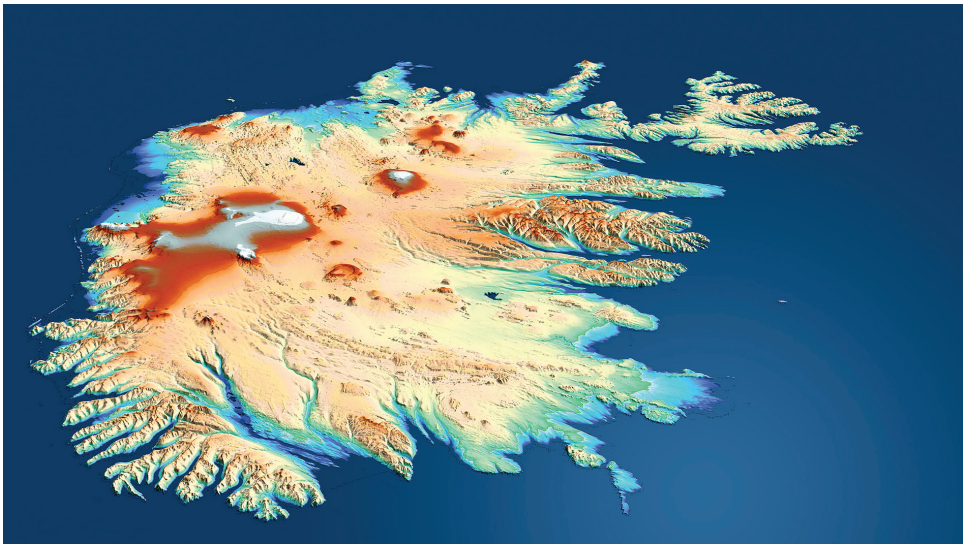

FIGURE 4.8 TanDEM-X topographic mosaic map of Iceland. SOURCE: Courtesy of DLR (The German Space Center); "A Step Closer to Mapping the Earth in 3D," News, January 13, 2012, http://www.dlr.de/dlr/en/desktopdefault.aspx/tabid-10081/year-2012/.

2011, the Tohoku, Japan, earthquake and tsunami in 2011, superstorm Sandy on the U.S. East Coast in 2012, and super-typhoon Hainan in the Philippines in 2013.

As examples, the analyses shown in Figures 4.2 and 4.5 demonstrate how non-U.S. assets were utilized to address land surface processes of intense interest within the borders of the United States; Figures 4.8 and 4.9 indicate how U.S. capabilities are being combined with data from non-U.S. programs to address global concerns.

SPECTRUM ISSUES FOR MICROWAVE REMOTE SENSING OF THE LAND SURFACE

For the broad variety of applications discussed in the earlier sections of this chapter, microwave remote sensing of the land surface requires the use of a wide range of frequencies. The HF, VHF, UHF, L-, S-, C-, X-, K_u-, and K_a-bands are all currently in use. Cases where scientists have either had difficulty accessing bands due to transmit restrictions or experienced extreme interference due to other radio services are discussed in detail in Chapter 7. For researchers involved in land remote sensing, the main spectrum issues may be summarized as follows:

FIGURE 4.9 Interferometric "change map" derived from Italian Space Agency Cosmo-Skymed radar depicting damage done by Supertyphoon Haiyan in the Philippines, November 8, 2013. Areas in red reflect the heaviest damage to cities and towns in the storm's path. SOURCE: ASI/NASA/JPL-Caltech. See NASA, "NASA Damage Map Helps in Typhoon Disaster Response," November 13, 2013, http://www.nasa.gov/centers/jpl/news/typhoon20131113.html#.VZ15xvlVhBf.

- There is currently no HF or VHF spectrum allocation for Earth science remote sensing from space. This will be a region of intense interest for subsurface sounders in the future.
- There is a UHF allocation for spaceborne remote sensing, but it is a secondary allocation. This is proving to be a difficult band to use due to transmit restrictions. The ESA BIOMASS mission, which will operate at the UHF band, has been denied permission to radiate over much of North America and Europe because of perceived interference with the U.S. Department of

Defense's (DOD's) Space Object Tracking Radar (SOTR) system. Wider-band airborne instruments operating at the UHF band apply to use radiolocation bands but are also subject to severe geographical and spectral restrictions.

- There has been increased incidence of RFI at the L-band over the last decade. This has spawned the development of interference mitigation techniques, which are thus far successful. Transmit restrictions have also increased at the L-band, occasionally resulting in requirements for expensive design features.
- There is a strong concern that new commercial Radio Local Access Network (RLAN) services proposed by industry at the C-band will severely impact current and planned SAR systems operating in that region of the spectrum.
- Non-radar techniques—such as satellite-to-satellite radio ranging for gravity field measurements and differential GPS for the detection of surface motion—are also susceptible to spectrum concerns such as RFI. In 2011, many in the Earth science community (along with other users) weighed in heavily against a broadband service proposal that threatened to cause significant interference in the GPS spectrum. From a regulatory perspective, these techniques may occupy a gray area between Earth remote sensing and radiolocation, but they nevertheless represent key measurements that warrant vigilance from the science community.

Radar measurement techniques are always advancing in order to meet growing science needs. In general, the more bandwidth a radar transmits, the better the spatial resolution and accuracy associated with the land surface phenomena being measured. An explicit proposal for an expansion of the X-band allocation is expected at the ITU World Radiocommunication Conference in late 2015. Bandwidth expansions of the allocations at several other bands are also being explored.

FINDINGS AND RECOMMENDATIONS

Finding 4.1: Radar remote sensing of the global environment is becoming an increasingly international collaborative endeavor. Data from each country's programs are being used by other countries' scientists in order to address regional and global issues.

Finding 4.2: Active microwave remote sensing of the land has proven valuable across a number of science disciplines and practical applications, including geology, urban planning, agriculture and crop management, forestry and biomass assessment, hydrology and water resource management, weather forecasting, generation

of topographic maps, sea ice mapping and glacier studies, earthquake and volcano studies, archaeological investigations, and postdisaster assessment.

Recommendation 4.1: The Office of Science and Technology Policy should adjudicate the possibility of time and frequency sharing between ESA BIOMASS and the U.S. DOD SOTR system.

Recommendation 4.2: Spectrum usage by active airborne remote sensing platforms and airborne test beds is inherently very sparse in both time and space, amounting to a few dozen to a few hundred hours of on-time per year, with the maximal spatial extent typically less than 50 km from the illumination point. Special consideration should be given to accommodating these few but important low usage systems.

Recommendation 4.3: The current frequency allocations for active remote sensing for land applications should be preserved and strongly protected to ensure their continued contribution to the nation and to scientists' understanding of Earth and its processes.

5

Active Earth Remote Sensing for Space Physics

INTRODUCTION

Space physics is a broad discipline that encompasses studies of magnetospheric physics, ionospheric/thermospheric physics, and space weather; it also overlaps with the discipline of radio science. Space physics active remote sensing primarily consists of ground-based radars making observations of the ionospheric plasma, but has application in each of the areas.

Ionospheric studies using radio transmitters date to the early part of the last century and are intimately tied to the early development of radio communications. Marconi's early attempts at long-distance radio transmissions suggested the presence of a reflecting layer in the upper atmosphere,[1] which was published nearly simultaneously by Arthur Kennelly and Oliver Heaviside in 1902. The suggestion was confirmed experimentally in 1924 through the experiments of Appleton[2] and his succeeding work, for which he was awarded the Nobel Prize in 1947. In those experiments, Appleton observed the fading of radio signals received from a distant transmitter and concluded that the fading was caused by interference of signals arriving at the receiver by two paths: one path directly along the ground, and the other via reflection from the ionosphere. Through these experiments, active remote sensing of the ionosphere using radio waves was born. While ionospheric studies

[1] P.J. Nahin, *Oliver Heaviside: The Life, Work, and Times of an Electrical Genius of the Victorian Age*, JHU Press, Baltimore, Md., 2002, p. 13.

[2] E.V. Appleton and M.A.F. Barnett, On some direct evidence for downward atmospheric reflection of electric rays, *Proceedings of the Royal Society of London A* 109, doi:10.1098/rspa.1925.0149, 1925.

have a long history, they remain relevant today. Increasing reliance on satellites for communication and navigation—global positioning systems (GPS) and global navigation satellite systems (GNSS)—means that ionospheric impacts on these signals has an increasing societal impact. Ionospheric studies help us to understand these impacts and potentially how to mitigate them.

Space physics active remote sensing focuses on observations of the ionosphere because physical limitations hinder observations of either the magnetosphere or the thermosphere. Radio waves reflect from discontinuities in the index of refraction of the medium in which they propagate. In the upper atmosphere the primary source of such discontinuities is gradients of the plasma density. Hence, upper atmospheric active remote sensing is primarily sensing of the ionospheric plasma. It is, however, possible to study both the magnetosphere and the neutral atmosphere using those ionospheric observations. Ion-neutral collisions produce measurable effects in radar returns. At altitudes where those effects are significant, it is possible to estimate thermospheric properties from the plasma observations. Magnetospheric research using ionospheric observations is made possible by the high conductivity of the magnetic field lines that connect the two regions (Figure 5.1). Because of the high conductivity, the field lines are nearly equipotentials, which means that the structure of the electric fields in the magnetosphere continues into the ionosphere. Further, the magnetosphere is the source of the energetic particle precipitation that influences the ionosphere. By observing the fields and particles in the ionosphere, a great deal of information can be gained about the magnetosphere.

The relatively low plasma densities in the magnetosphere require the electromagnetic waves used for direct sensing to be in the VLF and ELF bands. Such low frequencies are difficult to generate and cannot reliably penetrate the ionosphere, so their use for magnetospheric observations from the ground has been fairly limited. There have been a few space-based missions that used such low-frequency transmission for observation of the magnetospheric plasma. However, since those transmissions do not penetrate the ionosphere and they do not reach the ground, they neither suffer nor cause interference from or to terrestrial sources and therefore are not germane to this report.

In order to provide the reader with background to understand the application of active remote sensing to space physics, this chapter begins with a discussion of the scientific disciplines. The discussion begins with the ionosphere/thermosphere, followed by the magnetosphere, radio science, and, finally, space weather. In each section, a general background is provided along with some pertinent issues to which active remote sensing is applied. Following the scientific background, spectrum usage is discussed beginning with the lowest active remote sensing frequencies

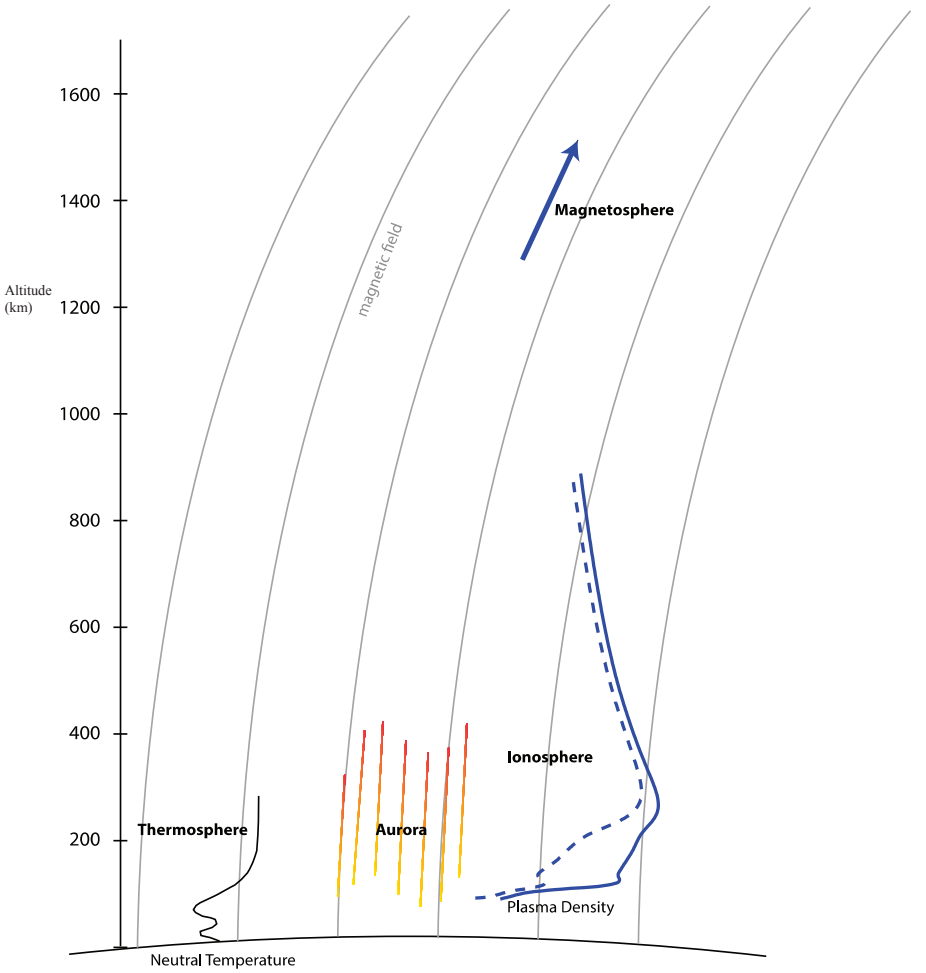

FIGURE 5.1 Approximate altitude ranges of the ionosphere, thermosphere, and base of the magnetosphere. The neutral temperature and plasma density profiles (solid, day; dashed, night) are representative of typical conditions. SOURCE: William A. Bristow, University of Alaska, Fairbanks.

used in space physics (VLF) and working upward through the HF, VHF, and UHF bands, and finally the L-band. Table 5.1 summarizes the spectrum usage based upon currently operating instruments. The chapter concludes with a brief discussion of radio spectrum issues experienced by space physics active remote sensing.

TABLE 5.1 Characteristics of Space Physics Remote Sensing Transmitters

Radar	Location	Frequency (Bandwidth)	Power	License
Arecibo HF	Arecibo, Puerto Rico	5.1 MHz and 8.175 MHz	600 kW	NTIA
Arecibo ISR	Arecibo, Puerto Rico	430 MHz, 500 kHz BW	2.5 MW	NTIA
Digisonde	Global	2 MHz–30 MHz	300 W	
GPS/GNSS	Global/space-based	1100 MHz to 1600 MHz		
HAARP	Gakona, Alaska	2.6 MHz-9.995 MHz instantaneous BW 200 kHz	3.6 MW CW	NTIA
Homer VHF	Homer, Alaska	29.795 MHz 100 kHz BW	15 kW	FCC experimental noninterference
Jicamarca ISR	Jicamarca, Peru	49.92 MHz 1 MHz BW	6 MW	Peruvian
Millstone Hill ISR	Westford, Massachusetts	440.0, 440.2, 440.4 MHz, 1.7 MHz BW	2.5 MW	NTIA noninterference
PFISR	Poker Flat, Alaska	449.5 MHz 1 MHz BW	2 MW	NTIA primary
RISR	Resolute Bay, Nunavut, Canada	442.9 MHz 4 MHz BW	2 MW	Industry Canada
Sondrestron	Kangerlussuaq, Greenland	1287-1293 MHz 1 MHz BW	3.5 MW	
SuperDARN	Global	8 MHz-20 MHz instantaneous BW 60 kHz	10 kW	Within United States, FCC experimental noninterference

NOTE: Acronyms are defined in Appendix D.

SCIENTIFIC AND OTHER APPLICATIONS

Ionosphere-Thermosphere Science

As illustrated in Figure 5.1, the ionosphere and thermosphere are atmospheric regions that occupy the same volume of space: one is ionized (the ionosphere) and the other, neutral (the thermosphere). The thermosphere is the region of Earth's atmosphere above the mesopause (~90 km), making it the highest-altitude region of the atmosphere. It is characterized by a mass density profile that decreases exponentially with increasing altitude and a temperature profile that increases with increasing altitude. The ionosphere is the ionized portion of the atmosphere ranging from an altitude of about 50 km up to about 2,000-3,000 km. The ionosphere and thermosphere regions are coupled by collisions between ions and neutral molecules, which influence the energetics and dynamics of both regions.

The ionosphere is formed by the ionization of the neutral atmosphere, primarily by solar ultraviolet radiation, which varies with time of day, the seasons, geographic location, and level of solar activity. The lowest ionization energy (and hence longest wavelength) of the major atmospheric constituents is 12.1 eV for molecular oxygen. The corresponding wavelength is 102.6 nm, which is classified as extreme ultraviolet (EUV). Ionization of the other major constituents requires shorter wavelengths, ranging from 79.6 nm for molecular nitrogen, up to 91.1 nm for atomic oxygen. While solar irradiance peaks in the visible wavelength range, there is sufficient power spectral density at EUV wavelengths to produce the ionosphere. The spectral density below 100 nm is in the range of 10^{-3} to 10^{-2} W/m^2/nm,[3] which is about five or six orders of magnitude lower than the spectral density in the visible wavelengths. At these wavelengths, however, the temporal variability can be orders of magnitude larger than that at visible wavelengths. The temporal variability in solar activity includes changes in the long-term average value over a sunspot cycle, as well as short-term bursts during events like solar flares. This variability of the ionization source gets reflected into corresponding variations in the height profiles of the plasma density and atmospheric temperature.

Another major ionization source is energetic particle precipitation, which can come from either the solar wind or the magnetosphere. Typically solar wind particles entering the upper atmosphere are relatively low energy (approximately hundreds of electron volts) and result in high-altitude ionization. Occasionally, these particles can reach MeV energies, in which case they are referred to as solar energetic proton events, and can produce ionization at altitudes as low as 50 km. Such events cause shortwave radio blackouts, preventing communication at HF frequencies that are used by, for example, airliners flying on polar routes and military patrols on remote deployments. Energetic particles of magnetospheric origin arise from regions with structure of the plasma pressure or velocity. Depending on the region and dynamics, these particles can reach energies of tens of kilo-electron volts or more and can cause ionization over the full range of ionospheric altitudes. In addition to creating ionization, these particles are responsible for creating the aurora.

While solar EUV radiation and energetic particle precipitation produce ionization, the resulting distribution of plasma density is determined by various chemical reactions taking place in the ionosphere, along with plasma motions, which can transport the plasma across latitudes, longitudes, and altitudes. Figure 5.2 shows typical altitude profiles of electron density and temperature calculated by a

[3] See, for example, J. Lean, Solar ultraviolet irradiance variations: A review, *Journal of Geophysical Research* 92(D1):839-868, 1987.

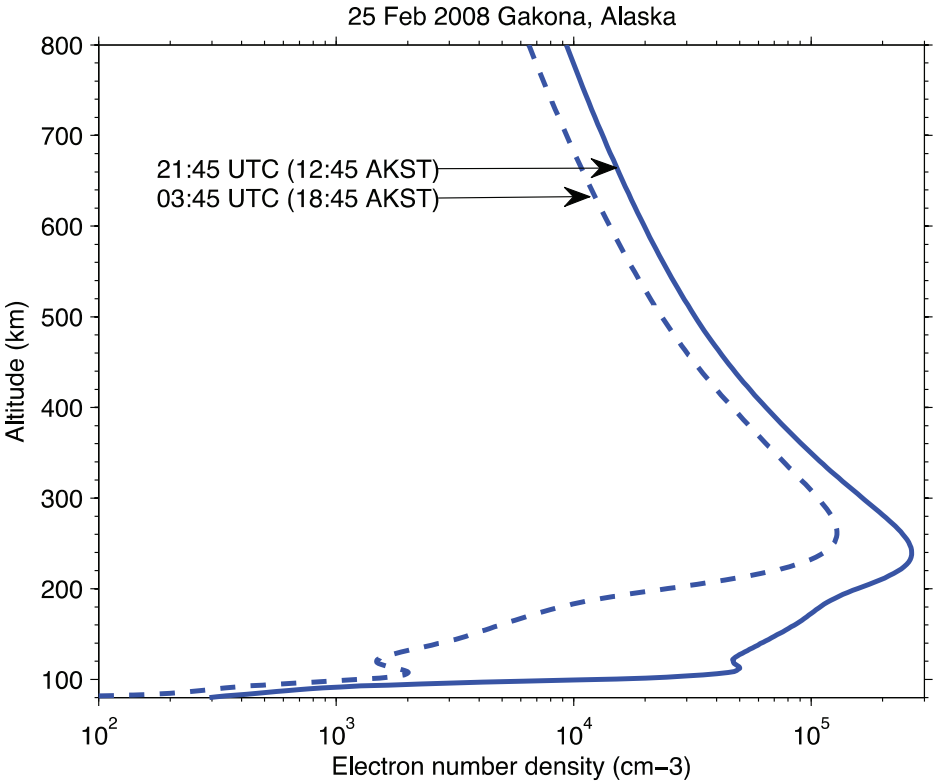

FIGURE 5.2 Profile of ionospheric electron density as calculated by the Self-Consistent Ionosphere Model (SCIM). SOURCE: Courtesy of Christopher Fallen, University of Alaska, Fairbanks, see C.T. Fallen, J.A. Secan, and B.J. Watkins, In-situ measurements of topside ionosphere electron density enhancements during an HF-modification experiment, *Geophysical Research Letters* 38:L08101, 2011, doi:10.1029/2011GL046887.

numerical ionospheric model.[4] The density is insignificant below about 100 km, increases rapidly to a local peak at around 130 km (E-region), then, after a local minimum, rises to its peak value at around 250 km (F-region). Above the peak, it decreases gradually until at very high altitudes it levels off at the magnetospheric plasma density.

Remote sensing of the ionospheric plasma density and temperature profiles coupled with observations of the solar irradiance at altitudes above the ionosphere

[4] C.T. Fallen, J.A. Secan, and B.J. Watkins, In-situ measurements of topside ionosphere electron density enhancements during an HF-modification experiment, *Geophysical Research Letters* 38(8):L08101, doi:10.1029/2011GL046887, 2011.

enable studies of the physics and chemistry that govern the formation of the ionosphere and its characteristics. Coupling the observations with magnetospheric satellite observations enables studies of magnetospheric dynamics.

The two main active remote sensing instruments used for observing the ionospheric plasma density are ionosondes and incoherent-scatter radars (ISRs). Ionosondes are swept frequency devices that measure plasma density as a function of altitude up to the altitude where the density peaks. They transmit short pulses at a series of frequencies below the peak plasma frequency of the ionosphere and observe the time between transmission and reception of each pulse to determine the altitude from which it was reflected. They cannot provide information on the plasma above the altitude of the peak. ISRs are single-frequency radars that observe backscatter from thermal fluctuations of the plasma at all altitudes with significant density up to the point where returns become too weak to detect. These observations, when coupled with the well-developed theory of incoherent-scattering from plasmas, provide altitude profiles of a number of parameters, including plasma density, plasma temperature, plasma velocity, ionic composition, and ion-neutral collision frequency. Figure 5.3 shows an example of observations from the Poker Flat, Alaska, Incoherent-Scatter Radar (PFISR) during an interval that included the effects of a solar flare. The four panels of the figure show the total plasma density (Ne), and the densities of the three major ion species O^+, O_2^+ and NO^+. The rapid increase in plasma density observed just prior to 0100 UT was due to x rays generated by the impulsive X-class solar flare and resulted in a blanking of short-wave radio over a large portion of the side of Earth illuminated by the Sun at the time.

While ISRs provide significantly more information than do ionosondes, the information comes at a cost. A typical ISR costs tens of millions of dollars, while an ionosonde costs on the order of a hundred thousand dollars. The high cost of ISRs has resulted in relatively few being built, while ionosondes are widely distributed. Hence, ISRs provide detailed high-fidelity information at a few strategic locations, and ionosondes provide less detailed information over broad geographic regions.

Ionospheric dynamics are driven by a variety of forces that also vary in time and space. In the lowest altitude region, collisions between the ionized and neutral constituents are the primary influence, while at the highest altitudes there are essentially no collisions, and the dynamics are governed entirely by the electric fields imposed from the magnetosphere. At the altitudes in between, the transition from collisional to collisionless leads to a rich environment for study.

Dynamical processes in the ionosphere lead to plasma instabilities that cause irregularities of the plasma density and temperature. Such irregularities diffuse along the magnetic field to produce what are referred to as field-aligned irregularities (FAIs), which can scatter electromagnetic waves. FAIs have a scattering cross section that can be orders of magnitude larger than the incoherent-scatter cross section, which means that radars of significantly lower sensitivity than an ISR can

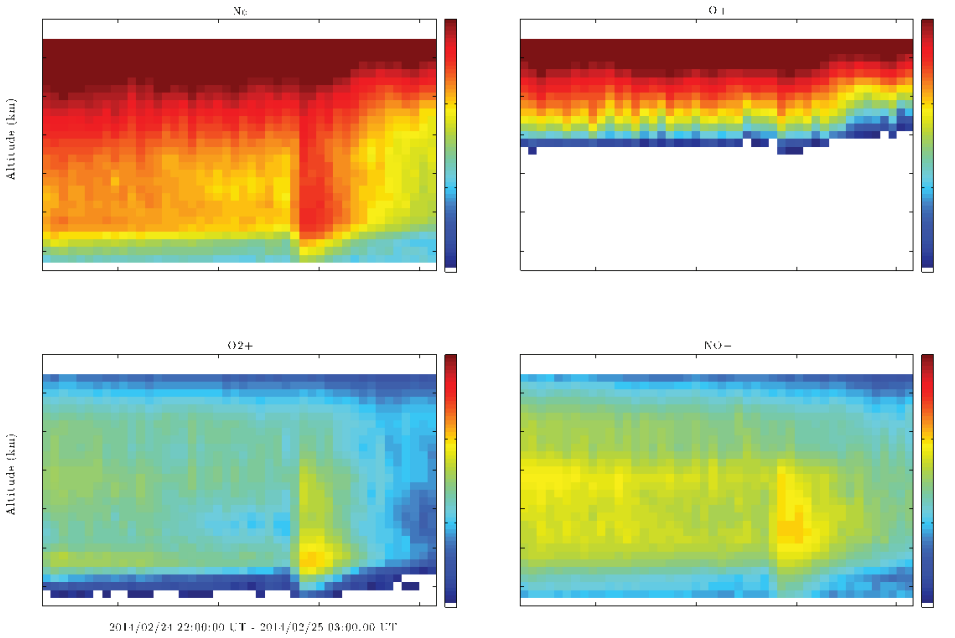

FIGURE 5.3 Observations from the PFISR from 2200 UT February 24, 2014, to 0300 UT February 25, 2014. Top-left: total plasma density; top-right: O^+ ion density; bottom-left: O_2^+ ion density; and bottom-right: NO^+ ion density. SOURCE: The Poker Flat Incoherent Scatter Radar (PFISR) is operated by SRI International on behalf of the U.S. National Science Foundation under NSF Cooperative Agreement AGS-1133009.

detect them. Radars that observe scatter from FAIs are referred to as coherent-scatter radars. Coherent-scatter observations provide information not only on the scattering cross section but also on the Doppler shift produced by the irregularities, which can be used to study the dynamical processes that generate the irregularities. In addition, at high altitudes (F-region), the FAIs convect with the bulk plasma, which means that observations of their velocity provide information about the bulk-plasma velocity. At lower altitudes (E-region) the irregularities do not drift with the bulk plasma velocity but can provide detailed information on the plasma instability mechanisms that led to their creation.

Magnetospheric Physics

The magnetosphere is the volume of space formed by the interaction of Earth's magnetic field with the solar wind and the interplanetary magnetic field (IMF). It surrounds Earth, extending from about 10 Earth radii from Earth's center on the

sunward side to as much as 200 Earth radii on the antisunward side. Magnetospheric plasma comes from two sources: capture of solar wind plasma at the boundary, and upwelling of plasma from the ionosphere. Within the magnetosphere, plasma dynamics and energetics are determined by internal processes driven by interactions with the solar wind and IMF at the outer boundary, which is referred to as the magnetopause. Figure 5.4 shows a sketch of the magnetosphere including some of its subregions. Within these subregions the plasma and/or the magnetic field exhibit characteristic properties (such as open or closed field lines, hot plasma or cold plasma, etc.) usually related to the internal dynamics or the driving. For example, the region identified as the Cusp derives its name from the topology of the magnetic field within the region. Magnetic field lines in the cusp are identified as open, having a footpoint on Earth and mapping out to the magnetopause. It is a region of strong interaction between the solar wind/IMF and the magnetosphere and drives much of the dynamics of the entire magnetosphere.

The primary goal of magnetospheric physics is to understand the complex chain of interactions that couple solar wind energy and momentum into the upper atmosphere. Doing so requires understanding the processes occurring at the mag-

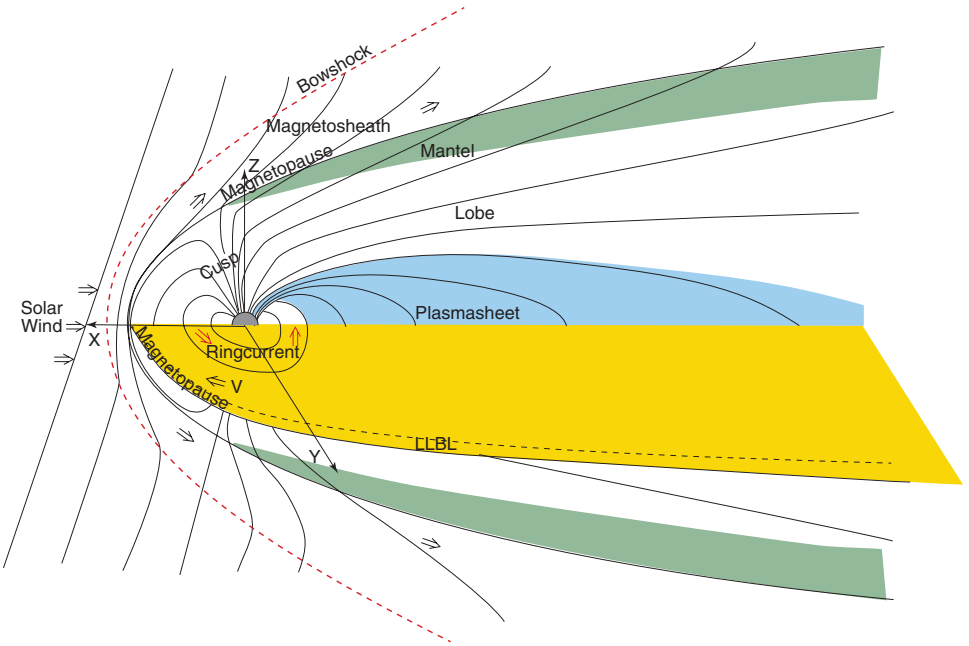

FIGURE 5.4 Sketch of Earth's magnetosphere identifying various regions. SOURCE: Courtesy of Antonius Otto, University of Alaska, Fairbanks.

netopause and the internal dynamics of the magnetospheric regions. It is necessary to understand and observe how plasma and magnetic flux are transported within the system, and how the magnetosphere and ionosphere are coupled. In addition, there are events known as magnetic storms and auroral substorms that are characterized by rapid global-scale configuration changes in the magnetosphere that can have significant impacts on technological systems. Understanding the causes and characteristics of these events is another focus of magnetospheric physics.

Ground-based active remote sensing uses observations of the ionosphere to study the magnetosphere, which is possible because the patterns of particle precipitation and plasma velocities observed in the ionosphere can be mapped to the magnetosphere. As discussed in the section covering ionospheric science, energetic particle precipitation from the magnetosphere produces plasma in the ionosphere that can be sensed using ISRs. The ISR measurements provide regional patterns of the precipitation morphology and can be used to infer the energy flux and characteristic energy of the precipitation. The observations are spatially and temporally resolved, with resolutions on the order of kilometers and time resolution on the order of seconds. ISR observations also provide information on the flow of ions from the ionosphere to the magnetosphere. This ionospheric outflow is at times the major source of magnetospheric plasma. Understanding the conditions under which it occurs and the mechanisms by which it occurs are topics of considerable current research.

One of the most significant ways in which ground-based active remote sensing contributes to magnetospheric research is through observations of the high-latitude plasma flow patterns. Characterizing the patterns requires observations over broad regions in both the northern and southern hemispheres, from midlatitudes to the poles. An international network of coherent-scatter radars known as the Super Dual Auroral Radar Network (SuperDARN)[5] has evolved to provide these observations. Pairs of SuperDARN radars measure line-of-sight components of the F-region plasma velocity in common volumes from different directions. By combining the observations from all of the radars in the network, maps of velocity vectors are created. The maps cover both hemispheres from about 50° magnetic latitude to the poles with spatial resolutions of about 100 km and temporal resolution of about a minute. Observations from SuperDARN are used in nearly all aspects of magnetospheric research.

[5] R.A. Greenwald et al., DARN/SuperDARN: A global view of high-latitude convection, *Space Science Reviews* 71:763-796, 1995.

Radio Science

Broadly speaking, radio science is a scientific and engineering discipline focusing on the generation and propagation of electromagnetic waves. Space physics aspects of radio science address how space plasmas affect the propagation of waves, or conversely, how the waves can affect space plasmas. While radio science is identified as a distinct discipline, it is closely related to both ionospheric research and magnetospheric research. There are direct practical applications of radio science, including the understanding of impacts on transionospheric propagation of satellite communication, navigation, and remote sensing signals.

When a radio signal passes through a plasma, its propagation is influenced by the index of refraction along its path. The index of refraction of a plasma is different from that of free space and depends on the frequency and polarization of the signal, the density of the plasma, and the strength and direction of the ambient magnetic field. The index of refraction determines the velocity of propagation of signals and, hence, the time it takes for signals to propagate from their source to their point of reception. For signals that are used for timing and navigation (GPS and GNSS), knowledge of the propagation time is critical for proper operation. When a signal encounters a smooth gradient of the index of refraction, it is refracted, changing its propagation direction. Radar signals that rely on knowledge of the signal line of sight must be able to account for such refraction. In regions of turbulent changes of the index of refraction, interference among different signal paths creates constructive and destructive interference that lead to amplitude and phase fluctuations referred to as scintillations.

Just as plasmas affect electromagnetic wave propagation, electromagnetic waves can affect plasmas. The electric field of a wave accelerates the charged particles of the plasma, which can lead to a variety of plasma phenomena. The most basic result of electromagnetic wave passage is a general heating of the plasma. The heating is caused by collisions among the accelerated charged particles, which randomizes the particle velocities. In addition to heating, a variety of plasma instabilities can be excited, generating a plethora of plasma wave modes. Studying these effects has led to the construction of facilities, colloquially known as ionospheric heaters, that transmit high-power high-frequency waves into the ionosphere and diagnose the impacts using remote sensing instruments.

Space Weather

Space weather is a relatively new discipline that encompasses the other disciplines of space physics but focuses on societal impacts and on prediction of events with potentially adverse effects. Examples of such effects include increased level of ionospheric scintillation causing outages of GPS signals, induced currents in power

systems caused by ionospheric currents, and increased radiation belt particle fluxes causing damage to satellites.

Large space weather events can have severe societal impacts. One of the most cited examples is a March 1989 geomagnetic storm in which the Quebec power grid was disrupted, leaving over 800,000 customers without power for nearly 10 hours. During the event, currents flowing in the ionosphere induced currents in the power system of sufficient magnitude to trip circuit breakers in the grid's transmission lines, leading to the widespread outage.

The goal of space weather research is to predict the occurrence and intensity of such space phenomena, with the expectation being that the availability of such predictions would allow system operators to take steps to mitigate the potentially adverse effects. Making predictions with useable accuracy, however, is a rather daunting task.

Predicting space weather is difficult for several reasons. First, the volume of space that contributes to the impacts is large. As discussed in earlier sections, electric fields and particle precipitation map along Earth's magnetic field. As a result, conditions at one location are influenced by conditions in regions that may be many tens of Earth-radii away. Secondly, the evolution of the magnetosphere-ionosphere system in time is a strong function of the drivers, but also depends on the state of the system at the time the drivers become active. Changes of the main drivers, the solar wind and IMF, are communicated rapidly to the entire system and can induce effects within minutes after reaching the magnetopause. The precise nature of the effects depends critically on the state of the system. For example, if an IMF transition that would increase the level of driving arrives at the magnetopause at a time when the system is quiescent, it would likely induce increased convection and a general expansion of the auroral oval toward lower latitudes. If, however, the magnetosphere is in an excited state when the transition arrives, the effects will be quite different. Within a short time, the increased convection could result in a magnetospheric substorm, which is the rapid release of energy stored in the magnetotail, resulting in active auroral displays, large ionospheric currents, and highly structured ionospheric plasma.

The sheer volume of the magnetosphere makes characterization using in situ sensing impractical. Hence, observations of the magnetosphere-ionosphere state can be obtained only through remote sensing. As discussed above, the high conductivity of the magnetospheric magnetic field lines makes these observations possible. The same convection and particle precipitation measurements used in basic magnetospheric and ionospheric research apply to space weather as well. Remote sensing observations can be used for a variety of space weather measurements, including the strength of convection, the latitude of auroral precipitation, the location of auroral currents, and the location of potentially scintillation-causing irregularities.

SPECTRUM USAGE

Ionospheric active sensing observations use radio transmitters that operate at frequencies ranging from kilohertz up to a few gigahertz, with certain ranges being more actively used than others. The observations come primarily from ground-based radar systems but include satellite-borne radio beacons. This section provides a summary divided into ground-based and space-based systems, starting with the lowest frequencies and working upward. In each case, the choice of frequency is directly related to the type of information sought from the observations. In almost every case, the frequency is determined by the properties of the target medium. In order to sense the plasma for the desired measurement, it is necessary to use a signal that interacts with it in a specific way. Using a different frequency would not provide the same information. For example, an ISR operating in the UHF band provides information on the density and temperature of the plasma, while a coherent-scatter radar operating in the HF or VHF bands provides information on the spectrum of irregularities present in the plasma. While both instruments provide information on the same plasma, the measurements are distinct.

Ground-Based Radar

VLF Band

The lowest transmitter frequencies used in space physics research are in the VLF band. Though no longer operational, at one time the world's longest dipole was used to produce VLF signals that directly probed the magnetosphere. The Siple Station, Antarctica, antenna was a 40 km dipole transmitting signals at frequencies around 3 kHz, which were received at the conjugate point in the northern hemisphere at Roberval, Canada. When these transmissions reached the magnetosphere, they interacted with the trapped energetic particle populations, resulting in amplification of the signals and the triggering of other emissions. From the observed signatures it was possible to draw conclusions about the particle populations, and about the wave-particle interactions. No dedicated space physics transmitters operating at the VLF band exist today. To overcome this lack of dedicated transmitters, the research continues using other means. Magnetospheric research using the VLF band has been continued by using HF band heating facilities to generate the signals by modulating electrical currents flowing in the ionosphere. Ionospheric research using VLF signals currently relies on radio navigation and time signals transmitted by various government agencies in the 15-20 kHz band. These signals propagate for thousands of kilometers in the waveguide formed by the ionosphere as the upper boundary, and Earth's surface as the lower boundary. Small phase and amplitude

fluctuations observed at a fixed site are used to infer properties of the waveguide, which translate to properties of the ionosphere.

HF Band

The next most widely used band for space science is the HF band. As described in the preceding section, "Scientific and Other Applications," ionosondes measure the altitude profile of electron density in the lower ionosphere by observing reflections of swept frequency signals. When a wave propagates into a region where the plasma frequency is comparable to but below the wave frequency, the propagating wave experiences a decrease in velocity and a change in direction. As the wave approaches an altitude where the plasma frequency is equal to the wave frequency, the phase index of refraction approaches zero and the wave reflects. Usually an ionosonde begins its transmissions at a frequency of around 1 MHz or lower and steps to some upper frequency determined by the highest expected plasma frequency, which may be 20 MHz or higher. At each frequency step, short pulses are transmitted, then reflected by the plasma and received by the ionosonde receiver. The time between transmission and reception is used to estimate the altitude of the reflection boundary. Successively higher frequencies reflect from higher altitudes until a frequency is reached that is above the plasma frequency at the density peak altitude. Beyond this frequency, no more reflections are observed.

There are a few different ionosonde designs in use today. The most common model is the Digisonde, manufactured by Lowell Digisonde International. The system can transmit between 200 kHz and 30 MHz, with a peak power of 300 W. Over 150 Digisondes have been built since 1969, of which more than 60 remain in operation today and are part of the Global Ionospheric Radio Observatory (GIRO). GIRO is a distributed network of ionosondes that provide specification of the ionospheric electron density below the F-region peak altitude over much of the globe.

Ionospheric heating uses high-power transmitters to study the interaction of radio-frequency electromagnetic waves with plasmas, with waves of high enough amplitude to cause measurable effects. In heating experiments, energy is transferred from the electromagnetic waves to the plasma. The mechanism for the energy transfer depends on the properties of the plasma and the frequency and polarization of the waves. If the frequency of the wave is close to one of the resonant frequencies of the plasma, energy coupling is highly efficient, and the transfer can lead to explosive growth of plasma instabilities. Away from a resonant frequency, the energy transfer is less efficient, but because of collisions among the plasma constituents or between the plasma and the neutral gas, the energy transfer leads to a general heating of the plasma, modifying the properties of the plasma, such as its electrical conductivity. In addition, the heating can lead to motion of the plasma through diffusion and thermal upwelling. Because of energy coupling mechanisms,

ionospheric heating is possible only in the lower portion of the HF band; lower frequencies would not reach the ionosphere, and higher frequencies would pass through the ionosphere with little interaction.

In the process of radio-frequency ionospheric heating, interesting and useful effects can be produced. For example, under suitable ionospheric conditions, operating the transmitter in a mode that deposits energy into the D-region and lower E-region can alter the ionospheric conductivity and modulate the naturally occurring electrojet currents, which as a result radiate electromagnetic waves at the modulation frequency. ELF/VLF waves generated in this manner have been measured with significant amplitudes both on the ground and in space. Other effects include the generation of field-aligned irregularities in the plasma, artificial auroras, large-scale modification of the plasma density, and stimulated electromagnetic emissions.

In the United States, there are two HF band heating facilities. The High-Frequency Active Auroral Research Program (HAARP) facility at Gakona, Alaska, operates at frequencies between 2 MHz and 10 MHz and is capable of transmitting 3.6 MW of continuous power. The facility has a large phased-array antenna consisting of 180 crossed dipoles covering about 33 acres. It is the highest-power, broadest-frequency, and most flexible facility of its kind. The second U.S. facility is currently under construction at the Arecibo Observatory. The facility will use an array of dipoles below a wire subreflector suspended over the 300 m diameter dish. While the facility will not cover the same range of frequencies as HAARP or achieve the same power level, it will have the advantage of being colocated with the Arecibo Incoherent-Scatter Radar, which is the most sensitive ISR in the world. Having such a powerful diagnostic instrument is a significant advantage for detailed studies of the plasma processes under investigation.

SuperDARN is an international network of coherent-scatter radars used for observing plasma flows in the ionosphere. At present, the network consists of 33 radars distributed around the globe, with 22 in the Northern Hemisphere and 11 in the Southern Hemisphere. The observation mechanism used by coherent-scatter radars differs from that of ionosondes. While it is still necessary to use a frequency that interacts with the plasma, the scattering mechanism is Bragg scatter from field-aligned irregularities, which arises in regions where there are spatially periodic fluctuations of the plasma density with a wavelength equal to half of the probing wavelength. Regions of plasma turbulence have a broad spectrum of wavelengths, so usually if turbulence is present there will be a component with the appropriate spatial scale. Scattering occurs whenever the wavelength-matching criterion is met, but the scattered signal returns to the radar location only when it is directed along the line from which it came. SuperDARN uses the HF band because refraction of the signals bends them toward the horizontal, resulting in perpendicularity to the magnetic field over large regions of space and particularly in the F-region at

auroral-zone and polar cap latitudes. SuperDARN uses frequencies between about 8 MHz and 20 MHz, though at any given time, each radar operates on a single frequency and uses only about 30 kHz to 60 kHz of bandwidth.

VHF Band

Like HF coherent-scatter radars, VHF radars target field-aligned plasma irregularities. The lack of significant refraction at the VHF band, however, greatly impacts the focus of the research. As discussed in the previous section, observing the scatter from field-aligned irregularities requires the probing signal to be perpendicular to Earth's magnetic field. Without refraction, however, perpendicularity to the field at F-region altitudes cannot be achieved at high latitudes. The result is that research investigations using VHF coherent-scatter radars focus primarily on observations of E-region plasma irregularities.

In the United States, there are two currently operational fixed-location VHF radars for ionospheric remote sensing: one at Homer, Alaska, and one at St. Croix, U.S. Virgin Islands. The radars are operated by Cornell University on a campaign basis at a frequency of 29.795 MHz (technically in the HF-band) at a peak power of about 16 kW. Additional portable radars are operated during research campaigns at a variety of locations. These radars operate at 40.92 MHz and 49.8 MHz and use bandwidths from 200 kHz to 500 kHz and peak power of 30 kW.

UHF Band

The U.S. National Science Foundation supports the operation of six incoherent-scatter radar facilities, three of which are in the United States. Incoherent scatter is a misnomer referring to the scattering of radio waves by individual electrons, which is not the actual scattering mechanism that these radars exploit. The scattering actually comes from thermal fluctuations due to an array of plasma waves. The total scattering cross section is approximately the product of the classical electron scattering cross section and the number of electrons in the scattering volume, which results in very weak scattering, requiring transmit powers of megawatts and antenna gains of 30-50 dB or more.

A well-developed theory of ISR describes the shape of the frequency spectrum of the radar returns.[6] The spectrum is a function of several ionospheric parameters, which can be estimated by fitting theoretical curves to the observed spectra. The parameters include the electron density, the ion temperature and mass, the electron temperature, the ion-neutral collision frequency, and the ion velocity. Estimates of

[6] See, for example, J.P Dougherty and D.T. Farley, A theory of incoherent scattering of radio waves by a plasma, *Proceedings of the Royal Society of London A 259(1296):*76-99, 1960.

these parameters are obtained over the full range of ionospheric altitudes, including above the F-region peak.

Existing ISRs operate at frequencies between 50 MHz and 1290 MHz, although most use the band around 400-450 MHz. Analysis of ISR theory shows that this band is nearly optimum in terms of the altitude coverage and radar sensitivity. Lower frequencies would require larger antennas to achieve the same antenna beamwidths, and the noise from external sources would increase greatly. At higher frequencies the wavelength approaches the Debye length (a length scale below which collective effects no longer shield individual charges) and the spectrum becomes that of simple Thompson scattering. The result is that many of the ionospheric parameters cannot be determined using such frequencies.

Satellite-Borne Radar

Satellite-borne beacon transmitter signals and GPS/GNSS signals are used for ionospheric science and radio science by studying the integrated effects of propagation from the satellites to receivers on the ground. These effects relate to the total time a signal takes to propagate from the satellite to the ground, and how the amplitude and phase of the signals vary in time. Both effects are related to propagation through ionospheric plasma and can be used to infer ionospheric properties.

Time variations of the amplitude and phase of the signals are related to spatial variations of the index of refraction along the path. Variations with scales on the order of the diameter of the Fresnel zone at ionospheric altitudes cause constructive and destructive interference of the signals. Passage through regions with irregularities of this size can lead to rapid fluctuations of the signals, referred to as scintillation. When scintillations become severe, as may occur during geomagnetic storms, they can cause loss of receiver lock, leading to outages of the system.

The total time between transmission and reception is proportional to the integration of the index of refraction along the path, which is related to the total number of electrons along the path, referred to as the total electron content (TEC or slant TEC). Precise measurements of the signal propagation times are used to estimate TEC along the transmission paths. By observing multiple satellites from multiple ground locations, maps of TEC are produced covering large areas of the globe. In addition, in some regions there are dense arrays of receivers that use the line-of-sight TEC observations in a tomographic inversion to produce three-dimensional volume estimates of electron density.

Satellite beacons have used frequencies from the HF band through the L-band (Table 5.1).

RADIO SPECTRUM ISSUES

The characteristics of the various space physics active remote sensing instruments vary significantly from instrument to instrument, which means that the spectrum issues also vary significantly. In the VLF band, the instruments use navigation and timing signals generated by others. The band is not heavily used for other purposes, and there are few spectrum issues. While the primary interference signals in the HF band are environmental (cosmic background and terrestrial lightening), increased usage for communication and broadcasting means that at times no clear frequencies are available that can be used by the HF radars. At the UHF and L-bands, crowding of the bands has become a significant problem. The most telling example is the allocation of a band near 900 MHz for telecom use in Finland and Sweden, resulting in the loss of the band for use by the European Incoherent Scatter Radar (EISCAT). Their operations now rely entirely on their VHF system. In the United States, radars operating in the band near 430 MHz share the band with Department of Defense (DOD) radars, which have priority. The PFISR system is allowed to operate at the edge of the band occupied by the DOD radar at Clear Air Force Station, Alaska, but was allowed to do so only after extensive testing showed that it did not interfere with that system. Even at the edge of the band, the PFISR system experiences significant RFI at times.

Future advances in space physics research will rely on increasing spatial and temporal resolution and sensitivity, which will increase bandwidth and power requirements for active remote sensing. To some extent, the future demands are unknown and will be driven by individual investigators proposing new instruments or enhancements to the existing ones.

FINDINGS AND RECOMMENDATIONS

Finding 5.1: Active remote sensing plays a vital and central role in space physics research, which provides societal benefits. These benefits are both direct, in characterizing impacts on technology critical to government and industry, and indirect, in providing a fundamental understanding of our space environment.

Finding 5.2: The choice of frequencies and associated bands used in space physics active remote sensing are determined primarily by the physical properties of the medium being probed.

Finding 5.3: The information provided by ionospheric active remote sensing cannot be obtained by other means.

Recommendation 5.1: Access to the spectrum currently used in space physics remote sensing should be maintained.

Recommendation 5.2: The next decadal survey in solar and space physics should address the future spectrum needs for the space physics research community.

Recommendation 5.3: NASA and the National Science Foundation should conduct a formal survey of the space physics research community to determine future spectrum needs.

6

Planetary Radar Astronomy

INTRODUCTION

Radar studies of the planets and smaller bodies in the solar system are driven by the desire to understand how our solar system formed and evolved and, in the case of near-Earth asteroids (NEAs), by the concern that some of these small objects may pose a threat to Earth. This chapter will give a brief historical introduction to planetary radar astronomy, a description of the technical needs of the field, and a brief survey of current U.S. planetary radar systems, including their use of the spectrum. This is followed by a discussion of the techniques used to obtain and analyze the data. The section "Science Applications" discusses the research programs with some emphasis on studies of near-Earth asteroids due to Earth-based radar's unique capability to obtain detailed information about the orbits and characteristics of these objects. Finally, the sections "Future Science Drivers and Technical Requirements" and "Frequency Assignment Requirements" look to the future, discuss plans for new radar systems, and speculate on possible requirements for additional spectrum assignments.

The rapid development of radar during World War II opened the possibility of utilizing this new technology to learn more about our solar system by detecting radar echoes from large and small solar system bodies. With today's ability to image our sister planets from orbiting spacecraft, it is hard to realize how little was known about our solar system until the early 1960s with the advent of the first space missions and the development of more capable ground-based instruments, including radar. The overall scale of the solar system, as represented by the astronomical unit

(AU), the mean distance between Earth and the Sun, was still imperfectly known; Venus was postulated to have rain forests below its clouds; science fiction had not given up on the idea that Mars had canals; and there was continuing discussion as to whether lunar craters were of impact or volcanic origin.

In 1946, radar systems in Hungary and the United States first detected echoes from the Moon. However, detecting echoes from our nearest planet, Venus, required an improvement in radar sensitivity by a factor of over a million. This was achieved in the late 1950s, resulting in detections of the planet at its close approach to Earth in 1961 by five different radar systems in the United States, Great Britain, and the Soviet Union. By the mid-1960s, three new, much more powerful radar systems were available for this new field of planetary radar astronomy. These were the 305 m Arecibo telescope of the National Science Foundation (NSF) in Puerto Rico, the 37 m Haystack antenna in Massachusetts, and the 64 m Deep Space antenna of NASA in Goldstone, California. Progressive upgrades of the NASA Goldstone and NSF Arecibo systems, primarily by moving to higher frequencies and more powerful transmitters, have made these two radar systems the dominant instruments for current radar studies of the solar system (Figure 6.1). Until recent events shuttered its scientific work, the Russian 70 m Evpatoria telescope in the Crimea was the only other currently operating planetary radar system. The telescope's limited sensitivity restricted it to rare observations of NEAs. However, there are discussions underway that may lead to one or two more transmitting systems in the United States and further upgrades to the Arecibo and Goldstone systems aimed, primarily, at orbit determination and characterization of NEAs.

CURRENT RADAR ASTRONOMY SYSTEMS

The sensitivity of a planetary radar system is proportional to the average transmitter power and the effective area of the transmitting and receiving antennas, which are the same for a monostatic system but may be different for a bistatic system (Figure 6.2), and inversely proportional to $\lambda^{3/2}$, where λ is the operating wavelength, and to the system temperature, which characterizes the noise contributions from the receiver, Earth's atmosphere, our galaxy, and the cosmic microwave background. For a particular target body, the ability to detect an echo is dependent on R^{-4}, where R is its distance from the radar, plus the size, surface electrical and physical properties, and rotation state of the body. The very large distances of solar system bodies from Earth dictate the need for very high transmitter powers and large transmitting/receiving collecting areas and very low system temperatures. Table 6.1 lists the characteristics of the currently operating planetary radars and the antennas that are occasionally used during bistatic observations.

FIGURE 6.1 (*Left*) the 305 m NSF Arecibo antenna. The 2.38 GHz transmitter is housed in the dome, while the 430 MHz transmitter is in the operations building with the power being delivered to the line feed to the left of the dome via a waveguide coming up the catwalk from the base of the tower in the image. (*Right*) The 70 m NASA Goldstone DSN-14 antenna. SOURCE: (*Left*) Courtesy of NAIC/Arecibo Observatory, a facility of the NSF. (*Right*) Courtesy of NASA/JPL.

TECHNIQUES

The great advantage of radar versus passive observations is the ability to control the properties of the transmitted waveform and measure the changes in these properties in the received echo. These properties are the following:

- The time origin of the transmitted waveform,
- Frequency or wavelength,
- The effective isotropic radiated power (EIRP), and
- Polarization state.

The time origin allows precision measurement of the distance to the target body, while the frequency of the echo relative to the transmitted frequency, the

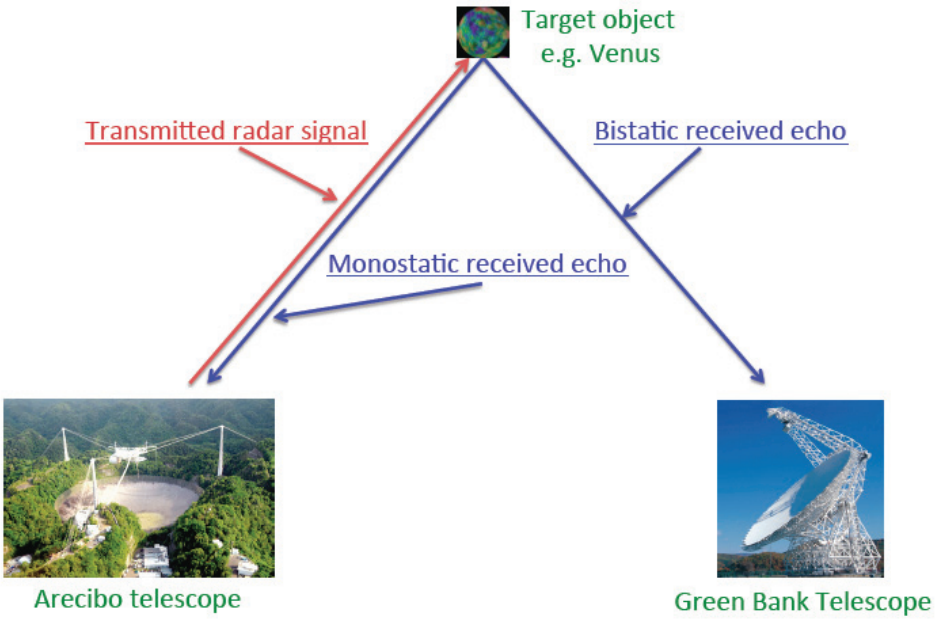

FIGURE 6.2 Monostatic and bistatic configurations for radar observations of Venus and near-Earth asteroids. SOURCE: *Lower left:* Courtesy of Donald B. Campbell, Cornell University; *lower right:* National Radio Astronomy Observatory; *image of Venus:* Courtesy of NASA/JPL/USGS (PIA00157: Hemispheric View of Venus Centered at 0 Degrees East Longitude).

Doppler shift, allows the radial velocity of the target body to be determined. It was these radar astrometric measurements to Venus that refined the value of the AU, and they are now primarily used to obtain precise orbits for potentially hazardous NEAs. The width and shape of the rotationally Doppler broadened echo provides information about the rotation state and surface roughness of the body (Figure 6.3). Given the distance to the target body and its size, the strength of the echo, combined with the shape of the Doppler-broadened echo, gives insight into the electrical properties of the surface material. Measuring the echo power as a function of time delay and Doppler shift relative to the sub-Earth location on the target body provides an image of echo power versus these two coordinates, which can be converted into a more normal latitude-longitude image if the size, shape, and spin vector of the body are known. However, as is clear from Figure 6.3, two locations symmetrically placed north and south of the equator have the same time delay and Doppler shift relative to the radar and the sum of the echo powers from these locations is imaged, leading to what is known as the N-S ambiguity problem (Figure 6.4). Irregular bodies such as near-Earth objects can have two or more

TABLE 6.1 Current U.S. Planetary Radar Systems

Transmitting Location	Frequency (GHz)	Bandwidth (MHz)	Power (MW)	Receive Location
Arecibo, Puerto Rico	2.380	20	1.0 (CW)	Arecibo, Puerto Rico GBT, Green Bank, West Virginia VLA, Socorro, New Mexico LRO, Lunar orbit
	0.430	0.6	2.5 (pulsed)	Arecibo, Puerto Rico GBT, Green Bank, West Virginia
Goldstone, California DSS-14	8.560	50	0.5 (CW)	Goldstone, California GBT, Green Bank, West Virginia Arecibo, Puerto Rico VLA, Socorro, New Mexico 10 VLBA sites
Goldstone, California DSS-13	7.190	80	0.08 (CW)	Goldstone, California GBT, Green Bank, West Virginia Arecibo, Puerto Rico

NOTE: Close asteroid observations require bistatic operation. Goldstone DSS-14 has NTIA assignment of 8.50 to 8.70 GHz. Goldstone DSS-13 has NTIA assignment of 7.150 to 7.230 GHz. Acronyms are defined in Appendix D.

locations with the same delay and Doppler shifts, and multiple observations at different aspect angles are needed to obtain a true shape.

Normally, the transmitted signal is circularly polarized, and both senses of circular polarization are received, allowing the polarization Stokes parameters of the received echo to be computed. For a surface normal to the incident wave and smooth at the radar wavelength, the echo power will be in the opposite sense of circular polarization to that received—the "expected" sense. Echo power at non-normal incidence angles arises from scatter from surface and/or subsurface wavelength-scale "roughness" within the penetration depth, typically about 10 wavelengths for the very dry surfaces of all solar system bodies apart from Earth, dependent on the loss tangent of the surface material. These scattering processes also couple power into the same (unexpected) sense of circular polarization, and the ratio of this power to that in the expected sense is used as a measure of relative surface/subsurface roughness. At moderate to high incident angles, the transmission coefficients into the surface for linear polarizations parallel and perpendicular to the plane of incidence diverge, so that the presence of a linearly polarized component in the radar echo is indicative of subsurface scatter and can be used to estimate the dielectric constant of the surface material.

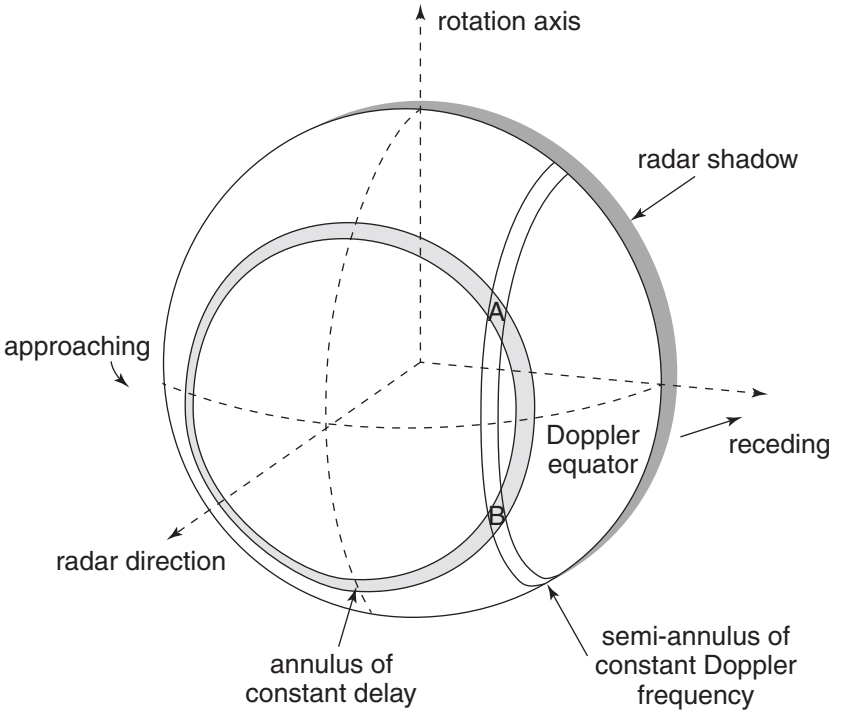

FIGURE 6.3 Radar imaging geometry for a spherical target. Lines of constant delay are concentric with sub-Earth point (the location on the sphere closest to Earth), and the lines of constant Doppler shift intersect these concentric delay circles at two locations. Measuring the radar echo power as a function of time delay and Doppler shift relative to the sub-Earth location provides an image in time delay and Doppler shift coordinates. When, as is usual, the angular resolution of the radar telescope is larger than the angular diameter of the target object, two locations, A and B in the diagram, have the same delay and Doppler shift, and what is measured is the sum of the echo powers from these two locations (Figure 6.4). SOURCE: A. Vardy (ed.), *Codes, Curves, and Signals: Common Threads in Communications*, Springer, New York, 1998, doi:10.1007/978-1-4615-5121-8, with permission of Springer Science+Business Media.

SCIENCE APPLICATIONS

During the 1960s, radar astronomy made major contributions to our knowledge of the solar system and to basic physics. These included a significant improvement in our knowledge of the AU, enabling accurate navigation of early spacecraft planetary missions; the discovery of the slow retrograde rotation of Venus and the very surprising 59.6-day rotation period of Mercury; the first low-resolution images of the surface of Venus below its cloud cover; the first radar detection of an asteroid,

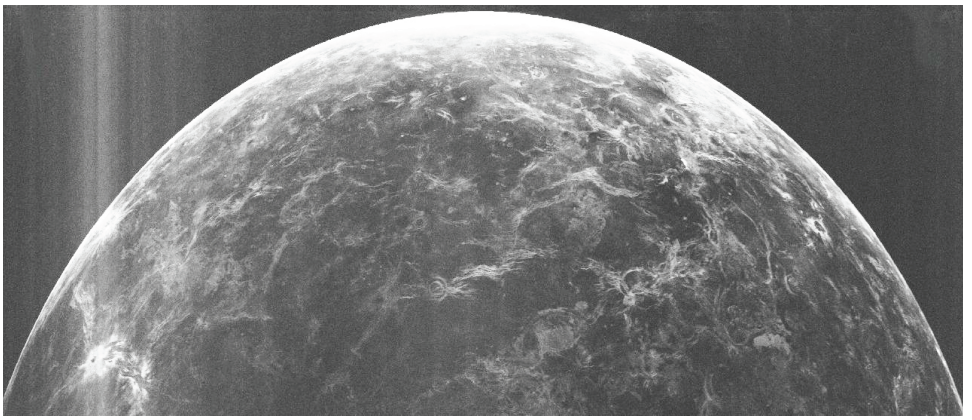

FIGURE 6.4 An image of Venus at about 1 km resolution in delay and Doppler coordinates made by transmitting at 12.6 cm wavelength with the Arecibo telescope in Puerto Rico and receiving the echo with the Green Bank Telescope in West Virginia. Because of the hemispheric ambiguity, it is not possible to tell in which hemisphere the various features are located. Increasing delay is from the top down and Doppler shift left to right, with the west limb of the planet to the left. The large volcano, Theia Mons, is at lower left. SOURCE: Courtesy of Bruce A. Campbell, Smithsonian Institution.

the NEA Icarus; imaging of the Moon and other investigations of the lunar surface in support of the Apollo missions; and tests of general relativity (GR) via time delay measurements to Venus as it passes behind the Sun (the fourth, or Shapiro, test of GR) and to Mercury to measure the rate of advance of its orbit's perihelion.

In the first half of the 1970s, the sensitivity of the Arecibo radar system was significantly increased by replacing the wire mesh surface of the telescope's reflector with 38,788 aluminum panels, allowing operation up to 5 GHz, and installing a 450 kW transmitter operating at 2.38 GHz (12.6 cm wavelength). At the same time, a 400 kW transmitter operating at 8.56 GHz (3.5 cm wavelength) was installed on the 64 m Goldstone antenna, greatly increasing its sensitivity. A major driver for the upgrading of Arecibo's radar system was the imaging of the surface of Venus at high resolution. Initial maps of the planet's surface had resolutions of about 15 km covering 40 percent of the planet's surface, allowing the first large-scale look at the surface of our nearest planetary neighbor and the first indication that its surface is very young compared to those of Mars, Mercury, and the Moon, about 700 million years. The Galilean satellites of Jupiter were detected in the 1970s, resulting in the discovery of the unusual radio wavelength scattering properties of the low-temperature water ice surfaces of Europa, Ganymede, and Callisto. These surfaces are radar retroreflectors due to internal scattering in the ice, which has very low loss at radio wavelengths. The sense of received circular polarization is also

inverted, with the unexpected sense dominant over the expected sense. It was these properties that led to the discovery in the early 1990s of ice deposits at the poles of Mercury and a continuing "discussion" as to whether similar multiwavelength-sized deposits exist in the permanently shadowed parts of impact craters at the poles of the Moon. This period also saw the first radar detection of the rings of Saturn, clearly demonstrating that the rings were composed of centimeter- and larger-sized particles and not small millimeter-sized ones.

Through the mid-1990s, about 50 NEAs, almost 40 main-belt asteroids, and several comets were studied by the Arecibo and the Goldstone radar systems. These studies were a harbinger for the current emphasis of the Earth-based planetary radar program on astrometric and characterization observations of NEAs.

Incremental improvements in the Goldstone planetary radar system were obtained by the expansion of the NASA Goldstone antenna from 64 m to 70 m in 1988 and a small increase in transmitter power due to improved X-band klystrons in the 1990s. In the mid-1990s, a major modification of the optics of the Arecibo 305 m antenna and installation of a 1.0 MW transmitter at 2.38 GHz increased its sensitivity as a planetary radar system by a factor of 10 to 20, depending on the target. This left the Arecibo radar system with about 20 times the sensitivity of the Goldstone system. However, the Arecibo telescope has limited steerability, so it can only observe about 33 percent of the sky (declinations from 2 degrees S to 38 degrees N). The Goldstone antenna is fully steerable and can observe declinations of ~40 degrees S to the North Pole. This makes the two radar systems very complementary, especially for observations of NEAs.

Current Science Programs

Current science activities revolve around three observational modes: (1) astrometry based on precision distance and radial velocity measurements, (2) imaging based on measuring echo power as a function of position on the surface of a solar system body, and (3) speckle interferometry (see Box 6.1). Much of the emphasis of planetary radar observations is now directed to the characterization of NEAs and the determination of their orbits. However, radar's sensitivity to centimeter-scale and larger surface roughness, its ability to penetrate dry surfaces, and its unique ability to detect water ice has kept it relevant to investigations of the Moon and terrestrial planets as well. Furthermore, its ability to make precision measurements of rotation vectors via speckle interferometry is providing information about the interior structure of planets and satellites and potentially giving insight into phenomena such as the transfer of angular momentum between the atmosphere and the solid body of Venus.

The interest in NEAs is driven by scientific curiosity, by what NEAs can tell us about the formation and evolution of our solar system, by concern about the poten-

BOX 6.1
Radar Speckle Interferometry

The ability of radar to measure range and range rate (Doppler shift), and to image solid surfaces in two and three dimensions is well known. However, a recently introduced technique called radar speckle interferometry (RSI) is less well known. RSI can be used to make very precise measurements of the rotation vectors of Mercury, Venus and, perhaps, the icy Galilean satellites of Jupiter and estimates of the spin state direction of near-Earth asteroids. The reflected radar echo from a rough surface can be thought of as the incoherent sum of the echoes from a large number of point reflectors (e.g., wavelength-scale rocks on the surface). Since the point scatterers (rocks) do not move on the surface, the resulting speckle (diffraction) pattern, corresponding to the radar echo power as a function of direction, rotates with the planet, and part of it sweeps over Earth at a rate primarily determined by the rotation period of the planet and its distance. In angle, the speckle pattern changes very rapidly, on the scale of approximately λ/D, where λ is the wavelength of the radar signal and D is the diameter of the area that contributes to the radar echo. In the case of, say, Mercury, D is about 2,000 km and, assuming a wavelength of 3.5 cm, the scale over which the speckle pattern changes is ~3.5 milliarcsec. At Mercury's close approach to Earth of about 0.7 AU (~10^8 km), this corresponds to a distance on the surface of Earth of ~2 km.

The technique is implemented by transmitting from one antenna and receiving the echo with two widely spaced antennas, preferably several thousand kilometers apart. If the apparent rotation axis of the body being observed and projected on the sky is perpendicular to the vector joining the two receiving antennas, then the same speckle pattern determined, in the case of Mercury, by the ~2 km scale of change, sweeps over both antennas and the received signals are correlated at a time delay dictated by the rate at which the diffraction pattern sweeps over Earth. Because of the very small scale of the speckles, the time at which correlation occurs gives the orientation of the projected rotation axis to high accuracy and the time delay gives the rotation period with, in some instances, an accuracy of 1 part in 10^5. Multiple observations at different orbital orientations for Earth and the target body allow the full rotation vector to be determined.

tial threat posed by large and small NEA impacts with Earth, and by the potential of NEAs as resources for minerals for use on Earth or in space. NEAs are also being considered as possible stepping stones for human exploration of the solar system.

Over the past two decades, there has been an increasing awareness of the potential hazards posed by small asteroids in the inner solar system with orbits that may allow them to impact Earth. The impact histories on Earth, the Moon, and other bodies in the solar system, as evidenced by the large number of impact craters on their surfaces, make the threat very real. For Earth, the best-known impact is the one that likely caused the extinction of the dinosaurs about 65 million years ago. The roughly 10-km-sized asteroid that crashed into the Yucatan peninsula of Mexico at about the same time is generally believed to have been the cause.[1] The

[1] P. Schulte, L. Alegret, I. Arenillas, J.A. Arz, P.J. Barton, P.R. Bown, T.J. Bralower, G.L. Christeson,

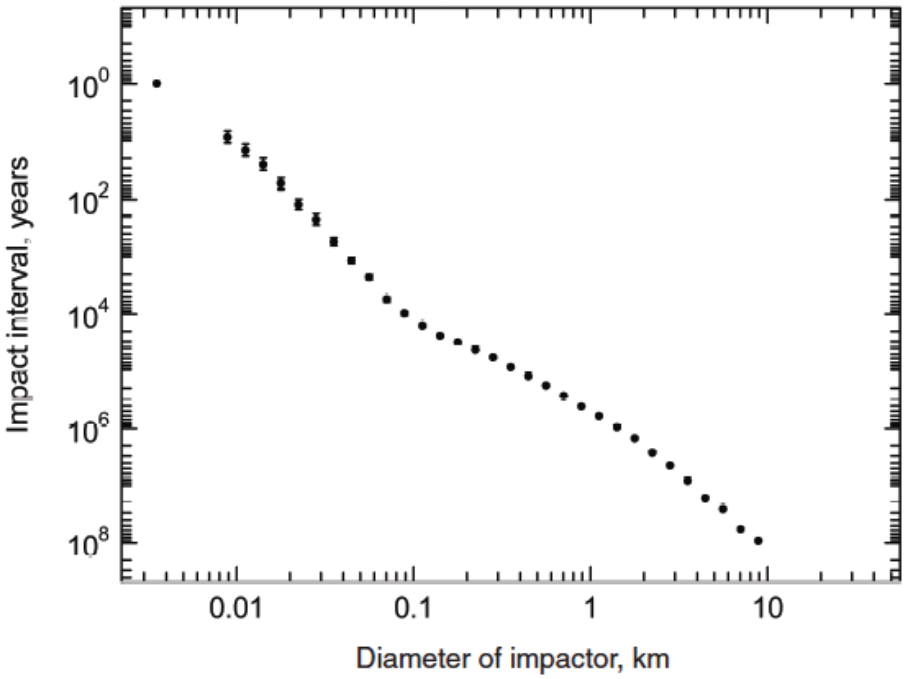

FIGURE 6.5 Current estimates of the average interval in years between collisions with Earth of near-Earth objects (NEOs) of various sizes from about 3 m to 9 km in diameter. (NEOs comprise comets as well as asteroids.) SOURCE: Alan W. Harris, Space Science Institute.

February 15, 2013, airburst of a ~20 m asteroid over Chelyabinsk, Russia, releasing energy equivalent to approximately 500 kilotons of trinitrotoluene (TNT) and injuring about 1,500 people, has highlighted the potential threat from very small NEAs, which are vastly more numerous than large ones.

Figure 6.5 shows the expected interval between impacts of NEAs on Earth as a function of their size. However, there have been recent suggestions based on analysis of the Chelyabinsk event and the number of small impact events in the interval 1984-2013 that the number of NEAs between 10 and 50 m in size may be considerably greater than previously thought, increasing the risk from the airbursts of these objects.[2]

In the 1990s, as awareness increased of the potential hazard from NEAs,

P. Claeys, C.S. Cockell, G.S. Collins, et al., The Chicxulub asteroid impact and mass extinction at the Cretaceous-Paleogene boundary, *Science* 327(5970):1214-1218, 2010.

[2] P.G. Brown, J.D. Assink, L. Astiz, R. Blaauw, M.B. Boslough, J. Borovička, N. Brachet, D. Brown, M. Campbell-Brown, L. Ceranna, W. Cooke, et al., A 500-kiloton airburst over Chelyabinsk and an enhanced hazard from small impactors, *Nature* 503:248-251, 2013.

Congress placed a mandate on NASA to find 90 percent of NEAs with diameters greater than 1 km by 2008. Known as the Spaceguard survey, the NASA project largely achieved this goal by 2009. However, in 2005 Congress established a second mandate for NASA via the George E. Brown, Jr. Near-Earth Survey section of the 2005 NASA authorization bill to find 90 percent of the potentially hazardous NEAs larger than 140 m by 2020.

The 2010 National Research Council report *Defending Planet Earth: Near-Earth Object Surveys and Hazard Mitigation Strategies*[3] strongly supported the use of both the Arecibo and Goldstone radar systems for orbit determination and characterization of near-Earth objects (NEOs). The report describes search programs for NEAs, plus orbit determination, characterization and mitigation strategies for potentially hazardous NEOs, primarily NEAs.

Earth-based radars are not effective at finding NEAs; they are discovered either optically via reflected sunlight or at infrared wavelengths via their thermal emissions. However, once found, radar is by far the best means for characterizing their sizes, shapes, rotation states, surface properties, and whether they are in multiple-body systems. No other technique short of a spacecraft flyby or orbiter can achieve the 4 m to 15 m image resolution on NEAs offered by the Goldstone and Arecibo radars. Figure 6.6 shows a series of Arecibo radar images, in delay and Doppler coordinates, of the NEA 1999 JM8 at different orientations as viewed from Earth. A series of such images at different aspect angles can be used to construct a detailed shape model of the NEA.

Radar can provide physical characterization and precise orbit information for spacecraft mission planning and navigation. Figure 6.7 shows delay-Doppler images and the derived shape model for 101955 Bennu, the target of NASA's OSIRIS-Rex orbiting and sample return mission scheduled for launch in 2016. Bennu was discovered in 1999 by the LINEAR NEA survey. Its orbit varies from 0.90 to 1.36 AU from the Sun crossing that of Earth and making it both the most accessible carbonaceous asteroid and one of the most potentially hazardous asteroids (PHAs) known. Analysis of precise radar astrometric measurements gives Bennu a cumulative probability of impact with Earth of order 10^{-3} through the 22nd century, with most of the risk associated with a potential encounter with Earth in 2182.[4]

Radar observations have shown that NEAs come in a multiplicity of sizes, shapes, and configurations—single body, contact binary, binary, and triple systems (Figure 6.8). Approximately 15 percent are in a binary configuration, and another

[3] National Research Council, *Defending Planet Earth: Near-Earth Object Surveys and Hazard Mitigation Strategies*, The National Academies Press, Washington, D.C., 2010.

[4] S.R. Chesley, Michael C. Nolan, D. Farnocchia, A. Milani, J. Emery, D. Vokrouhlický, D.S. Lauretta, P.A. Taylor, L.A.M. Benner, J.D. Giorgini, M. Brozovic, et al., The trajectory dynamics of near-Earth asteroid (101955) 1999 RQ36, American Astronomical Society Division of Dynamical Astronomy Meeting 43, Mt. Hood, Ore., Paper 7.08, 2012.

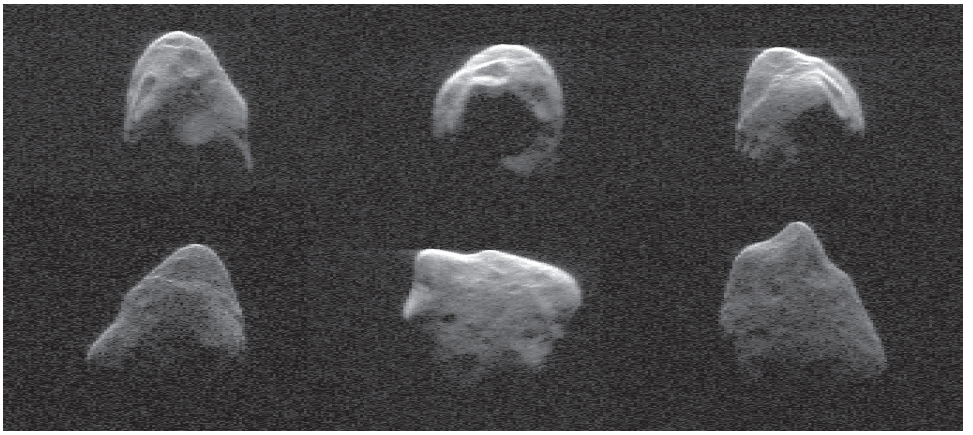

FIGURE 6.6 Arecibo delay-Doppler images of the ~3 km NEA 1999 JM8 taken at different aspect angles at a resolution of 15 m. Delay is measured from the top. SOURCE: Courtesy of Jean-Luc Margot, UCLA.

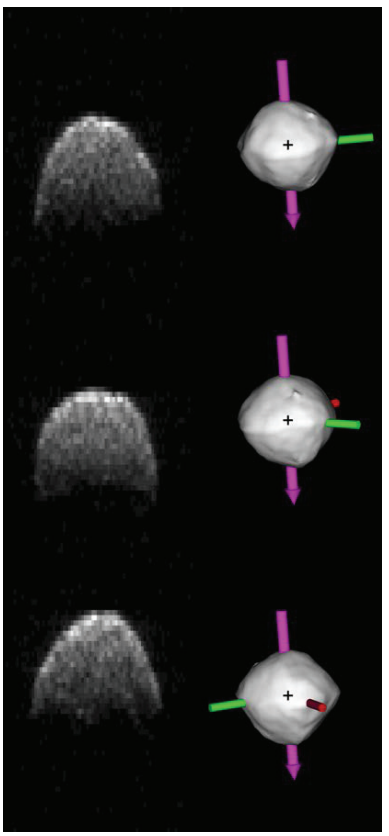

FIGURE 6.7 The Arecibo delay-Doppler images of the ~500 m diameter NEA 101955 Bennu, the target of NASA's OSIRIS-Rex mission; right column, the shape model derived from the delay-Doppler images shown at the orientation of the observations. SOURCE: Courtesy of Michael C. Nolan, Arecibo Observatory.

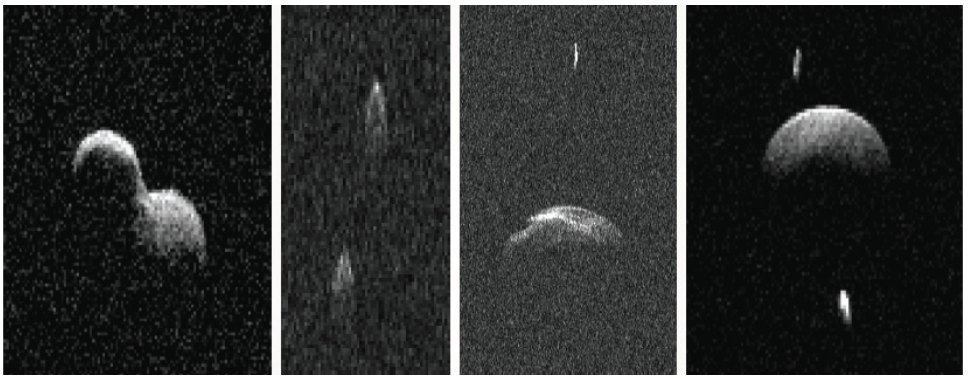

FIGURE 6.8 NEA multiple system types, delay-Doppler images. From the left, contact binary, binary with the two bodies of roughly equal size (rare), binary with a small companion, triple system with two small companions. SOURCE: Courtesy of Michael C. Nolan, Arecibo Observatory.

~16 percent are contact binaries. Only two triple systems have been discovered. Earth-based radars provide the orbit information needed to determine whether a NEA is potentially hazardous to Earth and characterization information, including whether the NEA is a multiple object system, needed to design a mitigation efffort.

For binary and triple systems, analysis of the orbits of the bodies about the center of mass of the system allows their masses to be derived. Their densities can then be determined from their volumes derived from the shape models. Density information provides insight into whether an NEA is a "rubble pile" body with high porosity or whether it is a solid body, usually a remnant of larger asteroid disrupted by a collision with another asteroid. This is critical information for designing a mitigation procedure for a potentially hazardous NEA.

Distance (time delay) and velocity (Doppler shift) measurements to NEAs can be made with a precision of about 10 m and a few mm sec^{-1}, respectively. This precision has a long-term practical value as it allows accurate orbits of NEAs to be projected into the future (and past) for about 5 times longer than is possible based on just optical position measurements. This translates roughly from about 80 years to 400 years. High-precision radar astrometry, when combined with optical plane of sky measurements, can identify which NEAs are truly potentially hazardous to Earth. The biggest uncertainty in this determination is the Yarkovsky effect (see Box 6.2),[5] and one of radar astronomy's major achievements was the confirmation that

[5] J.D. Giorgini, S.J. Ostro, L.A.M. Benner, P.W. Chodas, S.R. Chesley, R.S. Hudson, M.C. Nolan, A.R. Klemola, E.M. Standish, R.F. Jurgens, R. Rose, et al., Asteroid 1950 DA's encounter with Earth in 2880: Physical limits of collision probability prediction, *Science* 296:132-136, 2002.

BOX 6.2
The Yarkovsky and YORP effects

The Yarkovsky effect is the very small nonradial acceleration on a solar system body due to the absorption of solar radiation and its re-emission as heat. For the same reason that hot days on Earth are hottest in the early afternoon and not at midday, for an asteroid the re-emission is not back toward the Sun but rather centered on an angle that, depending on the spin state and surface properties of the asteroid, is typically about 30 degrees producing, owing to the momentum carried by the emitted infrared photons, a tiny force in the opposite direction (Figure 6.2.1). Over very long time spans, this force can significantly modify the orbit of a small solar system body and is the greatest source of uncertainty in the long-term prediction of the orbits of near-Earth asteroids (NEAs). The possibility of this effect has been known for a long time, but its effectiveness was only demonstrated in 2003 by precise distance and velocity radar measurements to a small NEA, Golevka, over a number of years. Golevka's distance and velocity during the last measurement could only be accounted for if the Yarkovsky effect was real. Apart from its effect on NEA orbits, the confirmation of the Yarkovsky effect had profound implications for our understanding of how small bodies in the main asteroid belt between Mars and Jupiter are translated into the inner solar system.

The YORP (Yarkovsky, O'Keefe, Radzievskii, Paddack) effect is similar to the Yarkovsky effect except that it acts over very long time scales on surface irregularities to spin up or down a small body and, potentially, change its spin axis direction. It was confirmed by a combination of optical and radar observations in 2007. The YORP effect is thought to be responsible for producing binary NEAs by spinning them up until they become gravitationally unstable.

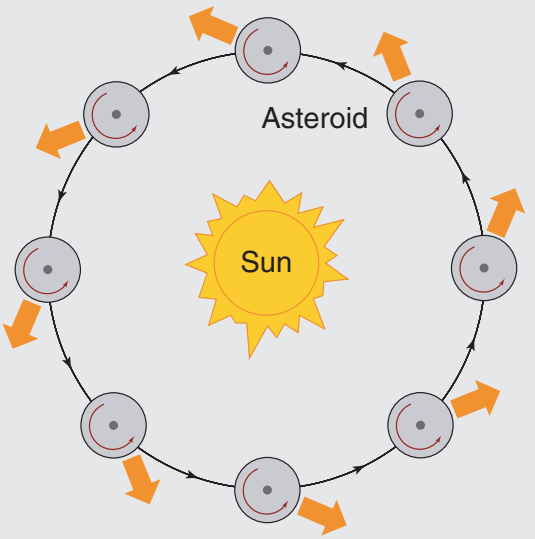

FIGURE 6.2.1 A diagram showing the direction of the force due to the Yarkovsky effect on a small body orbiting the Sun. The direction is dependent on the near-Earth asteroid's rotation direction and period. SOURCE: D.P. Rubincam, Yarkovsky thermal drag on small asteroids and Mars-Earth delivery, *Journal of Geophysical Research: Planets* 103(E1):1725-1732, 1998.

the Yarkovsky effect can alter the orbits of small bodies in the solar system.[6] This resolved a long-standing issue in solar system research, namely how the population of NEAs is replenished from the main asteroid belt between Mars and Jupiter since the average life of an NEA is only a few million years due to collisions with the Sun, planets, and smaller bodies. The Yarkovsky force on small bodies in the main asteroid belt is capable of moving them into resonance orbits with Jupiter, from which they can be transported into the inner solar system.[7]

Estimates of the Yarkovsky force based on estimates of the mass and thermal inertia of an NEA allows improved orbit predictions. Alternatively, measurements of the Yarkovsky drift rate for a NEA can be used to estimate its mass and rotation direction.[8] Knowledge of its approximate size allows its density to be estimated, providing, in the case of a hazardous object, critical information for mitigation planning that is not biased by the requirement that the NEA be in a binary or triple system.

Radar observations from Earth continue to provide new information about the terrestrial planets and the Moon despite the many spacecraft flybys, orbiters, and landers. The unique radar back-scattering properties of water ice led to the discovery by ground-based radar of ice deposits in the permanently shadowed portions of impact craters at Mercury's poles. High-resolution (1.5 km) radar imaging of these deposits has mapped out their distribution with high precision[9] (Figure 6.9). Further study of the deposits was a high priority of NASA's current Messenger mission to Mercury. Radar speckle interferometric measurements of Mercury's spin vector revealed the presence of a liquid outer core, a major advance in our understanding of this planet (Figure 6.10).

Radar is the only effective means for detailed studies of the surface of Venus due to its optically opaque cloud cover. With no new radar missions planned for the foreseeable future, only Earth-based radars, primarily the one at Arecibo, are capable of monitoring the planet's surface. Major objectives for continuing observations of Venus are the confirmation of current volcanic activity by direct observation of new surface lava flows; the investigation via the polarization properties of the reflected echo of potential landing sites, especially those on tesserae terrain,

---

[6] S. R. Chesley, S.J. Ostro, D. Vokrouhlický, D. Čapek, J.D. Giorgini, M.C. Nolan, J.-L. Margot, A.A. Hine, L.A.M. Benner, and A.B. Chamberlin, Direct detection of the Yarkovsky effect by radar ranging to Asteroid 6489 Golevka, *Science* 302:1739-1742, 2003.

[7] W.F. Bottke, D. Vokrouhlicky, D.P. Rubincam, and D. Nesvorny, The Yarkovsky and YORP effects: Implications for asteroid dynamics, *Annual Review of Earth and Planetary Sciences* 34:157-191, 2006.

[8] C.R. Nugent, J.L. Margot, S.R. Chesley, and D. Vokrouhlicky, Detection of semi-major axis drifts in 54 near-earth asteroids: New measurements of the Yarkovsky effect, *The Astronomical Journal* 144:60, 2012.

[9] J.K. Harmon, M.A. Slade and M.S. Rice, Radar imagery of Mercury's putative polar ice: 1999-2005 Arecibo Results, *Icarus* 211:37-50, 2011.

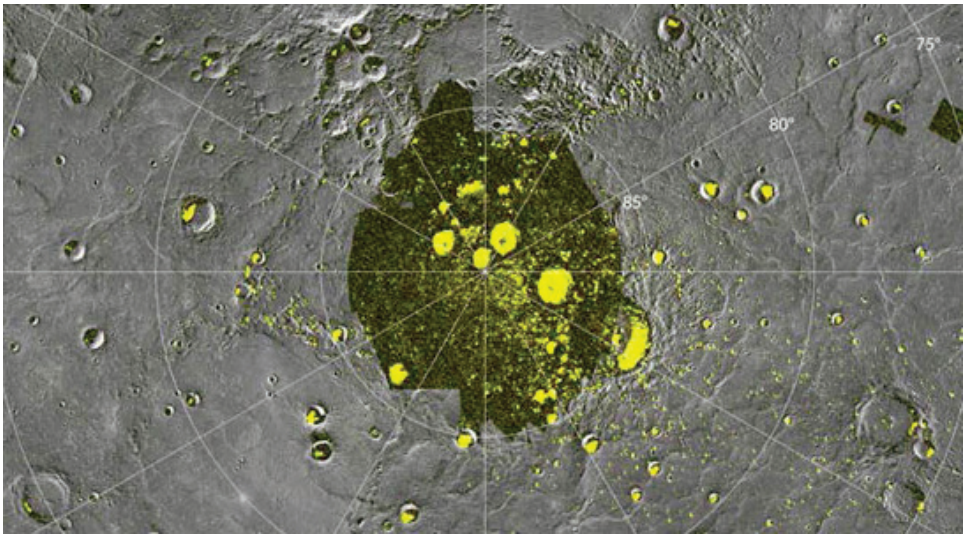

FIGURE 6.9 Arecibo radar image of the distribution of ice deposits at the north pole of Mercury (yellow), superimposed on a mosaic of Messenger orbiter images showing the coincidence of the ice deposits with the shadowed portions of impact craters. SOURCE: NASA/Johns Hopkins University Applied Physics Laboratory/Carnegie Institution of Washington.

believed to be the oldest extant surfaces on the planet; and radar speckle interferometric measurements of the planet's spin vector to monitor changes thought to be due to the transfer of angular momentum between the atmosphere and the solid planet. New Arecibo/Green Bank Telescope (GBT) bistatic observations of Venus were made in 2012 (Figure 6.11) and compared with reprocessed Arecibo imagery from 1988 and Magellan images to look for possible surface changes due to volcanic activity, but, to date, no evidence of change has been detected. Arecibo to the Very Large Array (VLA) bistatic observations have the potential to provide high resolution radar imagery of Venus free of the North-South (N-S) range-Doppler ambiguity issues apparent in Figure 6.11.

Radar's ability to penetrate into dry, low-electrical-loss surfaces enables the investigation of the near subsurface. This is especially useful for the Moon, where the regolith, the upper 5 m to 15 m of the surface that has been pulverized into fine material by meteoritic impacts, masks the underlying stratigraphy, and for Mars, where dust deposits over many areas also mask the underlying rocky surface. Figure 6.12 shows an Arecibo radar image of Mare Serenitatis on the Moon made at 70 cm wavelength, where the penetration depth is 5 to 10 m, compared with an optical image. Extensive subsurface structure is apparent in the radar image, sug-

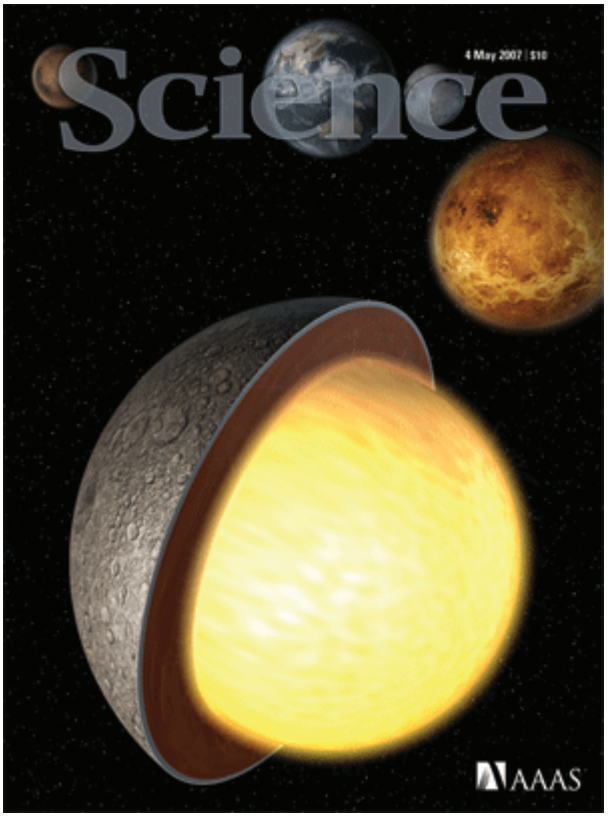

FIGURE 6.10 Cover page of *Science* magazine from May 4, 2007, highlighting the paper "Mercury librations measured by Earth-based radar" by J.L. Margot, S.J. Peale, R.F. Jurgens, M.A. Slade, and I.V. Holin (Volume 316, No. 5825, pp. 313-330), which showed that Mercury has a liquid outer core. Reprinted with permission from AAAS.

gesting volcanic flow fronts, channels, and the like. The demonstrated ability of Arecibo's 70 cm wavelength radar to probe several meters below the surface of the Moon (Figure 6.12) will be used to study layered volcanic ash and lava deposits, potentially ice-bearing polar craters, and early mare-forming volcanic deposits now buried by basin debris. High-resolution (~20 m) 2.38 GHz imagery will be obtained to complement the similar resolution and frequency imagery from the mini-radio frequency (RF) radar that was on the Lunar Reconnaissance Orbiter.

Moon sensitivity is not an issue, but the range resolution of the radar images is limited by the bandwidth of the transmitter system, in this case about 200 m, due to the small bandwidth of the Arecibo 70 cm wavelength transmitter.

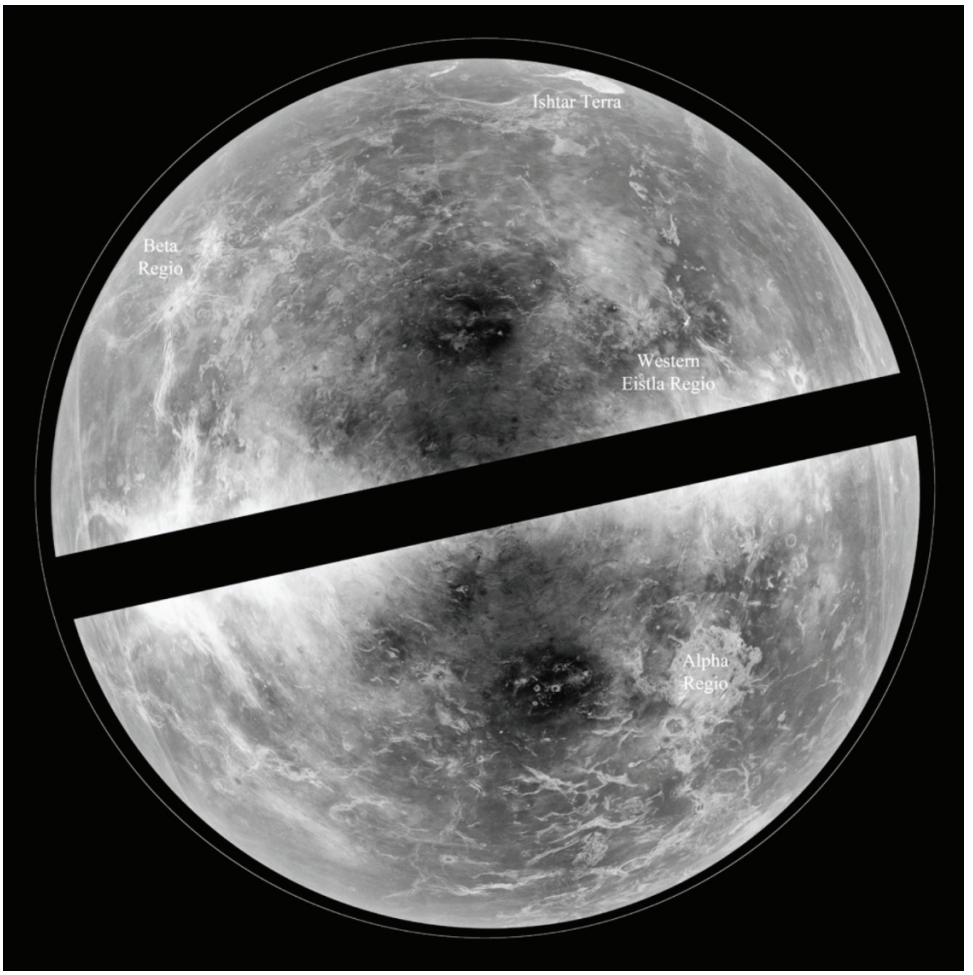

FIGURE 6.11 Arecibo/GBT radar image of Venus made from data acquired in 2012. The resolution is 1 to 2 km. Problems related to the N-S range-Doppler ambiguity causes ghost images in the opposite hemisphere, especially for radar bright features such as Alpha Region. The black bar is the location of the Doppler equator, which is perpendicular to the apparent rotation axis as viewed from the radar. It is not possible to image the surface close to this equator. The outer line is the edge of the planet's projected disk. SOURCE: Courtesy of NASA/GSFC/Arizona State University.

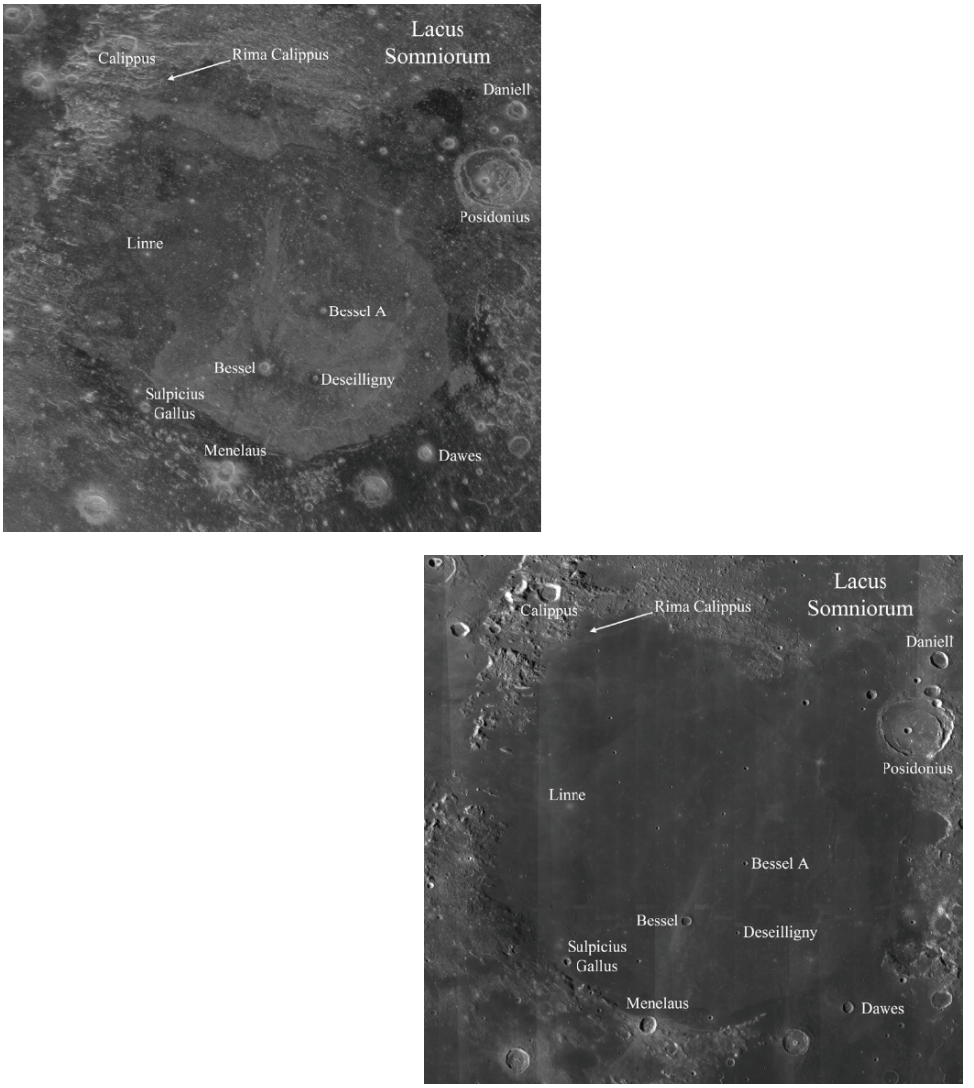

FIGURE 6.12 (*Left*) An Arecibo 70 cm wavelength image of Mare Serenitatis on the Moon showing echo power differences thought to arise from the blocky transition zone between the upper lunar regolith and the solid bedrock. The backscatter differences highlight lava flow units, lobes, channels and what is thought to be a large graben that has been flooded by lava flows. (*Right*) A lunar reconnaissance orbiter wide-angle camera mosaic optical view of the same region. There is little evidence of the structures apparent in the radar image. SOURCE: NASA/GSFC/Arizona State University; see B.A. Campbell, B. Ray Hawke, G.A. Morgan, L.M. Carter, D.B. Campbell, and M. Nolan, Improved discrimination of volcanic complexes, tectonic features, and regolith properties in Mare Serenitatis from Earth-based radar mapping, *Journal of Geophysical Research-Planets* 119:313-330, 2014, doi:10.1002/2013JE004486.

FUTURE SCIENCE DRIVERS AND TECHNICAL REQUIREMENTS

Near-Earth Asteroids

For at least the next decade, the emphasis of the Earth-based planetary radar program will be on astrometric and characterization observations of NEAs. None of the kilometer-sized and above known NEAs pose a risk to Earth over the foreseeable future.[10] It is from the vast number of smaller bodies, as small as a few tens of meters, that the perceived near-term threat arises. It is this threat that is driving the desire for higher-resolution radar imaging and, due to the lower echo strength from each resolution cell as the resolution improves, higher sensitivity to improve the characterization capabilities.

The required modulation bandwidth of the transmitter to achieve a range resolution of ~8 m is 20 MHz. This is the current limit of the Arecibo 2.38 GHz radar system set by the maximum bandwidth of its klystrons of ~25 MHz. The maximum bandwidth of a klystron is normally a fraction, about 1 percent, of its operating frequency but can be increased at the cost (apart from dollars) of lower gain, lower efficiency, and greater weight. The two 250-kW 8.56-GHz klystrons currently in the transmitter on the Goldstone antenna have a bandwidth of 50 MHz, allowing a range resolution of ~4 m. New signal-processing instrumentation is allowing researchers to take advantage of this bandwidth with spectacular results (Figure 6.13), and a new klystron design has been developed that would have a bandwidth in excess of 100 MHz, allowing range resolutions of about 2 m. In the direction orthogonal to range, the azimuth or Doppler direction, the Doppler broadening of the radar echo from a rotating NEA is linearly dependent on the transmitter frequency. This means that achieving the spectral resolution corresponding to the size of the desired resolution cell is easier at higher frequencies.

For a given antenna, higher resolution in both range and Doppler plus increased sensitivity can be achieved most easily by moving the radar to a higher frequency, since sensitivity is proportional to $\lambda^{-3/2}$ and the klystron bandwidth is about 1 percent of the transmitted frequency. For the 70 m Goldstone antenna, surface accuracy is a limitation to going to significantly higher frequencies. For Arecibo, doubling the frequency to 4.6 GHz, where there are existing high-power klystrons used by the particle accelerator community, is being considered. This would allow a bandwidth of about 50 MHz, giving a range resolution of ~4 m.

For the current Arecibo and Goldstone radar systems, two other means for increasing their sensitivities are to increase transmitter power and/or to use a

[10] It is estimated that there remain approximately 1,000 undiscovered kilometer-sized NEAs. As of February 17, 2015, there were approximately 866 km-sized (or above) NEAs known (per http://neo.jpl.nasa.gov/stats/). The population is believed to contain 1,090 ± 180 objects (per Stuart and Binzel 2004), or about 940 (per Harris 2008).

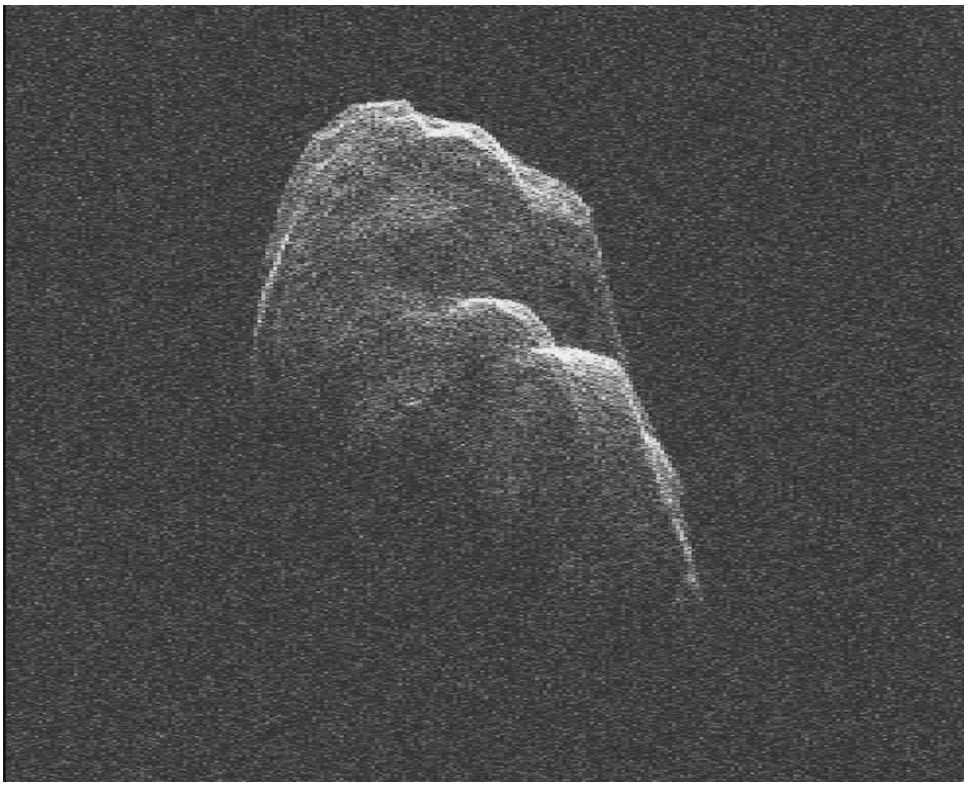

FIGURE 6.13 Goldstone radar image at 4 m resolution of the 4.8 km sized NEA Toutatis made on December 12, 2012 as it passed within 18 lunar distances from Earth. SOURCE: NASA/JPL-Caltech; see PIA16599: Tumbling Asteroid Toutatis, http://photojournal.jpl.nasa.gov/catalog/PIA16599.

larger antenna for reception. For Arecibo, neither of these options is possible as no other antenna has a larger collecting area, and it is already transmitting close to a megawatt. Any increase in power would require an unacceptable increase in weight on the suspended structure of the antenna. Doubling the power of the Goldstone transmitter to 1 MW is being considered, utilizing four of the newly designed wideband klystrons. Utilizing the 100 m GBT in West Virginia for echo reception would increase the sensitivity of the Goldstone radar by a factor of two to three, and utilizing Arecibo for reception for those objects that are within Arecibo sky coverage would increase sensitivity by a factor of about four.

The possibility of an 8.6 GHz radar system on the 100 m GBT is being discussed. Assuming a 500 kW transmitter similar to that on the Goldstone 70 m antenna, a GBT-based radar system would have about four times the sensitivity of

TABLE 6.2 Possible Upgrades to Current Radar Systems and Potential New Systems

Transmitting Location	Frequency (GHz)	Bandwidth (MHz)	Power (MW)	Receive Location
Green Bank Telescope, West Virginia	8.6	100	0.5	GBT, West Virginia VLA, New Mexico Goldstone, California
Arecibo, Puerto Rico	4.6	50	0.5	Arecibo, Puerto Rico GBT, West Virginia
Goldstone DSS-14, California	8.60	120	1.0	Goldstone, California GBT, West Virginia Arecibo, Puerto Rico

the Goldstone radar and would be more available since the 70 m Goldstone antenna is a prime component of NASA's Deep Space Network (DSN).

For NEAs that pass very close to Earth, within a few lunar distances, nimbleness is more important than sensitivity because of the R^{-4} dependence on echo strength, where R is the distance to the NEA. These are typically small NEAs that are discovered only a short time before their close approach to Earth, so it is important to be able to react quickly. To foster this, NASA/Jet Propulsion Laboratory (JPL) has recently equipped one of its 34 m DSN antennas with an 80 kW transmitter operating at 7.210 GHz. Reception will be with another nearby 34 m DSN antenna, DSS-28.

Table 6.2 lists possible upgrades to the current planetary radar transmitting systems, and one potential new system, in the United States. None of these systems is currently funded, except for the new NASA Goldstone radar at 7.210 GHz.

Venus, the Moon, and the Galilean Satellites

Owing to the difficulty of seeing through its cloud cover, Venus remains the least-explored terrestrial planet. Yet, given how close it is to Earth in size, we clearly have much to learn from it related to Earth's evolution. Since the atmosphere of Venus is relatively transparent for radio waves at frequencies below about 3 GHz, radar is the only method for obtaining large-scale imagery and topographic information for the planet. With no radar-equipped spacecraft mission currently planned, a program of Earth-based radar imaging at 1 to 2 km resolution searching for active volcanism (Figure 6.14) and studying potential landing sites for future lander missions will continue over the next decade. Observing small changes in the surface of Venus over time requires high-quality imaging. The quality of the current monostatic, Arecibo to Arecibo, and bistatic, Arecibo to the GBT, imaging is compromised by the N-S ambiguity problem (Figure 6.11). The recent upgrading

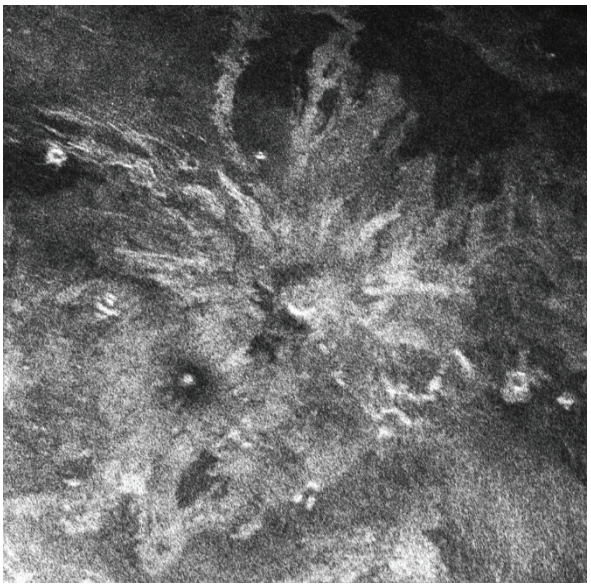

FIGURE 6.14 An Arecibo radar image of the volcano Sif Mons on Venus made in 1988. Future Arecibo radar images will be used to look for changes indicating very recent volcanic activity. SOURCE: Courtesy of Donald B. Campbell, Cornell University.

of NSF's VLA in New Mexico has equipped it with receivers at the S-band, the frequency of the Arecibo radar system, allowing a return to the use of interferometry to resolve the N-S ambiguity and provide very-high-quality, 1- to 2-km imagery free of ambiguity defects. Some modification of the VLA's data acquisition system will be needed before this technique can be implemented.

Radar speckle interferometric measurements of Europa and Ganymede, two of the icy Galilean satellites of Jupiter, are providing measurements of their obliquities, the angles between the rotation axis and the plane of their orbits about Jupiter. These measurements have the potential to reveal the presence of subsurface oceans and to generally help in constraining interior models of these satellites.[11] The sensitivity of these measurements is about 3,000 times smaller than for the equivalent measurements on Mercury, so any increase in sensitivity of the Goldstone radar system or the installation of an equivalent system on the GBT would help resolve some of the most important issues regarding these satellites.

[11] J.-L. Margot, S. Padovan, D.B. Campbell, S. Peale, and F. Ghigo, Measurements of the spin states of Europa and Ganymede, American Astronomical Society Division for Planetary Sciences Meeting 45, Paper 504.02, 2013.

FREQUENCY ASSIGNMENT REQUIREMENTS

Over a wide range of wavelengths, the optimum frequency for almost all Earth-based planetary radar observations is driven by the need to maximize sensitivity and, to a lesser extent, the transmitting bandwidth. The exceptions are observations of Venus, where the atmosphere is highly absorptive at frequencies much above 3 GHz, and of the Moon, where long wavelengths allow penetration into the surface and sensitivity is not normally an issue. Since very large antennas are required, the optimum frequency is dictated by the maximum frequency at which the antenna can efficiently operate and the availability of klystrons capable of providing between 250 kW and 500 kW of output power.

Transmitting Stations

The only two transmitting locations currently in operation are NSF's Arecibo Observatory in Puerto Rico and NASA's Goldstone complex in California. For the two transmitters used for planetary radar astronomy at Arecibo, the National Telecommunications and Information Administration (NTIA) frequency assignments are the 20 MHz bandwidth centered on 2.380 GHz and the 0.5 MHz bandwidth centered on 0.430 GHz.

For the two transmitting stations used for planetary radar astronomy at NASA's Goldstone site, there are NTIA assignments of 200 MHz centered on 8.60 GHz at the 70 m DSS-14 antenna, and an 80 MHz allocation centered on 7.210 GHz at the 34 m DSS-13 antenna.

A transmitting capability at NSF's GBT in West Virginia could be based on the redesigned 8.60 GHz klystron if a NTIA frequency assignment of ~120 MHz bandwidth centered on 8.600 GHz is requested and approved, or it could utilize the currently available 8.56 GHz klystrons. Any upgrade of the Arecibo transmitter would likely want to utilize an existing klystron at 4.60 GHz, and the request would be for a 60 MHz assignment about this center frequency. Alternatively, if a suitable klystron can be developed, the bandwidth of the Arecibo 2.38 GHz system could be increased to 50 MHz, and a wider bandwidth frequency assignment would be needed.

Reception at these stations would be at the same frequencies, so radio frequency interference (RFI) is a significant concern. With the exception of the 430 MHz band at Arecibo, there have been no serious RFI issues to date at either the Goldstone or Arecibo locations. For the 430 MHz Arecibo system, interference is a major concern but primarily for the use of the system as an incoherent scatter radar for studies of Earth's upper atmosphere. The lunar radar studies are conducted bistatically with reception with the GBT, where interference is not an issue owing to its siting in the Radio Quiet Zone straddling part of the border between West Virginia and Virginia.

Bistatic Reception

Radar astronomy makes use of several antennas for reception, apart from the transmitting stations. For Arecibo transmissions, these are NSF's GBT and VLA in New Mexico. For Goldstone, they are NSF's GBT, Arecibo, and the antennas of the Very Long Baseline Array (VLBA). Goldstone transmissions also use other 34 m antennas at NASA's Goldstone complex for reception. Of these, the GBT is the most heavily used for reception, and its location in the Radio Quiet Zone keeps it largely free of terrestrial interference. The VLA and VLBA antennas are in relatively remote locations, and terrestrial interference in the bands being used for radar astronomy has not been a problem.

FINDINGS AND RECOMMENDATION

Finding 6.1: Active remote sensing through planetary radar astronomy continues to make important contributions to our understanding of the solar system, planning for space missions to extraterrestrial objects, and in particular for the tracking and characterization of NEAs that may pose a threat to society.

Finding 6.2: Radio frequency interference has not been a significant impediment to planetary radar astronomy observations to date. However, as bandwidth requirements increase due to the need to image NEAs at high spatial resolution, RFI could pose a significant problem in the future. To facilitate high-spatial-resolution imaging of small NEAs, frequency assignments with bandwidths of 60 MHz to 120 MHz are required. The NASA JPL Goldstone radar currently has an assignment of 200 MHz centered at 8.600 GHz.

Recommendation 6.1: If deemed worthwhile by the astronomy community, and if the National Science Foundation (NSF) considers it appropriate, NSF should seek frequency assignments in the relevant bands for the proposed Green Bank Telescope and upgraded Arecibo radar systems to facilitate high-spatial-resolution imaging of small near-Earth asteroids.

7

Spectrum Access: Allocation Policies and the Assignment Process

INTRODUCTION

The radio frequency (RF) spectrum has many uses beyond the popular mobile communications and TV broadcasting. The onset of smart phones, tablets, and machine-to-machine communications has created great demand for wireless broadband and digital data to support numerous mobile applications. This increased demand for mobile broadband creates a derived demand for additional RF spectrum for mobile broadband. Some of the many examples include smart phone applications, as well as wireless broadband deployed in support of applications in agriculture, automotive, education, energy efficiency, health, commerce, and smart cities. The largest increase in mobile broadband use has been in video. By the end of 2013 it was estimated that greater than 50 percent of wireless broadband use was for video.[1] This is expected to continue to be the greatest driver of additional wireless broadband demand.

[1] Sandvine, *Global Internet Phenomena Report*, 2013, https://www.sandvine.com/downloads/general/global-internet-phenomena/2013/2h-2013-global-internet-phenomena-report.pdf.

RADIO SPECTRUM POLICIES

U.S. Radio Spectrum Policies

U.S. spectrum policy is driven by its broader broadband policy, which can be summarized as "more is better." In 2010, the U.S. Federal Communications Commission (FCC) issued a National Broadband Plan (NBP).[2] This plan set a goal of allocating an additional 500 MHz of RF spectrum to mobile broadband uses over the next 10 years. Two significant reallocations meet a portion of this goal and will be available in the next few years:

- *Advanced Wireless Services, Band 3 (AWS-3)*. This will extend the existing wireless broadband AWS band and make 65 MHz of spectrum available through a combination of reallocating and sharing with federal users.
- *TV Incentive Auction*. This will simultaneously buy out TV broadcasters and sell the reclaimed RF spectrum to mobile broadband providers. The amount of spectrum reallocated will be determined in the auction by a combination of what mobile wireless providers are willing to pay and how much TV broadcasters demand for their licenses. If properly designed and executed, this auction should reallocate up to 120 MHz from TV to mobile broadband uses.

These two allocations, however, comprise less than 200 MHz of new spectrum for mobile broadband. Meeting the remainder of the NBP's goal of 500 MHz of spectrum will be difficult because it will involve significant transfers of spectrum currently dedicated to various uses by federal government agencies.[3] Much of this spectrum is likely to be made available to the private sector only on a shared basis.

International Radio Spectrum Policies

The United States is not alone in its desire to have more RF spectrum available for commercial uses. Table 7.1 is a snapshot across the world indicating the amount of spectrum in the pipeline for mobile broadband, and Figure 7.1 depicts the large and growing global use of mobile phones. Finding this additional spectrum is a challenge for policy makers and may be unattainable. The tools available to policy makers to meet these goals consist of reallocation, spectrum sharing, and developing higher spectral efficiencies.

[2] FCC, "National Broadband Plan," https://www.fcc.gov/national-broadband-plan, accessed June 4, 2015.

[3] It is also possible that spectrum allocated to satellite uses that could be used terrestrially could go toward this 500 MHz.

TABLE 7.1 Summary of Total Available Licensed Spectrum Available for Mobile Broadband (in megahertz)

Country	Total (Current + Pipeline)
United States	663+ (608 + 55)
Australia	708 (478 + 230)
Brazil	554 (554 + 0)
China	587 (227 + 360)
France	605 (555 + 50)
Germany	615 (615 + 0)
Italy	560 (540 + 20)
Japan	510 (500 + 10)
Spain	600 (540 + 60)
United Kingdom	618 (353 + 265)

NOTE: U.S. Pipeline numbers do not include the significant amount of spectrum that will be made available for mobile broadband from incentive auctions and federal repurposing.
SOURCE: Federal Communications Commission, "The Mobile Broadband Spectrum Challenge: International Comparisons," FCC White Paper, Wireless Telecommunications Bureau, Office of Engineering and Technology, Washington, D.C., February 26, 2013.

Outside the United States, it is common to allocate spectrum to a specific cellular technology (2G, 3G, or 4G). Reallocation, sometimes referred to as refarming, could involve moving from 3G to 4G services and enabling higher efficiencies, exploiting the digital dividend from more efficient TV broadcasting technology, or finding bands of low usage and thus reallocating them to a higher use. Exploiting the digital dividend by migrating from analog to digital TV, and freeing up spectrum for other uses in the process, is a primary means of providing additional spectrum.[4] The Mobile Satellite Services (MSS) spectrum is also under consideration for terrestrial uses.

The European Union (EU) has been addressing the potential for spectrum sharing through the TV Whitespace, as well as Licensed Shared Access (LSA) and Authorized Shared Access (ASA) for both the 2.3 GHz and the 3.5 GHz band.

With additional capital investments, higher spectral efficiencies can be obtained by waveform and network optimization as well as higher spatial reuse (cell splitting). Moving from waveforms for voice services to data services can provide sig-

[4] Over the past decade, interest was expressed by both the private sector and government institutions in several countries, including the United States, to develop high-speed communication using the power grid instead of towers and repeaters. To date, the concept has not materialized, but should such an approach become feasible, its potential RFI effects on active sensing could be detrimental.

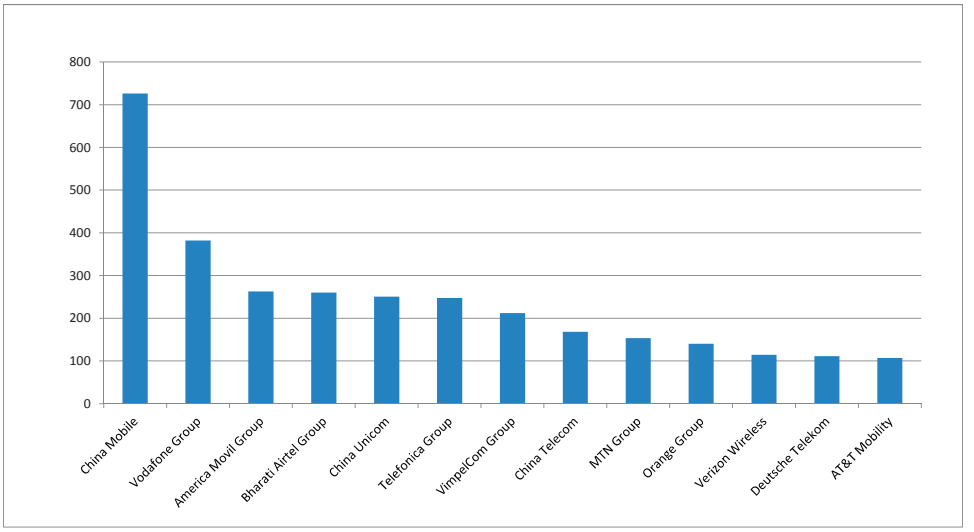

FIGURE 7.1 Top 13 mobile operators. SOURCE: Data from J. Groves and W. Croft, "Operator Group Ranking, Q1 2013: Chinese Carriers Continue Strong Growth; Egypt Deal Lifts Orange," Research, GSMA Intelligence, July 4, 2013, https://gsmaintelligence.com/research/.

nificant improvements in spectral efficiency. Enabling greater use of femtocells[5] and tower access and thus higher spatial reuse can also have significant positive impacts.

SPECTRUM ALLOCATION AND ASSIGNMENT

The entire radio spectrum is divided into blocks or bands of frequencies that are used for specific types of services. The spectrum management process is broken up into two general areas: spectrum allocation and spectrum assignment.

Spectrum allocation determines what blocks of frequencies are used for what specific purpose under a set of technical and operational rules. For example, spectrum managers in some countries have allocated 698 to 793 MHz band (a.k.a. 700 MHz band) for mobile services that eventually became 4G/LTE mobile broadband. Spectrum can be allocated on a primary basis in which that service is given priority and is protected from other services that may come in at a later date and create interference to the operations of the primary allocated service. Spectrum can be allocated on a coprimary basis in which its use is also protected in the same manner as a primary service. Secondary allocations are for services that are allowed but must protect all primary (and co-primary) services. For example:

[5] Femtocells are discussed in Chapter 9.

- Primary allocation in the 3.1 to 3.3 GHz band is Radio Location Service (RLS), which includes S-band radars.
- Secondary allocation in the 3.1 to 3.3 GHz band is Earth Exploration Satellite Service (EESS) and Space Research Services (SRS).

Spectrum assignment determines who gets to access blocks of the spectrum over a specific geographic region in support of a specific service. This comes in the form of a license or an assignment. A typical example of this would be a major cellular service provider (e.g., Verizon Wireless, AT&T, T-Mobile) licensed to operate specific blocks of spectrum in the 700 MHz band, or the military being assigned a band for its exclusive use. In some cases, spectrum can be accessed through "license by rule" in which a specific entity is allowed to operate but does not have a license. This is also called unlicensed spectrum (United States) and license-free spectrum (EU). One well-known example is the Wi-Fi band at 2.4-2.483 GHz.

U.S. Framework

Radio regulation in the United States began in 1910 with the Wireless Ship Act requiring ocean going ships to have transmitting equipment. The sinking of the Titanic in 1912 precipitated international obligations in wireless communications and eventually in the Radio Act of 1912. The Radio Act provided regulation for licensing all transmitters for interstate and foreign commerce to be overseen by the Secretary of Commerce.

During the 1920s there was an explosion of requests for licenses and burgeoning interference concerns, which were addressed by then Secretary of Commerce Herbert Hoover. The Radio Act of 1927 established a new temporary independent agency, the Federal Radio Commission, with the stated purpose to resolve these numerous interference issues.[6] The commission was empowered to impose rules and regulations for both the licensing and operations of the radio spectrum.

In 1934 Congress passed the Communications Act, which put both wired and wireless communications under the regulatory control of a permanent agency called the Federal Communications Commission. Ever since, the FCC has been directed by five commissioners appointed by the President and confirmed by the

[6] Some argue that its ulterior purpose was to protect incumbent interests and limit competition. See T. Hazlett, The wireless craze, the unlimited bandwidth myth, the spectrum auction faux pas, and the punchline to Ronald Coase's big joke—An essay on airwave allocation policy, *Harvard Journal of Law and Technology* 14(2), 2001.

Senate for 5-year terms. The President designates one commissioner to serve as chairman. Today the Commission has 7 bureaus and 11 staff offices.[7]

The United States has a separate administrative office that manages federal use of the RF spectrum. The Office of Spectrum Management within the NTIA of the Department of Commerce provides this function. Therefore the United States has two separate organizations providing spectrum management: an independent agency, the FCC, for all nonfederal uses and the executive branch office of NTIA for federal uses. In addition to the two regulatory agencies, the U.S. Congress also intervenes in spectrum policy—for example, by directing the reallocation of a band of spectrum and then mandating that the reallocated frequencies be auctioned.

International Framework

Spectrum policy and management at the international scale is broken into cooperative activities across borders in the shape of treaties and regulatory activities within a sovereign nation. The use of RF spectrum is very different than use of other national resources. First of all, RF transmissions cannot be contained at the borders, and thus border agreements between nations to address potential interference scenarios must be addressed. Secondly, uses of the RF spectrum in space (for example, satellite systems) need to be coordinated because the actual transmitters cross international borders.

Cooperation at the international scale for spectrum management occurs both at the global level, in the form of agreements made at the International Telecommunications Union (ITU), and at the regional level, such as the European Conference of Postal and Telecommunications (CEPT) Administration.

The ITU is a specialized agency within the United Nations. It specializes in promoting cooperation for spectrum allocation and global regulation of the radio spectrum. Individual countries sometimes deviate from ITU rules and spectrum allocations, however, because the organization does not have an effective enforcement mechanism for its rules and allocations and thus largely depends on countries to abide by the rules because it is in their own long-term self-interest to do so. The ITU has divided the world into three regions to enable specific rules and spectrum allocations customized to those geographies (see Figure 7.2). This methodology may no longer be appropriate because of the global nature of the telecommunication marketplace.

One division of the ITU, the ITU-R (Radio Communication Sector), holds

[7] The seven bureaus are Consumer and Government Affairs, Enforcement, International, Media, Public Safety and Homeland Security, Wireless Telecommunications, and Wireline Communications (see Federal Communications Commission, "Bureaus and Offices," http://www.fcc.gov/bureaus-offices, accessed June 4, 2015).

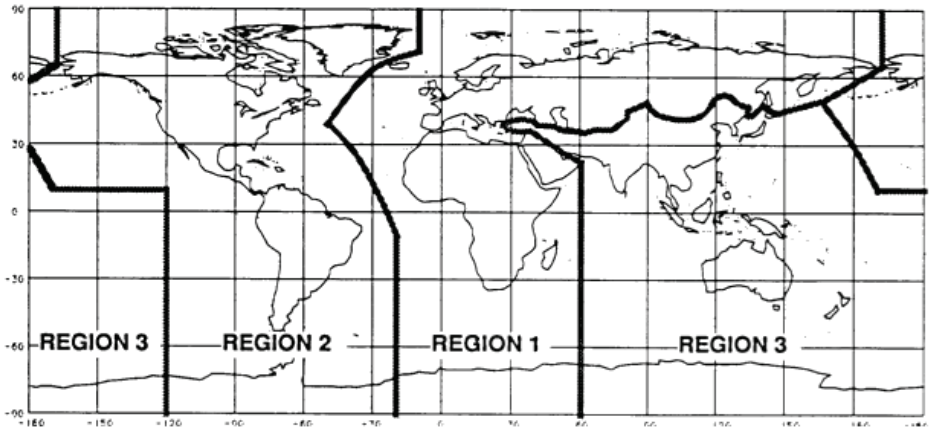

FIGURE 7.2 International Telecommunication Union geographic regions. SOURCE: NASA, *NASA Radio Frequency (RF) Spectrum Management Manual*, NASA Procedural Requirement (NPR) 2570.1B, effective date December 5, 2008, Figure 1-1, http://nodis3.gsfc.nasa.gov/npg_img/N_PR_2570_001B_/N_PR_2570_001B_.pdf.

the World Radiocommunication Conference (WRC), where it proposes intergovernmental treaties on spectrum allocations. The most recent WRC was held in 2012, and the next conference is scheduled for 2015. The U.S. delegation is led by a term-limited ambassador specifically appointed for the WRC. The results of a conference are sets of treaties on spectrum allocations and equipment rules. Any such treaties need to be ratified by the U.S. Senate if they are to become binding within the U.S. regulatory framework. There have been multiple occasions where only a limited number of the treaties from a specific WRC are ratified. Therefore the rules and allocations adopted by either the FCC or NTIA are not always in agreement with those of the ITU.

Regional organizations, such as CEPT, are voluntary associations across the member communities. They attempt to develop common policies and regulations across their community and are a focal point for information on spectrum use among its members. An example of regulations would be a series of recommendations for the technical rules for specific services and/or recommendations for how to perform interference analysis on specific systems. Many of the technical rules that are implemented by regulators across the world are based, at least in a small part, on these analyses and recommendations.

U.S. Federal Assignments

Federal frequency assignments are provided by the Office of Spectrum Management within NTIA. NTIA has a formal process in which all federal spectrum users provide advisory support through the Interdepartmental Radio Advisory Committee (IRAC). The following two examples demonstrate how federal departments provide support in securing frequency assignments:

- *National Science Foundation (NSF).* The Electromagnetic Spectrum Management (ESM) unit at NSF is responsible for assisting projects and systems to gain access to the radio spectrum for research. ESM is represented in IRAC and participates in ITU committees. Spectrum uses that come under its rubric include radio telescopes and radio astronomy, radar astronomy, incoherent scatter radar arrays, HF radars, micro- and nanosatellites, S-band radars, and telecom systems for polar programs.
- *National Oceanic and Atmospheric Administration (NOAA).* The Radio Frequency Management Division is responsible for assisting users within the entire Department of Commerce in obtaining access to the RF spectrum. It is represented in IRAC and participates in the ITU, the Organization of American States Commission for Inter-American Telecommunications, the Space Frequency Coordination Group, and a steering group on radio frequency coordination of the World Meteorological Organization.

The federal government maintains software and informational resources to assist in applying for spectrum assignments for federal use. The Spectrum XXI (SXXI) software was developed to fulfill a need to automate many processes and to standardize spectrum management processes throughout the federal government.[8] SXXI assists in the process of obtaining a frequency assignment and also carries out other support functions, including interference analysis. NTIA also keeps current a Government Master File that catalogs the frequencies assigned to all U.S. federal government agencies in the United States.[9] Nevertheless, security and other concerns obscure how some spectral bands are used.

[8] See DISA, *SPECTRUM XXI: Spectrum Management in the 21st Century*, ITT Advanced Engineering and Sciences, http://www.disa.mil/mission-support/spectrum/jsc-joint-spectrum-center/~/media/files/disa/services/jsc/spectrumxxi_jsc.pdf, accessed June 4, 2015.

[9] See "National Telecommunications and Information Administration," http://www.ntia.doc.gov/, accessed June 4, 2015.

U.S. Nonfederal Assignments

Nonfederal spectrum use licenses are obtained through the FCC via multiple mechanisms: by rule, direct assignment, auction, or acquisition. There also are means of obtaining experimental and Special Temporary Authority (STA) licenses.

- *License by rule (unlicensed access).* This is commonly used for accessing the spectrum by unlicensed devices such as those used in Wi-Fi local area networks. The ability to access the spectrum is defined by the technical rules stipulating that any piece of equipment that follows technical rules may access that portion of the spectrum. The 2.4-2.483 GHz band for Wi-Fi is an example of where such an approach is applied. A variant of license by rule are the nonexclusive licenses now proposed in the 3.5 GHz band.
- *Direct assignment.* This is used for systems in which an auction may not be applicable or desirable, such as when there are no competing commercial demands for the band. In this case, the FCC directly provides a license based on requirements that are specific to the band and service type. For example, the mobile satellite service (MSS) spectrum was licensed in this manner.
- *Auction.* Since the mid-1990s when Congress first directed the FCC to use auctions, this has been the most commonly understood mechanism for obtaining a commercial RF spectrum license. Since 1994 the FCC has held approximately 100 auctions for spectrum licenses. Each auction has specific rules such as who can participate, bidding mechanisms, and credits for small businesses or new entrants. Almost $100 billion has been generated through auctions in the United States.[10]
- *Acquisition.* Licenses are often traded between companies. Furthermore, the spectrum holdings of a company that is being acquired is transferred to the parent entity. In both cases, this requires FCC approval. There are cases in which the FCC may not approve such an acquisition if it believes that harm will be done to the consumer. An example of this is when an acquisition would reduce competition and thus increase the potential for monopolistic or duopolistic behavior.[11]
- *Experimental license.* The FCC allows for scientific research and technical

[10] See FCC, "FCC Auctions: Band Plans," http://wireless.fcc.gov/auctions/default.htm?job=bandplans, accessed June 4, 2015.

[11] See, for example, Federal Communications Commission, "Order Dismissing Applications and Staff Report: Staff Analysis and Findings," https://apps.fcc.gov/edocs_public/attachmatch/DA-11-1955A2.pdf, accessed January 26, 2015.

development without an explicit long-term license. An STA is an experimental license that is not expected to last more than 6 months.[12,13]

The FCC maintains software and information resources to assist users in applying for spectrum licenses and to understand the current state of licenses across the country. Two resources are particularly useful: the Universal Licensing System[14] (ULS) and the Spectrum Dashboard.[15] The ULS allows a user to search for all of the licenses that have been assigned for a specific frequency band, geographic area, and/or service type. The Spectrum Dashboard allows a user to look at specific frequency bands and to determine which services are allowed, which technical rules are enforced, and which licenses have been assigned.

Challenges of New Allocations

Gaining access to the spectrum for new uses can be a difficult and time-consuming process. As noted, uses of RF spectrum that cross country borders require international coordination. The WRC process, required for new international allocations, can take years if not decades.[16] Even for purely domestic allocations, finding spectrum for new uses is very difficult. Virtually all readily usable RF spectrum has some incumbent user with an interest in maintaining current allocations. Consequently, any new allocation and subsequent assignment will displace the rights of some existing entity, generating opposition to change. As a result, spectrum allocation tends to be an inherently political process with many competing interests. For example, the digital TV transition that ultimately led to the 700 MHz allocation was begun in the 1980s and took two laws—one in 1997 and another in 2006—before the reallocation could be consummated in 2009, with services beginning to be deployed a couple of years later.

[12] See Part 5 of the FCC rules governing the usage of the experimental radio service (47 CFR Part 5, available at http://ecfr.gpoaccess.gov/).

[13] The committee is aware of possible changes to the rules regarding FCC experimental licenses, but the impact on remote sensing systems is unclear at present.

[14] FCC, "Universal Licensing System," http://wireless.fcc.gov/uls, accessed June 4, 2015.

[15] FCC, "Spectrum Dashboard: Exploring America's Spectrum," http://reboot.fcc.gov/reform/systems/spectrum-dashboard, accessed June 4, 2015.

[16] An example of this process would be the allocation of spectrum for mobile satellite services (MSS). Initial work in ITU-R in the 1980's precipitated the WRC-1992 to allocate 1980-2010 MHz and 2170-2200 MHz for MSS worldwide. FCC completed the allocation of the sub-band 1990-2025 MHz and 2165-2200 MHz for MSS in 1997. The technical rules were completed by the FCC in 2000. In 2001 the FCC assigned eight licenses. By 2010 six licenses had been revoked and the remaining two license holders had filed for bankruptcy. By 2012 the band had be reduced to 30 MHz and reallocated to allow mobile terrestrial service and now called AWS-4 (Advanced Wireless Services, Band 4).

SPECTRUM ALLOCATION ISSUES FOR CUBESATS

One of the most important advances in educating the future science and aerospace workforces has been the introduction of the CubeSat program by NSF. In this program, students under faculty supervision design, build, launch, and analyze data from a small satellite, usually a 10 cm cube, with a mass of no more than 1.33 kg. The sounding rocket and balloon programs of NASA were for many generations the vehicles by which future experimentalists were trained. With the advent of CubeSats, that educational experience, for both scientists and engineers, has been extended to actual satellites.

The introduction of CubeSats has also led to a burst of creativity from which it is now being recognized that CubeSats in larger versions, either individually or through constellations, can make important scientific measurements, particularly of Earth and geospace. For example, the 2013 National Research Council report *Solar and Space Physics: A Science for a Technological Society*[17] anticipates and promotes the concept that constellations of CubeSats will be essential to understanding the space environment of Earth.

The emergence of this new satellite technology, with its unique and in some ways challenging needs for spectrum, has been difficult to accommodate within the deliberative and cumbersome spectrum allocation process. The issue is particularly acute for CubeSats that are for educational purposes, which are, by definition, extremely low-cost and run by students. A complicated bureaucracy for getting a communication license runs counter to the education intent and is a serious impediment to the success of the educational CubeSat program.

There is also confusion about what license to seek. If the educational CubeSat is deemed a government satellite, which most are not, one must download to government ground stations, for which the cost normally exceeds the budget of a low-cost CubeSat. Alternatively, if the CubeSat is not considered to be a government satellite, a license can be sought in the amateur radio band. However, this has become more difficult, since the VHF band for CubeSats has been eliminated, leaving only the UHF band as a possibility.

ESTIMATING THE VALUE OF ACTIVE SENSING

This report offers a number of different ways in which the value of active sensing for research can be estimated. Table 2.5 provides the estimated financial savings to the U.S. economy to which active atmospheric sensing contributes, according to NOAA. Finding 3.2 says, "Active microwave sensors provide unique ocean measure-

[17] National Research Council (NRC), *Solar and Space Physics: A Science for a Technological Society*, The National Academies Press, Washington, D.C., 2013.

ments for scientific and operational applications that are vital to the interests of the United States." Chapter 4 adds that active microwave remote sensing of the land has proven valuable across a number of science disciplines and practical applications, including geology, urban planning, agriculture and crop management, forestry and biomass assessment, hydrology and water resource management, weather forecasting, generation of topographic maps, sea ice mapping and glacier studies, earthquake and volcano studies, and postdisaster assessment. Chapters 5 and 6 also state that active sensing of the near-Earth environment is essential to understanding space weather and identifying near-Earth objects.

Other benefits certainly flow from this research. Basic research begets advanced research; technologies spin off from research; and training the next generation of scientists and engineers spurs society's technological progress.

However, many of these benefits are not easy to fully internalize in a market system, so the value of active sensing is very difficult to compare with commercial systems. For example, benefits from advances in weather prediction might be hard to internalize such that private entities would not invest sufficiently in the prediction systems. Also, basic research such as this develops knowledge, which is a public good that is again hard to fully internalize in a market system. Early scientific discoveries can also lead to many different paths of social benefits.

When considering the relative values of various potential services for a given spectrum band, regulators should take into account that the value of the scientific uses of the spectrum is not easy to establish and thus difficult to compare against the value of the commercial uses.

DECADAL SURVEYS OF SCIENTIFIC FIELDS

The National Academies of Scineces, Engineering, and Medicine conducts large surveys of each of the space science disciplines, called decadal surveys, about every 10 years. The surveys, executed by members of the research community, set science and mission priorities for the coming decade. The effort results in a report that provides guidance to the federal agencies supporting the discipline, and the agencies typically set about executing the priorities to the extent possible. The two disciplinary surveys most relevant to this report are the solar and space physics survey and the Earth science and applications from space survey.[18] To date, neither decadal survey has addressed spectrum needs for these communities, although it would be beneficial to do so in the future.

[18] The most recent survey of solar and space physics is *Solar and Space Physics*, 2013. The most recent survey of Earth science is NRC, *Earth Science and Applications from Space: National Imperatives for the Next Decade and Beyond*, The National Academies Press, Washington, D.C., 2007.

FINDINGS AND RECOMMENDATIONS

Finding 7.1: The U.S. approval process for transmit assignment for environmental radar is too cumbersome, lengthy, and inefficient. The U.S. Interagency Radio Advisory Committee operates by consensus of its members and thus provides numerous opportunities to table or veto applications. Specifically, the allocation for P-band radar allocations is ineffective and encourages only voluntary self-compliance by the applicant.

Finding 7.2: Merit alone will not assure that the spectrum required is available for the scientific community. Scientific interests must be actively engaged in the spectrum allocation and assignment process to assure that science needs are met.

Improving this situation will require ongoing effort in two complementary areas.

Recommendation 7.1: The science community should increase its participation in the International Telecommunications Union, the National Telecommunications and Information Administration, and the Federal Communications Commission spectrum management processes. This includes close monitoring of all spectrum management issues to provide early warning for areas of concern. It also requires regular filings in regulatory proceedings and meetings with decision makers to build credibility for the science community and ensure a seat at the table for spectrum-related decision making that impacts the science community.

This increased participation could be encouraged by organizations such as the International Radio Science Society, the American Astronomical Society, the Institute of Electrical and Electronics Engineers, and the American Geophysical Union, and supported by the relevant funding agencies.

Recommendation 7.2: For participation in the spectrum management process to be effective, the science community, NASA, the National Oceanic and Atmospheric Administration, the National Science Foundation, and the Department of Defense should also articulate the value of the science-based uses of the radio frequency spectrum. Such value will include both economic value, by advancing commerce or reducing the adverse economic impact of natural phenomena, and noneconomic values that comes from scientific research.

Finding 7.3: CubeSats that are undertaken for education are essential for the training of the nation's aerospace workforce. They are at the forefront of the revolution in small satellite technology that is becoming essential to understanding the envi-

ronment of Earth and geospace. However, the spectrum allocation process creates impediments to the success of the educational CubeSat program.

Recommendation 7.3: Given the importance of the educational CubeSat program for the development of the aerospace workforce and for the development of small satellite technology, the National Science Foundation, NASA, the Federal Communications Commission, and the National Telecommunications and Information Administration should undertake a concerted and coordinated effort to eliminate impediments in the spectrum allocation process that are currently inhibiting the success of educational CubeSats.

Recommendation 7.4: The next decadal surveys in solar and space physics (see Recommendation 5.2) and Earth science and applications from space should address the future spectrum needs of those communities.

8

Radio-Frequency Interference Issues for Active Sensing Instruments

INTRODUCTION

The objective of this section is to give an overview of current spectrum issues encountered with active science sensors, the resultant impact to the objectives of the science investigations, and the nature and limitations of mitigation strategies that may be employed.

For the purposes of this discussion, "spectrum issues" essentially fall into two categories:

1. *Radio-frequency interference (RFI).* This is the interference from other radio services impacting the performance of active science sensors. Unlike passive science systems, where regulatory effort is made to keep the allocated band free of other emitters, active science systems are often expected to share the band with other services, so signals from other radio services are often present to varying degrees. Various mitigation techniques may be employed to lessen the impact of this interference.
2. *Sensor transmit restrictions.* Active sensors emit radiation and thus may interfere with other services that share the band. National and international regulatory bodies can place limits on how science systems operate.

RADIO-FREQUENCY INTERFERENCE

As noted in earlier chapters, a radar system senses a medium of interest (atmosphere, land, ocean surface, or others) by extracting information from the "echo," or "radar return," received from that medium. Radar sensors operate in a variety of bands ranging from 2 MHz to 300 GHz (with potential applications outside this range).

When a signal from other radio sources (communication systems, aircraft tracking radars, etc.) is present with the echo, this is termed RFI. RFI can corrupt the desired science measurement in a number of ways, depending on what the sensor is intended to measure and how the sensor system is designed (Figure 8.1). Depending on the application, a sensor extracts information based on one or more of the following signal characteristics of the echo: (1) amplitude, (2) frequency, (3) time delay, (4) polarization, (5) Doppler shift, or (6) phase. The sensitivity of a given sensor to RFI is also a function of the specific nature of the RFI experienced. The existence of a wide range of active sensor techniques, as well as a wide variety of RFI environments encountered globally, conspire to make it difficult to characterize the RFI problem and the associated solutions.

In general terms, RFI may be described as follows:

- *Narrow-band RFI.* These sources have spectra that are narrow relative to the bandwidth of the sensor and may typically be described as continuous in time relative to the sensor integration time. A classic example of such a signal is a single-frequency sinusoidal tone. Commonly encountered cases include commercial land-mobile radio and amateur radio.
- *Pulsed RFI.* These sources are pulsed in time, with on/off cycling that may be longer or shorter than the sensor integration time and may have bandwidths narrow or wide relative to the sensor bandwidth. A typical example is a ground-based radiolocation radar.
- *Broadband, noiselike RFI.* These sources are composed of signals modulated to relatively broad bands, and usually are continuous in time relative to the radar integration time. Examples of such systems include broadband communication and data systems, as well as other coded signals such as GPS. Over the bands in which they operate, these sources have noiselike characteristics.
- *Heterogeneous RFI environments.* Particularly for airborne and spaceborne sensors that have a wide geographic field of view—either within the main antenna beam or within the extended side lobes—multiple RFI emitters of multiple different types can be viewed simultaneously.

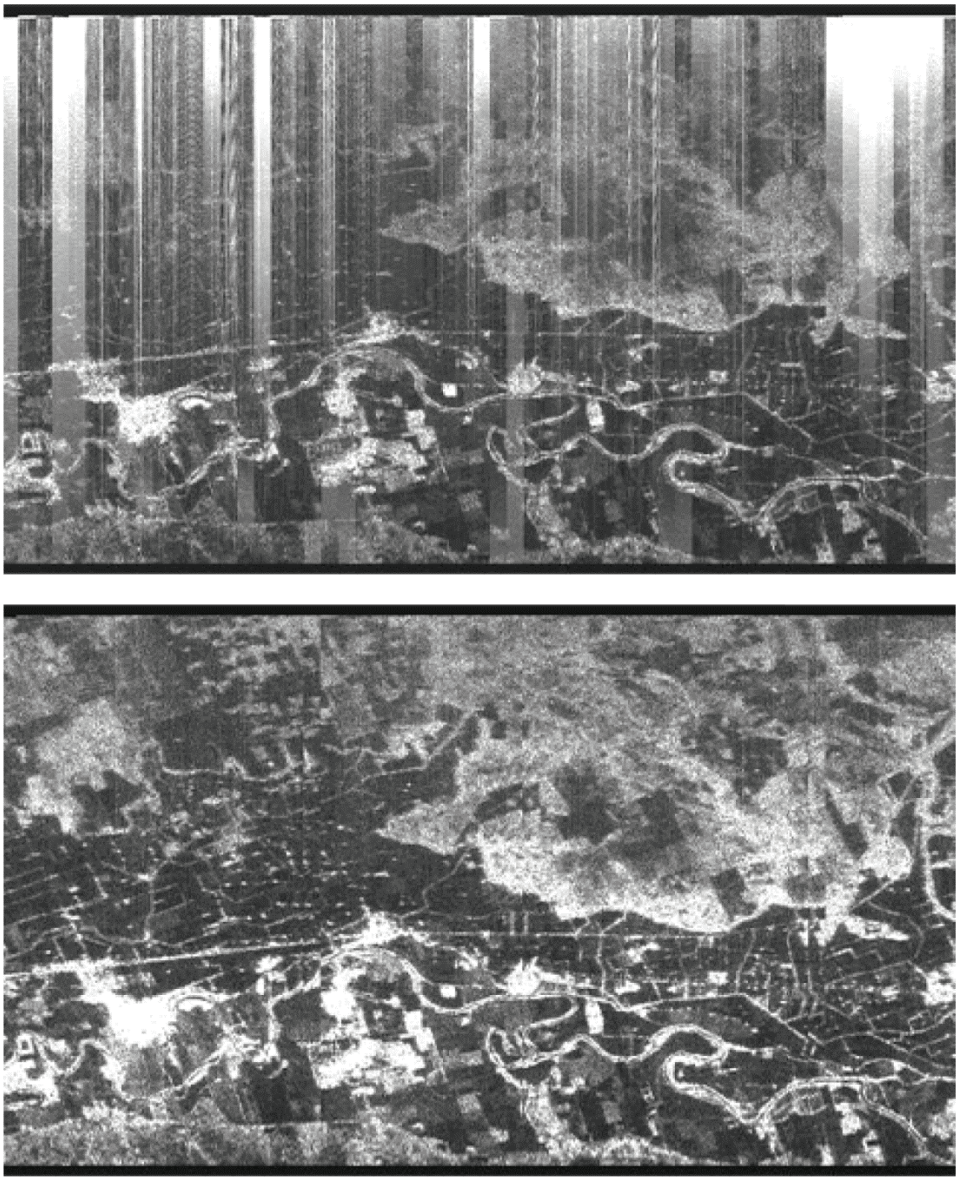

FIGURE 8.1 Sample images collected with the Jet Propulsion Laboratory's (JPL's) AIRSAR P-band radar system. The top image shows scene heavily contaminated with radio-frequency interference (RFI), which is often present at the P-band. The bottom image shows same scene after RFI mitigation is employed, in this case largely successfully because of the narrow-band nature of the interference encountered. SOURCE: Courtesy of NASA/JPL-Caltech.

RFI MITIGATION

Because science sensors share bands with other services, and because the global RFI environment has generally been growing worse over time, the science community has employed a variety of RFI mitigation methods to protect its sensors from damage or to improve science performance in the presence of the RFI environment. Generally, these mitigation techniques include one or more of the following:

- *Receiver protection.* At some frequencies, there are emitters that are sufficiently powerful to damage the sensitive receivers of active systems (such as military radars). Consequently, the sensor receiver electronics must be designed to survive such levels if they are expected to be encountered. A limiter placed in front of sensitive components is a common protective measure.
- *Out-of-band filtering.* It is desirable to reject RFI signals outside the sensor band. In addition to protecting the receiver against potential damage from strong signals, undesired nonlinear effects such as receiver saturation and spurious harmonics can occur during the reception of the in-band signal even when the RFI occurs out of band if sufficient rejection is not achieved.
- *Geographic avoidance.* The simplest way to avoid RFI is to operate the sensor in a location where RFI is not present. Although it might be possible to locate some types of science measurements in sufficiently remote locations, this may be impractical for most airborne systems, and even more difficult for spaceborne systems.
- *Frequency avoidance.* It may be possible to operate a science sensor in a band where no interference is present. Since the bands used by active science sensors are often well-used by other services sharing the band, it can be difficult to choose a single fixed frequency a priori, and consequently, some sort of tuning capability is often required to realize this technique.
- *RFI detection.* Although not a mitigation technique per se, the ability to detect and characterize RFI is important in implementing various measures. In cases where interference present in the science data is sufficient to corrupt the desired measurement accuracy, it is necessary to detect the presence of RFI so that the data can be discarded. Detection is also a necessary first step if the RFI is to be removed. In general, RFI detection techniques focus on identifying the presence of signals significantly different from the expected echo return. Examples of interference detection are the presence of narrow-band interference appears as a conspicuous spike in the Fourier transform domain; pulsed RFI appears as statistically significant spikes in the time domain; also, many radar returns from the surface have Gaussian statistics due to speckle, and thus the presence of RFI may be detected by

signal statistics exhibiting non-Gaussian behavior. Note that RFI detection techniques are most effective when the raw science data are available (the original A/D samples of the echo return). If, for example, there is significant compression of the raw radar echo by onboard processing or averaging, the detection of low to moderate RFI signatures may be much more difficult.

- *RFI removal.* When adequate raw data exist, it is sometimes possible to remove offending RFI signals and consequently recover science data of improved quality. The simplest example of this is the notch filtering of a very narrowband interfering signal or the excision of time-domain outliers consistent with interference from pulsed radars. Under certain conditions, it may also be possible to estimate the offending interference and attempt to directly subtract it from the science data. All of these techniques come with some cost in that the process of interference excision and/or subtraction also corrupts the desired science signal to some degree. There is also often a significant added cost in terms of designing, implementing, and operating the RFI removal steps. In general, the more sparsely an interfering signal occupies the time or spectrum domain, the easier it is to detect and excise without corrupting the underlying science data. Examples of very sparse signals would be a single narrowband tonelike signal in the frequency domain, which can be notched while retaining most of the wider-band science data, or that from a single ground surveillance radar with pulses at a rate much slower than the active sensor samples, where the blips associated with this interfering source can be detected and excised from the sensor averaging or processing. Wideband, noiselike sources and heterogeneous environments present more difficult problems for removal techniques. First, such signals are harder (or, in some cases, impossible) to detect because they are not neatly concentrated at discrete times or frequencies, or may have "more Gaussian" statistics that are less easily discriminated from the science sensor echo. Secondly, the removal of such wideband or complex signals would necessarily involve the removal of significant portions of the desired echo and compromise the science measurement.
- *Cooperative operation.* The preceding mitigating techniques are "unilateral" in the sense that the active science system reacts to the existing RFI environment without trying to modify it in any way. In some circumstances, it may be possible for science sensors to operate cooperatively with other services. For instance, a ground radar or communication system may agree to turn off or switch frequency when a science sensor is known to be present.

It should be noted that the above mitigation techniques are most effectively implemented in the design phase of the sensor with a specific RFI environment in mind. Some sensor systems have been deployed without full knowledge of the RFI

environment, but, luckily, the nature of the interference was such that removal techniques could be implemented in postprocessing. To ensure effectiveness, however, the RFI environment to be mitigated should be clearly understood before sensor deployment, flight, or launch. This understanding can be a very difficult objective to achieve given the varied and evolving RF environment around the world today.

SCIENCE SENSOR TRANSMIT RESTRICTIONS

Through the spectrum regulatory process, operational restrictions are often imposed upon active science sensors so that they do not interfere with incumbent radio services. Examples of operational restrictions include the following:

- *Geographical restrictions.* An active science sensor may be restricted from operating near another service—for instance, a military radar "keep out" zone imposed on an airborne sensor. This can be a severe restriction for a spaceborne sensor because it typically has a very large field of view, particularly if the antenna side lobes of the science sensor are considered a problem for the other service. Consequently, such geographic restrictions on spaceborne sensors may result in significant loss of science data coverage, potentially denying coverage of entire continents.
- *Transmit power restrictions.* The maximum radiated power of science sensors, expressed in terms of effective isotropic radiated power (EIRP) or flux density incident in the vicinity of other receivers, may be restricted to certain levels, which may limit the detection of signals from weak scattering media.
- *Transmit waveform modifications.* An active sensor may be required to modify its transmit waveform to avoid interfering with other services. For narrowband science sensors, this may be accomplished by tuning the transmit carrier frequency away from the service potentially being interfered with. For broadband sensors, some measurements may allow the spectral "notching" of the transmitted waveform. For example, some synthetic aperture radars (SARs) operating in crowded spectral environments have the ability to generate an FM linear-chirped signal with both narrowband and wideband notches at specific frequencies. Such a waveform modification requires advanced coordination to know which frequencies must be suppressed and a sophisticated arbitrary waveform generation capability; moreover, depending on how much the transmit spectrum is required to be notched, the science measurement may be significantly compromised due to resolution loss and increased side lobes.

CURRENT SPECTRUM ISSUES BY FREQUENCY BAND

The intent of this section is to provide specific examples of some of the spectrum issues currently being encountered by science researchers, in terms of both RFI and operational restrictions. This section is organized by frequency band, starting at 3 MHz and going up to 300 GHz. A variety of different types of active sensing systems are illustrated. Spaceborne systems are treated with perhaps the most thoroughness because they are sensitive to RFI on a global basis, provide data to a very large number of users, and are relatively few in number (presenting a manageable set in terms of a more comprehensive treatment). Spaceborne systems also are subject to well-defined spectrum allocations from the International Telecommunications Union's (ITU's) Earth Exploration Satellite Service Active (EESS-Active) bands, as shown in Table 8.1. Some airborne and ground-based sci-

TABLE 8.1 EESS-Active Allocated Bands and Other Services Operating in Bands

Band Designation	Frequency (MHz)	EESS-Active Allocation Status	Other Services in Band	Sharing Considerations by Service and by Band
P-band	432-438	Secondary	Radiolocation, amateur, amateur satellite, fixed, mobile, ISM, space operation service (Earth-to-space), aeronautical radio navigation	RS.1260: wind profiler radars, space object tracking radars, launch vehicle range safety command destruct receive frequency RS.1282: avoid FM pulsed wind profiler radars RS.1749: mitigation techniques to share with radiolocation and radio navigation radar systems
L-band	1215-1300	Primary	Radiolocation, RNSS, amateur (secondary)	RS.1280: processing gain of search radars RS.1347: increase in loop SNR of RNSS receiver
S-band	3100-3300	Secondary	Radiolocation	RS.1280: processing gain of search radars
C-band	5250-5460	Primary	Radiolocation (active and secondary), Aeronautical RNSS	RS.1280: processing gain of search radars RS.1632: sharing feasible with RLANs having constraints

continued

TABLE 8.1 Continued

Band Designation	Frequency (MHz)	EESS-Active Allocation Status	Other Services in Band	Sharing Considerations by Service and by Band
C-band	5460-5570	Primary	Radiolocation	RS.1280: processing gain of search radars
X-band	8850-8650	Primary	Radiolocation	RS.1280: processing gain of tracking radars
X-band	9300-9800 9800-9900	Primary Primary	Radiolocation, radio navigation Fixed	RS.1280: processing gain of tracking radars Compatible with fixed, but only for bandwidths > 500 MHz
K_u-band	13250-13750	Primary	Aeronautical RNSS, radiolocation	RS.1281: Constraints on EESS (active) for "short dwell" and "long dwell"
K_u-band	17200-17300	Primary	Radiolocation	
K-band	24050-24250	Secondary	Radiolocation, amateur (secondary)	
K_a-band	35500-36000	Primary	Radiolocation, MET-AIDS, fixed, mobile	RS.1628: Constraints on pfd of EESS (active) to share with radiolocation radars, compatibility with fixed service
W-band	78000-79000	Primary	Radiolocation, amateur, amateur-satellite, space research (space-to-Earth)	
W-band	94000-94100	Primary	Radiolocation	RS.1261: mitigation technique to protect radio astronomy in 86-92 GHz, feasible to share with radiolocation, limit band to cloud profile radars
mm-band	133500-134000	Primary	Radiolocation	
mm-band	237900-238000	Primary	Radiolocation	

NOTE: Acronyms are defined in Appendix D.

ence sensors also are addressed, with the goal of capturing a representative sample of the issues encountered by these systems, which are typically sensitive to more localized problems. In general, airborne and ground-based systems use a wider spectral range than that prescribed for satellites, typically using the bands identified for radiolocation but not necessarily limited to those bands when authorization to radiate on a "noninterference basis" is granted. Much of the resource material for this section came from an active sensing RFI workshop held at the Jet Propulsion Laboratory (JPL) on November 8, 2013, under the auspices of the committee.[1]

HF and VHF Bands

Band Usage

The IEEE Standard Letter Designations for Radio-Frequency Bands defines the HF band as between 3 and 30 MHz and the VHF band as being between 30 and 300 MHz. As discussed at length in Chapter 5, active science sensors operating in the HF and VHF bands constitute an important measurement tool for understanding the physics and chemistry of Earth's upper atmosphere. Space physics transmitters operate at HF and VHF frequencies to take advantage of the natural interactions between the transmitted electromagnetic wave and the ionospheric plasma. These low-frequency bands are also used by radar sounders to probe glaciers, sea ice, coastal ocean regions, and the land subsurface. Earth remote sensing systems share the HF and VHF region of the spectrum with other important services worldwide. Globally, these bands are used for military and government communications, aviation air-to-ground links, amateur radio, shortwave broadcasting, maritime sea-to-shore radio, over-the-horizon radar, and the Global Maritime Distress and Safety System (GMDSS).

Interference Environment for Active Sensors at the HF and VHF Bands

RFI is a well-known issue for science sensors operating at the HF and VHF bands. Owing to the large number of applications in these bands, and the long distance propagation properties of electromagnetic waves, particularly at HF with sky wave reflections, there is an inherently dense RF interference environment present at all times. The interference from remotely located transmitters is most noticeable at night, when the reflection properties of the ionosphere are favorable for multiple-bounce signal propagation. In practice, the impact of RF interference on the operation of active RF sensors for space physics in the HF and VHF bands can be successfully mitigated by determining and selecting a clear operat-

[1] See Appendix C.

ing channel. The interfering sources are typically narrowband relative to a 3 kHz channel, and even in periods of maximum congestion, the HF band is less than half occupied. A further mitigating factor is the directionality of the interfering signals, which tend to arrive at low angles due to multiple bounce reflections off the ionosphere. The space physics sensors described in Chapter 5 typically utilize high-directivity antennas pointed at high elevation angles and thus have greatly reduced susceptibility to incoming RF interference at low elevation angles. For airborne radar sounders exploring the depths of polar ice sheets and glaciers, no report of significant deleterious interference from external sources has come to the attention of the committee.

Transmit Restrictions for Active Sensors at the HF/VHF Bands

HF radars used for sensing ocean currents have encountered some issues with operational restrictions, but among other science operating sensors, no significant operational restrictions have come to the attention of the committee. This is likely due to the remoteness of the areas at which many of these sensors operate. Although there is currently no EESS-Active allocation for spaceborne science sensors to operate at VHF, there is some interest in the science community for pursuing one, or at least obtaining authorization to radiate on a noninterference basis. This is due to an interest expressed by both the U.S. and the European science communities for flying ice and subsurface sounding radars on spaceborne platforms. As previously mentioned, because satellites have an inherently wide field of view (often thousands of kilometers), not only would transmit restrictions need to be resolved, but RFI issues would likely be encountered.

UHF Band and P-Band

Band Usage

The IEEE Standard Letter Designations for Radio-Frequency Bands defines the UHF band as between 300 and 1000 MHz, of which the P-band is a subset. The EESS-Active allocation at the P-band is from 432 to 438 MHz, which is a secondary user allocation and therefore has lower priority relative to other users. Multiple airborne radar systems operate in the UHF band. UHF is becoming increasingly important for scientific remote sensing because electromagnetic waves at these frequencies exhibit good penetration properties through foliage, making UHF band radars popular for biomass studies in densely vegetated areas, as well as for applications in which the ground must be viewable in the presence of vegetation. Also, UHF is used when a moderate degree of subsurface penetration is needed,

such as observing soil moisture in the root zone. The UHF frequency is also being explored as a means to penetrate ice sheets.

Examples of airborne SAR systems operating at UHF include the Fugro GeoSAR system (which operates in the band 270-430 MHz) and the NASA/JPL AirMOSS system (which operates in the band 420-440 MHz). The European Space Agency (ESA) BIOMASS radar mission due to launch in 2020 will utilize the full EESS allocation, from 432 to 438 MHz. There are a wide variety of other nonscience services that operate at UHF. The EESS band is also occupied by ground-based radiolocation radars for tracking aircraft and space objects (e.g., the U.S. PAVE PAWS). In addition to radiolocation systems, the wider frequency range typically utilized by airborne sensor systems may also overlap the spectra used by land and mobile communication systems, amateur radio, and other science and meteorological services.

Interference Environment for Active Sensors at the UHF Band/P-Band

In the heavily used UHF band, RFI is routinely observed near populated areas by airborne systems (see, for example, Figure 8.2). In many regions, RFI can cause heavy contamination of a SAR image, rendering it unusable for the intended application if the RFI is not mitigated in postprocessing. The extent of RFI contamination is related to the bandwidth of the science sensor. Narrower band systems such as AirMOSS may observe less interference than much wider band systems such as GeoSAR.

Many of the observed interference signals over the UHF band are narrowband communication signals. For aircraft-based systems, these signals are also observed to be highly nonstationary in time as the aircraft moves from scene to scene. The problem of removal or enhancement of dynamic narrowband interference from wideband signals has long been an active research topic in various disciplines. The most popular adaptive filtering technique is the least-mean-square (LMS) algorithm, which is frequently used to remove the often-encountered narrowband interference present in science measurements at UHF. The AirMOSS project reports that, in the instances where a limited number of narrowband interferers is observed to degrade the image, the LMS RFI removal technique is very successful at cleaning up the data to allow their specific science requirements to be met. Interference from pulsed radars is observed less frequently in the data, but the impact from these systems is readily identified by time domain techniques that search for statistical pulse outliers in the data (i.e., brief events with anomalously high power), and can relatively easily be removed. The wider-band GeoSAR system must invoke a similar RFI removal algorithm more frequently, but measurement objectives are nevertheless met the majority of the time with the cleansed data. The RFI environment to

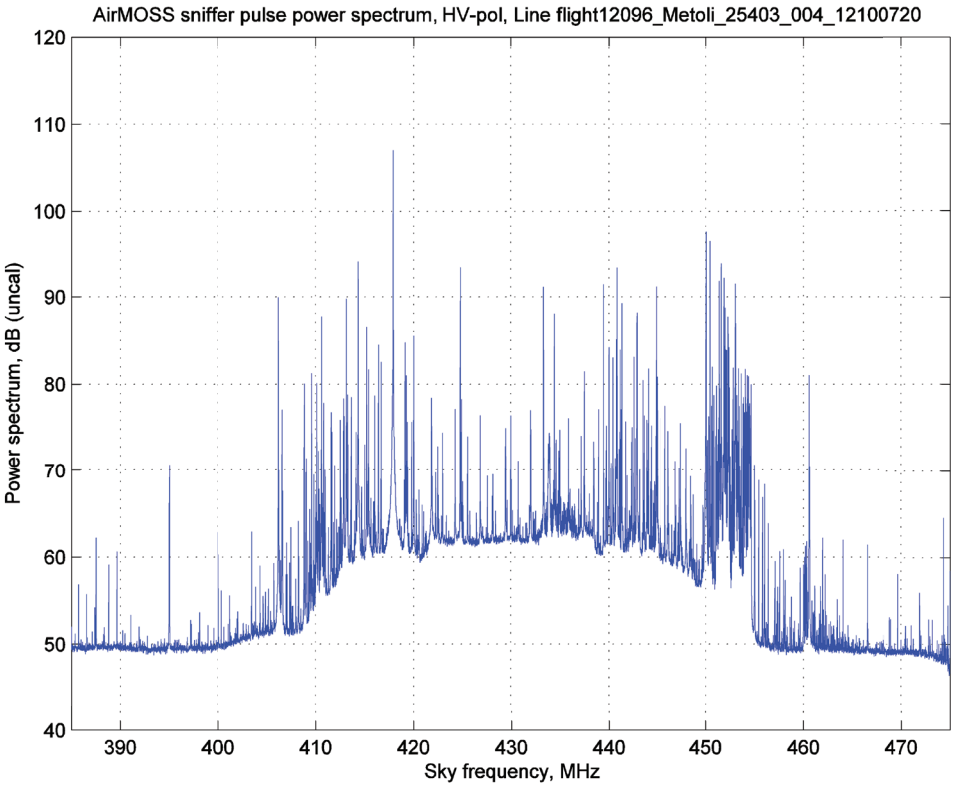

FIGURE 8.2 AirMOSS "sniffer pulse" spectrum containing radar thermal noise with RFI observed by the AirMOSS radar for a flight near Metolius, Oregon. This area has a relatively low population density but nevertheless exhibits significant RFI "hair," composed of multiple narrowband signals. SOURCE: Courtesy of NASA/JPL-Caltech.

be encountered for a spaceborne sensor is as of yet somewhat uncertain, but no doubt the BIOMASS mission will shed light on this topic.

Transmit Restrictions for Active Sensors at the UHF Band/P-Band

In general, airborne active sensors have been allowed to operate in the UHF band but are subject to some severe restrictions. The GeoSAR system is a case in point. GeoSAR was originally granted a Stage 4 (operational) approval to operate over the continental United States (CONUS) but has since been subject to an evolving series of transmit restrictions that have made consistent operation difficult. The GeoSAR system is required to employ frequency notching of its wideband

transmit signal. The severe notching requirements imposed on GeoSAR can significantly degrade science effectiveness, and appear to be getting worse over time. The AirMOSS system, which operates at a much narrower bandwidth and spatial resolution, has been allowed to operate over all required science sites without notching the spectrum, but is nevertheless subject to severe transmit restrictions near government radars.

The ESA BIOMASS UHF SAR radar, which operates in accordance with the EESS-Active frequency allocation of 432-438 MHz, has been denied permission to operate within line-of-sight field of view of the space object tracking radars in North America and Europe. Figure 8.3 shows the coverage restriction contours where BIOMASS is not allowed to operate, which includes all of North America and most of Europe. ESA has documented numerous attempts to reach an agreeable cooperative operating strategy, but it was ultimately unsuccessful at obtaining even limited access to the denied coverage areas.

While acknowledging the necessity to avoid interfering with critical government services related to national defense or human health and safety, in general there is a sentiment amongst researchers that the licensing process for UHF science radars—which also have significant societal benefits—are in many cases extremely restrictive. The ability to deploy future spaceborne UHF systems is in question.

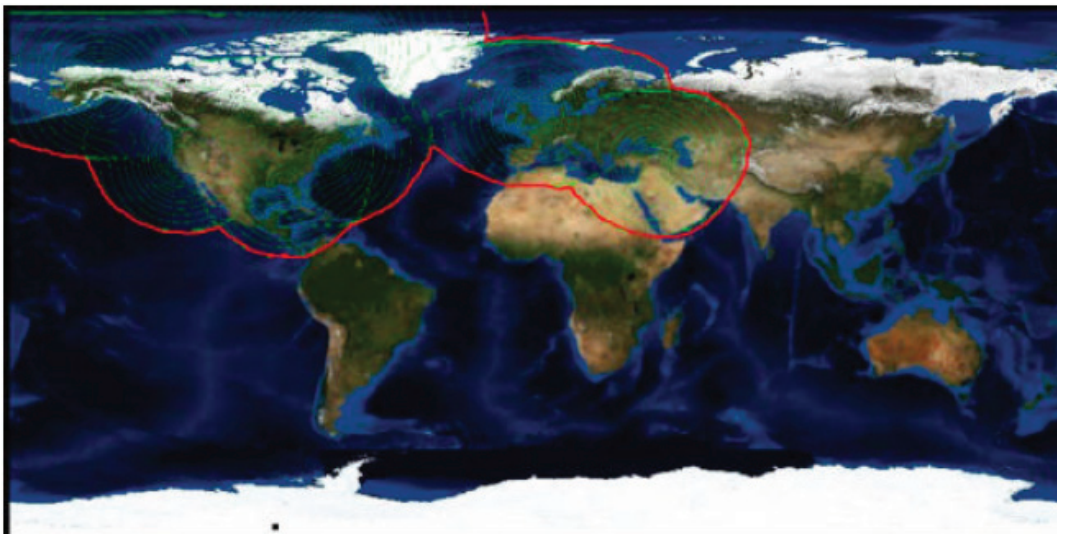

FIGURE 8.3 Denied access area contours. SOURCE: European Space Agency.

(It should be noted that no documented instances or reports of operating UHF radars actually having deleterious effects on incumbent services have come to the attention of the committee.)

L-Band

Band Usage

The IEEE Standard Letter Designations for Radio-Frequency Bands defines the L-band as between 1 and 2 GHz. The EESS-Active allocation at the L-band is from 1215 to 1300 MHz. The L-band has been extensively used for scientific remote sensing for many years. Because the L-band is insensitive to clouds and rain and offers a moderate level of vegetation and surface penetration, it is ideal for many scientific measurements, including soil moisture mapping, sea ice mapping, and soil moisture and biomass estimation. In addition to various environmental science applications, the L-band is also used for various civil applications, including detection of surface deformations associated with seismic and other natural hazards, land-use assessment, and crop characterization.

There is an expansive body of knowledge regarding the retrieval of geophysical data from radar measurements at the L-band, and a large technology investment in both airborne and spaceborne L-band systems. The first SAR to fly in space was an L-band system flown on Seasat in 1978. Successive L-band sensors have flown on both U.S. missions (SIR-A, 1981; SIR-B, 1984; SIR-C, 1994) and Japanese missions (JERS-1, 1992; ALOS/PALSAR, 2006; ALOS-2/PALSAR-2, 2014). Current or planned systems include the U.S. Aquarius, SMAP, and NISAR missions and the Argentine SAOCOM. In addition, numerous airborne L-band radars are operated around the world, including the NASA UAVSAR system.

Earth remote sensing systems share the L-band region of the spectrum with other important services worldwide. In the United States, the EESS allocation overlaps with radiolocation services (primarily ground-based Federal Aviation Administration (FAA) and Department of Defense air surveillance radars) as well as radio navigation satellite systems (GPS). Globally, the band is used by air surveillance radar and the radio navigation satellite systems of other nations, among others.

Interference Environment for Active Sensors at the L-Band

RFI is a well-known issue for science sensors operating at the L-band, particularly over the world's developed population centers: North America, Europe, and East Asia (see Figure 8.4). Most of the interference over North America is from relatively narrowband pulsed emitters, indicative of ground-based radars (see Figure 8.5), but emissions over other regions of the world are indicative of different

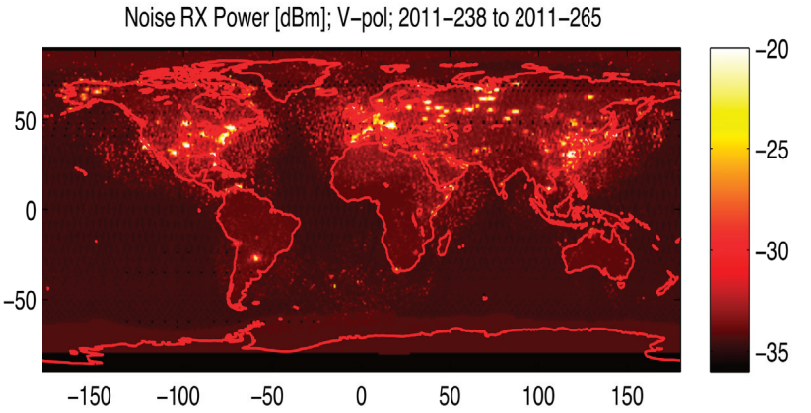

FIGURE 8.4 RFI observed by the Aquarius L-band instrument in 2011. The Aquarius radar operates in a 4 MHz band centered on 1260 MHz. Image courtesy NASA/JPL-Caltech.

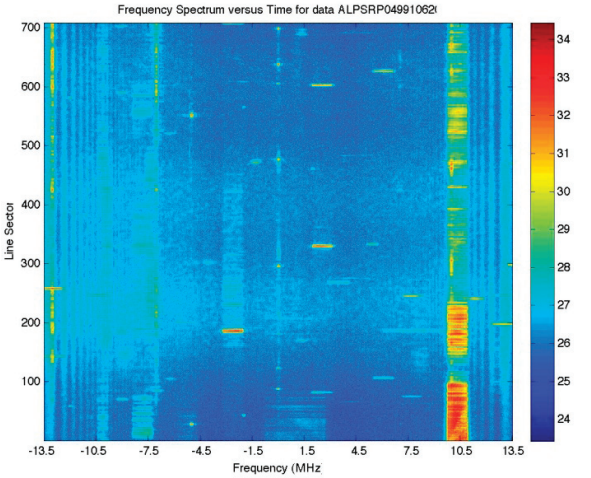

FIGURE 8.5 A time spectrogram of observed RFI taken from ALOS/PALSAR data. Frequencies are referenced relative to the PALSAR center frequency, which is 1270 MHz. Image courtesy NASA/JPL-Caltech and JAXA.

types of systems. Globally, the RFI environment at the L-band has been observed to be growing steadily worse with time. The Japanese Aerospace Exploration Agency (JAXA) conducted a study in which the percentage bandwidth contaminated by RFI from the JERS-1 mission, which flew in the 1992-1998 time frame, was compared to the same metric from the ALOS mission, which flew in the 2006-2011 time frame. JAXA found that significantly more of the spectrum was contaminated more of

the time during the ALOS mission. L-band airborne systems also routinely report observing RFI.[2]

L-band data are often sufficiently corrupted by RFI that science can be seriously compromised. Because of the importance of the L-band spectrum for many geophysical measurements, mitigation techniques for remote sensing radars are highly developed. For the JAXA L-band missions (previously, JERS-1 and ALOS/PALSAR, and now ALOS-2/PALSAR-2), these strategies are being implemented operationally as part of the ground radar processing and are seen as largely preserving the scientific quality of the data. Regions where RFI removal is successful share two primary characteristics:

- *Relatively "sparse" time/bandwidth occupancy of the RFI.* Many of the interfering systems are observed to be either narrow-band systems, whose energy can be notched out in frequency as part of the mitigation process, or pulsed sources with relatively low duty cycles, where time-domain detection and excision is effective at removing the offending events.
- *Many sources that are observed to be quite stationary in geographical position and over long periods of time (months, years).* This allows mitigation techniques to be finely tuned.

RFI mitigation techniques have enabled JAXA science objectives to be met over most of the globe. The NASA L-band SMAP and planned NISAR missions are planning to use similar techniques for RFI mitigation.

Though successful, it is important to point out that most of the RFI mitigation efforts at the L-band have been largely reactive in nature in that the interference environment was not fully understood until the sensor was in orbit. In the case of the JAXA sensors, for instance, it is fortuitous that both the design of the sensor and the precise nature of the interference environment have combined to allow RFI mitigation to be successful. Still, there are some regions of the globe where the RFI time/bandwidth occupancy of RFI is sufficiently "non-sparse"—that is, the environment is sufficiently populated with many emitters—that current RFI removal techniques are not effective. Noteworthy cases include some urban areas of East Asia. There is also concern that the band in general is filling up with more and more interferers, which are exhibiting increasingly "non-sparse" time/frequency characteristics. An example is the FAA's deployment of the new Common Air Route Surveillance Radar (CARSR) system), which utilizes longer transmit pulses and a higher overall duty cycle and is consequently less sparse in time/frequency than predecessor systems.

[2] See Appendix C for more detail.

Transmit Restrictions for Active Sensors at the L-Band

Although L-band remote sensing systems have not experienced the severe transmit restrictions that have occasionally been imposed on P-band systems, they appear to be coming under increased scrutiny in the spectrum approval process. This is likely due to the fact that the L-band spectrum overall is becoming more crowded with time, and "incumbent" services such as air surveillance radars and global positioning systems are concerned about the potential negative impact of these spaceborne systems. Although no proposed spaceborne system has so far been denied the ability to operate, the burden of proof imposed on such systems to demonstrate that they will not adversely impact incumbent systems appears to be growing heavier in recent years. Examples include costly hardware design changes required for SMAP late in its development phase and certain operational restrictions requested for the PALSAR system. Airborne systems have likewise been impacted. For instance, although UAVSAR has generally not had difficulty operating over the United States, the full Stage 4 certification approval has nevertheless been delayed due to concerns of agencies that operate incumbent systems. Although these measures can be seen as justifiable means to demonstrate that critical incumbent services will not be interfered with, the perception of many in the science community is that the criteria for interference are often ill defined, and, consequently, extreme conservatism is invoked at the expense of science measurements. (Again, it is noted that no instances or reports of L-band science sensors actually having interfered with incumbent services have come to the attention of the committee.)

S-Band

Band Usage

The IEEE Standard Letter Designations for Radio-Frequency Bands defines the S-band as between 2 and 4 GHz. The EESS-Active allocation at the S-band is from 3.1 to 3.3 GHz, and it is a secondary allocation. The S-band is a good intermediate frequency that has many of the long-wavelength advantages of the L-band (good penetration of low vegetation, low temporal decorrelation, low tropospheric propagation losses), as well as some of the advantages of higher frequencies (smaller antennas, lower degree of ionospheric effects, ability to measure rain when operated at high power in ground-based applications). ESA's ENVISAT mission utilized an S-band altimeter channel that operated over a bandwidth of 3.1-3.3 GHz in order to make ionospheric corrections for sea surface topography measurements. Otherwise, science users of this band spaceborne are primarily China, which is currently operating the HJ-1C SAR mission, and India, which plans to fly an S-band SAR on the joint ISRO/NASA NISAR mission to be launched around 2020. Whereas the

entire S-band region encompasses a variety of services—including radiolocation, spacecraft communication links, fixed and mobile communications, and radio astronomy—the 200 MHz EESS band overlaps a band currently allocated only for radiolocation systems.

Interference Environment for Active Sensors at the S-Band

No information regarding RFI experienced at the S-band has come to the attention of the committee. The ENVISAT S-band altimeter preprocesses its raw data onboard, so that all but the most extreme RFI is not likely to be easily seen in the downlinked data. Little information regarding the Chinese SAR observations has been available to the committee.

Transmit Restrictions for Active Sensors at the S-Band

No ongoing difficulties with spectrum access at the S-band have come to the attention of the committee.

C-Band

Band Usage

The IEEE Standard Letter Designations for Radio-Frequency Bands defines the C-band as between 4000 and 8000 MHz. The EESS-Active allocation for the C-band is from 5250 to 5570 MHz. The C-band is one of the most important bands for radar science imaging, and there has been substantial technological investment for the C-band by many of the world's space and science agencies. The choice of the C-band offers a suitable compromise between the antenna aperture size required to achieve a desired beamwidth (which decreases with frequency) and the attenuation of the radar signal as it propagates through rain and clouds (which increases with frequency). The C-band is also used for Doppler weather radar, which detects the motion of rain droplets in addition to the intensity of precipitation. Examples of satellite SAR systems operating at the C-band include the Canadian Radarsat-1, which was launched in 1995, and Radarsat-2, which was launched in 2007. Canada's next-generation Radarsat Constellation Mission (RCM) will be launched in 2018. ESA's Sentinel-1 satellite was launched in April 2014. All of these SAR radars operate in the 5350-5470 MHz band. Examples of satellite ocean altimeter systems operating at the C-band include the French SSALT on JASON, which was launched in 2001, ESA's Sentinel 3, which was launched in 2013, and the Chinese HY-2A, which was launched in 2011. Examples of satellite

ocean wind scatterometer systems operating at the C-band include ESA's ASCAT on Metop, which is to be launched in 2016, and the Chinese FY-3E wind radar, which is to be launched in 2018. C-band ground-based weather radars operate in the primary radiolocation band of 5600-5650 MHz.

Interference Environment for Active Sensors at the C-Band

ESA reports a limited number of RFI events at the C-band in scatterometer and SAR data, although there is evidence that it is increasing. For SAR data, the RFI appears as short, strong bursts indicative of ground-based radar. As previously discussed, such events fall into the "sparse" time/bandwidth occupancy category, and the ESA experience is that they have (thus far) been readily mitigated to recover clean SAR imagery.

The biggest concern for C-band science radar interference is the proliferation of wireless access systems, which include radio local access networks (RLANs). At the World Radiocommunication Conference 2003 (WRC-2003), the decision was made to provide a primary allocation to the mobile service in the bands 5250-5350 MHz and 5470-5725 MHz. As a preventative measure, ESA and the Canadian Space Agency (CSA) chose to move their Sentinel, RadarSat-2, and RCM sensors to the band 5350-5470 MHz, which was not open to RLAN, in order to avoid RFI from such systems in the future. There has been a subsequent push by the wireless industry, however, for the addition of the 5350-5470 MHz band for RLAN use. ESA studies show that the RLAN deployment in the frequency band 5350-5470 MHz will create harmful interference to Sentinel-1 satellites, as well as Canada's Radarsat-2 and RCM (three satellites). A major concern is that extension of mobile services to the 5350-5470 MHz band would eventually be applied worldwide. Studies by ESA and CSA suggest that no mitigation would be possible because the aggregated effect of the RLAN RFI is entirely different from that of "classical" (for example, pulsed, or narrowband) RFI experienced with SAR in that it appears as continuous, broadband, noiselike interference, and consequently is distinctively "nonsparse" in the time/bandwidth domain. The RLAN bands consist of 10 channels, each with 18 MHz of bandwidth. Figure 8.6 shows the frequency spectrum of a simulated 18 MHz RLAN signal.

As an interference mitigation approach, it has been proposed that radar and wireless access system (WAS) technologies will coexist in the same environment through a frequency abandonment protocol implemented in the RLANs. The RLANs are required to utilize dynamic frequency selection (DFS), whereby radio frequencies are monitored and the RLAN selects frequencies that are not in use. Before using a channel, the RLAN would check for the presence of radar signals. If any signal is detected, the RLANs would vacate the channel for a 30-minute period. In addition, before reusing the channel, the RLANs must continuously monitor

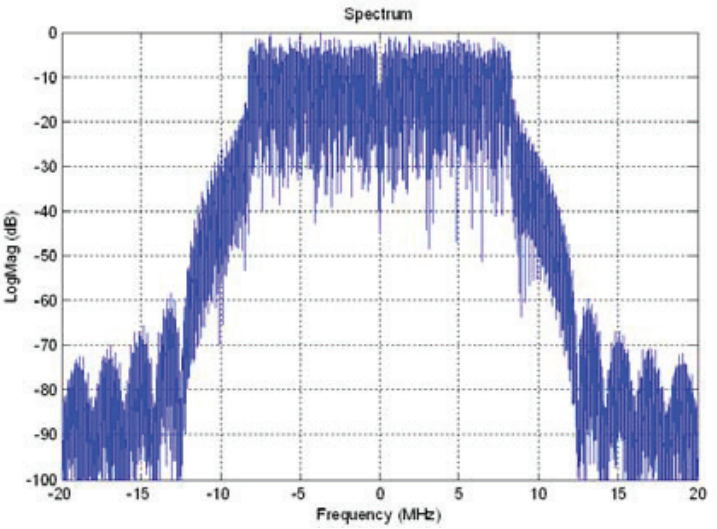

FIGURE 8.6 The frequency spectrum of a simulated 18 MHz RLAN signal.

the channel for 10 minutes. An analysis performed recently by ESA (presented in June 2014 at the SFCG-34 meeting in Boulder, Colorado) disputes the claim by the wireless industry that the RLANs can safely coexist with C-band SAR satellite radars using this method. An ESA analysis, presented under WTC-15 agenda item 1.1, indicates that even two outdoor RLANs in the active footprint of the radar will exceed the interference maximum defined in ITU-R RS 116-4. Furthermore, the expected density of RLANS in a suburban environment will exceed the maximum interference limit by over 24 dB. This presents a significant degradation to C-band SAR performance over major areas of coverage

It has also been well documented that RLANs can severely interfere with the operation of ground-based weather radars. Early versions of the DFS algorithm used in commercial RLAN units were incapable of detecting the waveforms common to C-band Doppler weather radars. A detailed study was performed by NTIA on the interference of RLAN's on the C-band WSR-88D weather radar in Puerto Rico. The study identified a set of problems with the commercial DFS implementations, which were remedied in subsequent versions of the RLANs.

Transmit Restrictions for Active Sensors at the C-Band

The ITU Radio Regulations have several footnotes at the C-band stating that the EESS-Active shall not claim protection from the radiolocation service in the 5250-5350 MHz band and that the EESS-Active shall not cause harmful interfer-

ence to the aeronautical service in the 5350-5460 MHz band, to the radio navigation service in the 5460-5470 MHz band, or to the maritime radio navigation service in the 5470-5570 MHz band. Compatibility studies with simulation results have shown that the EESS-Active does not cause harmful interference to the other services in the C-band. Overall, no ongoing difficulties with spectrum access at the C-band have come to the attention of the committee.

X-Band

Band Usage

The IEEE Standard Letter Designations for Radio-Frequency Bands defines the X-band as being between 8000 and 12000 MHz. The EESS-Active allocation for the X-band is 8550-8650 MHz and 9300-9900 MHz. The X-band is another important band for scientific radar imaging. Like the L-band and the C-band, the X-band is also extensively used for "applications," including seismic hazard analysis, environmental disaster monitoring, and infrastructure assessment. Examples of satellite SAR systems operating at the X-band include the German two-satellite TerraSAR on Tandem-X, launched in 2007; the Italian five-satellite constellation COSMO-SkyMed, launched from 2007 to 2010; the Israeli TECSAR, launched in 2008; the Italian CSG, to be launched in 2015; the Spanish Paz SAR-X, launched in 2013; and the Russian Meteor-M SAR, to be launched in 2015. X-band science sensors share the band with terrestrial radio navigation radars and radiolocation tracking radars operating between 9300-9900 MHz.

Interference Environment for Active Sensors at the X-Band

Although some anecdotal discussion of RFI observed by X-band SAR came to the attention of the committee, this has not been reported to be much of a current problem. At least over North America, most of the current radio navigation and radiolocation radars at the X-band have either unmodulated pulses or frequency modulated pulses with relatively narrow bandwidths of 1 MHz or less. As previously discussed, mitigation techniques have been demonstrated for this type of interference at the L-band and the C-band.

Transmit Restrictions for Active Sensors at the X-Band

There are no known restrictions on spectral access for science sensors in the X-band. The pulsed radars of the EESS-Active are generally very compatible with the pulsed radars of the radio navigation and radiolocation service radars. Compat-

ibility studies with simulation results have shown that the EESS-Active does not cause harmful interference to the other services in the X-band.

Driven by the desire to achieve higher spatial resolution for science and applications, there is an Agenda Item (AI 1.12) for WRC 2015 to expand the EESS-Active from 600 MHz bandwidth to 1200 MHz bandwidth. This is proposed to be accomplished by expanding in a contiguous lower band, in a contiguous upper band, or in a combination of lower and upper bands. Although there has been interest in creating new allocations for EESS-Active in other regions of the spectrum, this proposal at the X-band represents perhaps the most significant near-term effort to expand the EESS-Active allocation rather than simply defend it.

K_u-Band and K-Band

Band Usage

The IEEE Standard Letter Designations for Radio-Frequency Bands defines the K_u-band as between 12000 and 18000 MHz. The EESS-Active allocations for the K_u-band are 13250-13750 MHz and 17200-17300 MHz. Most of the current EESS-Active systems operate in the 13250-13750 MHz band. (In previous years the K_u-band allocation was from 13400 MHz to 14000 MHz, but the upper band 13750-14000 MHz was taken from EESS-Active and given to satellite link usage, and at the same time the lower band 13250-13400 MHz was added to EESS-Active). The K_u-band is an important band for spaceborne altimeters, scatterometers, and precipitation radars, as well as many airborne systems making similar measurements on a more regional basis over the years. Examples of satellite altimeter systems operating at the K_u-band include the French SSALT on JASON, which was launched in 2001; ESA's Sentinel 3, which was launched in 2013; and the Chinese HY-2A, which was launched in 2011. Examples of satellite scatterometer systems operating at the K_u-band include NASA's Seawinds on Quickscat, which was launched in 1999; the replacement Rapidscat on the International Space Station, which was launched in 2014; the Chinese HY-2A scatterometer, which was launched in 2011; and the Chinese FY-3E wind radar, which is to be launched in 2018. Examples of satellite precipitation radar systems operating at the K_u-band include NASA/JAXA's TRMM, which was launched in 1997, and NASA/JAXA's GPM DPR, which was launched in 2014. The K_u-band is also being used for a relatively new measurement of snow depth and snow water equivalent by airborne systems. There is interest among European and U.S. investigators in deploying a snow measurement system from space that potentially would utilize the allocation 17200-17300 MHz band in space for the first time.

The IEEE Standard Letter Designations for Radio-Frequency Bands defines

the K-band as between 18000 and 26000 MHz. The EESS-Active allocation for the K-band is 24050-24250 MHz. There are currently no plans to operate an EESS-Active system in space at the K-band.

Interference Environment for Active Sensors at the K_u-Band and the K-Band

No reports of significant RFI at the K_u-band have come to the attention of the committee. It should be noted that K_u-band sensors that have been deployed to date have either (1) been primarily ocean missions and thus primarily concerned with areas away from land-based RFI sources or (2) performed significant amounts of onboard processing or averaging (in either time or frequency) that would tend to "wash out" any evidence of low to moderate RFI of the type typically observable in the "raw" data provided by SARs. It is largely unknown if future sensors seeking to make more sensitive measurements could observe RFI in the future, but that is certainly possible. K_u-band radar interference could come from aeronautical radio navigation radars operating in the 13250-13400 MHz band and radiolocation radars operating in the 13400-13750 MHz band and the 17200-17300 MHz band. An NTIA report indicates that emitters at the K_u-band show occupancy by high-power, long-range air search radars and terrestrial point-to-point communications.[3]

There is an Agenda Item (AI 1.6.1) for WRC 2015 to consider possible additional primary allocations to the fixed satellite service (Earth-to-space and space-to-Earth) in the 10-17 GHz range, which includes the EESS-Active band 13.25-13.75 GHz. There is also an Agenda Item (AI 1.6.2) for WRC 2015 to consider possible additional primary allocations to the fixed satellite service (Earth-to-space) in the 13-17 GHz range for Regions 2 and 3, which includes the EESS-Active band 13.25-13.75 GHz. Moreover, there is also an Agenda Item (AI 1.17) for WRC 2015 to consider possible spectrum requirements to support wireless avionics intracommunications (WAIC) in the EESS-Active band 13.25-13.4 GHz. These services represent a potential threat to science sensors either as future interference sources or as future spectral co-occupants that could impose transmit restrictions on active science systems. Sharing studies are being performed in the various ITU study groups including SG7 to protect the EESS-Active bands.

[3] F.H. Sanders, B.J. Ramsey, and V.S. Lawrence, *Broadband Spectrum Survey at San Francisco, California May-June 1995*, NTIA Technical Report TR-99-367, National Telecommunications and Information Administration, Washington, D.C., 1999.

Transmit Restrictions for Active Sensors at the K_u-Band and the K-Band

Although compatibility with existing services must always be established before flying any new sensor, no current significant barriers to operating active sensors at these frequencies have come to the attention of the committee.

K_a-Band

Band Usage

The IEEE Standard Letter Designations for Radio-Frequency Bands defines the K_a-band as between 26000 and 40000 MHz. The EESS-Active allocation for the K_a-band is at 35500-36000 MHz. The K_a-band is employed for altimeters, SARs, and cloud and precipitation radars. Multiple airborne systems exist to make these measurements for regional science or as demonstration platforms for space missions. Examples of satellite altimeter systems operating at the K_a-band include the French SARAL AltiKa, which was launched in 2012, and the U.S./French SWOT KaRIN, to be launched in 2020. A current example of a satellite precipitation radar system operating at the K_a-band is NASA/JAXA's GPM DPR, which was launched in 2014. The use of the K_a-band is somewhat "young" relative to the lower frequencies discussed thus far. Because of the relatively compact electronics and antennas, as well as the sensitivity to atmospheric hydrometeors associated with this high RF, the K_a-band is expected to be a significant growth area, seeing more and more sensors flown in the near future.

Interference Environment for Active Sensors at the K_a-Band

No reports of significant RFI at the K_a-band have come to the attention of the committee. Like other frequencies, there are some known, very-high-power ground radars that K_a-band sensors must take care to protect themselves against. Similar to the K_a-band, many current sensors either predominantly operate over the ocean or significantly process the data onboard, making a characterization of low to moderate RFI difficult. As with the K_u-band, it is currently difficult to assess the prospects of future measurements with respect to RFI.

Transmit Restrictions for Active Sensors at the K_a-Band

There are some restrictions on transmitted signals for science sensors at the K_a-band. In particular, there are limitations on the mean power flux density at Earth's surface that these sensors are allowed to produce in order not to interfere

with ground-based defense radars. Modern sensors (such as KaRIN on SWOT) meet this criterion, but not with a large amount of margin, perhaps suggesting that significant operational limitations may exist if the science community wishes to employ higher-power or higher-gain systems in the future.

W-Band

Band Usage

The IEEE Standard Letter Designations for Radio-Frequency Bands defines the W-band as being between 75000 and 110000 MHz. The EESS-Active allocations for the W-band are 78000-79000 MHz and 94000-94100 MHz. The W-band is used primarily for cloud profiling radar (CPR) systems. Examples of satellite CPR systems operating at the W-band include the U.S. CloudSat mission, which was launched in 2012, and ESA/JAXA's Earthcare CPR, which is to be launched in 2015, both of which operate within the 94000-94100 MHz band. The committee is unaware of any EESS-Active system planned for the 78000-79000 MHz band.

Interference Environment for Active Sensors at the W-Band

W-band radar interference could potentially come from radiolocation radars operating in the 78000-79000 MHz band and the 94000-94100 MHz band. Operators of CloudSat have not reported any RFI issues.

Transmit Restrictions for Active Sensors at the W-Band

There are restrictions on spectral access for science sensors in the W-band related to possible interference with radio astronomy (a passive radio science technique). An ITU Radio Regulations footnote states that "the use of the band 94-94.1 GHz by the Earth exploration-satellite (active) and space research service (active) is limited to spaceborne cloud radars." This apparently means that other applications at the W-band are allowed only in the lower W-band at 78-79 GHz, a potentially limiting restriction. Another Radio Regulations footnote (5.562 A) states that because W-band transmissions at 94 GHz from space "have the potential to damage some radio astronomy receivers … space agencies operating the transmitters and the radio astronomy stations concerned should mutually plan their operations so as to avoid such occurrences to the maximum extent possible."

Millimeter-Wave Band

Band Usage

The IEEE Standard Letter Designations for Radio-Frequency Bands defines the millimeter (mm)-band as between 110000 and 300000 MHz. The EESS-Active allocations for the mm-band are 133500-134000 MHz and 237900-238000 MHz. These bands have been proposed for possible spaceborne use for more sensitive cloud radars, but no satellite remote sensing EESS-Active system currently operates in this spectral region. These bands, however, are a potential new frontier for science sensors, and there is danger of potentially losing these bands to other services if they are not used.

Interference Environment for Active Sensors at the Millimeter-Band

Interference in the mm-band could potentially come from fixed, intersatellite, and mobile service systems operating in the 133500-134000 MHz band.

Transmit Restrictions for Active Sensors at the Millimeter-Band

There are restrictions on spectral access for science sensors in the mm-band. The lower mm-band at 133.5-134.0 GHz falls into the 130-134 GHz band, where the radio astronomy service has a primary allocation. The upper mm-band at 237.9-238.0 GHz band falls into the 235-238 GHz band, where the EESS (passive) has a primary allocation. There is a restriction similar to the W-band for "spaceborne cloud radars only" for the upper band 235-238 GHz. There is no such restriction in the lower band at 133.5-134.0 GHz, where the radio astronomy service has a primary allocation, but for this lower band the mutual planning of operations would avoid damaging radio astronomy receivers.

FINDINGS AND RECOMMENDATIONS

Finding 8.1: There are primarily two spectrum issues that can impact active science sensors. Like passive sensors, active sensors can experience RFI from other radio services. Conversely, and unlike passive systems, active systems also transmit signals and are hence subject to operational restrictions to ensure that they do not interfere with other services. With demand for and use of the spectrum growing rapidly, both of these spectrum issues are generating concerns for the successful operation of current and planned active science sensors.

Finding 8.2: In several cases, transmit restrictions imposed on active science sensors have significantly impeded the ability to collect the desired science data (as in the operational restrictions imposed on ESA's BIOMASS mission), degraded the science data (an example being the deep spectral waveform notches required on the GeoSAR sensor flown on aircraft), or significantly driven up costs (as for the NASA Soil Moisture Active-Passive mission). Conservative interference standards in some bands can make science operations difficult. Restrictions imposed in the lower-frequency UHF and L-bands are increasing with time.

Finding 8.3: Whereas active science sensors routinely report interference from other nonscience sources, science sensors appear to rarely interfere with other services. The only documented instance to come to the attention of the committee of an active science sensor actually interfering with the operations of another service was the CloudSat radar, which can interfere with the radio astronomy service (another science service).

Finding 8.4: The RFI environment has been observed to be growing worse in some bands. Within the heavily used and well-studied L-band allocation of 1215-1300 MHz, the amount of RFI observed worldwide has steadily increased over time. This trend has been detected by a series of L-band SARs operated by JAXA spanning the years 1992-2011. ESA has reported an increase in RFI at the C-band.

Finding 8.5: As of yet, few problems with RFI have been experienced with the specific science measurements made at frequencies above the C-band.

Finding 8.6: RFI mitigation techniques have been successfully employed at the UHF, L-, and C-bands to significantly reduce the impact of interference on science. Current RFI mitigation techniques, however, work best for interfering signals that have "sparse spectral/temporal occupancy" (e.g., signals closest to being continuous wave or short, widely separated pulses). The more that sources, or aggregates of sources, resemble broadband white noise, the more difficult the interference is to mitigate with known techniques. Consequently, active remote sensing is able to more effectively share with some services than others.

Finding 8.7: Established, high-value science radar measurements at the C-band face near-term threats due to the planned expansion of commercial services in the EESS-Active allocation. The proposed 5350-5470 MHz

RLAN service will severely limit science performed by ESA's Sentinel 1 satellite and Canada's Radarsat-2 and RCM constellations. The broadband, noiselike nature of RLAN emitters is difficult or impossible to mitigate.

Finding 8.8: Particularly for spaceborne missions, the RFI environment is difficult to characterize a priori for a given instrument. Consequently, RFI measures are often only fully implemented reactively when the true nature of the interference environment is encountered after a new sensor is deployed. This is due to both the incompleteness of information regarding current emitters worldwide and the evolving nature of the RFI environment over time.

Finding 8.9: There is currently a lack of good metrics for quantifying the degradation of science measurements for the full variety of active instrument types (for example, scatterometers, altimeters, synthetic aperture radars, interferometers, sounders, and others). This, coupled with Finding 8.7, often makes it difficult to predict accurately how a given active sensor might be impacted by RFI, how the RFI might be mitigated, and how the spectrum might be shared.

Finding 8.10: There are multiple bands allocated to EESS-Active where only portions, of the band are being used or that are not being used at all. With constant pressure to accommodate new services, it may be more difficult to establish new science in these bands in the future.

Recommendation 8.1: NASA should lead an effort to significantly improve characterization of the radio-frequency interference environment that affects active science measurements. This effort should also involve other agencies involved in active remote sensing, including the National Oceanic and Atmospheric Administration, the National Science Foundation, and perhaps the Department of Defense, as well as the agencies regulating these activities—the Federal Communications Commission and the National Telecommunications and Information Administration. The effort could be coordinated by the Office of Science and Technology Policy. It should include the use of (1) modeling, (2) dedicated ground-based and airborne characterization campaigns, and (3) data mining of currently operating science sensors. To the extent possible, this effort should be a collaborative one with other space and science agencies of the world.

Recommendation 8.2: NASA should lead a community effort to construct a set of metrics that relate the various radio-frequency interference environments encountered to the associated degradation in science performance for each major class of instruments employed in active remote sensing.

9

Technology and the Opportunities for Interference Mitigation

INTRODUCTION

Fundamentally, every active sensing system, be it monostatic or bistatic in configuration, is a communication system consisting of a transmitting source and a receiver. Owing to advances realized in the past decade in the technology used in cellular mobile phone applications, opportunities for improving coexistence with radio-frequency interference (RFI) have improved significantly. However, these benefits offer more to the world of communications than to sensing applications. Each communications link has a definable signal-to-interference-plus-noise ratio (SINR) threshold, and any signal above the threshold level meets the minimum requirements for the establishment of robust data transfer. If interference exceeds this threshold, it is sometimes still possible to apply technological remedies that reduce the interference to a level below the threshold, thereby recovering the data without loss of information. In a sensing application, however, the target environment has many thresholds because the strength of the signal scattered from the atmospheric volume or the land or ocean surface may vary over a wide range, so there is no clear or absolute level for successful interference mitigation. Even so, there are opportunities for the better use of established approaches to reduce interference. The opportunities include both unilateral methods, wherein no cooperation between users in the same spectrum is needed, and sharing methods, wherein coordination between users in the same spectrum is required.

UNILATERAL TECHNIQUES AND STRATEGIES

Active remote sensing implies the use of a transmit signal, whereas passive remote sensing implies that the sensing operation uses a receive-only mode. In the case of unilateral methods, there are two techniques for dealing with other signals in the sensing spectrum. In the first technique, the potentially interfering signal is used directly as the source for active sensing. In the second, mitigation techniques to reduce the level of interference are applied without cooperation from the source of the interference.

If an active remote sensing system relies on the transmission of an independent signal that is already present in the spectrum, allocation of additional spectrum is not necessary for the sensing function. Two key examples are provided to illustrate the process: (1) global navigation satellite system (GNSS) signals and (2) TV and radio broadcast signals. In both cases, the sensor operates in a bistatic mode by measuring the signal transmitted by such sources, after reflection/scattering by the medium or surface of interest.

The Global Positioning System (GPS) provides between 24 and 32 L-band space-based transmit signals radiating towards Earth. GNSS signals from other systems, such as GLONASS, Galileo, and Beidau, are also available in the same frequency band. These forms of radio and microwave signals are analogous to multiple low-power "suns" for optical passive remote sensing (i.e., taking a picture with a camera). The distribution of these signals provides multiple sources for sensing at any time, and to continue the same optical analogy, these signals ensure that there is daylight with four or more "suns" continuously at every spot on Earth.

The state of the ionosphere is important in predicting the possible degradation of space-ground communication signals. Signals from the GPS to ground-based receivers provide a measurement of the total electron content (TEC) along multiple paths through the ionosphere. The website at www.swpc.noaa.gov/ustec provides daily reports like that shown in Figure 9.1, along with trends and historical data.

Upward-looking ground-based microwave radiometers can provide accurate information on the height profiles of temperature, air density, and other atmospheric parameters, but the technique is essentially limited to the lowermost 10 km in altitude. Downward-looking satellite-borne radiometers are also best suited for profiling approximately the same altitude range, but they can do so globally. Higher-altitude profiles can be measured by radiosondes launched on balloons, but the information is specific to the geographic location of the radiosonde launch position. While there are hundreds of sites worldwide that perform sensing of the atmosphere with balloon-based sensors, the information is geographically sparse, especially over the maritime environment. To improve the coverage and fidelity of this atmospheric data, a new method was developed using the space-based reception of the occultation of a space-based radio signal to profile atmospheric

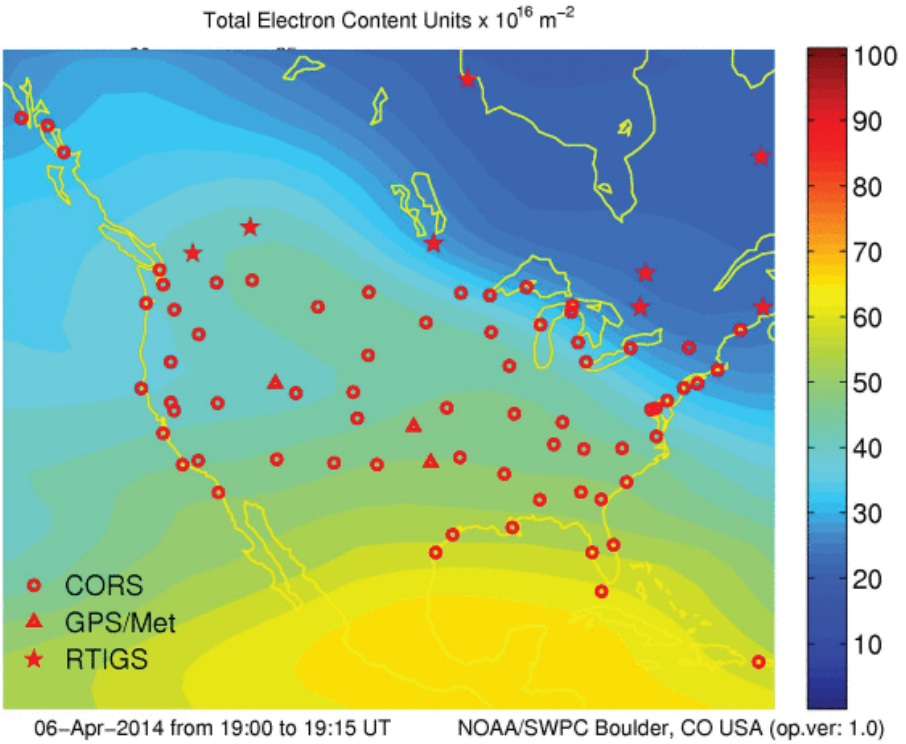

FIGURE 9.1 Current total electron content levels and the locations of ground receivers are shown for April 6, 2014, for North America. NOTE: CORS, Continuously Operating Reference Station; RTIGS, Real Time International GNSS Service. SOURCE: NOAA Space Weather Prediction Center, "U.S. Total Electron Content," http://www.swpc.noaa.gov/products/us-total-electron-content, accessed August 3, 2015.

density and temperature, and the GPS signal is an important part of this technique. Figure 9.2 shows how a low Earth orbit (LEO) satellite can observe the GPS signal as the geometry causes occultation of the signal.

After inversion of the measured data using the geometry of the occultation, high-resolution profiles are generated for a wide range of altitudes extending between 8 and 30 km or higher. The indirect occultation measurements are compared to the direct radiosonde sensors on a weather balloon in Figure 9.3.

The temperature estimates based on occultation are more accurate than those predicted by the current European Centre for Medium-Range Weather Forecasts (ECMWF) model, which is based on the combination of inputs from ground, aircraft, ships, weather balloons, and other space instruments without occultation inputs. The improved data collection that led to these operational systems

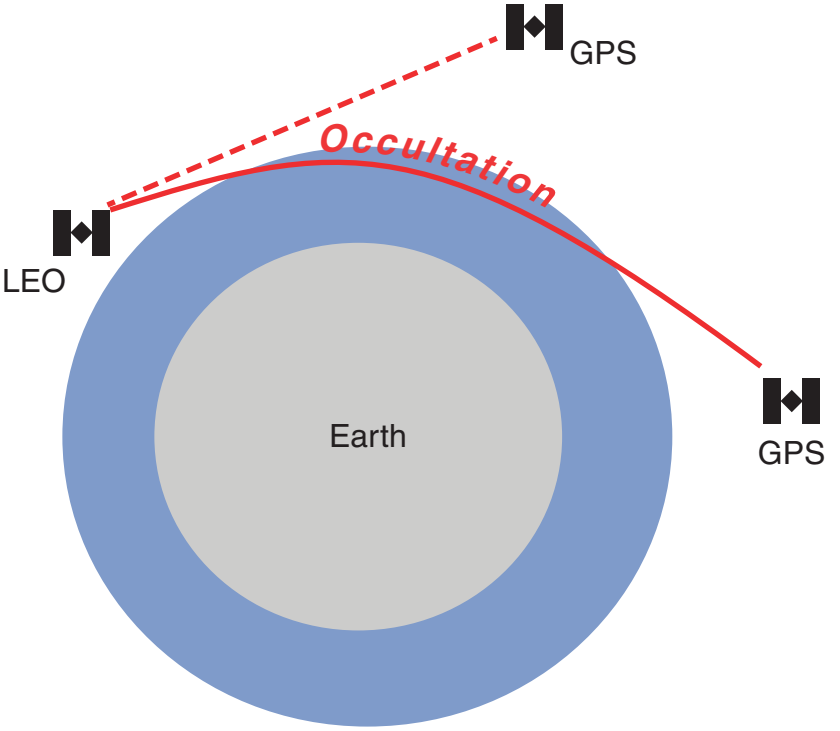

FIGURE 9.2 Variations in the GPS signal as the rays pass through the lower atmosphere are used for determination of atmospheric density, temperature, and pressure profiles.

was accomplished without the allocation of additional radio spectrum. Instead, these accomplishments can be attributed to novel technologies that reuse existing "signals of opportunity."

Another example of a bistatic radar that uses an external source for illumination is shown in Figure 9.4.

The two approaches to wind vector measurements—backscatter and bistatic—agree to within 1-2 m/s, and the bistatic system has an enhanced ability to detect the low-level divergence under the cell owing to better clutter filtering and shorter range to target.[1] The signal source for both measurements is the S-band multimission hemispheric radar (MHR), which is a NEXRAD prototype radar.

A second approach to unilateral sharing of the spectrum involves using tech-

[1] J. Wurman, M. Randall, C.L. Frush, and E. Loew, Design of a bistatic dual-Doppler radar for retrieving vector winds using one transmitter and a remote low-gain passive receiver, *Proceedings of the IEEE* 82(12):1861-1872, 1994.

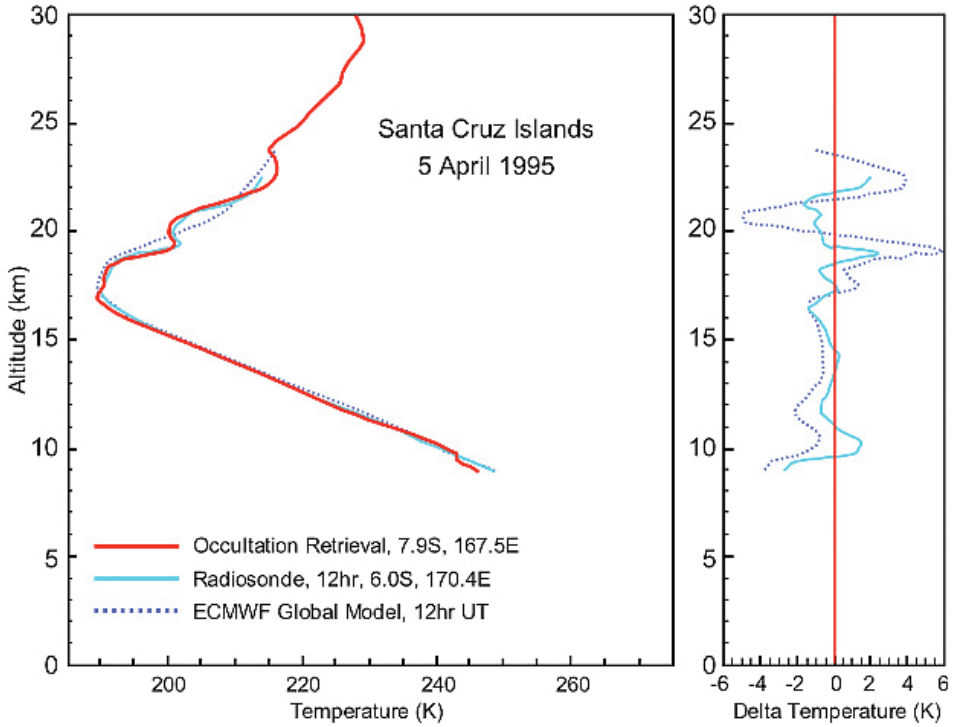

FIGURE 9.3 Comparison of temperature profile based on occultation and radiosonde measurements. SOURCE: Tom Yunck, Jet Propulsion Laboratory.

niques and methods to reduce or mitigate interference. Examples of RFI reports and the application of notch-filtering to mitigate RFI effects are available in Chapter 8.

Unilateral approaches to interference mitigation are used when appropriate. In some applications, however, there is no effective method of cooperation. In other cases, the sources of interference are too numerous for effective enforcement of the actual spectrum allocation and/or authorization. Better remote sensing in the presence of other users of the spectrum comes from sharing the spectrum cooperatively.

SHARING TECHNIQUES AND STRATEGIES

Frequency, time, and space are the three fundamental domains for the presence of an electromagnetic (EM) signal. Within these three domains, an EM signal has one more degree of freedom—namely, its polarization. Furthermore, a powerful combination of frequency and time used for signal isolation is coding, and while coding is not a unique domain, it is widely used and well characterized in com-

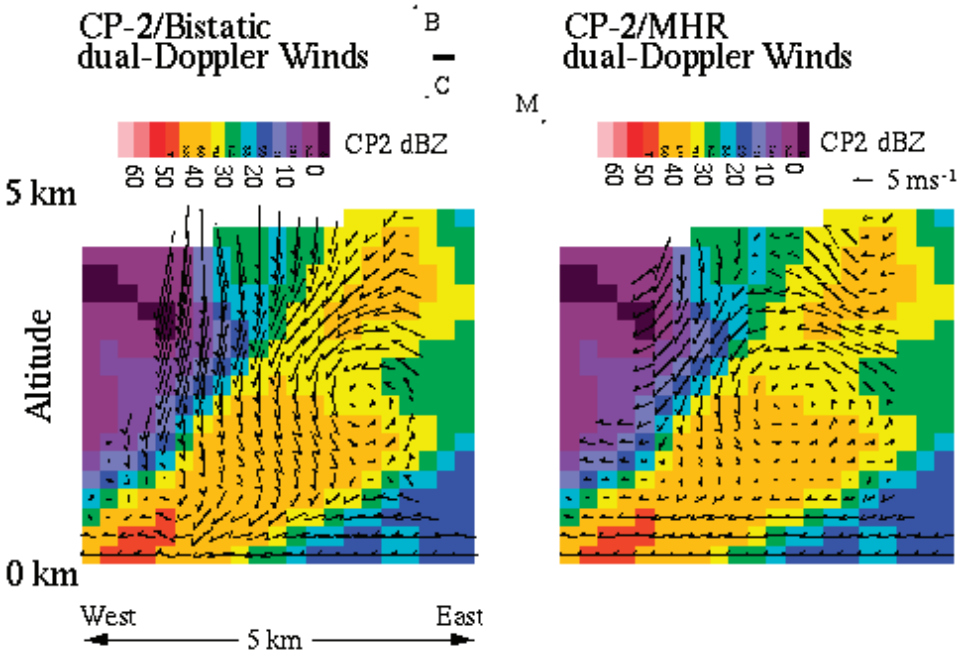

FIGURE 9.4 Comparison of wind vector profile data obtained in bistatic mode (*left*) with the mile high radar (MHR) in backscatter mode (*right*). SOURCE: Joshua Wurman, Center for Severe Weather Research, Research; see J. Wurman, M. Randall, C.L. Frush, and E. Loew, Design of a bistatic dual-Doppler radar for retrieving vector winds using one transmitter and a remote low-gain passive receiver, *Proceedings of the IEEE* 82(12):1861-1872, 1994. Reprinted, with permission.

munications and some sensing applications. Finally, the power of a signal impacts the level of that signal at other ranges, and this impacts the spatial domain. This section examines all of the six dimensions of frequency, time, space, polarization, code, and power control (Figure 9.5).

Frequency Domain

The frequency domain is assumed to be limited to only allocated and assigned users (Figure 9.6). It should be noted that there are practical limitations to this assumption, which creates a form of sharing even when there is no desire to share. For example, the frequency spectrum of signals radiated by faulty or poorly designed equipment may drift outside the desired band of operation and infringe on other portions of the spectrum. Older receive equipment may lack proper front-end filtering, and the presence of two or more signals from other spectral

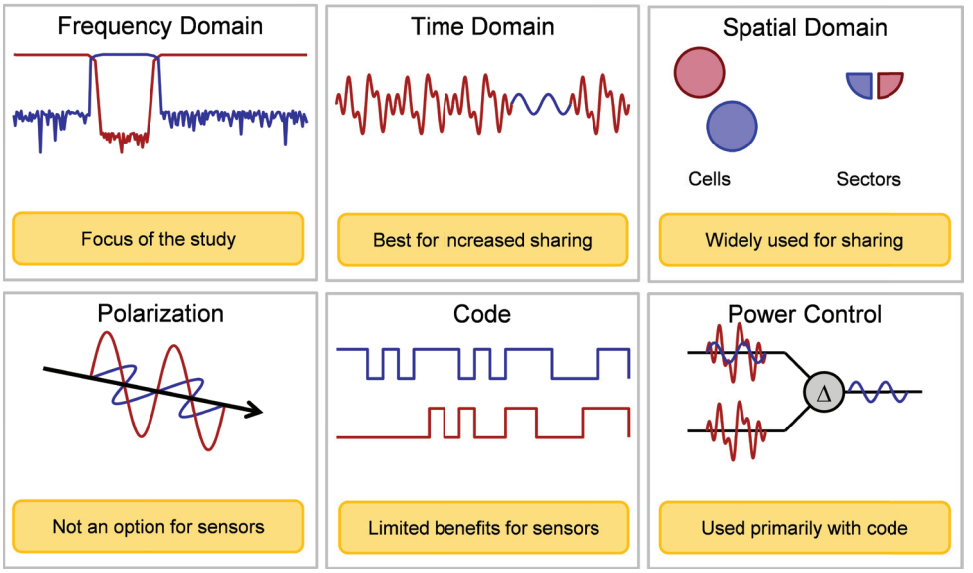

FIGURE 9.5 Six domains of potential sharing are considered. SOURCE: FIRST RF Corporation.

allocations at the front end of this equipment may mix via nonlinear effects to cause interference in, or partially outside, the spectrum served by this equipment. Older transmitting equipment may lack the filtering to meet adjacent spectral allocations, and/or the wave shaping, especially for pulsed signals, may be insufficient to reduce transient creation of spurious products that fall outside the spectral allocation for this equipment. As technology advances, these issues tend to decrease.

Time Domain

The most powerful form of cooperative sharing is in the time domain. In its simplest form, a single user has full use of a segment of the spectrum for a specific time slot, and no other signals are present during the assigned time period, so there is effectively no interference. With longer time slots or "slow" time, there is little issue with alignment accuracy of the time slots or transient effects of users moving into or out of assigned slots. Figure 9.7 illustrates this concept.

When the time slots occur very quickly, more serious issues may occur in dealing with the timing accuracy and transient effects. In general, sharing fast time slots, as shown in Figure 9.8, is best implemented by a single-spectrum user, as there is a monetary value to better control of these effects.

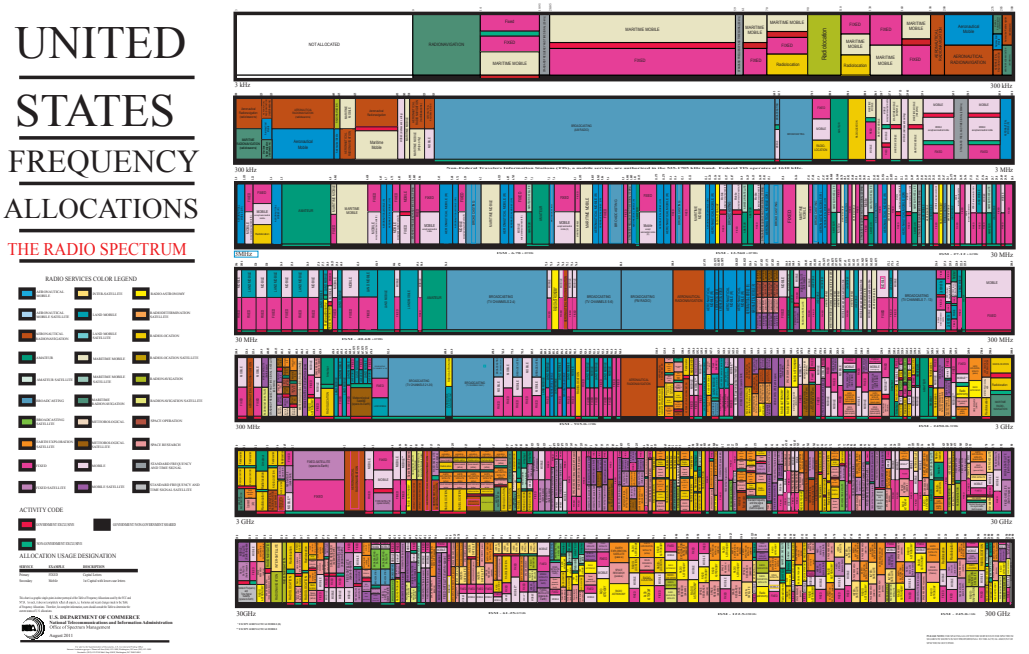

FIGURE 9.6 Frequency (spectrum) allocation is shown in this chart. SOURCE: U.S. Department of Commerce.

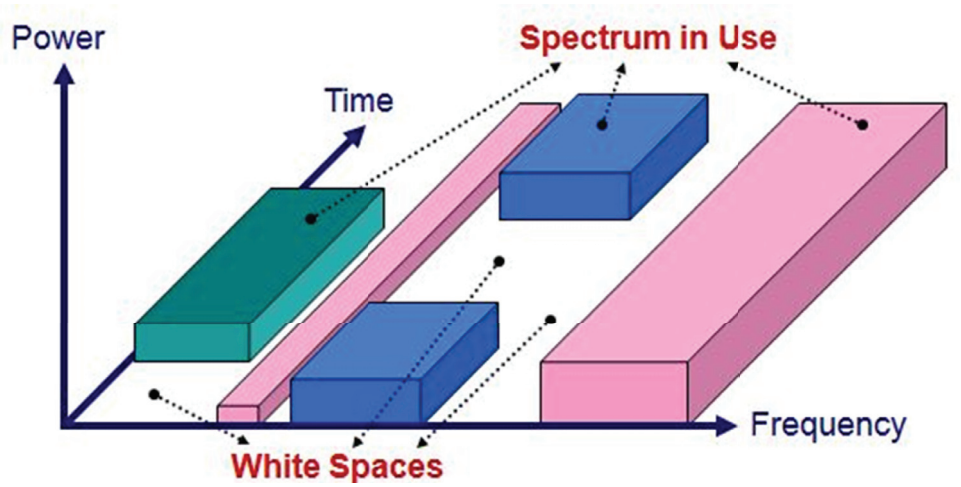

FIGURE 9.7 Sharing in "slow" time has nearly infinite isolation. SOURCE: Electronic Communications Committee, European Conference of Postal and Telecommunications Administrations (CEPT), *ECC Newsletter*, June 2011, http://www.cept.org/ecc/who-we-are/ecc-newsletters; diagram reproduced with permission of the CEPT.

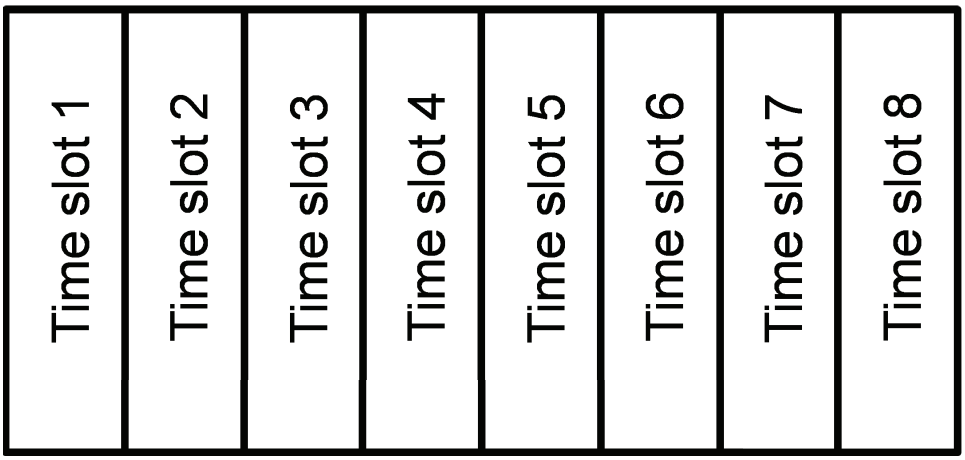

FIGURE 9.8 Sharing in fast time is called time division multiple access (TDMA). SOURCE: Dean Paschen, First RF Corporation.

Spatial Domain

In a manner similar to temporal sharing, a given spectrum allocation can be shared spatially. The rapid increase in data rates to mobile users is directly a result of efficient spatial sharing of the spectrum, as illustrated in Figure 9.9 for the early layout of the cellular mobile phone system.

Sharing in space can be nearly as effective as sharing in time. The limitations, which are best managed by a single motivated user, are primarily due to leakage of the signal from one spatial cell into an adjacent cell. The motivated user generally implements some form of power control, so that only the required power for the communication link is used, and this reduces the potential for leakage relative to the case where all signals operate at full power. Much of the foreseeable future gains in data bandwidth to mobile users will be due to spatial sharing. The cell diameters will be reduced, and the cells will be split into subsectors, as shown in Figure 9.10.

Progress in spatial sharing can be seen in the terminology used in the cell phone industry. The largest cell size is called a macrocell. Microcells, picocells, and even femtocells are terms that indicate the decreasing size of each spatial cell. As the cell size decreases, the benefits of spatial sharing increase.

A femtocell is a low-power device that handles very localized wireless traffic. Femtocells allow wireless coverage to be extended from the edges of the areas covered by larger cells into small but high-demand areas (for example, buildings) for less cost than deploying a partially redundant larger cell.

A recent development in spatial sharing, which falls outside the cell phone

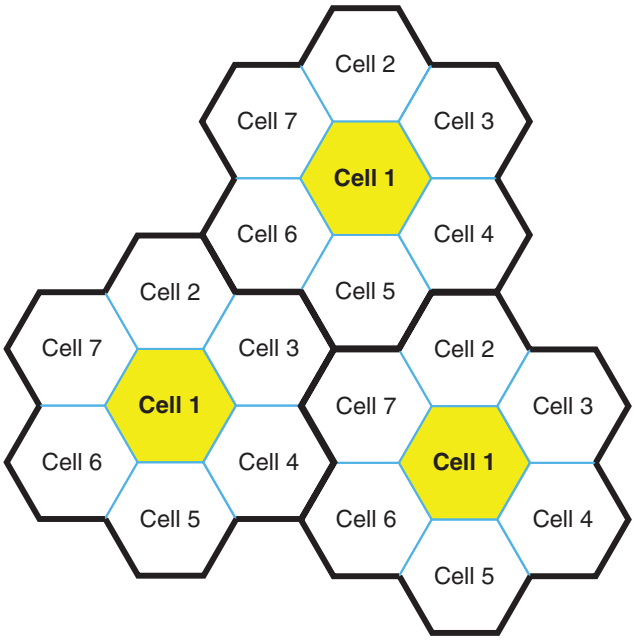

FIGURE 9.9 Early cellular systems achieved a frequency reuse factor of 7 through spatial sharing.

industry, is the April 1, 2014, release of modifications to Part 15 of the Code of Federal Regulations, Title 47 (ET Docket No. 13-49) to support the Unlicensed National Information Infrastructure (U-NII). Two features are implemented to protect the spectrum, with the first being a security feature to prevent simple modification of the hardware to change the frequency. The second feature is a new implementation of spatial sharing between different users of the spectrum: devices within 35 km of a terminal Doppler weather radar (TDWR) location must be separated by at least 30 MHz (center-to-center) from the TDWR operating frequency, and the rule includes procedures for registering the devices in an industry-sponsored database.

Polarization Diversity

Polarization is another sharing domain that offers the potential for doubling the amount of data in a single spectral allocation. In satellite communications (SATCOM), this domain is nearly always used. In SATCOM links, polarization is used to tighten the spacing between frequency slots without total overlap of the spectrum used between the two orthogonal polarizations, as illustrated in Figure 9.11 for C-band operation.

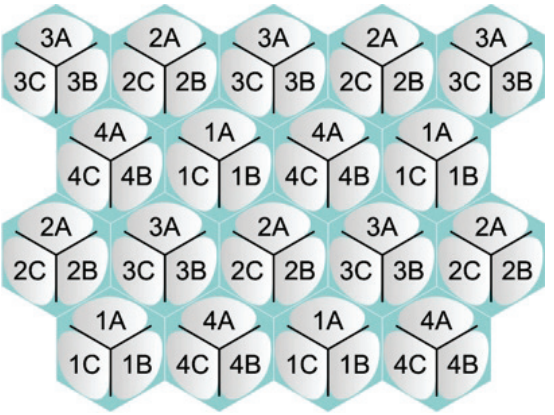

FIGURE 9.10 Spectral sharing efficiency is improved with the use of three sectors within a cell and a frequency-reuse factor of 4 between cells. SOURCE: Courtesy of TruTeq Wireless, truteq.com.

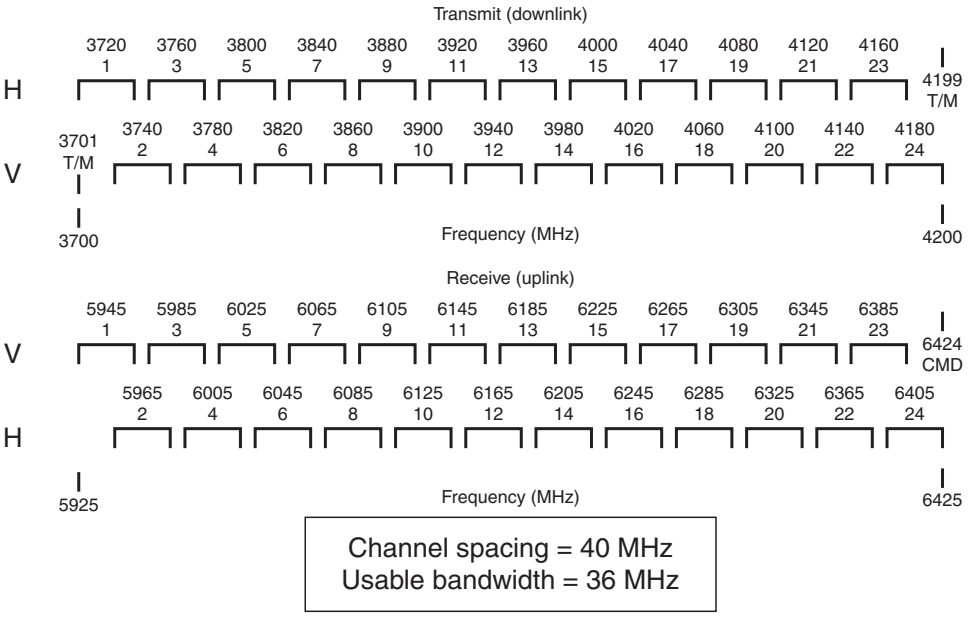

FIGURE 9.11 The basic 24-channel transponder alignment is shown at the C-band (3.7-6.5 GHz).

However, polarization is not always a good candidate for sharing between active sensors and other users of the same spectrum. In ground-based weather radar, for example, measurements of the backscatter from a precipitating volume made at orthogonal polarizations are used to distinguish between rain and snow and to determine the precipitation rate, so sensor control over the polarization domain is required.

Code Domain

In cellular communication systems, a subset of the spectrum may be allocated to separate users, and this is called frequency division multiple access (FDMA). As discussed earlier, time slots within each frequency slot may be used by multiple users, and this is called time division multiple access (TDMA). Time and frequency are orthogonal domains. An alternative form of sharing spectrum that combines time and frequency into a set of codes is called code domain multiple access (CDMA) (Figure 9.12).

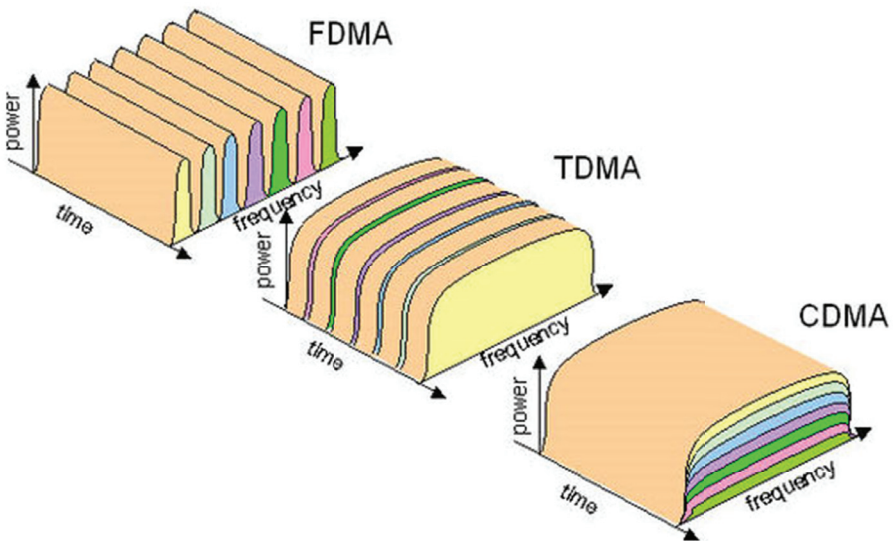

FIGURE 9.12 CDMA is the combination of time and frequency into codes that overlap in both the time and frequency domains. SOURCE: J. Zhang,Y. Liu, Ş.K. Özdemir, R.-B. Wu, F. Gao, X.-B. Wang, L. Yang, and F. Nori, Quantum internet using code division multiple access, Nature's Scientific Reports 3:2211; licensed under a Creative Commons Attribution 3.0 Unported License, http://creativecommons.org/licenses/by/3.0/.

In the code domain, each bit of data for different users is encoded with a unique code. The coding of a single bit of data with multiple bits of code spreads the bandwidth of the original signal. This spread-spectrum approach takes a given bit in time and spreads the spectral content. Since the codes are isolated from each other, the individual signals can be recovered by mixing them with the same spreading code during reception and detection, so there is no effective loss to the number of users in the same time and frequency.

The code domain is not a new domain. Rather, it is a transformation of two existing orthogonal domains (time and frequency). While orthogonal or independent codes do exist, there is a limited number of codes, and they require time synchronization to achieve true orthogonality. To avoid synchronization issues, modern CDMA systems use nonorthogonal codes. These practical codes operate without the need for precise synchronization, but the isolation is less than that obtainable for an orthogonal code. This limitation in isolation, coupled with the larger dynamic range required in active sensor systems, means that there is limited benefit for the use of the code domain in active sensing systems. However, if there are known interferers using a known code set, there are opportunities for both unilateral and cooperative sharing using this technology.

Power Control

In conjunction with spatial sharing, power control is very important. If too much power is used, leakage occurs into nearby spatial regions. In CDMA systems, power control becomes even more important, and the issue is known as the "near-far problem." The isolation between two codes is based on the cross-correlation of the codes as designed or selected. This isolation assumes equal power at the receiver/detector. When the power levels are different, as illustrated in Figure 9.13, the expected isolation from the cross-correlation of the code can be compromised.

To deal with this loss in isolation, each phone in a CDMA communication system is controlled to provide equal power at the base station to minimize the reduced orthogonality of the near-far problem.

Sharing the spectrum works best when all users of a particular portion of the spectrum are motivated to use the spectrum efficiently. Cell phone systems are examples of excellent spectral utilization. Each telecommunication company is assigned a segment of the spectrum, and all sharing of that segment is designed specifically for that company and its customers. The financial benefits to each company motivate the best sharing practices.

The sharing of the spectrum by less motivated users is not as promising. As mentioned earlier, a communication user may be unaware of another signal in the same spectrum as long as the detected data have few uncorrected errors. An active sensor, however, can miss the detection of long-range or low-visibility targets at

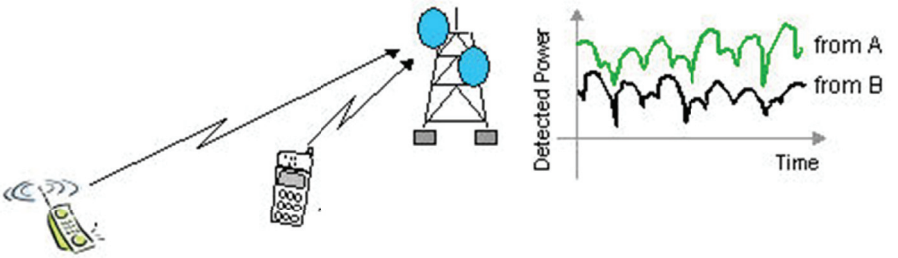

FIGURE 9.13 The detected power for different ranges at equal transmit power is different. SOURCE: Shimada Masanobu, Tokya Denki University.

much lower levels of interference. The limitations to sharing for active sensing applications comprise the topic of the next section.

BEST OPPORTUNITIES FOR SHARING

As discussed previously, wireless communication systems have already demonstrated the ability to share the spectrum. Spatial sharing in this community has provided more gains in capacity than increases in spectrum. The wireless communication industry is moving to continue the capacity gains by a migration to smaller cells at higher frequencies. These femtocells operating at millimeter wavelengths will dramatically increase system capacity.

In the world of active sensors, radar systems are also known to share well, and there is an opportunity to conserve spectrum by better sharing. As discussed in Chapter 2 (see the section "Future Trends and Concepts—Ground-Based Radar"), the National Oceanic and Atmospheric Administration (NOAA) and the Federal Aviation Administration (FAA) are considering a proposal to move the Air Route Surveillance Radar (ARSR) and TDWR systems, which are currently in different frequency bands across the L-, C-, and S-bands, into the existing S-band spectrum (2.7-3.0 GHz) for air traffic control and weather radar, with the use of phased array methods in place of existing mechanically steered radar systems.[2] The MPAR concept would enable rapid-update weather observations that are fundamentally important for severe weather safety, among other significant improvements, benefiting both the active sensing community and the public. Another advantage of an MPAR system would be its improved spectral efficiency, since radars operating

[2] *Multifunction Phased Array Radar (MPAR),* Notional Functional Requirements Document, Version 2.2, April 18, 2013.

across different frequency bands would be replaced with radars in a single band. From an economic standpoint, an advanced radar network with a common design would inherently have much lower maintenance and operation costs.

It is important to make the technology transition to support the multiple functions from a single radar site in the single frequency band. In addition, the existing S-band radar spectrum may be reduced further through the use of similar techniques to wireless communication systems.

Although active sensor systems are sensitive to interference from communication systems, the opposite case of radar system interference to modern communication systems using forward error correction (FEC) is very limited. In fact, for radar waveforms with narrow pulse widths and low duty cycles that impact less than 0.5 percent of the symbols in a communication system, it is necessary for the radar signal level to be 50-70 dB higher than the carrier level of the communication system to cause failure.[3] It should be possible for Earth imaging systems to operate in existing communication bands when certain waveform features are used in the radar system. The radar systems will still need to apply notching in the areas of high spectral power density, but this adherence to waveform guidelines would eliminate interference to any communication devices present in portions of the spectrum that are still considered to be effective for the radar system.

The National Science Foundation's (NSF's) Enhancing Access to the Radio Spectrum (EARS) program funds multidisciplinary research in technologies and techniques with potential to greatly increase the efficiency of spectrum, including sharing. For example, since space-based, active remote sensing sensors typically observe a single spot on Earth only a few times per day, they could coordinate with other transmitting services to more efficiently use the spectrum otherwise reserved only for remote sensing when not in use by remote sensing. Vice versa, when incumbent transmitting services are not using a band, active remote sensing sensors could do so. This example is but one sharing possibility based in the time domain. As the program proceeds and research is conducted, it is likely that many new sharing techniques will be developed.

LIMITATIONS OF MITIGATION TECHNIQUES AND STRATEGIES

While both unilateral methods of interference mitigation and cooperative approaches to sharing the spectrum offer benefits, it is important to also understand their limitations. In the unilateral case, the limits of mitigation are dictated

[3] F.H. Sanders, *Measurements of Pulsed Co-Channel Interference in a 4 GHz Digital Earth Station Receiver*, NTIA Report 02-393, National Telecommunications and Information Administration, Washington, DC., 2002.

by the physics of the interference process. In contrast, with cooperative sharing, mitigation is limited more by issues of management.

For unilateral interference mitigation, the optimum approach is to probe the channel and adjust the transmit waveform for minimum correlation with the channel interference characteristics. A simple form of this (previously discussed) is notch filtering. Basic notch filtering removes high-level aspects of the interference as determined by spectral analysis of the channel. The technique is not always successful, however. An example of a synthetic aperture radar (SAR) image before and after basic notch filtering is shown in Figure 9.14.

While RFI may be mitigated for the conventional SAR image, there are other data products that may still be impacted. Interferometric SAR (InSAR), which compares the phase information between two or more images, can be degraded at a much lower residual RFI levels. The closely related data product of coherent change detection (CCD), which compares the complex correlation between two or more images, is also dependent on the phase information and can be impacted at much lower levels of residual, and effectively unmitigated, RFI.

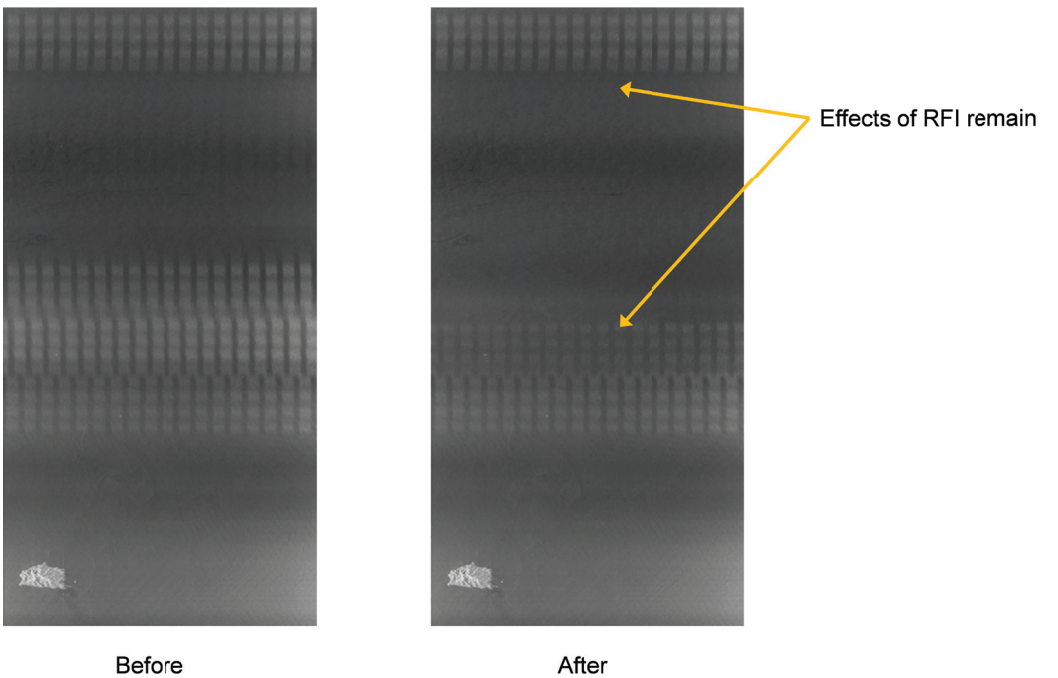

FIGURE 9.14 While spectral notching reduces radio-frequency interference (RFI) effects to active sensors, the RFI may not be completely eliminated. SOURCE: Shimada Masanobu, Tokya Denki University.

When sharing spectrum between cooperative users, there are many logistical issues that may limit the quality of the signals for the various stakeholders. The following examples illustrate some of the issues that arise when time and space sharing are used.

Sharing that occurs over relatively slow periods of time (e.g., minutes or longer) is generally based on established schedules. If a schedule is not properly communicated to all users, there can be deviations that might cause interference. There can be breakdowns in managing a schedule across time zones, especially at transition points like changing from Standard Time to Daylight Saving Time or crossing over fractional time zones.

When sharing over faster time intervals, timing accuracy becomes an issue. This may be due to the frequency stability of a reference oscillator, although current technology provides many high-accuracy clocks. More likely, this is due to spatial separation of the various users, which creates a time offset that is difficult to coordinate between multiple users. For example, a time slot set up to synchronize with a close user may be out of sync with a user further away. Even with precise information about the location of all users, there may be no solution other than to increase the guard band of the channel to avoid collisions, which would decrease the spatial/temporal efficiency.

Spatial sharing has similar issues. If a ground-based sensor is located beyond the line of sight to another ground-based sensor in the higher frequency bands where ionospheric scattering is not present, a large scattering object (e.g. blimp, aircraft, and so on) can still provide a reflected path from one sensor to the other. In cases where power control is used to limit the interference between two sensors, a variety of mechanisms exist to convey power at a much higher level (e.g., ducting, scattering by large objects, multipath, and the like).

Although radar systems are known to share well with other radar systems of a similar type, ground-based radar systems do not share well with airborne and spaceborne radar systems, even though Earth-imaging airborne and spaceborne radar systems share well. Therefore, specific radar bands are best allocated for either ground-based systems or Earth-imaging systems.

FINDINGS AND RECOMMENDATIONS

Finding 9.1: From the perspective of efficient spectrum usage, the active sensing community would benefit from consolidating the L-, C-, and S-band radar assets of NOAA and the FAA to a single multifunction radar at the S-band, as proposed by the Multifunction Phased Array Radar program.

Recommendation 9.1: The committee recommends an investigation of spatial frequency reuse techniques (for example, 7-to-1 spatial frequency saving) to reduce

the total S-band spectrum requirements. The existing L-band spectrum should be maintained for Earth-imaging radar use.

Finding 9.3: The use of millimeter-wave frequencies for shortwave, femtocell-sized communications would increase network capacity by an order of magnitude, thereby reducing pressure on the spectrum and on the active sensing science services, as well.

Recommendation 9.2: The wireless industry should pursue the femtocell approach by developing towers, networks, and the like to add the use of millimeter-wave frequencies for communications in 6G communication standards and up.

Finding 9.4: Communications systems are highly resistant to interference from radar systems with narrow pulse waveforms and low duty cycles, which are typical characteristics of scientific and operational radars.

Recommendation 9.3: The Federal Communications Commission or the National Telecommunications and Information Administration should permit radar systems meeting specific criteria for pulse repetition, maximum pulse width, and duty cycle to operate in communications bands as secondary users, where minimal interference to the communications operations would be expected to occur.

Appendixes

A

Statement of Task

The committee will prepare a report exploring the scientific uses of the radio spectrum by radio frequency transmissions and the measurement thereof. In carrying out the study, the committee will:

- Describe the science that is currently being conducted using the radio spectrum for transmission and measurement of these active signals and identify the spectrum requirements necessary to conduct this research;
- Identify the anticipated future spectrum requirements necessary to continue to conduct and expand this research for the next 10-20 years, taking into account trends in overall active use of the spectrum;
- Discuss the value to the nation of accommodating the active scientific use of the spectrum, recognizing the need to balance the needs of multiple communities;
- Assess the active science communities' current and anticipated future access to the spectrum required for research; and
- Recommend strategies to accommodate the continued active use of the spectrum for scientific purposes in order to maintain the needed science capabilities identified above.

The committee will comment on the spectrum use by the relevant scientific communities for applications such as active microwave remote sensing (i.e., airborne and space-based radars) of Earth to observe environmental phenomena, incoherent scatter radar studies of Earth's ionosphere and radar astronomy of solar

system objects, but will not make recommendations on the allocation of specific frequencies. The committee will not make recommendations on communications operations (i.e., transmission of data) that support the scientific uses of the spectrum described above. The committee should consider proven and potential unilateral and cooperative mitigation techniques in its analysis of access to spectrum.

B

Committee Meeting and Workshop Agendas

MEETING 1

August 15-16, 2013
Keck Center of the National Academies
Washington, D.C.

August 15, 2013

CLOSED SESSION

8:30 a.m. Committee Discussion

OPEN SESSION

12:30 p.m. Working Lunch

1:00 Opening Remarks on the Study
Vic Sparrow, NASA
Director, Spectrum Policy and Planning

1:20	Active Earth Remote Sensing: NASA Perspective—Study need, context, scope, desired outcomes Tom vonDeak, NASA
	Spectrum Management Bryan Huneycutt, JPL
	Committee discussion with NASA Betsy Edwards, NASA Earth Sciences
3:15	Spectrum Management for Active Radio Science—Study need, context, scope, desired outcomes Andrew Clegg and Glen Langston, NSF ESM
	Committee Discussion with NSF
4:30	RFI Mitigation Techniques Under Study at DARPA John Chapin, DARPA Strategic Technology Office
	CLOSED SESSION
5:15	Committee Discussion

August 16, 2013

OPEN SESSION

8:30 a.m.	Working Breakfast
9:00	FCC Perspective Julie Knapp, FCC, Chief, Office of Engineering and Technology
9:30	NTIA Perspective Karl Nebbia, NTIA, Associate Administrator, Spectrum Management
10:00	OSTP Perspective Tom Power, OSTP, Deputy CTO, Telecommunications

10:45	Perspective from Congress TBD Hill Staff
11:15	General Discussion Public Comment Session

CLOSED SESSION

11:45	Committee Discussion
3:00 p.m.	Adjourn

MEETING 2

Active Sensing Radio-Frequency Interference Workshop[1]
November 8, 2013
Jet Propulsion Laboratory
Pasadena, California

8:30 a.m.	Visitor Badging at JPL
9:00	Welcome and Goals for the Workshop Fawwaz Ulaby, Workshop Co-organizer and Committee Chair
9:15	Perspective from the European Space Agency Pierluigi Silvestrin, ESA (by WebEx)
9:45	Perspective from the Canadian Space Agency Dean Sangiorgi, CSA (by WebEx)
10:15	Perspective from the Japan Aerospace Exploration Agency Masanobu Shimada, JAXA
11:00	Frequency Allocation Challenges for UWB Radars Mark Davis, Consultant
11:30	NTIA Perspective Frank Sanders, NTIA

[1] See Appendix C for a summary of the workshop.

12:00 p.m.	Working Lunch
1:00	NASA Active Remote Sensing Spectrum Overview Bryan Huneycutt, JPL
1:30	JPL Radar RFI Experience Steve Durden, JPL Leif Harcke, JPL Scott Hensley, JPL Mike Spencer, JPL
3:45	RFI in P-Band and X-Band Seen by the GeoSAR System Jim Reis, Fugro EarthData
4:15	Group Discussion; Conclusions
5:30	Adjourn
6:30	Working Dinner

MEETING 3

November 14-15, 2013
Arnold and Mabel Beckman Center of the National Academies
Irvine, California

November 14, 2013

CLOSED SESSION

8:00 a.m.	Committee Discussion

OPEN SESSION

11:00	European Perspective on User Requirements andAssociated Applications for Future Spaceborne SAR Systems (including discussion) Kostas Papathanassiou, German Aerospace Center (DLR)
12:00 p.m.	Working Lunch

1:00	The Economic Issues of Spectrum Sharing (including discussion) Coleman Bazelon, Committee member
1:45	Atmospheric Radar: Science Applications, Frequency Usage, Interference Issues (including discussion) Bob Palmer, Committee member
2:45	Ionospheric Radar: Science Applications, Frequency Usage, Interference Issues (including discussion) Bill Bristow, Committee member
3:30	Radar Astronomy: Science Applications, Frequency Usage, Interference Issues (including discussion) Don Campbell, Committee member
4:15	Current and Future Techniques for Increasing Capacity (including discussion) David Borth, University of Illinois at Chicago
5:00	Break for Working Dinner
6:00	Working Dinner
8:00	Adjourn

November 15, 2013

OPEN SESSION

8:30 a.m.	Breakfast
9:00	Multi-Function Phased Array Radar: Program Plans and Frequency Usage (including discussion) Kurt Hondl, NOAA

CLOSED SESSION

9:45	Discussion
1:00	Adjourn Meeting

MEETING 4

February 10-11, 2014
Keck Center of the National Academies
Washington, D.C.

February 10, 2014

CLOSED SESSION

8:30 a.m.	Breakfast Available
9:00	Discussion Fawwaz Ulaby, Chair

OPEN SESSION

9:15	Summary of the Observations and Conclusions from the Last Meeting David Lang, NRC
11:00	Another Perspective on the Future of Wireless Communications Networking Paul Kolodzy, Committee member
12:00 p.m.	Working Lunch

CLOSED SESSION

1:00	Discussion
8:00	Adjourn

February 11, 2014

CLOSED SESSION

8:30 a.m.	Discussion
1:00 p.m.	Adjourn Meeting

MEETING 5

June 11-12, 2014
J. Erik Jonsson Woods Hole Center
Woods Hole, Massachusetts

June 11, 2014

CLOSED SESSION

8:30 a.m.	Working Breakfast
9:00	Discussion Fawwaz Ulaby, Committee Chair
6:15 p.m.	Dinner at Meeting Site

June 12, 2014

CLOSED SESSION

8:30 a.m.	Working Breakfast
9:00	Discussion Fawwaz Ulaby, Committee Chair
12:00 p.m.	Lunch Available and Adjourn

C

Summary of the Radio-Frequency Interference Workshop

Meeting 2 of the Committee on a Survey of the Active Sensing Uses of the Radio Spectrum

November 8, 2013
Jet Propulsion Laboratory
Pasadena, California

The National Academies of Sciences, Engineering, and Medicine's Committee on a Survey of the Active Sensing Uses of the Radio Spectrum convened a 1-day workshop of experts in the area of radio frequency interference (RFI) and active users from the radio frequency spectrum scientific community on November 8, 2013, at the Jet Propulsion Laboratory (JPL) in Pasadena, California. The purpose of the workshop was to obtain information from experts working in the area of active remote sensing of Earth's environment on the problems being encountered in the use of radars for such purposes. Radio-frequency interference has been increasingly observed in data recorded by several airborne and spaceborne radar remote sensing systems. The Academies established the Committee on a Survey of the Active Sensing Uses of the Radio Spectrum to study this problem.

The workshop was organized by committee chair Fawwaz Ulaby and committee member Mike Spencer. Attendees included the following:

NOTE: The notes on which this summary is based were taken by committee member Albin J. Gasiewski, University of Colorado. Acronyms not defined in the text are defined in Appendix D.

Fawwaz Ulaby, University of Michigan, workshop co-organizer and committee chair
Mike Spencer, JPL, workshop co-organizer and committee member
Mark Davis, Independent Consultant
Steve Durden, JPL
Albin Gasiewski, University of Colorado, committee member
Leif Harcke, JPL
Scott Hensley, JPL
Bryan Huneycutt, JPL
Jim Reis, Fugro EarthData
Frank Sanders, National Telecommunications Industry Association (NTIA)
Dean Sangiorgi, Canadian Space Agency (CSA) (by telecon)
Masanobu Shimada, Japan Aerospace Exploration Agency (JAXA)
Pierluigi Silvestrin, European Space Agency (ESA) (by telecon)

BACKGROUND

The workshop was opened by Fawwaz Ulaby, who discussed the context and defined the charge for the workshop. The workshop purpose stemmed from the following charges to the committee:

1. Describe the science that is currently being conducted using the radio spectrum for transmission and measurement of these active signals and identify the spectrum requirements necessary to conduct this research;
2. Identify the anticipated future spectrum requirements necessary to continue to conduct and expand this research for the next 10-20 years, taking into account trends in overall active use of the spectrum;
3. Discuss the value to the nation of accommodating the active scientific use of the spectrum, recognizing the need to balance the needs of multiple communities;
4. Assess the active science communities' current and anticipated future access to the spectrum required for research; and
5. Recommend strategies to accommodate the continued active use of the spectrum for scientific purposes in order to maintain the needed science capabilities identified above.

RFI has been identified by the committee as an important issue. Even though several research institutions and space agencies have reported RFI observations, and in some cases techniques were developed to remove or filter out the interfering signals, there is a need to generate a comprehensive report to document the

RFI issue across all radar-frequency allocated bands from the P-band through the K_a-band as part of this study.

Accordingly, the purpose of the workshop was to answer the following questions for all radar bands between the P-band and the millimeter-wave part of the spectrum:

1. What is the extent of the RFI problem? Where does it occur geographically, and who is the interfering source? Conversely, are remote sensing radars interfering with other users?
2. How does the RFI impact the quality of the information extracted from the radar data?
3. What mitigation techniques, if any, are used to deal with the RFI problem?
4. Projecting 20 years into the future, what future missions are likely to be negatively impacted by the RFI issue?

Prof. Ulaby reminded the attendees of the timeline of the study, which should be completed by approximately the middle of 2014.

PERSPECTIVES FROM THE EUROPEAN SPACE AGENCY

The first presentation was by Pierluigi Silvestrin of ESA, assisted by Elena Daganzo, and presented via teleconference. He described the ESA Earth Observation Programme, which included radar altimeters (e.g., Cryosat-2, Sentinel-3 series), a cloud profiling radar on EarthCare (2018), and synthetic aperture radars on the Sentinel-1 series, and scatterometers on the MetOp operational series of satellites. Silvestrin reminded the attendees of the operation of the K_u- and C-band radars on EnviSat, which operated for 10 years. The Sentinel series is meant to establish a long-term, continuous monitoring capability. A set of interference criteria was presented based on ITU RS 1166. The issue of RFI is an increasing problem for both passive and active ESA sensors. Management of the spectrum by the national authorities is more reactive than pro-active, and pro-active management is urged. Silvestrin proceeded to describe the ESA active microwave sensor bands of interest ranging from 0.435 GHz (P-band synthetic aperture radar (SAR) for surface biomass) to 238 GHz (multimillimeter wave cloud radar). RFI cases for ERS-1/2 SAR were rare (10 cases in 20 years), and also in ENVISAT/ASAR. RFI to ASCAT scatterometer on MetOp were also very low, but increasing after ~mid-2012. Occurrences are in the Middle East and (less so) the Far East and North America. He also reported about RFI to the (passive) SMOS synthetic aperture radiometer, which has seen more than 500 cases. More than 50 percent of these cases have been resolved, but high RFI is still seen in the Middle East, China, and Japan.

Examples of RFI cases in ESA C-band SAR (ERS-2 SAR) and EnviSat (5250-5350 MHz, burst RFI) were presented. It seemed that these cases were possibly due to a military radar. Random position and duration suggests radar pulses, possibly a countermeasure radar. Silvestrin noted that the problems may not be seen in the Level 1 data, and processing of RFI at the Level-0 data is needed to identify RFI. RFI mitigation on the Level-0 data in the time domain was able to be used to remove this RFI based on statistics. However, the mitigation algorithm was not implemented in the ground segment as there was no guarantee of the accuracy of the algorithm.

Silvestrin further described the ESA/European Union Sentinel series' radio band needs from 5250 to 5570 MHz. He indicated that reallocation of local area network allocations by WRC-2003 within this band prompted reassignment of the Sentinel C-band from 5250-5350 MHz to 5350-5470 MHz. In preparation for WRC-2015, he noted with concern that discussions are occurring to expand radio local area network (RLAN) allocations to 5350-5470 MHz, which would hasten the likelihood of SAR interference to Sentinel. The tolerable interference to the Sentinel SAR would be exceeded by 30 dB, and even a single outdoor wireless RLAN would be detectable. He noted that the Sentinel design stemmed from 10 years of effort, while the request to use the new subband for RLAN arose only over the previous year. A relevant question in this regard is this: Will future C-band SARs have the capability to frequency hop from one sub-band to another to avoid RFI? The requisite technology may become available in the future, but it is also likely that the entire C-band range may become a source of RFI, thereby making the frequency hopping capability irrelevant. Also, the C-band RFI sources are anticipated to be nonstationary, and difficult to predict and sense around. How wide a bandwidth would be ultimately needed by C-band SARs? At least 90-100 MHz is needed for data continuity (e.g., for surface topographical change detection using SAR interferometry, InSAR), and higher-resolution design would demand even wider bandwidths. He noted that the original C-band allocation was 320 MHz, and so current systems are operating at reduced bandwidths from even this specification.

The potential for interference between ESA active remote sensing SARS systems operating at 420-450 MHz and other services, such as Space Object Tracking Radars (SOTRs) at the P-band, was also discussed. Silvestrin noted the existence of a proposed approach for sharing which is being discussed with the U.S. Department of Defense, but no reciprocal coordination by the United States has been offered. As a result, secondary mission objectives (e.g., ice sounding) are strongly impacted. Missions using the X-, K_u-, and K_a-bands are also being studied, but no RFI concerns have yet been identified.

PERSPECTIVES FROM THE CANADIAN SPACE AGENCY

Dean Sangiorgi of CSA discussed the needs and current RFI situation of the CSA and, specifically, the use of the C-band. Radarsat-1 used a carrier centered at 5300 MHz, and the Radarsat-2 Constellation Mission (RCM) will use 5405 MHz center frequency. A bandwidth of up to 100 MHz is used. Launch of three satellites is due in 2018. A two-part study with MacDonald Dettwiler Associates (MDA) was undertaken to assess current and past RFI and to simulate RFI. The study used Ottawa as the primary scene with 85 scenes between 1996 and 2012. A consistent backscatter increase was seen in 4 of 9 scenes between 2001-2002; all of these were covered by water and close to urban centers. These were likely a result of RFI increases. Overall an average increase of 3 dB was noted over the 15-year period, although there was no definite way to identify what was the source of the increase.

Sangiorgi also discussed the impact of World Radiocommunication Conference (WRC)-2015 RLAN reallocations on the 5305-5470 MHz band. A joint task group has been formed to discuss this issue, and the MDA study considered additive Gaussian noise to study the potential impact. A scene from May 2010 of the Victoria, British Columbia, airport was used as a baseline. Small detectable noise features are seen at an interference-to-noise level (I/N) of 0 dB in Radarsat-2 images. The additive interference is visible in areas of low backscatter such as runways. Eventually, runways and highways become undetectable at levels of ~6 dB, and at ~12 dB the image becomes useless. Such interference impacts the use of the data for change detection, specifically with respect to archival imagery observed without interference. An experiment using actual RLANs to study the impact empirically is being considered. A graph of number of RLAN connections required to exceed an interference threshold was presented. Approximately 1,050 RLAN connections with an equivalent (or effective) isotropically radiated power (EIRP) between 25 mW and 1 W over the 225 km^2 can be tolerated within a 100 MHz bandwidth. A –6 dB I/N threshold was concurred as a rough threshold for observing an effect on InSAR topography. The conclusion of the study is that sharing between RLANs and Radarsat Constellation Mission (RCM) measurements is not practical. Potential use of RLANS in 5350-5450 MHz is thus a growing concern.

CSA foresees continued use of C-band SAR sensors in future missions to ensure data continuity beyond 2025. RCM launches are scheduled to begin in 2018.

PERSPECTIVES FROM THE JAPAN AEROSPACE EXPLORATION AGENCY

Masanobu Shimada of JAXA provided an assessment of RFI concerns to the JAXA L-band SAR missions, including ERS-1/SAR (1992-1998), ALOS/PALSAR (2006-2011), and ALOS-2 (2013-). A bandwidth of 28 MHz is used by PALSAR, and 85 MHz is used by ALOS-2. He also discussed the airborne Pi-SAR radars.

RFI has been recognized as the noise source for the JAXA L-band SAR imaging problem. The contamination bandwidth as become wider as time has progressed. A possible correction is zero padding the contaminated frequency components, resulting in a contamination ratio that has been increasing in time. The RFI for examples shown was believed to be due to ground radars operating over Japan. Both JERS-1 (15 MHz bandwidth about 1.275 GHz center frequency) and PALSAR (28 MHz bandwidth over 1.270 GHz center frequency) were both shown to be affected. Shimada noted that the RFI depends on observation angle. Notch filters are applied to the spectral data to produce images that have RFIs of ~3 MHz in width removed. Significant image improvement over Hawaii and Alaska were shown after RFI mitigation, including changes in overall backscatter baseline. RFI over Korea was shown to be quite large and not removed by notch filtering. The notch filter is applied automatically; however, it also removes some noticeable geophysical features.

Global maps of RFI observed by JERS1-SAR and PALSAR from 1992-2011 using the notch filtering methods were shown. Up to a few percent bandwidth contamination was observed from 1992-1998, increasing to up to 10 percent in 2011. Contamination is noted in Western Europe, Middle East, China, Korea, and a radar line across northern Canada. Contamination also occurs over water. Sidelobe coupling of RFI from over land (for water observations) was also noted. Major increases in contaminated areas are observed from JERS-1 to PALSAR, although differences in radar bandwidth and power level would warrant a major reprocessing effort to ensure consistency between the two data sets.

FREQUENCY ALLOCATION CHALLENGES FROM UWB RADARS

Frequency Allocation Challenges from ultra wideband (UWB) radars were discussed by Mark Davis, an independent consultant and representative of the Institute of Electrical and Electronics Engineers (IEEE) Aerospace and Electronic Systems Society (AESS). He noted that advanced radar techniques are demanding more bandwidth and frequencies, but wideband communications for government and personal/business use are being allocated more bandwidth. The economics for frequency allocation are presenting a serious impediment for radar frequency allocation. AESS has the charter for maintaining the IEEE radar definitions and standards. A subpanel on radar waveform diversity has been established to explore the impact of spectrum allocations. IEEE standard 1675 defines UWB as being either "500 MHz bandwidth or a percentage bandwidth greater than 25 percent" of the carrier frequency. Two examples of airborne UWB radars: FOPEN ATD (100 percent and 120 percent bandwidth for the UHF band and the VHF band, respectively), and GeoSAR (50 percent bandwidth for the UHF band and 2 percent bandwidth for the X-band) were discussed. Both systems experienced a 3-year frequency approval process.

Davis discussed the UWB intercept power measurement concept. The NTIA Part 15 UHF Frequency Avoidance Table shows very few open bands within UHF, with –70 to –90 dBm sensitivity thresholds. All UWB airborne systems must use a very conservative approach to notching across the UHF band in order to get permission to operate. The range from 960 to ~1470 MHz is particularly important for GPS and other critical applications. However, the NTIA requirements cause significant loss of bandwidth due to excessive notching. Linear frequency-modulated notching or frequency jump bursts are used for notching. Significant loss of resolution occurs for current notching requirements. Bridging notched frequencies can improve resolution, as can use of cognitive radar techniques. The cognitive radar approach senses and adapts to the radio frequency environment, and uses adaptive transmit waveforms to achieve greater average bandwidth.

The conclusion is that compliance standards are conservative and inflexible, and that new technologies need to be considered. The international radar community needs to adapt and develop new technologies analogous to cognitive radio. Systems demonstrating cognitive radio include those developed by the U.S. Army and the Defense Advanced Research Projects Agency, but only now are these technologies being studied for use in radar.

NATIONAL TELECOMMUNICATIONS INDUSTRY ASSOCIATION PERSPECTIVE

Frank Sanders of the NTIA provided the issue of RFI between active L-band long-range search radars and satellites. Terrestrial radar usually transmit upwards at angles of ~0.5 to 20 degrees above the horizon and, thus, can scan across many satellites. The high sensitivity of satellite and radar receivers suggests that RFI may potentially occur in both directions. Propagation distances are generally in the range of 440 to 900 km. Dr. Sanders presented typical solid-state air-search radar EMC characteristics. These radars operate between 1200-1400 MHz, and have very gain antennas (30-40 dBi). Scan rates are ~1 rotation per second. Unintentional out-of-band (OOB) emissions may only be 40 dB down at 1400 MHz due to a non-conservative OOB spectral emission mask. Sanders noted that the P(Y) channel frequency of GPS receivers at 1227.60 MHz are not affected by long-range search radars since they integrate over the brief search radar pulse. Peak EIRP at 1425 MHz and 440 km distance would be approximately -83 dBm/MHz into a 0 dBi satellite receiver (see NTIA report TR-06-444, available at http://www.its.bldrdoc.gov/publications/2481.aspx). A transmit power of ~250 W might be possible without exceeding a typical –6 dB I/N limit.

Interference to long radars from satellite can also occur, as shown in a plan position indicator (PPI) long-range radar image with ~5 degree blanked azimuthal sector. Interference as part of NASA SMAP design studies were performed showing

reductions of the probability of detection (P_d) at interference levels of ~20 dB I/N for three long-range radar types. SMAP has a 1-MHz transmit bandwidth, which is comparable to the long-range radars (a few MHz).

In summary, RFI can occur in both directions, and the U.S. recommendations on OOB rolloff provides some protection. Satellite transmitters can provide RFI into long-range radars, potentially causing loss of tracked aircraft. Occurrence of loss of tracking is more frequent that 1 in 10^6, but difficult to further specify.

NASA ACTIVE REMOTE SENSING SPECTRUM OVERVIEW

Bryan Huneycutt of JPL provided as overview of NASA JPL satellite experiment, beginning with Seasat in 1978. Sensor types are SARs (e.g., Seasat, AIRMOSS), altimeters (e.g., JASON, SWOT), scatterometers (e.g., QuikSCAT, Aquarius), precipitation radars (e.g., TRMM TMI or GPM GMI), and cloud radars (e.g., CloudSat). Applications impact viewing geometry and required bands, but requirements include frequencies from the P-band (0.432-0.438 GHz) to the millimeter wave spectrum (237.9-238.0 GHz). This is frequency range of over 500 (or ~9 octaves). Several current and planned missions use bands that do not necessarily have primary allocations for EESS active remote sensing. The EESS-Active allocated bands and their current uses were discussed, specifically radiolocation. Interference criteria for missions range from –3 to –10 dB I/N, and data availability criteria are between 95 and 99 percent.

JPL RADAR RFI EXPERIENCE WITH ATMOSPHERIC RADARS

Steve Durden of NASA JPL provided a synopsis of airborne and satellite atmospheric radar missions. The ARMAR radar operated at 13.4 GHz, and later (APR-2) at 13.4, and 35.6 GHz. The Airborne Cloud Radar (ACR) at 94.9 GHz was developed in the 1990s was a forerunner of CloudSat. This allocation was rooted in historical continuity. Getting a temporary assignment has been straightforward. Bandwidths required are ~100 MHz. The CloudSat allocation was originally at 78 GHz, but moved to 94 GHz to improve sensitivity to small cloud particles and take advantage of the availability of extended interaction klystron amplifier technology. Potential damaging interference from CloudSat to radioastronomy facilities (e.g., Haystack) remains a concern, but has apparently never occurred since most radio astronomy facilities do not observe at zenith. In summary, there are no major interference problems occurring with cloud radars, and the frequency allocations and bandwidths currently allocated are adequate for current and future missions. However, the possibility that automobile collision avoidance radars are being built to operate at the W-band raises some concerns about the future viability of this band.

JPL RADAR RFI EXPERIENCE WITH P-BAND RADARS

Leif Harcke of NASA JPL provided a synopsis of AirMOSS P-band radar RFI experience. AirMOSS is capable of operating from 280 to 450 MHz with an instantaneous bandwidth of 80 MHz. Only a 20 MHz chirped operating bandwidth without notching has currently been approved. The CleanRFI code has been used for RFI removal. The algorithm was illustrated using 430-450 MHz P-band data from AIRSAR in 1998 where significant RFI was successfully removed. Narrowband amateur radio communication sources at 450 MHz were cited as likely sources. The Point Target Simulator (PTS) for simulating interference was described. It was noted that the interference was often so time dynamic (for a number of reasons, including frequency hopping, multipath fading, sidelobe reception) that derived least mean square filter coefficients could not readily be reused from pulse to pulse. Changes of 2-3 dB in backscattering cross section were noted upon filtering. Data obtained using 32,000 fast Fourier transform samples over 80 MHz reveal many interference sources that are 20-30 dB above the radar receiver noise floor. Most of these sources are narrowband and are ubiquitous over all AirMOSS calibration sites. The strongest RFI was observed in the United States from 406-420, 450-470, and 440-450 MHz. The 420-440 MHz spectrum has been observed to be the quietest. Some wideband sources are present from time to time and at certain locations (Duke Experimental Forest).

JPL PERSPECTIVES ON L-BAND RADAR INTERFERENCE

Mike Spencer of NASA JPL provided a discussion of the impact of RFI on L-band active remote sensing. The science applications include soil moisture, salinity, biomass measurement, disaster management, and polar studies. Sensors include Aquarius (~1260 MHz) and SMAP (~1230 MHz), and NI-SAR and UAVSAR (~1280 MHz). A number of radionavigation and radar systems operate over the bands of these instruments. Aquarius observations provided a global map of radar RFI in dBm. The interference is globally conspicuous. Over North America the strongest sources are known emitters, most of which are long-range radars. The current interference environment seems mostly manageable from a science perspective. However, there are worrisome trends, including lower power/longer pulses and higher pulse repetition frequency Common Air Route Surveillance Radars, which are harder to remove. Also worrisome is the general increase of the urban noise floor, which was illustrated by PALSAR measurements over Hong Kong.

The SMAP frequency approval process required changing from low-power long pulses (200 W/40 usec) to higher-power shorter pulses (500 W/15 usec). The process required 11 months and extensive testing against Federal Aviation Administration (FAA) radars in Oklahoma City, compatibility testing against GPS systems,

and an extensive dynamics analysis. A short duty cycle is preferred to minimize interference to long-range radars. Some operational restrictions on SMAP may yet be imposed. SMAP is scheduled to be launched in January 2015.[1] It is noted that Aquarius has been operating for 2 years without incurring any interference to ground-based radars.

In summary, the status quo is acceptable, but there are concerns about the long-term future. There are also ill-defined spectral acceptability criteria that hinder the approval process, thus carrying operational risk deep into the project life cycle.

JPL PERSPECTIVES ON SCIENCE DEGRADATION METRICS TO TRACK THE IMPACT OF AN EVOLVING RFI ENVIRONMENT

Scott Hensley of NASA JPL provided a discussion of metrics to track the impact of an evolving RFI environment and observations of increasing RFI over the past decades of active science studies. A goal is that NASA develop a standard way of setting RFI criteria. NASA operates a variety of sensors over a wide range of frequencies that cannot be shifted in frequency due to the physics of the measurement. Hensley's fundamental recommendation is for NASA to fund development of metrics addressing the impact of RFI on active sensor science. Questions such metrics need to quantitatively answer are the following: (1) What is the impact of RFI to science? (2) When is RFI so great that precludes useful science? and (3) What is the benefit of this science to society? Anecdotal evidence is insufficient to track these impacts.

Hensley next outlined the qualities of a good metric. It needs to be relatively easy to compute, measure degradation in way that is easy to explain, accurately reflect the loss of science to changes in the RFI environment, be able to be tracked over a mission lifetime to inform future missions, and be meaningfully averaged both spatially and temporally. With radars, every aspect of the received signal is used (amplitude, frequency, time delay, Doppler shift, and phase). The impact to science depends on the character of the RFI. The full characteristics of the RFI signals should be characterized empirically. He suggested a table that would begin a means of archiving RFI.

Hensley considered the example of SMAP, which offers a simple metric for quantifying the impact of RFI on the error standard deviation (STD) of the backscattering cross section. This error STD can be directly related to soil moisture error. In radar interferometry the signal-to-noise ratio (SNR) correlation is also a straightforward function of the SNR and RFI signal-to-interference ratio (SIR). Carrying these degradation ratios back to the accuracy of the science product depends on the differential relationship between backscattered signal and geophysi-

[1] As of January 24, 2015.

cal quantity of interest. The example of RFI impact on topography and deformation measurements was suggested.

RFI IN THE P-BAND AND THE X-BAND SEEN BY THE GEOSAR SYSTEM

Jim Reis of Fugro EarthData discussed a user's perspective on a commercial SAR system, including the licensing issues associated with allocations. The GeoSAR is a wideband, interferometric, fully polarimetric P- and X-band system that has been in continuous commercial use since 2003. It uses a Gulfstream II aircraft to provide a 20 m interferometric baseline. Reis provided a number of examples of RFI occurring at various locations, including Papua New Guinea, Columbia, Central Alaska, Maryland, and Barrow Alaska. Notch filters over the ~160 MHz GeoSAR bandwidth (from 260 to 440 MHz) are required to in some regions to remove some authorized and unauthorized RFI. Both cases of narrowband and broadband RFI are observed, some of which is persistent over at least 2 years.

Certification of the GeoSAR system to Stage 4 through NTIA and Federal Communications Commission (FCC) was a lengthy process. Since it was a system that had routinely licensed over the last 8 years, it was considered for allocation. An early RFI study led to a requirement for mandatory notching of all users within a 20 nmi zone from nadir to prevent communications disruption. However, the Air Force Spectrum Management Office (AFSMO) imposed an umbrella standard requiring matching of all users up to 500 nmi from the acquisition site. Overall, the final notching requirements became more strict. Also, an active U.S. government contract was required at the time of allocation. The new process for allocation is through the FCC, which submits the request for a 30-day suspension with affected government agencies (NTIA, AFSMO, FAA, etc.), followed by a special temporary authorization. Such slow and uncertain allocation processes inhibits the regular operation of the system required to maintain operational readiness.

DISCUSSION AND SUMMARY

A brief workshop discussion session was held after the last presentation. It was requested by Prof. Ulaby that the attendees share with the organizer the three most important observations and recommendations from the workshop.

WORKSHOP OBSERVATIONS

General observations from discussions held during the workshop presentations and afterwards during the discussion session follow:

1. The approval process for transmit allocations is too cumbersome, lengthy, and ill-advised. The U.S. Interagency Radio Advisory Committee (IRAC) operates by consensus of its members and, thus, provides numerous opportunities to table or veto applications. The allocation for GeoSAR radar allocations is ineffective and encourages only voluntary self-compliance by the applicant.
2. The development of a common set of standardized metrics connecting RFI levels to science product accuracies would be useful in assessing the costs of observing with increasing levels of RFI.
3. The associated problems of adaptive notching and how notch variation on a pulse-to-pule basis affects SAR resolution and processing are open areas that need engineering investigation.

D

Acronyms

ADEOS	Advanced Earth Observing Satellite
ALOS	Advanced Land Observing Satellite
ALT	radar altimeter
AMSR	Advanced Microwave Scanning Radiometer
ARM	Atmospheric Radiation Measurement
ASA	Authorized Shared Access
BLR	boundary layer radar
CASA	Collaborative Adaptive Sensing of the Atmosphere
CCD	coherent change detection
CCN	cloud condensation nuclei
CDMA	Code Domain Multiple Access
CITEL	Commission for Inter-American Telecommunications
CNES	French Space Agency
CODAR	Coastal Ocean Dynamics Applications Radar
CONUS	continental United States
CYGNSS	Cyclone Global Navigation Satellite System
DARN	Dual Auroral Radar Network
DEM	Digital Elevation Model
DOD	Department of Defense
DPR	Dual-frequency Precipitation Radar

ECMWF	European Centre for Medium-Range Weather Forecasts
EESS	Earth Exploration-Satellite Service
EIRP	Effective Isotropic Radiated Power
EISCAT	European Incoherent Scatter Radar
ELF	extremely low frequency
EM	electromagnetic
ERS-1	European Remote Sensing Satellite
ESA	European Space Agency
ESM	Electromagnetic Spectrum Management
EUV	extreme ultraviolet
FAA	Federal Aviation Administration
FAI	field-aligned irregularity
FCC	Federal Communications Commission
FDMA	Frequency Division Multiple Access
GBT	Green Bank Telescope
GCM	General Circulation Model
GIRO	Global Ionospheric Radio Observatory
GMDSS	Global Maritime Distress and Safety System
GMF	Government Master File
GNSS	Global Navigation Satellite Systems
GPM	Global Precipitation Mission
GPR	ground-penetrating radar
GR	general relativity
GRACE	Gravity Recovery and Climate Experiment
IMF	interplanetary magnetic field
InSAR	Interferometric SAR
IOOS	Integrated Ocean Observing System
IRAC	Interdepartment Radio Advisory Committee
ISR	Ionosondes and Incoherent-Scatter Radar
ISS	International Space Station
ITU	International Telecommunications Union
ITU-R	Radiocommunication Sector of the International Telecommunications Union
JAXA	Japan Aerospace Exploration Agency
LAN	local area networks
LMS	least mean square

LSA	Licensed Shared Access
MetSat	Meteorological Satellite Services
MHR	Mile High Radar
MPAR	Multifunction Phased Array Radar
MSS	Mobile Satellite Service
MST	mesosphere-stratosphere-troposphere
NASA	National Aeronautics and Space Administration
NASDA	National Space Development Agency
Ne	total plasma density
NEA	near-Earth asteroid
NEO	near-Earth object
NEXRAD	WSR-88D radar network
NISAR	NASA/ISRO L-band SAR mission
NPB	National Broadband Plan
NRC	National Research Council
NSCAT	NASA Scatterometer
NSF	National Science Foundation
NTIA	National Telecommunications and Information Administration
NWP	Numerical Weather Prediction
OSTM	Ocean Surface Topography Mission
PALSAR	Phased Array type L-band Synthetic Aperture Radar
PFISR	Poker Flat, Alaska, Incoherent-Scatter Radar
PHA	potentially hazardous asteroid
PMSE	Polar Mesospheric Summer Echoes
PR	precipitation radar
PRF	pulse repetition frequency
RFI	Radio Frequency Interference
RLAN	Radio Local Access Network
RLS	Radio Location Service
RSI	Radar Speckle Interferometry
SAR	synthetic-aperture radar
SASS	Seasat-A Satellite Scatterometer
Scat	scatterometer
SINR	signal-to-interference-plus-noise ratio
SLAR	systems/side-looking airborne radar

SMAP	Soil Moisture Active Passive
SMMR	Scanning Multichannel Microwave Radiometer
SMS	Spectrum Management for Science in the 21st Century
SOS	Space Operation Services
SOTR	Space Object Tracking Radar (DOD)
SRS	Space Research Services
SRTM	Shuttle Radar Topography Mission
SST	sea surface temperature
STA	Special Temporary Authority
SWE	snow water equivalent
SWOT	Surface Water Ocean Topography
SXXI	Spectrum XXI
TEC	total electron content
TNT	trinitrotoluene
TRMM	Tropical Rain Mapping Mission
U.S. WP7C	U.S. Working Party 7C
ULS	Universal Licensing System
VLA	Very Large Array
VLBA	Very Long Baseline Array
VLF	very low frequency
WRC	World Radiocommunication Conference